THE ROLE OF INTEGRINS IN THE ACTIVATION OF FIBROBLASTS FROM SKIN, LUNG AND BREAST TISSUE

Zareen A. Khan

This thesis is submitted for the degree of Doctor of Philosophy

Queen Mary, University of London

2016

Declaration

I confirm that the research included within this thesis is my own work, with contributions from others properly cited and acknowledged. The work presented in this thesis was completed at the Centre for Tumour Biology, Barts Cancer Institute, Barts and the London School of Medicine and Dentistry, Queen Mary, University of London.

This study was funded by the Biotechnology and Biological Sciences Research Council (BBSRC) and GlaxoSmithKline.

Zareen Khan

October 2016

Acknowledgements

Firstly, I would like to thank my supervisor John. Thank you for giving me the opportunity to work on a great project and providing new and exciting ideas along the way. Thank you for being available whenever I needed advice and for all your helpful suggestions and guidance. Additionally, thanks to Dr Rob Slack and Dr Steve Ludbrook (GSK) for their advice and allowing me to spend time at GSK. I am also very grateful to have been part of the great 'β6 group'; to John, Kate, Ami (aka 'Ms Moneypenny'), Caroline, Claire, Ketan and Banu, thank you for all your support over the last four years and for all the laughs we've had at our group meetings! I feel so lucky to have worked alongside you all, and to not only call you colleagues, but friends.

As probably expected, the past four years have not been easy, though there were always lots of great times amongst the harder ones. A particular thank you goes to Myrto, Delphine and Mike for all your great PCR advice to get me started! And additionally, thanks to Stella for your patience, advice and sense of humour when our experiments didn't go as planned. I would also like to thank the following people for their friendship throughout this time. Again, thank you to Claire, Ketan, Caroline, Ivan, Natalia, Prabs, Abbie Fearon, Bakhouche, Liz, Abigail, Tash, Ed, Yasmine, Alex and Sara for making the lab such a fun place to work. I know from Debbie, how much our laughter use to fill up the lab.

Particularly special thanks go to Ami for sharing all the lab highs and lows with me throughout the four years. Thanks for keeping me sane. To Elisabete, thank you for making time for our tea breaks; your unwavering support and friendship means a lot to me. To Francesca, thanks for taking me on lots of adventures outside the lab, you are now a member of the Khan clan. To Fevzi, thanks for keeping me laughing through those long hours and weekends in the lab. To my friends outside the lab who have had to listen to me talk a lot of science/complain over the last four years; Angela, Ami, Rafeah, Kafia, Reena and Yasmin, you are more like sisters to me, as our decade long friendship already proves.

And finally, a big thank you to my siblings, Ambreen and Kamran for your continued love and support, and to my parents. To my late father, for always being so passionate about education and to my mum, there are not enough words for me to describe my gratitude. Thank you for supporting me throughout these four years. You made the journey much easier for me and I'm sorry if I did not always show how much I appreciated that.

Abstract

Fibroblasts are abundant mesenchymal cells present in all tissues in a quiescent state, which contribute to wound healing when activated. Cytokine transforming growth factor-β1 (TGF-β1) stimulates fibroblast-myofibroblast differentiation, which induces extracellular matrix secretion, tissue contraction and promotes cancer cell migration. Hence, chronic activity of stromal myofibroblasts correlates with a poor prognosis for cancer and organ fibrosis patients. Therefore, modulating myofibroblast activity may reduce the severity of these diseases. Previous research suggests blockade of transmembrane integrin receptors expressed by fibroblasts prevents TGF-β1-induced differentiation, indicating integrins are attractive therapeutic targets. However, fibroblasts derived from different organs exhibit heterogeneity, although their integrin expression and integrin-regulated differentiation has not been directly compared. The aim of my research was 1) to understand and compare how integrins regulate TGF-β1-induced activation of fibroblasts derived from normal skin, lung and breast tissue; 2) to examine the global gene expression of TGF-β1-treated lung fibroblasts; 3) to identify novel therapeutic targets that modulate TGF-β1-induced activation of lung fibroblasts using a drug library.

qPCR showed skin, lung and breast fibroblasts differentially expressed TGF-β1-induced activation markers, including ACTA2, FN1, TIMP3, CTGF and SERPINE1, in addition to integrin genes for α1, α4, α11 and β3. Small-molecule inhibitors of αv integrins only reduced the invasion of TGF-β1-exposed skin fibroblasts, but not lung or breast fibroblasts. siRNA against α11, β3 and β5 decreased TGF-β1-induced collagen contraction and activation marker expression in skin and lung fibroblasts, while α1 siRNA prevented collagen contraction by breast fibroblasts only. RNA sequencing of TGF-β1-treated lung fibroblasts revealed pro-inflammatory and pro-fibrotic pathways were significantly enriched, while screening TGF-β1-treated lung fibroblasts with a FDA-approved drug library identified 46 hits that significantly reduced α-smooth muscle actin and fibronectin expression.

Overall, genes are differentially expressed in TGF-β1-treated skin, lung and breast fibroblasts, while different integrins in each fibroblast appear to regulate invasion,

TGF-β1-induced collagen contraction and gene expression. RNA sequencing revealed TGF-β1 promotes the expression of a pro-tumour signature in lung fibroblasts and several novel therapeutic targets that modulate the activation of lung fibroblasts have been identified. Understanding these integrin-dependent and independent mechanisms will facilitate the generation of myofibroblast-targeted treatments for cancer and organ fibrosis.

Table of Contents

List of Figures

List of Tables

CHAPTER I. INTRODUCTION

1.1. Fibroblast biology

Fibroblasts are mesenchymal, spindle-shaped cells that are present in a quiescent state in most mammalian tissues. In response to various cytokines and changes in stiffness of their surrounding environment, fibroblasts differentiate into myofibroblasts[1], where they coordinate the synthesis, organisation and maintenance of the extracellular matrix, which functions as a scaffold that binds together organ tissue. Myofibroblasts maintain tissue homeostasis and hence, demonstrate prominent roles during embryonic development and wound repair, but also undergo activation in pathological states, such as cancer and organ fibrosis[2].

1.1.1. The role of fibroblasts during wound healing

The term 'myofibroblast' was originally suggested after the discovery that fibroblasts located within a newly secreted matrix of a healing wound, named granulation tissue, displayed distinct contractile apparatus within the cell cytoplasm. These consisted of densely packed bundles of actin stress fibres that were organised into microfilaments, indicating cells had adopted a contractile phenotype[3]. These findings were further illustrated by plating human skin fibroblasts obtained from healing wounds on to collagen gels, which were contracted to 50% of their original size within 24-hours. This was in contrast to healthy dermal fibroblasts derived from non-wounded skin, where prominent actin stress fibres were absent and cells took at least three times longer to achieve the same level of contraction, demonstrating fibroblasts undergo phenotypic changes during wound healing[4].

Universally, α-smooth muscle actin (α-SMA), which is a constituent of these stress fibres is predominantly used as a molecular marker of fibroblast-to-myofibroblast differentiation[1]. However, the identification of myofibroblast-specific markers is required, as smooth muscle cells and contractile cells surrounding vasculature called pericytes may also express α-SMA[5].

Wound healing is a dynamic process involving multiple stages and cellular contributions. In brief, this process has three primary stages: inflammation, granulation tissue formation and regeneration. Initial tissue injury causes damaged

capillaries to activate circulating platelets, which initiate the formation of a fibrin-based blood clot. Platelets release cytokines and chemotactic factors, such as transforming growth factor-β1 (TGF-β1) and platelet-derived growth factor (PDGF) which recruit inflammatory cells, including neutrophils, to remove debris from the site of injury and circulating monocytes, which mature into macrophages after infiltrating the wound from the local tissue and blood supply[6]. Macrophages are an additional source of TGF-β1 and PDGF, which promote endothelial cell recruitment and fibroblast proliferation and migration into the wound site, as displayed in **Figure 1.1a**[7]. The importance of this cytokine environment is typified by macrophage ablation in mice, which display defective wound repair[8].

The second stage of wound repair involves the formation of new blood vessels at the site of injury and the differentiation of recruited fibroblasts into α-SMA-expressing myofibroblasts, which generate granulation tissue by secreting extracellular matrix proteins to stabilise the wound, 3-4 days after injury[6]. The predominant extracellular matrix (ECM) component deposited in the initial fibrin clot is myofibroblast-secreted fibronectin that constitutes the scab covering the wound site[9]. This provides a framework for myofibroblast-secreted collagen type III fibrils that are gradually replaced by collagen type I to facilitate rebuilding of the wound space, which is a key structural component of dermal tissue[10].

Myofibroblasts then contract this underlying connective tissue to bring wound margins closer together[11]. Fibroblasts are mechanoresponsive cells as increases in the tension of granulation tissue also promotes α-SMA expression, which corresponds with the level of contractility. This phenomenon was demonstrated by Hinz and colleagues, who subjected tissue strips from wound sites to tension, which correlated with higher expression of α-SMA and fibronectin splice variant ED-A, compared to control tissue strips exhibiting lower levels of tension[12]. Contraction of the granulation tissue permits re-epithelialization, whereby local keratinocytes migrate along the wound edge and begin to proliferate (**Figure 1.1b**). Previous studies demonstrate that double paracrine signalling occurs between keratinocytes and fibroblasts, whereby IL-1 secreted from these epidermal cells stimulates the release of cytokine IL-6 from fibroblasts, which promotes keratinocyte

proliferation[13]. Moreover, wounds of IL-6 knockout mice exhibit less infiltrating leukocytes and angiogenesis culminating in delayed wound closure[14, 15].

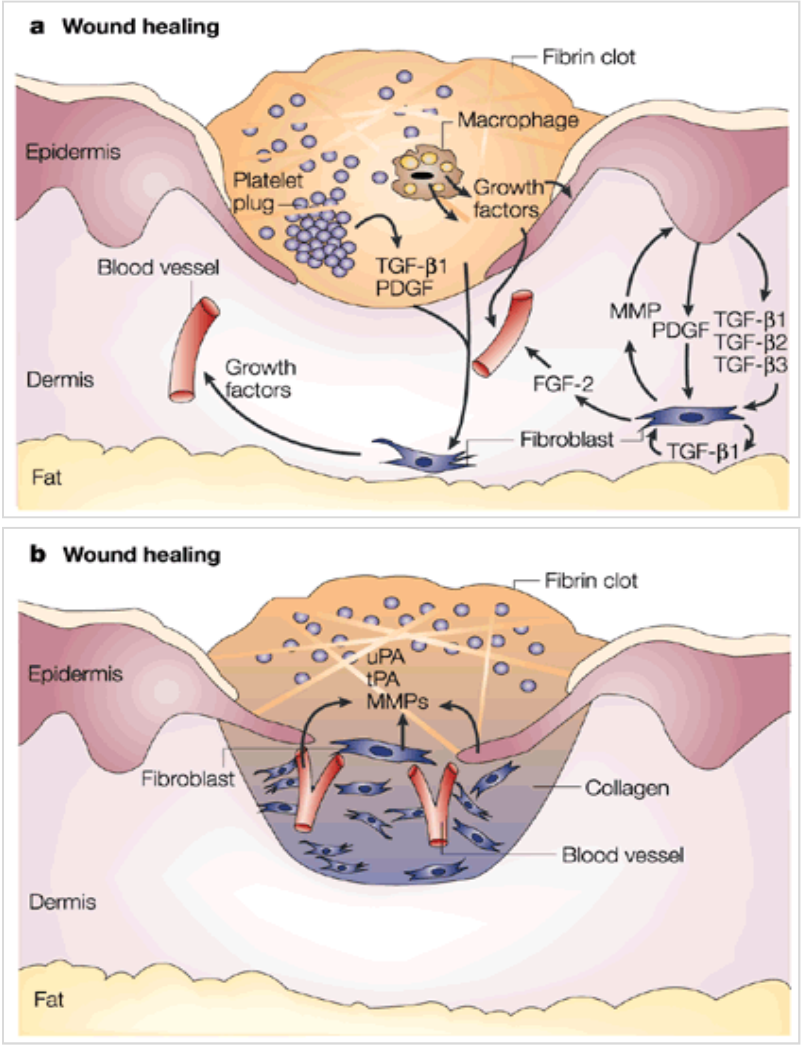

Figure 1. 1. Stages of wound healing during the inflammatory and remodelling phase.

A) The initial phase of wound healing results in fibrin clot formation and infiltration of inflammatory cells, which stimulate and recruit local fibroblasts. B) Remodelling of the wound involves production of proteases such as matrix metalloproteinases (MMPs) and urokinase/tissue plasminogen activator (uPA/tPA) by epidermal cells and granulation tissue formation and contraction by fibroblasts, which facilitates re-epithelialisation and angiogenesis. TGF-β: Transforming growth factor-β. PDGF: Platelet derived growth factor. FGF-2: Fibroblast growth factor. Image adapted from Bissell and Radisky, 2001.

In the final phases of wound healing the mechanical tension is lowered, which induces a reduction of myofibroblast numbers by apoptosis[5], although it is unknown whether myofibroblasts can revert into quiescent non-α-SMA-expressing fibroblasts[6].

The process of wound healing encapsulates key functions of myofibroblasts, including migration, the production of inflammatory mediators and the secretion and contraction of the extracellular matrix. Many of these functions, begin with TGF-β1 stimulation, which is a potent inducer of this active phenotype.

1.2. TGF-β1 activation

TGF-β1 is a pleiotropic cytokine with wide ranging biological effects, including cell proliferation, differentiation and apoptosis[16]. It is a component of the TGF-β superfamily of related signalling molecules, which contain common features such as the positioning of 7 cysteine residues in their core structure. This family includes 3 TGF-β isoforms (TGF-β1, TGF-β2 and TGF-β3), Activins, Nodal and bone morphogenetic proteins (BMPs), each with differential effects[17]. As TGF-β1 is the more abundant isoform and a potent inducer of fibroblast-to-myofibroblast differentiation[18], it was solely used in this study, therefore following literature is focused on this isoform.

TGF-β1 is secreted by damaged epithelial cells, immune cells, myofibroblasts and tumour cells[19], though it is initially translated as a precursor protein that is intracellularly processed via proteolytic cleavage into a latent form. This comprises homodimeric TGF-β1 that is non-covalently bound to the amino-terminal of 'latency-associated peptide' (LAP) and latent TGF-β binding protein (LTBP)[16, 20], which is secreted in this inactive complex that binds fibrillin-1 and fibronectin in the ECM (**Figure 1.2A**)[21]. Active TGF-β1 is then released from matrix-bound LAP-LTBP via various mechanisms, including proteolytic degradation of LAP via proteases localised to the cell surface of epithelial cells, particularly matrix metalloproteinase-2 (MMP-2)[22] and MMP-9[23] and myofibroblast-mediated contraction of the matrix, which primes latent-TGF-β1 for activation. In 2014, Klingberg and colleagues demonstrated

that when myofibroblasts contract the ECM, they reorganise LTBP-fibronectin into dense fibrils, whereas undifferentiated fibroblasts are unable to do so. This appears to facilitate more efficient activation and hence, higher levels of active TGF-β1 are generated by myofibroblasts[24]. Transmembrane integrin receptors also represent a key mechanism by which epithelial cells and fibroblasts bind and activate latent TGF-β1, as further detailed in section 1.3.

1.2.1. TGF-β receptor signalling in fibroblasts

Once released from its latent complex, active TGF-β1, -2 and -3 are each capable of binding to the type II TGF-β receptor expressed by fibroblasts, epithelial cells, inflammatory cells and endothelial cells. This dimeric receptor exists as a constitutively active serine-threonine kinase, and upon binding the cytokine, dimerises with the type I receptor dimer, inducing autophosphorylation (**Figure 1.2B**)[16]. This permits the recruitment and activation of canonical TGF-β signalling proteins, namely receptor-activated Smad2 and Smad3, that when phosphorylated bind Smad4 (**Figure 1.2C**) and translocate to the nucleus, to induce the transcription of various genes[25].

In addition, several positive and negative regulatory proteins also exist, including Smad anchor for receptor activation (SARA), which facilitates the binding of Smad2 to TGF-β receptors, and inhibitory Smad7, which interferes with the phosphorylation of Smad2/3 and mediates TGF-β receptor degradation[26], preventing downstream signalling. To induce transcription of key TGF-β1 target genes, the complex of Smads2/3 and Smad4 bind to Smad-binding elements in DNA, though they require synergy with additional transcription factors. These include AP-1 or TFE3, which bind to specific DNA sequences within TGF-β response elements and initiate transcription of key myofibroblast genes, such as protease inhibitor plasminogen activator inhibitor-1 (SERPINE1)[27]. Another key set of genes induced by TGF-β1 stimulation are the cell surface receptors, integrins, whereby TGF-β1 also signals via integrins to activate non-canonical signalling pathways in fibroblasts[28].

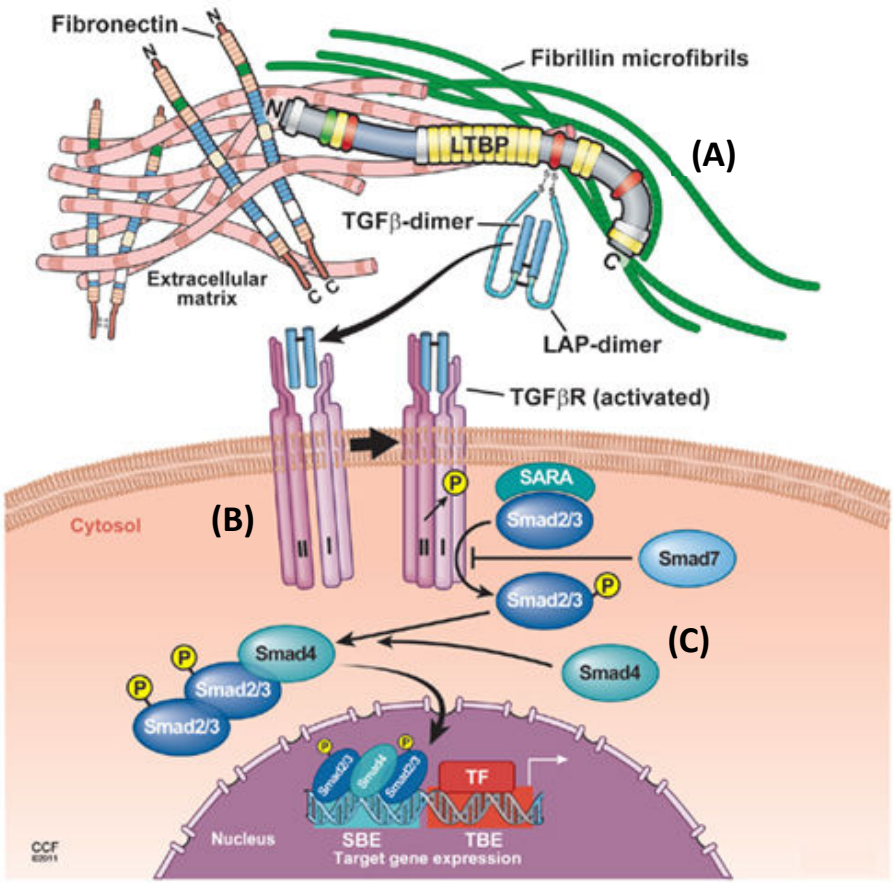

Figure 1. 2. Latent-TGF-β1 activation and TGF-β receptor signalling.

Fibronectin- and fibrillin-bound latency-associated peptide (LAP) and latent TGF-β-binding protein (LTBP) keep the TGF-β homodimer in an inactive complex (A). Various mechanisms release TGF-β, which binds to the corresponding type I and type II receptor, which undergo autophosphorylation (B). Smad anchor for receptor activation (SARA) promotes Smad2/3 phosphorylation, while Smad7 prevents this action. Phosphorylated Smad2/3 (C) binds to Smad4 and translocates to the nucleus to bind Smad-binding elements (SBE) in DNA. Recruitment of transcription factors (TF) to the T-box binding element (TBE) permits the transcription of target genes. Image from Hayashi and Sakai, 2012.

1.3. The role of integrins in cell biology

1.3.1. Integrin composition

Integrins are major adhesion receptors expressed on the plasma membrane of many cell types, including fibroblasts. They are heterodimers that consist of one α- and one β-subunit, whereby 18 α- and 8 β-subunits have been previously identified (**Figure 1.3**). Twenty-four combinations of heterodimers exist and some display restricted expression to specific cells types, for example β2 and β7 integrins are expressed only

by leukocytes, while αIIbβ3 integrins are restricted to platelets[29]. To note, there are no integrins exclusively expressed by fibroblasts.

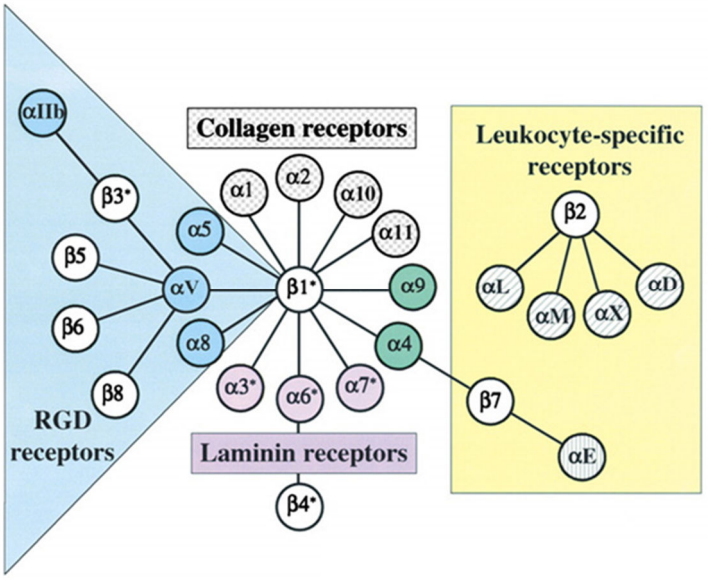

Figure 1. 3. Mammalian integrin subunit binding partners.

Integrin α- & β-subunits form heterodimers in various combinations to form receptors for particular ligands, e.g. collagen and laminin. RGD receptors are integrins that bind to proteins containing an arginine-glycine-aspartic acid sequence. Integrins can also exhibit restricted expression to certain cell types, e.g. only white blood cells express β2, β7. Image from Hynes et al, 2002.

In addition, each integrin binds particular extracellular ligands, as listed in **Table 1.1**. For example, ECM proteins, such as collagens are ligands for integrins α1β1, α2β1 and α11β1, or cell surface proteins, such as intracellular adhesion molecules (ICAMs) expressed by endothelial and inflammatory cells bind to αLβ2 integrins on leukocytes[30].

Integrins bind to corresponding ligands through the recognition of particular amino acid sequences. For example, collagens exhibit the GFOGER motif[31], while the arginine-glycine-aspartic acid (RGD) motif is expressed by many glycoproteins, in addition to fibronectin and the latency-associated peptide of TGF-β1[32]. The RGD sequence is recognized by eight integrins, including α5β1[33] and all αv-containing integrins, including αvβ3 and αvβ5, which are expressed by TGF-β1-activated fibroblasts[34]. It has previously been established that epithelial αvβ6 is a key

activator of latent TGF-β1, which physically binds to the RGD sequence and induces a conformation change in LAP by exerting force generated intracellularly, thereby releasing the TGF-β1 cytokine[35]. This function is particularly notable in damaged and cancerous tissues, where αvβ6 expression is upregulated[36]. In addition, αvβ8 displays a similar role using protease MMP-14 to release TGF-β1 by cleaving LAP in cerebral tissue[22] and regulatory T-cells[37], though its expression has not been extensively studied in fibroblasts. Sheppard and colleagues also recently documented αvβ1, which is expressed by lung fibroblasts and hepatic stellate cells, also directly binds and activates latent TGF-β1[38].

In addition, prior evidence suggests fibroblast integrins prime latent TGF-β1 for activation. Earlier studies by Wipff and colleagues suggested αvβ5, and to a lesser extent αvβ3 and β1 integrins expressed by myofibroblasts mediate TGF-β activation by contracting the matrix, which transmits conformational changes to ECM-bound LAP, releasing active TGF-β1[39].

Table 1. 1. Overview of the regulation of integrin expression by TGF-β.

Integrin	Main ligand	Effect of TGF-β	Cell type	Context
α1β1	Collagens, Laminins	Upregulation	Fibroblasts	Collagen remodelling and contraction, myofibroblast differentiation
α2β1	Collagens, Laminins	Upregulation, downregulation	Keratinocytes, fibroblasts	Collagen remodelling and contraction, myofibroblast differentiation, re-epithelialization
α3β1	Laminins	Upregulation, downregulation	Keratinocytes, fibroblasts, carcinoma cells, alveolar cells	Re-epithelialization during wound healing, EMT, cancer cell migration and invasion
α5β1	Fibronectin	Upregulation	Keratinocytes, fibroblasts, carcinoma cells, endothelial cells	Re-epithelialization, EMT, migration and invasion, endothelial cell migration and tube formation
α6β1	Laminins	Upregulation	Carcinoma cells, alveolar epithelial cells, leukaemia cells	Macrophage maturation, cancer cell migration and invasion
α8β1	RGD, fibronectin	Upregulation	Fibroblasts, vascular smooth muscle cells	Myofibroblast differentiation, vascular smooth muscle cell contraction
α11β1	Collagens	Upregulation	Fibroblasts, mesenchymal stem cell	Myofibroblast differentiation, contraction
αvβ3	RGD, fibronectin	Upregulation	Fibroblasts, carcinoma cells, endothelial cells	Myofibroblast differentiation, angiogenesis, carcinoma cell migration and invasion
αvβ5	RGD, vitronectin	Upregulation	Keratinocytes, fibroblasts	Myofibroblast differentiation, re-epithelialization, EMT, cancer cell migration and invasion
αvβ6	RGD, fibronectin	Upregulation	Keratinocytes, carcinoma cells,	Re-epithelialization during wound healing, EMT, cancer cell migration and invasion

EMT, epithelial-to-mesenchymal transition; ICAM1, intercellular adhesion molecule 1; RGD, arginine–glycine–aspartate; TGF-β, transforming growth factor-β. Adapted from Margadant and Sonnenberg, 2010.

1.3.2. Integrin structure and activation

Generally, the α- and β-subunits are transmembrane-localised glycoproteins, with an extracellular ectodomain, a transmembrane domain and a short cytoplasmic tail. In 2001, breakthrough electron microscope imaging of the αvβ3 crystal structure revealed different conformations of ligand-free and ligand-bound integrins[40], which displayed similarity to integrins αIIbβ3 and αxβ2. The current models of integrin activation propose that integrins exist in an inactive bent configuration, where the ligand binding site is near the plasma membrane and cell receptor stimulation induces the formation of an upright higher affinity structure of integrins (**Figure 1.4**). Furthermore, experimentally locking integrins in a bent state by inducing disulphide bonds prevented ligand binding by αvβ3 and αIIbβ3 integrins[41]. In addition, the upright extended configuration exists in a closed and open state, whereby the open state exhibits the highest affinity for ligand binding. The rationale for this conformation is best characterized by platelets, where integrins expressed by circulating cells are inactive to avoid potentially detrimental attachment and accumulation in blood vessels. In 2016, these various integrin configurations were also extended to α5β1 integrin, which only adhered to fibronectin in the extended-open conformation, but not while bent or extended-closed, demonstrating similarity to the mechanism of β2 and β3-containing receptors[42]. This concept is aptly named the 'switchblade' model and encompasses these 3 key states of integrin activation[43]. An alternative hypothesis named the 'deadbolt' model suggests more modest changes occur around the bent conformation, which can bind potentially ligands, although due to technical difficulties investigating the arrangement of solubilised integrins, the details of this model have yet to be defined. Nevertheless, the flexibility afforded to integrins derives from individual domains that comprise each α- and β-subunit.

The α-chain consists of 4-5 units; a 7-bladed 'β-propeller', which contains a calcium ion binding site that modulates ligand binding, a 'thigh' and 2 'calf' domains, as shown in **Figure 1.4**. Furthermore, 50% of integrins display an additional small 'α-I' domain that sits within the β-propeller. There are two chief regions of inter-domain flexibility, one is the linker between the β-propeller and the thigh and the second is

the bend between the thigh and calf-1 domain (the 'genu'), mirroring a similar region in the integrin β-subunit. The β-subunit consists of 7 domains; a β-I domain containing a significant α7 helix, a 'hybrid', a 'plexin-semaphorin-integrin' (PSI), 4 epidermal growth factor (EGF) modules and a β-tail that lacks enzymatic activity, though creates a platform where multiple signalling molecules interact and initiate downstream signalling cascades[44].

Extracellular ligand binding takes place at the interface between the α- and β-subunits. Binding is dependent on the conformation of the β-I head domain, as a downward movement of its α7 helix (visible in the β-I domain of the extended-closed and open structure in **Figure 1.4**) reveals the presence of metal ion-binding sites for magnesium and manganese cations, which promote ligand binding. There is also a separation of the dual transmembrane domains, facilitating 'outside-in' signalling.

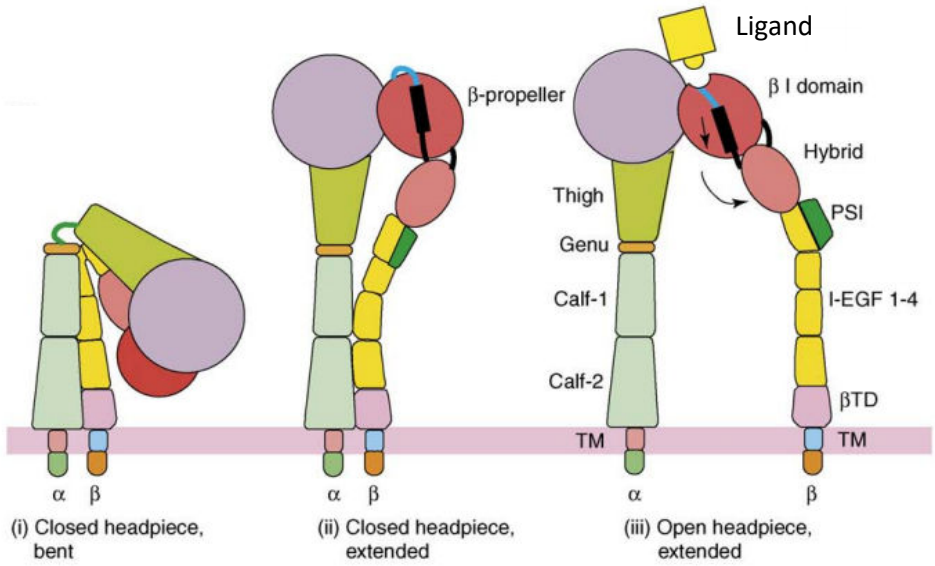

Figure 1. 4. The structure and activation of integrin heterodimers.

Three conformational states of integrins are shown during ligand binding (i, ii, iii). Ligand binding occurs when integrins display the extended-open conformation, where the α- and β- transmembrane domains are separated (iii). (iii) shows the name of each domain composing the α and β subunits. TM; transmembrane. Image adapted from Luo and Springer, 2006.

1.3.3. Integrin-mediated outside-in signalling

Extracellular ligand binding to integrins is associated with the recruitment of several cytoplasmic proteins to the short integrin β-tail[45]. In 2015, Horton and colleagues conducted data mining studies to identify proteins that constitute the integrin 'adhesome' when various cells lines, including foreskin and renal fibroblasts were plated on fibronectin. By integrating the proteome data from separate cell lines, they found 2,412 proteins were implicated in integrin adhesion complexes, where 60 proteins comprised a core signature in at least 5 cell types and included novel proteins in addition to well-known integrin-associated factors. These included kindlin, talin and vinculin[46], whereby previous studies have demonstrated kindlin and talin are important for mediating β1 and β3 integrin activation in platelets and fibroblasts[47, 48]. Talin and kindlin each bind to particular motifs in cytoplasmic integrin β-tails. This is supported by evidence of talin-bound integrins, which display extended structures, as opposed to bent, suggesting talin is associated with the activated heterodimer. In addition, vinculin[49] and talin[49] contain multiple actin-binding sites, enabling integrins to mechanically link proteins in the extracellular space to the intracellular actin cytoskeleton, which allows integrins to regulate cell shape and contractility.

Individual integrins exhibit weak interactions with the ECM and constitute 'nascent adhesions', which mature into larger focal adhesions containing clustered integrins, reinforcing adhesion sites[50]. This creates a hub for recruited intracellular signalling molecules, such as tyrosine kinase focal adhesion kinase (FAK)[51], which undergoes autophosphorylation or TGF-β1-mediated phosphorylation, and subsequently activates tyrosine kinase Src[52], facilitating the activation of various downstream signalling cascades, as displayed in **Figure 1.5**. This process is referred to as 'outside-in' signalling, where short-term changes induce cytoskeletal reorganisation to adapt cell shape and prepare for cellular migration, while long-term signalling (60 minutes plus) may affect the expression of genes that regulate survival, differentiation and growth of cells[45]. The Ras-ERK (extracellular signal-regulated kinase) pathway is a key cascade activated by the FAK-Src complex, which is implicated in regulating

transcription in myofibroblasts, while FAK was identified as a key protein involved in mediating TGF-β1-induced fibroblast α-SMA expression[28].

Depending upon the particular ECM protein and integrin engaged, integrins are capable of activating particular intracellular pathways. For example, when rat cardiac fibroblasts were plated on fibronectin, α4-, α5- and RGD integrins mediated the activation of ERK2 in response to stretch, whereas binding of integrins to vitronectin or laminin contributed to the activation of the c-Jun NH_2-terminal kinase (JNK1) pathway [53]. Consequently, downstream transcription factors induce gene expression in fibroblasts, indicating integrin signaling, as well as the TGF-β1 pathway is utilised to mediate fibroblast activity[54, 55].

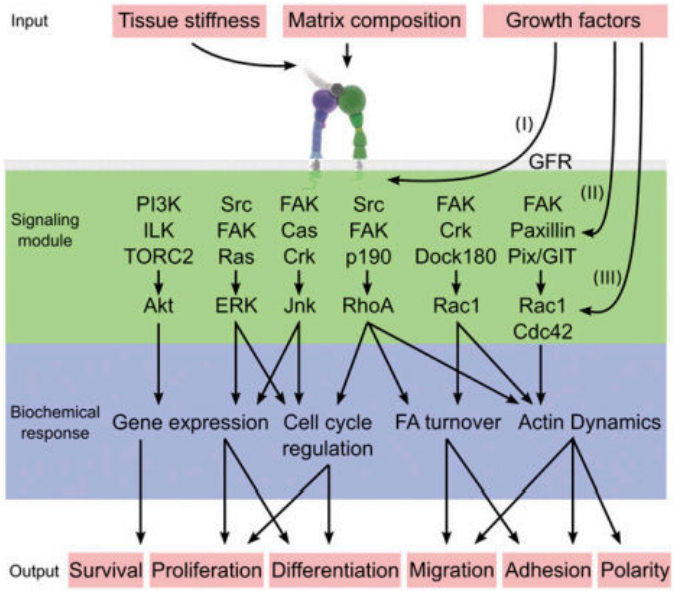

Figure 1. 5. Key downstream signalling pathways activated by integrins.
Tissue stiffness, matrix proteins and growth factor receptor (GFR) signalling promote integrin activation and several downstream signalling pathways that regulate cellular functions. Phosphatidyinositol-4,5-bisphosphate 3-kinase (PI3K), integrin-linked kinase (ILK), focal adhesion kinase (FAK), extracellular signal regulated kinase (ERK), c-Jun NH_2-terminal kinase (JNK). Image from Ledgate et al, 2009.

1.3.4. Inside-out signalling

Integrins are unusual as transmembrane receptors as they can signal bidirectionally. Inside-out signalling is important during embryonic development and in response to vasculature injury and inflammation[56]. This type of signalling is initiated by

cytokine and G-protein coupled receptor stimulation[57], producing intracellular signals that promote binding of cytosolic proteins, such as talin, kindlin and FAK to the integrin cytoplasmic β-tail. The talin head domain disrupts bonds between the α- and β-transmembrane domains, inducing separation that causes a conformational change to push integrins into a highly adhesive state, from the inside-outwards[58]. Moreover, kindlin contains similar structural domains to talin and supports talin-mediated integrin activation, by binding NXXY motifs in β1, β2 and β3 integrin tails, thereby functioning as a co-activator[59]. This inside-out-in signalling activates various intracellular signalling pathways to regulate a variety of cell functions summarised in **Figure 1.5**.

1.4. The role of integrins in TGF-β1-induced fibroblast activation and activity

1.4.1. Fibroblast differentiation

Previous studies have shown that TGF-β1 stimulation of human lung fibroblasts up-regulated specific integrin subunits, including α1, α2, α3, α5 and β1, which enabled regulation of cell adhesion and positioning[60]. Moreover, matrix stiffness may also promote integrin upregulation, as mechanical strain and TGF-β1 stimulation of mouse embryonic fibroblasts resulted in a 2-fold and 8-fold increase in α11 expression, respectively[61].

Localised scleroderma is a skin connective tissue disorder characterised by an abundance of collagen, where dermal fibroblasts derived from these tissues express a higher number of αvβ5 integrins, which enhance autocrine TGF-β1 signalling[62]. Endogenously secreted TGF-β is kept inactive by a latent complex and Asano and colleagues suggested that this latent complex is removed via an αvβ5-mediated pathway in dermal fibroblasts, which resulted in the release of active TGF-β into the ECM. Therefore, when an anti-αvβ5 antibody was applied *in vitro*, TGF-β1 remained inactive and myofibroblast activation was reduced, as noted by decreased type I procollagen, MMP-1 and Smad3 expression[63].

Integrin intracellular signalling is also a key mechanism of TGF-β1-induced differentiation. The administration of siRNA to collagen-binding integrin α11 in the

presence of active TGF-β1, prevented α-SMA expression by 50% in human corneal fibroblasts[61]. In fibroblasts derived from human oral mucosa and dermal tissue, anti-αvβ3 and anti-αvβ5 antibody blockade inhibited the expression of α-SMA and collagen gel contraction. Moreover, this also occurred in the presence of supplementary active TGF-β1, suggesting factors downstream of integrins were necessary to transmit TGF-β1 signals[64].

Thannickal and colleagues observed that TGF-β1-induced lung myofibroblast differentiation was prevented in non-adherent cells, suggesting integrin-dependent signalling was required. FAK was identified as a key signal transduction protein as inhibition of FAK's key phosphorylation site, tyrosine-397, prevented TGF-β1's ability to promote α-SMA expression and stress fibre formation. In addition, there was a correlation between TGF-β1-induced up-regulation of integrin subunits α4, α5 and β5 and the autophosphorylation of FAK, which was not observed when fibroblasts were plated on a non-integrin binding matrix[28]. In a separate study it was revealed that TGF-β1-mediated FAK phosphorylation was Smad3-dependent, while treatment of lung fibroblasts with an RGD-containing integrin inhibitor partially attenuated phospho-FAK expression after TGF-β1 stimulation[65]. Meanwhile, integrin β3 siRNA led to reduced phospho-FAK levels, while the addition of a FAK inhibitor to 3T3 murine fibroblasts culminated in significantly less type I collagen and connective tissue growth factor (CTGF)[66]. These studies suggest that TGF-β1 signals lead to phosphorylation of FAK and integrins enhance this phosphorylation, perhaps by creating docking sites for various signalling complexes.

Another key signalling component is integrin-linked kinase (ILK), a scaffold protein that can directly bind integrins or indirectly via kindlin-2, forging a link between integrins and the actin cytoskeleton[47]. ILK inactivation results in smaller focal adhesion sites, lower α-SMA and significantly inhibited collagen gel contraction. ILK-deficient dermal fibroblasts are unable to undergo differentiation into myofibroblasts in response to TGF-β1 and display impaired activity of TGF-β canonical and non-canonical signalling pathways, as observed by reduced phosphorylation of Smad2 and ERK, respectively[67]. Together, these data suggest

that integrin engagement is required for promoting TGF-β1-induced fibroblast differentiation.

1.4.2. Fibroblast-mediated contraction and invasion

Fibroblast-mediated remodelling and invasion are key functions during wound repair and constitute important measurements of myofibroblast activity. A key mediator of fibroblast contraction is GTPase RhoA, which is activated by both TGF-β1[68] and downstream of integrin-FAK interaction (**Figure 1.5**). RhoA activates Rho kinase (ROCK), which increases phosphorylation of the light chain of myosin II that is connected with the cell's actin filaments, forming an actomyosin network[69]. TGF-β1 contributes to this network by promoting stress fibre formation, while integrins are important for mechano-transduction activity, as the tension generated by a fibroblast's intracellular actin, including α-SMA, can be transmitted by integrins at focal adhesion sites, which pull on the outside ECM to aid contraction[70]. Furthermore, the continuous turnover of actin filaments at focal adhesion sites, allows integrins to sustain cell contraction[69].

As mentioned previously, integrin knockdown or blockade corresponds to a reduction in matrix contraction. The key contribution of non-canonical signalling was also recently demonstrated using tamoxifen, which impaired collagen contraction in TGF-β1-treated primary human skin and breast fibroblasts. The authors found that tamoxifen did not affect Smad-mediated signalling, but instead reduced ERK1/2 expression and downstream transcription factor AP-1, which significantly decreased the expression of α-SMA, actin-myosin regulator calponin and actin-crosslinker SM22α; each of which contribute to force generation in fibroblasts[71].

Separate integrins appear to regulate ECM remodelling depending on which matrix protein they detect. Huhtala and colleagues found that when fibroblast α5β1 bound intact fibronectin, MMP secretion was increased, though binding of α4β1 to a domain of fibronectin named connecting segment-1 (CS-1) suppressed the secretion of collagenase MMP-1 [72]. In addition, when breast fibroblasts were plated on collagen type I gels, they enhanced secretion of protease procathepsin B, which was mediated by collagen-binding integrins α1β1 and α2β1, as secretion was downregulated by

50% when these integrins were inhibited [73]. Furthermore, the knockdown of integrin α11 in periodontal ligament fibroblasts reduced their capacity to contract collagen gels by up to 40%. This capacity was partially dependent on MMP-13 expression, as α11 silencing resulted in more than 80% decline in MMP-13, while the application of an MMP-13 inhibitor to wild-type fibroblasts notably reduced contraction [74]. These studies suggest integrins regulate protease expression by processing cues from their immediate environment.

The actin-myosin machinery of fibroblasts also regulates cell migration and invasion, and expectedly, integrins are also key contributors to this process. Although there are few studies directly linking TGF-β1 to fibroblast invasion, TGF-β1 stimulation of fibroblasts may increase proteases that are required for ECM breakdown during cell invasion[68]. One example is MMP-2, which is localised to α6β1 on fibroblasts and mediates proteolysis of basement membrane protein collagen type IV. Moreover, α6β1 was upregulated on lung fibroblasts in response to matrix stiffness, while anti-α6β1 blocking antibody and siRNA knockdown significantly prevented invasion[75]. FAK is also known to regulate lung fibroblast migration, predominantly via β1 integrins[76], and 3T3 murine fibroblast invasion by activating transcription factor STAT3-dependent MMP-2 expression[77].

Again, these studies demonstrate that integrins are important for regulating TGF-β1-induced remodelling and invasion by fibroblasts. However, although fibroblast differentiation and activity is necessary during wound healing, these cells are inappropriately activated in diseases such as cancer and organ fibrosis.

1.5. The role of fibroblasts in disease

1.5.1. Cancer progression

In 2014, 29% of all deaths registered in England and Wales were due to cancer[78], while lung cancer remains the most common cause of cancer death in both males and females combined[79]. In addition, lung, breast, prostate and bowel cancers accounted for 53% of all newly diagnosed cancers in the UK in 2013[80]. Although the incidence of particular cancers, such as those originating in the bladder[81] and

stomach[82] are gradually decreasing, the incidence of cancer overall is steadily increasing each year[83].

Cancer becomes lethal if it metastasizes from the primary tumour site to other organs, making it more difficult to treat, resulting in a poorer prognosis. This is exemplified by the way cancer disease stage is linked with survival rates. For example, 87% of lung cancer patients presenting small tumours at stage I survived for at least one year, compared to the survival of only 19% of patients diagnosed with metastatic stage IV cancer[84]. Moreover, myofibroblasts identified in the tumour microenvironment are known to directly influence cancer spread[85].

The existence of a reactive stroma that actively supports angiogenesis, tumour growth and progression has been known for many years. Once a tumour has formed, it initiates a local inflammatory reaction and eventually modifies the microenvironment. Fibroblasts are key components of this reactive stroma and copious levels of TGF-β1 are released from tumour and inflammatory cells[86]. Eberlein and colleagues showed that integrin αvβ6 expressed by lung tumour cells was key in activating latent TGF-β1, which led to the TGF-β1-induced differentiation of normal fibroblasts into a cancer-associated fibroblast (CAF)-like phenotype. These effects were abrogated by an αvβ6-blocking antibody and a small molecule inhibitor of the TGF-β type I receptor[87].

Tumours appear to chronically activate a wound healing signature in resident fibroblasts, as recently characterised by the overlapping genes expressed by breast CAFs and TGF-β1-stimulated mammary fibroblasts[88]. Furthermore, paracrine interactions between tumour cells and fibroblasts promotes a cancer-promoting feedback loop. This was exhibited by colorectal and breast cancer cells that activated TGF-β/Smad signalling in adjacent CAFs, which increased secretion of hepatocyte growth factor (HGF)[89] and TGF-β1 (at a higher level than TGF-β2 and TGF-β3)[90]. These factors reciprocally promoted cancer cell proliferation and tumour cell invasion via EMT[91], respectively, also signifying that hyper-activated TGF-β1 signalling appears to be sustained by the secretion of TGF-β1 from myofibroblasts. Hence, it is unsurprising that the presence of α-SMA-positive myofibroblasts

correlates with a worse clinical outcome in many types of cancer, including breast[92], colorectal[93] and oral squamous cell carcinomas (SCC)[94].

Similar to their function during wound healing, activated fibroblasts secrete a variety of matrix proteins, such as fibronectin and collagens, in addition to matrix cross-linking proteins that produce a stiffened matrix; a characteristic feature of many tumours, which supports tumour proliferation and cell invasion[95]. A key cross-linking protein secreted by TGF-β1-stimulated fibroblasts is lysyl oxidase (LOX)[96], which catalyses post-translational modifications on ECM proteins that are essential to the structure of newly generated or repaired connective tissue. LOX initiates covalent crosslinking between elastin and collagen fibres by oxidising the amino acid lysine within these proteins. The oxidised lysine can then covalently attach to neighbouring fibres, thereby stabilising the ECM and producing stiffness when LOX is overexpressed[97].

Recent *in vivo* evidence shows LOX-mediated stiffness is associated with driving colorectal cancer proliferation and invasion by increasing FAK/Src phosphorylation in tumour cells, which may be mediated by tumour β1 integrin[95]. LOX expression also correlates with metastasis and a poor prognosis in various cancers, including squamous cell carcinomas[98]. Voloshenyuk and colleagues demonstrated that LOX expression is regulated by both canonical and non-canonical TGF-β1-induced signalling in cardiac fibroblasts, as the chemical inhibition of Smad3, PI3K, p38-MAPK, JNK and ERK1/2 each significantly reduced the expression of LOX in response to TGF-β1 stimulation[96].

Furthermore, changes in matrix tension also affects other cell types in the tumour microenvironment. Recent proteomic studies of endothelial cells cultured on matrices of increasing stiffness has shown endothelial cells upregulate matricellular protein CCN1. CCN1 then mediates the expression of endothelial cell adhesion molecule N-cadherin, and together these proteins promote the adhesion of tumour cells to endothelial cells, enhancing trans-endothelial migration of tumour cells into blood vessels. They further validated this *in vivo*, whereby inducible knockdown of vascular CCN1 reduced the number of circulating tumour cells and metastases in the

lungs[99], providing a defined mechanism by which exaggerated matrix stiffness could facilitate tumour cell invasion.

In addition, recent results demonstrated that breast CAFs exposed to matrix stiffness exhibit greater expression of pro-fibrotic genes, such as collagen (COL1A1, COL1A2, COL4A5) and LOX, in addition to increased intracellular tension, each of which were mediated by transcription factor SNAI1. These results suggest that stiffness is sustained in the tumour microenvironment by continued myofibroblast-induced fibrogenesis[100]. ECM contraction also accounts for increased matrix stiffness. Erler and colleagues recently found that prolonged hypoxia suppressed CAF-induced contraction and reduced levels of phosphorylated myosin light chain, which accounted for decreased matrix stiffness. Moreover, using organotypic invasion assays they showed that hypoxia prevented the ability of CAFs to remodel the ECM, which resulted in significantly lower SCC cell invasion[101].

Integrin function also contributes to the capacity of fibroblasts to promote tumour cell invasion. Gaggioli and colleagues showed that silencing of α3 and α5 integrin subunits in head and neck CAFs reduced contraction of organotypic gels, thereby fewer holes were created, which significantly decreased collective SCC cell invasion[102]. Paracrine factors secreted by activated fibroblasts also bind to local tumour cells. Tumour-derived TGF-β1 was found to activate fibroblasts *in vitro*, which induced SNAI1-dependent prostaglandin E2 secretion that correspondingly stimulated collective breast tumour cell invasion[103].

Particular integrins also appear to have an earlier role during tumour cell growth. The integrin subunit α11 expressed on stromal fibroblasts markedly increased the growth of lung adenocarcinomas compared to tumour cells co-injected with fibroblasts derived from α11-knockout mice. Further tests revealed tissue from α11-knockout tumours expressed 250-fold less insulin growth factor-2 (IGF-2) when compared to wild-type. IGF-2 is a potent stimulator of epithelial cell growth and when stably knocked down in wild-type fibroblasts and co-implanted with lung cancer cells, resulted in a significantly slower tumour growth rate[104]. These studies implicate integrins upon myofibroblasts as an exciting target for potential anti-cancer therapies.

Inflammation is also a hallmark of cancer and aside from activating fibroblasts in the tumour microenvironment, myofibroblasts secrete a variety of pro-inflammatory mediators that influence tumour growth, immune infiltration, invasion and metastasis[105]. Profiling of CAFs from ovarian and breast tumours showed high levels of pro-inflammatory transcription factor NF-κB, cytokine IL-6, cyclooxegenase-2 (COX-2) and CXCL1. This signature and the presence of infiltrating leukocytes was enhanced in invasive ductal carcinoma tissue compared to normal breast and ductal carcinoma tissue, demonstrating a correlation between inflammation and tumour progression[106]. These pro-invasive effects were also demonstrated recently, whereby chemokines CCL2 and CCL7 secreted by CAFs promoted the invasion of hepatic carcinoma cells *in vitro*. Further analysis to define this mechanism revealed that fibroblast-secreted chemokines promoted hedgehog and TGF-β1 signalling pathways in tumour cells, which increased the expression of EMT markers, such as vimentin, N-cadherin and Twist1[107].

Despite advances in developing targeted anti-tumour treatments, CAFs can promote drug resistance by a variety of mechanisms[108]. For example, Sahai and colleagues showed that inhibition of oncogene B-RAF in melanoma cells using drug PLX4720 actually activated CAFs. These CAFs contracted matrices, which increased β1 integrin/FAK/ERK signalling in melanoma cells, providing tolerance to the same drug[109]. Another mechanism involves the secretion of hepatocyte growth factor (HGF) from fibroblasts, which binds to its receptor, c-Met on adjacent tumour cells, while activation of c-Met signalling is associated with increased drug resistance to inhibitors of the epidermal growth factor receptor[110] and B-RAF[111], used in lung cancer and melanoma treatment, respectively. Conversely, addition of the c-Met inhibitor cabozantinib overcame gemcitabine-resistant pancreatic cancer cells and induced apoptosis[112].

Fibroblasts can also undergo senescence, which contributes to both tumorigenesis and tumour progression. Cellular senescence is an aging-associated process and can result from oncogenic-stress, oxidative stress, DNA damage and after repeated cell replications[113]. Although this is a tumour-suppressive mechanism to induce cell-cycle arrest in cells at risk of malignant transformation, senescent cells can

accumulate in tissues over time. Senescent and activated fibroblasts differ in growth potential, yet they can both stimulate proliferation and invasion of epithelial cells by the secretion of paracrine factors[113]. Studies suggest senescent fibroblasts acquire a permanent senescence-associated secretory phenotype (SASP), resulting in the secretion of many types of proteases, including PAI-1, MMP-3, collagenase MMP-1 and pro-inflammatory factors, such as chemokines and cytokine IL-6, which is a key inducer of senescence and is also secreted by senescent fibroblasts[114, 115].

The presence of the SASP phenotype has previously been linked to promoting the growth and invasion of tumour cells from different tissues, including premalignant and malignant breast epithelial cells (via MMP secretion)[116], and growth of prostate tumour cells via CTGF[117]. In addition, it was reported that senescent fibroblasts also promote angiogenesis via increased secretion of VEGF, as noted by greater blood vessel density when tumours formed alongside senescent fibroblasts compared with pre-senescent cells[118]. Furthermore, senescent fibroblasts also affect the balance of infiltrating immune cells, by promoting the recruitment of monocytes and regulatory T cells, which are associated with tumour progression[115].

These studies demonstrate the detrimental consequences of fibroblast activation and activity within the tumour microenvironment, as summarised in **Figure 1.6**, and supports the hypothesis that targeting fibroblasts/myofibroblasts may reduce the progression and lethality of cancer.

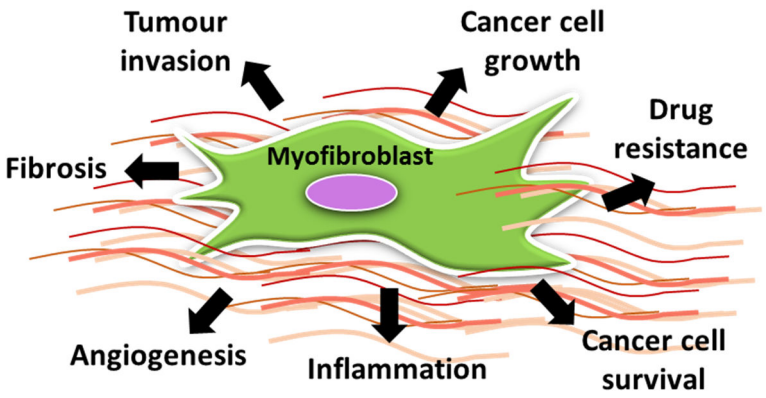

Figure 1. 6. Key contributions of myofibroblasts to cancer progression.

1.5.2. Organ fibrosis

Fibrosis occurs in organs such as the lungs, liver and heart and is often fatal as the condition worsens over time. Approximately 5000 new cases of pulmonary fibrosis are diagnosed every year in the UK, with the average survival only 3 years after diagnosis and lung transplant the only option if patients fail to respond to drug treatment[119]. Fibrosis results from an over-production of collagen, which surrounds organs reducing their functional efficiency and culminates in organ failure. In cases of idiopathic pulmonary fibrosis (IPF) the effectiveness of existing treatment options is disappointing and drug options are limited, as no particular cause of lung fibrosis is currently known, therefore current drugs only slow disease progression[120]. Though, fibrotic tissue is typically characterised by an overabundance of differentiated fibroblasts and these cells are thought to be crucial in its pathophysiology, particularly as they are the largest producers matrix proteins[121] and promote tissue stiffness via contraction and matrix crosslinking[122].

In fibrotic tissues, aberrant TGF-β1 signalling is present. Initially, damaged epithelia upregulate αvβ6 integrin, which culminates in excess levels of active TGF-β1 and subsequently promotes the differentiation of resident fibroblasts into α-SMA-positive myofibroblasts[123]. This critical step was demonstrated using β6 knockout mice and αvβ6 antibody blockade, which protected mice from lung fibrosis[124]. Tissue remodelling by myofibroblasts is also evident in cases of cardiac fibrosis. Sarrazy and colleagues found that integrins αvβ3 and αvβ5, as well as phospho-Smad3 were upregulated in porcine models of ventricular fibrosis, indicating the presence of enhanced TGF-β signalling. This increased integrin expression was also replicated with TGF-β1 treatment of human cardiac fibroblasts *in vitro*. Furthermore, by co-culturing cardiac fibroblasts with mink lung epithelial cells containing a PAI-1 promoter fused with a luciferase reporter gene, they found αvβ3 and αvβ5 mediated latent TGF-β1 activation, while this effect was abolished using small-molecule peptide inhibitors to αvβ3 (EMD 66203) and αvβ5 (cilengitide)[125].

Increased fibroblast proliferation also characterises organ fibrosis. Analysis of tissues from IPF patients identified an accumulation of myofibroblasts in the alveolar wall of the airways, which generate a rich collagen type I matrix that permanently damages the alveoli. In addition, in healthy lung fibroblasts, interaction of β1 integrins with polymerised collagen suppresses fibroblast proliferation by inhibiting the PI3K pathway via activation of its negative regulator PTEN. In contrast, IPF fibroblasts displayed pathological α2β1 integrin signalling in response to collagen, leading to chronic activation of the PI3K pathway promoting proliferation. Furthermore, the authors suggested that IPF fibroblasts attain a stable pathological phenotype that does not depend on continuous exposure to pro-fibrotic cytokines, supporting the hypothesis that alternative strategies outside direct TGF-β antagonism may be more beneficial for development of future therapies for IPF[126].

Liver fibrosis also is an increasingly common condition, which occurs as a consequence of chronic liver injury and inflammation, e.g. excess alcohol consumption, chronic hepatitis. Activated hepatic stellate cells (HSC) are a common source of hepatic myofibroblasts, which are localised to the lining of blood vessels in the liver. They display enhanced secretion of collagen, TGF-β1, PDGF and CTGF, which all contribute to fibrogenesis, resulting in liver failure[127]. Moreover, integrins expressed by these myofibroblasts play a prominent role in this process, as activated HSCs exhibit increased α5β1 integrin, active ERK signalling and enhanced collagen expression[128]. In addition, de-novo expression and upregulation of α8β1 integrin has been noted in myofibroblast-like HSCs and pulmonary interstitial fibroblasts, respectively, where this integrin has increased interaction with fibronectin, resulting in contraction-induced tissue stiffness[129].

In 2013, Henderson, Sheppard and colleagues highlighted the value of targeting integrins expressed by myofibroblasts in the treatment of organ fibrosis. Deletion of the integrin αv subunit in murine HSCs protected mice from liver fibrosis, most likely due to the declined TGF-β1 activity that was measured. This method of indirectly reducing TGF-β1 activity claims benefits over direct global TGF-β inhibition, which is expected to increase adverse side effects. The same results were also found using mouse models of lung and renal fibrosis[130]. Furthermore, recent work from the

Sheppard laboratory using a small-molecule inhibitor suggested these effects in lung and liver fibrosis models were mediated by integrin αvβ1, which they showed binds to the latency-associated peptide and activates TGF-β1[38].

These studies strongly suggest that myofibroblasts are important therapeutic targets due to their overwhelming contribution during cancer and organ fibrosis. Furthermore, transmembrane integrins expressed by myofibroblasts are potential therapeutic targets due to their ability to activate latent TGF-β1 and mediate TGF-β1 signalling intracellularly. However, targeting fibroblasts is complex, as fibroblasts from different organs are known to exhibit heterogeneity.

1.6. The heterogeneity of fibroblasts

Fibroblasts are not a uniform cell type, as those derived from different tissues display varied characteristics in features including proliferation, transmembrane protein expression and matrix production[131]. The presence of these subpopulations is highlighted by studies of the human dermis where three fibroblast subtypes have been identified, namely papillary, reticular and hair follicle-associated fibroblasts. Schafer and colleagues found that human papillary fibroblasts divide more rapidly than their reticular counterparts, while reticular fibroblasts are capable of contracting collagen matrices faster than those derived from the papillary dermis[132, 133].

More recently, analysis of fibroblasts from different organs demonstrated that cardiac fibroblasts had lower proliferation rates when compared with human dermal and lung fibroblasts. Production of matrix metalloproteinases was also variable, as the expression of MMP-1 was 24- and 17-fold higher in dermal and pulmonary fibroblasts when compared to cardiac fibroblasts, respectively. These tissue-specific differences were further highlighted in response to cytokine TNF-α stimulation, as each fibroblast displayed different levels of sensitivity[134].

Fibroblasts from distinct locations also appear to respond differently to TGF-β1 stimulation. In response to TGF-β1, lung myofibroblasts increased α-SMA and pro-

collagen type I expression, whereas TGF-β1-treated nasal fibroblasts showed no change in either factor[135]. While the addition of TGF-β1 to fibroblasts from the oral mucosa, dermis and kidneys also induced different levels of α-SMA expression, with renal fibroblasts exhibiting 2-4 times less α-SMA protein than oral mucosa and dermal fibroblasts. Moreover, these results correlated to differential levels of gel contraction in response to TGF-β1, as renal fibroblasts contracted collagen to the lowest degree. In addition, the investigators in the same study examined integrin-mediated regulation in each of the three fibroblast types. They found that both anti-αvβ3 and anti-αvβ5 blocking antibodies prevented TGF-β1-induced α-SMA expression in oral mucosa and dermal fibroblasts. However, blockade of only αvβ5 in renal fibroblasts prohibited differentiation, suggesting that fibroblasts from different organs rely on distinct integrins to regulate differentiation[64].

Although TGF-β1 is a key promoter of fibroblast-myofibroblast differentiation, very few studies have compared the responses of fibroblasts derived from separate organs to this cytokine. Furthermore, integrins appear to regulate TGF-β1-induced differentiation, in addition to myofibroblast functions, such as secretion, contraction and invasion. However, the complete integrin expression profile of different TGF-β1-treated fibroblasts has not been previously compared, therefore whether integrin function also produces heterogeneity and different integrins regulate myofibroblasts from separate organs, has not been examined extensively. These integrin characterisation studies in TGF-β1-exposed fibroblasts are required to further understand and manipulate myofibroblast biology, which my research aims to address.

Fibroblast phenotypes are also important to characterise, as their tissue of origin may dictate the mechanisms by which they enhance tumour progression. Sorell and colleagues demonstrated that co-culturing papillary dermal fibroblasts with human vascular endothelial cells *in vitro* supported the formation of highly branched, tube-like structures, whereas the same experiments using reticular dermal fibroblasts instead were unable to reproduce this result. HGF was identified as the key factor supporting blood vessel growth, which was secreted significantly more by papillary fibroblasts than reticular fibroblasts, indicating fibroblasts from separate sites have

specialised functions[136]. A similar phenomenon was also found in the context of cancer tissue, whereby breast tumour cell growth was only supported by IL-6-secreting breast, lung and bone fibroblasts, in contrast to skin fibroblasts that expressed little or no IL-6. Moreover, senescent skin fibroblasts that exhibited increased IL-6 production were able to promote breast tumour growth and invasion *in vivo*, which was inhibited with anti-IL-6 antibody treatment[137]. These studies indicate that fibroblasts from distinct sites may differentially support tumour progression by particular paracrine factors they express, thereby highlighting the need to characterise fibroblasts from different tissues, which could guide future drug treatments.

1.7. Potential therapeutic treatments in cancer and lung fibrosis

1.7.1. Targeting myofibroblasts

Due to their capacity to promote tumour growth, invasion, immune suppression, drug resistance and fibrosis, myofibroblasts comprise a key approach to therapeutically target the stroma.

In preclinical models of pancreatic cancer, hedgehog signalling was implicated as a key regulator of paracrine signalling, as tumour cells secreted hedgehog ligands that activated the pathway in stromal cells. Olive and colleagues found that hedgehog inhibitor IPI-926 depleted stromal fibroblasts in mouse models of pancreatic ductal adenocarcinoma and enhanced intra-tumoural vessel density, facilitating the delivery of cytotoxic drug gemcitabine[138]. However, clinical trials using hedgehog inhibitors in pancreatic cancer patients showed no clinical benefits, perhaps demonstrating limitations of mouse models and off-target effects. Moreover, it was noted that there was an absence of predictive stromal biomarkers, which could help assess therapeutic efficacy[139].

Matrix metalloproteinases secreted by stromal fibroblasts also represent potential therapeutic targets. Several pieces of promising pre-clinical data led to clinical testing of pan-protease inhibitors, such as tanomastat and marimastat (**Table 1.2**). However, these drugs showed no significant benefits over standard treatments in patients with

non-small cell lung cancers. Suggested reasons for this outcome were that early-stage tumours were more dependent on MMP function than later-stage tumours and that further research was needed to identify which specific MMP isoforms contribute to a poor prognosis[140].

Table 1. 2. Examples of small-molecule inhibitors that target the extracellular matrix (ECM)/fibroblasts for cancer treatment.

Molecule	Target	Status (reference)
Marimastat	MMP – broad spectrum	Phase III negative for NSCLC, SCLC and breast cancer (NCT00002911, NCT00003010, NCT00003011)
Prinomastat	MMP-2, 3, 9, 13, 14	Phase III negative for NSCLC and prostate cancer (NCT00004199, NCT00003343)
Tanomastat	MMP-2, 3, 9	Phase III terminated (NCIC-CTG trial OV12)
Neovastat	VEGFR2, MMP-2, 9, 12	Phase III negative for NSCLC (NCT00005838)
Rebimastat	MMP-1, 2, 8, 9, 14	Phase III negative NSCLC (NCT00006229)
Vismodegib	Smoothened receptor	Phase II negative for CRC and ovarian cancer and phase II for PDAC (NCT00636610, NCT00739661, NCT01064622)
Saridegib	Smoothened receptor	Phase II terminated for PDAC (NCT01130142, NCT01310816)
Sonidegib	Smoothened receptor	Phase III (NCT01708174)

NSCLC; non-small cell lung cancer, SCLC; small-cell lung cancer, CRC; colorectal cancer, PDAC; pancreatic ductal adenocarcinoma. Adapted from Junttila and Sauvage, 2013.

Tyrosine kinase receptors also reflect key therapeutic targets on both tumour cells and fibroblasts, which are paracrinally activated by excess ligands secreted by both cell types. Therefore, growth factor receptor signalling by mediators such as PDGF, vascular endothelial growth factor (VEGF) and fibroblast growth factor (FGF) is chronically activated in many tumour types. Lucitanib is an inhibitor of receptors FGFR1-3, VEGFR1-3 and PDGFRα and β, which inhibited tumour growth *in vivo*[141]. It is currently under investigation in phase II trials for the treatment of metastatic breast cancer (NCT02202746, NCT02053636) and lung cancer (NCT02109016), while

dovitinib is a non-specific receptor tyrosine kinase inhibitor in phase II trials for pancreatic (NCT01497392), urothelial (NCT01732107) and prostate cancers (NCT01741116). In addition, the multiple tyrosine kinase receptor inhibitor nintedanib improved progression-free survival and is currently being tested at phases I-III for several cancers, including monotherapy and combination treatment for ovarian cancer (NCT01610869, NCT01669798) and various solid tumours (NCT02835833)[142]. Furthermore, as the same pathways were known to be pro-fibrotic, nintedanib was investigated for the treatment of IPF. In preclinical tests, nintedanib counteracted the effects of TGF-β1 on myofibroblasts from IPF patients, as measured by reduced MMP expression, collagen secretion and cell proliferation, demonstrating the benefits of directly targeting myofibroblasts, even when already differentiation[143]. Encouragingly, in 2014 nintedanib was approved for use in the United States and Europe after it demonstrated the ability to slow the decline in lung function, though due to the limited number of current treatment options available for IPF, there is still a requirement for drugs that reverse fibrotic effects in lung tissues[144].

1.7.2. Targeting integrins

Due to their exposed extracellular ligand-binding sites, cell-type restricted expression and their association with certain diseases, integrins have long been attractive therapeutic targets in the pharmaceutical industry. Currently, there are only three heterodimers, αIIbβ3, α4β1 and α4β7, which are therapeutically targeted using monoclonal antibodies, peptides or small-molecule inhibitors in cases of thrombosis, Crohn's disease, multiple sclerosis and ulcerative colitis. In addition, at present, there are 80 clinical trials investigating integrins as therapeutic drugs, imaging agents and biomarkers[145].

Integrins are upregulated in many cancers and are known to facilitate metastasis. Overall, several compounds targeting integrins in cancers have been previously investigated for clinical development, while the majority of these drugs target integrins that recognise the RGD sequence (i.e. αv-, α5- or α8- containing integrins)[146]. One predominant example is cilengitide, a cyclic peptide that blocks αvβ3 and αvβ5 integrins. However, in contrast to preclinical data, cilengitide

detrimentally enhanced angiogenesis[147], though recently Wong and colleagues took advantage of this by administering low doses of cilengitide to mice, which aided the delivery of anti-cancer drugs inside perfused tumours, thereby reducing tumour growth[148]. Furthermore, this peptide was investigated for combination treatment of glioblastoma in phase II trials, where improved progression-free survival correlated with tumour αvβ3 expression, though there was no correlation with phospho-Smad2 levels, suggesting cilengitide was not regulating TGF-β activation[149].

Regulating TGF-β1 activation by indirectly targeting integrins, such as αvβ6 has shown positive results during *in vivo* treatment of breast cancer models[150]. Moreover, post-analysis of tissue from the recent phase I/II POSEIDON trial investigating the pan-αv blocking antibody abituzumab, demonstrated that colorectal tumours that exhibited high αvβ6 expression were predicative of overall survival, as survival was only higher in these patients, suggesting inhibiting αvβ6 provided therapeutic benefit[151]. In addition, αvβ6-blocking antibody STX-100 is currently under examination in phase II trials for IPF (NCT01371305). This approach of regulating TGF-β activity by targeting integrins may be beneficial as TGF-β1 activation would be locally controlled. This contrasts to direct global inhibition, which could be detrimental where TGF-β1 displays tumour-suppressive functions early in cancer pathogenesis.

In summary, although targeting fibroblasts is, perhaps, an obvious therapeutic strategy, a better understanding of mechanisms that regulate myofibroblast biology is required to identify new therapeutic targets to modulate the phenotype. This is particularly evident in the treatment of cancer and organ fibrosis, as many fibroblast-targeted agents have failed. Moreover, the identification of targets restricted to TGF-β1-activated fibroblasts would greatly enhance drug development. Furthermore, the use of anti-integrin therapies in various diseases and ongoing clinical trials suggests that integrins are also relevant drug targets.

1.8. Aims

TGF-β1 activated fibroblasts are key contributors to cancer progression and organ fibrosis, but these cells display heterogeneity depending on their tissue origin. Therefore, the first aim of this study was to compare fibroblast responses to TGF-β1 stimulation (Results Part I) and determine whether different integrins regulate myofibroblast biology (Results Part II). TGF-β1-treated lung fibroblasts were further examined to detect global gene expression changes (Results Part III) and identify integrin-independent mechanisms involved in regulating differentiation (Results Part IV).

This was investigated by the following:

1. To compare skin, lung and breast fibroblast responses to TGF-β1, the gene 'activation signature', integrin expression and collagen gel contraction was measured.
2. To examine whether different integrins regulate myofibroblast biology, integrins were targeted using small-molecule inhibitors and siRNA-mediated knockdown. The activation status of TGF-β1-treated fibroblasts was then re-examined by measuring invasion, collagen contraction and gene expression.
3. To examine which biological networks TGF-β1-stimulated fibroblasts contribute to, RNA sequencing of TGF-β1-treated lung fibroblasts was performed.
4. To identify additional mechanisms that regulate TGF-β1-induced lung fibroblast differentiation, a high throughput screen using a FDA-approved drug library was conducted.

CHAPTER II. MATERIALS AND METHODS

2.1. Cell culture

2.1.1. Human primary fibroblasts

All nine strains received were human primary fibroblasts derived from normal tissue (**Table 2.1**). For cell isolation, skin tissue was de-epidermised using dispase (Sigma, D4693-1G) and mechanical separation and fibroblasts were released from the dermis using collagenase D (Roche, 11088866001). Cells were then filtered through cell strainers (Fisherbrand, 22363548) and seeded in 75cm^2 dishes. Lung fibroblasts were originally sourced from National Disease Research Interchange (NDRI) resource and derived by explant culture, as described in [152]. Breast fibroblasts were isolated using an adapted method published by Gomm and colleagues[153]. Primary cells were isolated from segmented tissue using collagenase (1mg/ml, Sigma, C2674) and hyaluronidase (1mg/ml, Sigma, H3506) treatment. The resulting organoids and stromal fibroblast fractions underwent three sedimentation steps that separated fibroblasts into the supernatant, which was propagated in culture.

A light microscope (Olympus, IMT-2) was used to observe fibroblast morphology, which was expected as elongated cells with bipolar or multipolar processes when observed at sub-confluence and arranged in parallel patterns at confluence. Fibroblasts were also regularly examined for the presence of *Mycoplasma* using the polymerase chain reaction (PCR) method (see below).

Table 2. 1. Details of primary fibroblasts used.

Cell strain	Donor details	Tissue type	Provided by
Skin strain 1	Male, 28 days	Foreskin	Dr Su Marsh, (Blizard Institute, QMUL)
Skin strain 2	Male, 19 days	Foreskin	
Skin strain 3	Adult, unknown	Dermal	
Lung strain 1	Male, 60 years	Post-mortem	Dr Rob Slack (GlaxoSmithKline), cells from NDRI resource
Lung strain 2	Female, 22 years		
Lung strain 3	Male, 22 years		
Breast strain 1	Female, 27 years	Reduction mammoplasty	Dr Jenny Gomm (Breast Tissue Bank in Barts
Breast strain 2	Female, 58 years		

Breast strain 3	Female, 49 years		Cancer Institute, QMUL)

2.1.2. Human cancer cell lines

Cancer cell lines (**Table 2.2**) were solely used during mini-organotypic invasion assays.

Table 2. 2. Details of key cancer cell lines used.

Cell line	Donor details	Cell details	Reference
VB6 oral squamous cell carcinoma (OSCC)	-	Well differentiated, retroviral infection to overexpress β6 integrin	[154, 155]
H1299 lung carcinoma	Male, 43 years	Non-small cell lung cancer, lymph node metastases, NRAS mutation	[156]
MDA-MB-468 breast adenocarcinoma	Female, 51 years	Pleural effusion metastases, PTEN, RB1, SMAD4, TP53 mutations	[157]

2.1.3. Culture conditions and routine cell culture

All cells were cultured as adherent monolayers in sterile tissue culture flasks of various sizes (Corning 25cm^2, 75cm^2, 175cm^2) in a humidified atmosphere at 37^{o}C with 8% CO_2. Skin and lung fibroblasts and MDA-MB-468 cells were cultured in Dulbecco's Modified Eagle's Medium (DMEM, Sigma, D6429) and breast fibroblasts were cultured in a 1:1 mixture of DMEM and Ham's F12 (Sigma, N6658). VB6 OSCC cells were cultured in α-Minimum Essential Medium (α-MEM, Invitrogen, 22571-020) supplemented with 18mM adenine (Sigma, A2786-2SG), 0.5μg/ml hydrocortisone (Sigma, H4001), 10μg/ml insulin (Sigma, I1882), 10ng/ml epidermal growth factor (Sigma, E9644) and 1 x 10^{-10}M cholera toxin (Calbiochem 227035) and H1299 lung cancer cells were cultured in Roswell Park Memorial Institute (RPMI-1640, Sigma, R8758) medium. All media was supplemented with 10% (volume/volume) foetal bovine serum (FBS, Gibco, 10500-064) during routine culture.

To passage cells after reaching 80% confluence, medium was removed and trypsin-EDTA (Sigma, 59418C) was added for 2-5 minutes at 37^{o}C to detach adherent cells.

Once cells were in suspension, trypsin was inactivated by combining with medium containing 10% FBS and centrifuging the cell suspension at 1200rpm for 3 minutes. Cell pellets were resuspended in the appropriate medium and counted with a haemocytometer using a light microscope, before adding portions of the cell suspension to new tissue culture flasks. All fibroblasts used in experiments were between passages 2-7.

For cell preservation, cell pellets were resuspended in mixtures of 90% FBS and 10% dimethyl sulphoxide (DMSO) and placed in a cryovial freezing container at -80^{o}C. After 48 hours, cryovials were transferred to liquid nitrogen for long-term storage. To culture cells from storage, frozen cryovials were held in a 37^{o}C water bath until thawed (approximately 1.5 minutes) and diluted with 10ml cell culture medium and centrifuged (1200rpm for 3 minutes). Pellets were re-suspended with fresh medium and added in appropriate volumes to tissue culture flasks.

2.2. Reagents

2.2.1. TGF-β1 stimulation of fibroblasts

During experiments, cultured fibroblasts were either exposed to vehicle alone (control sample) composed of 10mM citric acid diluted in 0.1% bovine serum albumin (BSA, Sigma A8022) or 5ng/ml TGF-β1 (PeproTech, 100-21). During experiments, 'vehicle' and TGF-β1 was further diluted in 1% FBS in DMEM for specific time-points. Further details for each experiment are listed in relevant sections.

2.2.2. Antibodies

All antibodies and the final concentrations used are summarised in **Table 2.3**.

Table 2. 3. Details of antibodies used.

Target (Clone)	Species	Supplier (Cat No)	Dilution/Concentration
α-SMA (1A4)	Mouse	Dako (M0851)	**WB**: 1/1000, **IF-P**: 1/50, **IF-CS**: 1/200
CTGF	Rabbit	Abcam (AB6992)	**WB**: 1/500
PAI-1	Goat	Abcam (AB31280)	**WB**: 1/1000
HSC70	Mouse	Santa Cruz (sc-137211)	**WB**: 1/1000
Integrin αv	Rabbit	CST (4711)	**WB**: 1/1000

Integrin β3	Rabbit	CST (4702)	**WB**: 1/1000
Integrin β5	Rabbit	CST (4708)	**WB**: 1/1000
Anti-mouse HRP	Goat	Dako (P0447)	**WB**: 1/1000
Anti-rabbit HRP	Donkey	GE Healthcare (NA9340)	**WB**: 1/1000
Anti-goat HRP	Rabbit	Dako (P0160)	**WB**: 1/1000
Integrin α1	Mouse	Millipore (MAB1973Z)	**FC**: 10µg/ml
Integrin α2	Mouse	Millipore (MAB1950Z)	**FC**: 10µg/ml
Integrin α3	Mouse	Millipore (MAB1952Z)	**FC**: 10µg/ml
Integrin α4	Mouse	Millipore (MAB16983Z)	**FC**: 10µg/ml
Integrin α5 (P1D6)	Mouse	Millipore (MAB1956Z)	**FC**: 10µg/ml
Integrin αv (L230)	Mouse	Hybridoma, in house	**FC**: 10µg/ml
Integrin β1 (P4C10)	Mouse	Hybridoma, in house	**FC**: 10µg/ml
Integrin αvβ3 (LM609)	Mouse	Millipore (MAB1976Z)	**FC**: 10µg/ml
Integrin αvβ5 (P1F6)	Mouse	Millipore (MAB1961)	**FC**: 10µg/ml
IgG1 isotype	Mouse	Millipore (MABC002)	**FC**: 10µg/ml, **IF-CS**: 1/1000
IgG isotype	Rabbit	Santa Cruz (sc-2027)	**FC**: 10µg/ml, **IF-CS**: 1/1000
Cytokeratin	Rabbit	Dako (Z0622)	**IF-P**: 1/200
Nuclei, DAPI	-	ThermoFisher (D1306)	**IF-P/CS**: 1/5000
F-actin, Rhodamine Phalloidin	-	ThermoFisher (R415)	**IF-CS**: 1/1000
Anti-mouse Alexa Fluor-488	Donkey	ThermoFisher (A21202)	**FC**: 1/125, **IF-P**: 1/500, **IF-CS**: 1/125
Anti-rabbit Alexa Fluor-546	Goat	ThermoFisher (A11010)	**FC**: 1/125, **IF-P**: 1/500, **IF-CS**: 1/125

α-SMA: α-smooth muscle actin, CTGF: connective tissue growth factor, PAI-1: plasminogen activator inhibitor-1, HSC70: heat shock 70kDa protein 8, DAPI: 4',6-diamidino-2-phenylindole, FC: flow cytometry, WB: western blotting, IF-P/CS: immunofluorescent staining (-P: paraffin, -CS: coverslip), CST: Cell signalling Technology, HRP: Horseradish peroxidase.

2.2.3. Integrin inhibitors

Three small-molecule integrin inhibitors were applied to various fibroblast strains (**Figure 2.1**). Compound 1 was SC-68448, compound 2 was cilengitide and compound

3 was an αvβ1-selective inhibitor, which were provided by the Fibrosis and Lung Injury Discovery Performance Unit (DPU) Medicinal Chemistry group at GlaxoSmithKline (GSK) Medicines Research Centre (Stevenage, UK)[158]. SC-68448 (**Figure 2.1A**) is described as an αvβ3 RGD-mimetic antagonist in the literature[159], but was shown to target multiple αv-containing integrins by the GSK Fibrosis and Lung Injury DPU and is therefore described in this study as a pan-αv inhibitor. Cilengitide (**Figure 2.1B**) is a cyclic RGD peptide that selectively inhibits αvβ3/αvβ5 integrins by binding to a space between the integrin β-propeller and βA domain in the integrin head[160] and the integrin αvβ1-selective compound (**Figure 2.1C**) is 'compound 8', published by Reed and colleagues[38], which binds to the ligand binding α-I region[161]. Each inhibitor was dissolved in 100% (v/v) DMSO at stock concentrations of 10mM, aliquoted and stored at -20°C. During experiments, each compound was freshly diluted to the required concentration in tissue culture medium, as further detailed in relevant sections. Equal volumes of DMSO served as controls in each experiment.

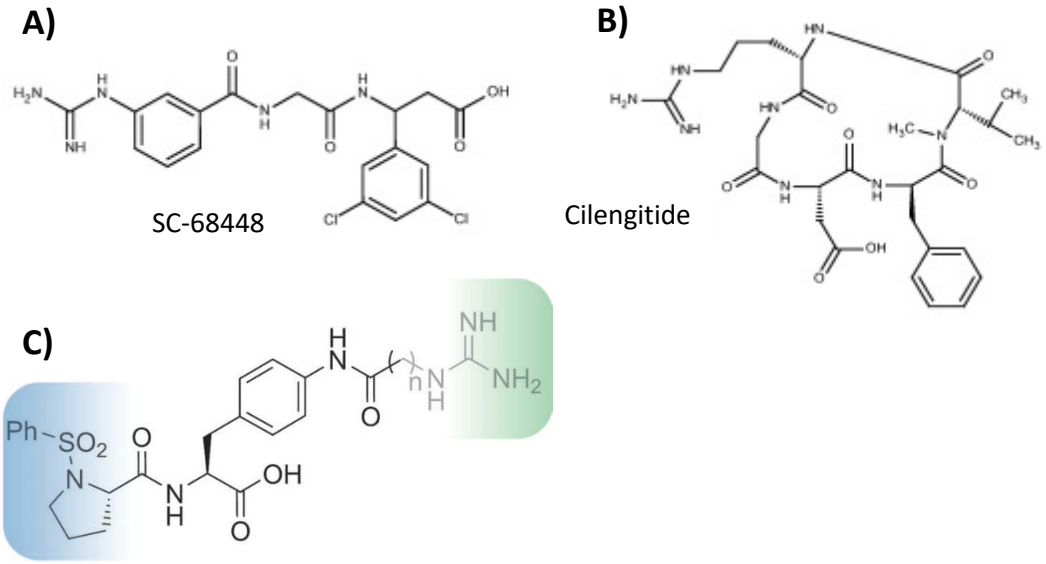

Figure 2. 1. Chemical structures of small-molecule integrin inhibitors used in this study.

Integrin inhibitors A) SC-68448 (pan-αv inhibitor), B) Cilengitide (targets αvβ3/αvβ5) and C) αvβ1-selective. This compound was designed by combining the positively charged guanidine moiety in an αvβ3 inhibitor (blue region) and a sulphonamidoproline moiety in an α2β1 inhibitor (green region). Images adapted from Hall et al, 2016 (A, B) and Reed et al, 2016 (C).

2.2.4. Small interfering RNA (siRNA) oligonucleotides

Fibroblasts were transfected with a pool of four siRNAs using the human SMARTpool siGENOME siRNA (Dharmacon CO).

Table 2. 4. siRNA product codes and target sequences.

Target (Cat. No)	Target sequences
Integrin α1 (M-008516-00-0005)	GAGGAGAGAUGGUAACUUU GAAUAACGUUGGACUUUAA AAAGAGAGCUUGCUAUUCA GAAACAGUAUGCAUAAAUG
Integrin α11 (M-008000-02-0005)	UCAAAUACAUCGCCAGUGA GAAUGGAGCUGUGCUAAAG GUUUAUAACGGAACGCUAA GAGGCAAGGUGUACGUCUA
Integrin β3 (M-004124-02-0005)	GAAAGUCCAUCCUGUAUGU GAAAAUCCGUUCUAAAGUA UUACUGCCGUGACGAGAUU CGUCUACCUUCACCAAUAU
Integrin β5 (M-004125-02-0005)	GAACAACGGUGGAGAUUUU GGAGGGAGUUUGCAAAGUU GGGAUGAGGUGAUCACAUG UACAAUAGUAUCCGGUCUA
Non-target luciferase duplex (P-002099-01-50)	GCCAUUCUAUCCUCUAGAGGAAUG

2.3. Primer design and optimisation

All primers were manually designed using the NCBI primer design tool (https://www.ncbi.nlm.nih.gov/tools/primer-blast/) and specificity was validated using the online Basic Local Alignment Search Tool (https://blast.ncbi.nlm.nih.gov/Blast.cgi). When designing primers, criteria included that primers should span exon-exon junctions to avoid amplification of genomic DNA and that the primer pair should be separated by at least one intron on corresponding genomic DNA. In addition, guanine-cytosine content in each primer was approximately 50% to regulate primer melting temperature and PCR product size was measured between 90-150 base pairs to ensure an efficient reaction.

All primers (Sigma-Aldrich, UK) used are detailed in **Tables 2.5-2.7**. Before experimentation, primers were tested to ensure they annealed at 60°C. Therefore, standard PCR using MegaMix-Blue (Microzone, 2MMB-5) was conducted using each primer (0.5µM) and positive control cDNA (see Section 2.4 for RNA/cDNA synthesis method). cDNA was derived from TGF-β1-treated (5ng/ml, 24 hours) fibroblasts to optimise myofibroblast activation marker primers and housekeeping genes, while cancer cells known to be positive for particular integrins were used to validate integrin subunit primers, as listed in **Table 2.7**. The PCR cycling conditions consisted of: one cycle of 30 seconds at 95°C, 35 cycles of 30 seconds at 95°C (denaturation), 30 seconds of a temperature gradient 55-65°C (annealing), 1 minute of 72°C (extension) and lastly one cycle of 1 minute at 72°C (final extension). PCR products were run on 1.5% agarose gels with ethidium bromide (Sigma, E1510) and visualised using ultraviolet light to confirm products were generated using an annealing temperature of 60°C. Subsequently, to determine the efficiency of primer binding to template DNA, qPCR (see Section 2.5.2 for qPCR method) was performed with 10-fold serial dilutions of positive control cDNA. The percentage of primer efficiency for each primer is listed beside primer sequences in **Tables 2.5-2.7**.

Table 2. 5. Primer details for myofibroblast activation markers.

Primers	Primer sequences	Primer efficiency
α-Smooth muscle actin: **ACTA2 – Forward (F)** **ACTA2 – Reverse (R)**	 CAGACATCAGGGGGTGATGG GGGCAACACGAAGCTCATTG	104%
Collagen Type I: **COL1A2 - F** **COL1A2 - R**	 TCGGCTAAGTTGGAGGTACTG AAAGATTGGCATGTTGCTAGGC	93%
Matrix metalloproteinase-1: **MMP-1 - F** **MMP-1 - R**	 GCTCAGGATGACATTGATGG TGCGCATGTAGAATCTGTC	104%
Tissue inhibitor of MMP(TIMP3): **TIMP3 - F** **TIMP3 - R**	 ACAGGTCGCGTCTATGATG ACAAAGCAAGGCAGGTAGTA	90%
Fibronectin: **FN1 - F** **FN1 - R**	 CACTCCCAAAAATGGACCAG AGGGCGATCAATGTTGGTTA	104%
Myosin heavy chain 9: **MYH9 - F**	 CCCAGAAGAGGAGCAAATGG	109%

MYH9 - R	TTTTGGGCAGCTGTGTTGT	
Connective tissue growth factor: **CTGF-F** **CTGF-R**	 CTGGAAGAGAACATTAAGAAGGGC GGTATGTCTTCATGCTGGTG	88%
Plasminogen activator inhibitor: **PAI-1 - F** **PAI-1 - R**	 TCATCCACAGCTGTCATAGTC ATCACTTGGCCCATGAAAAG	101%

Table 2. 6. Primer details for housekeeping genes.

Primers	Primer sequences	Primer efficiency
Glyceraldehyde 3-phosphate dehydrogenase **GAPDH-F** **GAPDH-R**	 CCATGACCCCTTCATTGACC TTGATTTTGGAGGGATCTCG	90%
Hypoxanthine phosphoribosyltransferase 1 **HPRT-1-F** **HPRT-1-R**	 GACCAGTCAACAGGGGACAT CCTGACCAAGGAAAGCAAAG	95%
β2 microglobulin **B2M-F** **B2M-R**	 AGTTAAGTGGGATCGAGAC GCAAGCAAGCAGAATTTGG	73%
Tripartite motif containing 27 **TRIM27-F** **TRIM27-R**	 CAGGCACGAGCTGAACTCT AGCTGCTCAAACTCCCAAAC	78%
Peptidylprolyl isomerase A **PPIA-F** **PPIA-R**	 GTTCTTCGACATTGCCGTCG GAAGTCACCACCCTGACACA	109%

Table 2. 7. Primer details for integrin subunits.

Primers	Primer sequences	Positive control cells	Primer efficiency
Integrin α1 **ITGA1-F** **ITGA1-R**	 CTCACTGTTGTTCTACGCTGC TGGCCAACTAACGGAGAACC	DX3-puro; melanoma	108%
Integrin α2 **ITGA2-F** **ITGA2-R**	 GGGACTTTCGCATCATCAACG ACTCCTGTTGGTACTTCGGC	DX3-puro; melanoma	75%
Integrin α3 **ITGA3-F** **ITGA3-R**	 AGCACCTTCATCGAGGATTACAG TCCACCAGCTCCGAGTCAAT	DX3-puro; melanoma	102%
Integrin α4 **ITGA4-F**	 AACCGATGGCTCCTAGT	DX3-puro; melanoma	103%

ITGA4-R	GTTCTCCATTAGGGCTAC		
Integrin α5 **ITGA5-F** **ITGA5-R**	TTTGTTGCTGGTGTGCCCAA CCAAAGTAGGAGGCCATCTGTTC	DX3-puro; melanoma	73%
Integrin α6 **ITGA6-F** **ITGA6-R**	TGATAACGATGCTGACCCCAC AGGACATAACACCGCCCAAA	DX3-puro; melanoma	96%
Integrin α7 **ITGA7-F** **ITGA7-R**	ACTCGGTCTGTGTGGACCTAA GTTCTTCCAGGTTACGGCTCA	Caov3; ovarian carcinoma	93%
Integrin α8 **ITGA8-F** **ITGA8-R**	TGCAGGCAGATACCGTTTGA ATAAAGGAGCACAGGCCACA	Caco-2; colon carcinoma	115%
Integrin α9 **ITGA9-F** **ITGA9-R**	ATGTGGCAGAAGGAGGAGATG CCAGACAGGTGGCTTGTATCA	Caco-2; colon carcinoma	113%
Integrin α11 **ITGA11-F** **ITGA11-R**	CTGGAAGGCACCAACAAGAAC ACTCGTCTCCTTTAGCACAGC	HT1080; fibrosarcoma	98%
Integrin αv **ITGAV-F** **ITGAV-R**	TGAACGCAGTCCCATCTCAA GATAACTGGTCTGGCCCTGTA	Capan-1; pancreatic cancer	70%
Integrin β1 **ITGB1-F** **ITGB1-R**	AGCCTGTTTACAAGGAGCTGA GCCTTCTGACAATTTGCCGT	DX3-puro; melanoma	92%
Integrin β2 **ITGB2-F** **ITGB2-R**	GCTGGCTGAAAACAACATCCA AGACCCTGGAGGAGAGTTTATTG	HL-60; promyelocytic leukemia	103%
Integrin β3 **ITGB3-F** **ITGB3-R**	TGACGAAAATACCTGCAACCG ACACTCTGGCTCTTCTACCAC	DX3-puro; melanoma	93%
Integrin β4 **ITGB4-F** **ITGB4-R**	ATGTCCATCCCCATCATCCCTG CAAAGTCCATCCGGCCATTCA	MCF-10A; fibrocystic disease	92%
Integrin β5 **ITGB5-F** **ITGB5-R**	TGCAAGGAGAAGATTGGCTG GCAAGGCAAGGGATGGATAG	DX3-puro; melanoma	86%
Integrin β6 **ITGB6-F** **ITGB6-R**	ATCACGTACAAGGTGGCTGTG GCTAAAAGGTTTGCTGGGGTATC	Capan-1; pancreatic cancer	101%
Integrin β7 **ITGB7-F** **ITGB7-R**	AGCAACGTGGTACAGCTCATC AAGTCACCGTCTGGTTGATTCG	HL-60; promyelocytic leukemia	70%
Integrin β8 **ITGB8-F** **ITGB8-R**	CCAAGGTGAAGACAATAGATGTGC CAACTGAGCAGCCTTTGCTTA	DX3-puro; melanoma	74%

2.4. RNA extraction and cDNA synthesis

To extract RNA from positive control cells listed in **Table 2.7** and fibroblasts at the end of each treatment period, cells were first trypsinised, centrifuged, washed with PBS and lysed at 4^{o}C using lysis buffer (RLT buffer) provided in the RNeasy Mini kit (Qiagen, 74104). Total RNA was then extracted according to the manufacturer's protocol and quantified using a NanoDrop 1000 spectrophotometer (ThermoFisher Scientific). Skin fibroblast RNA quality was assessed using the RNA 6000 Nano Chip (Agilent Technologies, 5067-1511) on the Agilent 2100 Bioanalyzer (all samples exhibited high RNA integrity) and RNA was stored at -80^{o}C. Total RNA (0.5-1µg) was reverse transcribed according to the manufacturer's protocol in a 20µl reaction volume using the QuantiTech Reverse Transcription kit containing random primers (Qiagen, 205311). The resulting cDNA was then diluted 1:40 in RNAase-free water (Sigma, W4502) and stored at –20^{o}C, ready for qPCR.

2.5. Quantitative real-time polymerase chain reaction (qPCR)

2.5.1. 384-well plate format

qPCR was conducted to allow housekeeping gene selection, TGF-β1 time-course analysis (4-, 8-, 16- and 24-hour treatments) and to assess integrin subunit expression in each vehicle and TGF-β1-treated skin, lung and breast fibroblasts. Initially, these qPCR experiments were performed manually over 6 months using a 96-well plate format. However, as there were hundreds of samples to be assessed, progress was improved by moving to a high throughput qPCR method using the 384-well format. Dr Steve Ludbrook and Dr Emma Koppe (GlaxoSmithKline, Stevenage) kindly permitted the use of their automated pipetting machine, the mosquito HV (TTP Labtech) to automatically pipette 4µl mastermix consisting of QuantiTech SYBR green (Qiagen, 204145), primers (0.5µM) and RNAase-free water into each well of a 384-well plate (Applied Biosystems, 4309849), followed by 1µl fibroblast cDNA (1.25ng/µl RNA). qPCR was performed at GlaxoSmithKline using the 7900HT Fast Real-Time PCR system (Applied Biosystems, 4329001). The cycling conditions involved one cycle of 2 minutes at 50^{o}C, 10 minutes at 95^{o}C to activate HotStarTaq DNA polymerase, 40

cycles of 15 seconds at 95^{o}C, 1 minute at 60^{o}C and 1 minute at 72^{o}C. At the end of each qPCR run, an additional step for melt curve analysis was added comprising 15 minutes at 95^{o}C and 15 minutes at 60^{o}C, to denature all the PCR products in each well, whereby the same PCR products have the same melting temperature, which is used to determine whether any non-specific amplification has occurred.

At the end of each qPCR run, a cycle threshold (Ct) value was generated, which is the number of cycles that was required for the fluorescence signal to cross the threshold/exceed background levels. These values were used for data analysis.

Housekeeping genes were required to act as internal controls to ensure the quality and quantity of cDNA was similar in each untreated/treated fibroblast sample. To select housekeeping genes per fibroblast strain, ten housekeeping genes were first investigated using qPCR. The $2^{-\Delta Ct}$ equation was used to determine which housekeeping genes produced similar Ct values between vehicle and TGF-β1-treated samples in each of the three independent repeats conducted per fibroblast strain. Only housekeeping genes that produced fold-changes between 0.5-1.5 in the TGF-β1-treated samples relative to vehicle were considered appropriate. The three housekeeping genes selected per strain are listed in **Table 2.8**. Data was analysed by normalising the TGF-β1-induced Ct value and vehicle-induced Ct value to the housekeeping gene Ct, as detailed here: Fold-change = 2^{-}[(**TGF-β1** Ct **- Housekeeping** Ct)-(**Vehicle** Ct – **Housekeeping** Ct)]. This is summarised by the equation $2^{-\Delta\Delta Ct}$, as described by Livak and Schmittgen[162].

Table 2. 8. Housekeeping genes used for each strain of skin, lung and breast fibroblast during qPCR.

Fibroblast strain	Housekeeping genes selected
Skin strain 1	B2M, GAPDH, PPIA
Skin strain 2	B2M, GAPDH, TRIM27
Skin strain 3	B2M, GAPDH, HPRT-1
Lung strain 1	GAPDH, HPRT-1, PPIA
Lung strain 2	B2M, HPRT-1, PPIA
Lung strain 3	GAPDH, HPRT-1, PPIA
Breast strain 1	B2M, HPRT-1, PPIA
Breast strain 2	B2M, HPRT-1, TRIM27
Breast strain 3	B2M, HPRT-1, PPIA

2.5.2. 96-well plate format

qPCR was conducted in the 96-well plate format (Applied Biosystems, 4346906) for all the additional qPCR experiments. This included initial primer efficiency testing, integrin siRNA-mediated knockdown and assessing the expression of myofibroblast activation markers after integrin knockdown. These qPCRs were performed in triplicate wells using 20µl total reaction volumes with SYBR green and 0.5µM primers, and run on the StepOne Plus system (Applied Biosystems, 4376598) at Barts Cancer Institute, using the same method of analysis described in Section 2.5.1, although only one housekeeping gene (HPRT-1) was used due to lack of space per plate. The cycling conditions were one cycle for 10 minutes at 95^{o}C, 40 cycles for 15 seconds at 95^{o}C, 1 minute for 60^{o}C, 30 seconds at 72^{o}C and one cycle for 15 seconds at 95^{o}C. An additional melt curve analysis step was included which ran for one minute at 60^{o}C and 15 seconds at 95^{o}C.

2.6. Western blotting

2.6.1. Protein Isolation and quantification

To collect proteins from fibroblasts, adhered cells were washed with ice cold phosphate-buffered saline (PBS, Severn Biotech Ltd, 20-7461-01) and lysed in a fresh mixture of protease inhibitor (Calbiochem, 539131) and phosphatase inhibitor (Calbiochem, 524625) diluted 1/100 in NP40 cell lysis buffer (Invitrogen, FNN0021). Fibroblasts were collected in microcentrifuge tubes by scraping cells in lysis buffer using a plastic scraper, which were placed on ice and vortexed every 5 minutes, 4 times. Lysates were spun in a microcentrifuge at 13,000rpm for 10 minutes at 4^{o}C to remove cell debris and supernatants were each transferred into new 1.5ml tubes for storage at -20^{o}C.

Protein concentration was quantified in 96-well plates (Corning, 3599) using Bio-rad Protein Assay reagents according to the manufacturer's instructions (Bio-Rad Laboratories, Reagent A, 500-0113, Reagent B, 500-0114, Reagent S, 500-0115), alongside a series of known concentrations prepared using BSA (0-5mg/ml). The absorbance of each sample was measured at 550nm using a microplate reader (Tecan, Infinite F50) and compared between samples of known BSA concentrations and cell lysates to determine the micrograms/ml of protein collected.

2.6.2. Sodium dodecyl sulphate polyacrylamide gel electrophoresis (SDS-PAGE)

To perform SDS-PAGE, lysates containing 15-25µg total protein were diluted in an appropriate volume of 2x laemmli sample buffer (Sigma, S3401) and heated to 95^{o}C for 10 minutes. Samples were then run on freshly made 8% polyacrylamide gels in gel cassettes (ThermoFisher Scientific, NC2010), where resolving gel for a 15ml gel consisted of 7ml distilled water, 4ml acrylamide (National Diagnostics, EC-890), 3.8ml Tris-HCl (1.5M, pH 8.8), 10% SDS (Fisher Scientific, BP1311-1), 10% ammonium persulphate (APS, Sigma, A3678) and 9µl TEMED (National Diagnostics, EC-503). Stacking gel (3ml) was composed of 2.1ml distilled water, 0.5ml acrylamide, 0.38ml Tris-HCl (1M, H 6.8), 10% SDS, 10% APS and 3µl TEMED and added above polymerised resolving gel with a 10-well comb until set. Cassettes were inserted into SDS-PAGE

chambers (ThermoFisher Scientific, EI0001) with 10x Tris-glycine SDS-PAGE buffer (Severn Biotech, 20-6300-100) diluted in distilled water and lysates were loaded into each well alongside a pre-stained protein ladder (ThermoFisher Scientific, 26616) and run at 120 volts for 95 minutes.

2.6.3. Immunoblotting

Proteins were transferred to nitrocellulose membranes (GE Healthcare, 10600003) for up to 3 hours at 35 volts and the resulting membranes were stained with Ponceau S (Sigma, P7170) to confirm protein transfer. Membranes were washed in distilled water briefly and blocked in 5% BSA and 0.1% tris-buffered saline (TBS)-Tween20 (TBS; Severn Biotech, 20-7301-10, Tween20; Sigma, P9416) for 30 minutes on a rotator. Primary antibodies were diluted in the blocking buffer and incubated with the membrane, rotating overnight at 4^{o}C. Subsequently, membranes were washed several times in 0.1% TBS-Tween20 and incubated with species-specific horseradish peroxidase (HRP) conjugated-secondary antibody for 30 minutes at room temperature. Protein bands were visualised by chemiluminescence using HRP substrate (Millipore, WBLUR0100) and the ChemiDoc Imager 600 (GE Healthcare).

2.6.4. Densitometry

Densitometric analysis was performed using Image J software (National Institute of Health, USA) to quantify band densities, which were normalised to the loading control (HSC70) for each sample.

2.7. Flow cytometry

Fibroblasts were trypsinised, counted and resuspended at 4 x 10^6 cells/ml in FACS buffer (0.1% BSA and 0.1% sodium azide diluted in DMEM). 50µl cell suspension was aliquoted per tube and incubated with anti-integrin antibodies for 45 minutes on ice. A species-matched IgG was also applied to cells as a negative control. Cells were washed twice with FACS buffer by centrifuging in between washes (1200rpm, 3 minutes) and then cells were incubated with species-specific secondary antibody AlexaFluor-488 for 30 minutes on ice in the dark. Cells were washed in FACS buffer,

resuspended in 400µl and fluorescence was determined with a flow cytometer (BD FACS Calibur, BD Biosciences) using Cell Quest Pro software, collecting 10,000 events. Data were plotted as geometric mean fluorescence intensity (MFI).

2.8. Collagen gel contraction

Collagen type I (Corning, 354236) was added at an 8x ratio to 1x concentrated DMEM 10x (Sigma, D2429) and 1x FBS and neutralised with 0.1M sodium hydroxide on ice until the mixture became magenta-coloured. The cell suspension (40,000 cells per gel) was resuspended in 100µl DMEM and mixed into the gel mixture. Subsequently, 400µl gel mix was added to each well of a 24-well plate and initially kept at 37^{o}C for 2 hours to set, and then incubated overnight to allow cells to adhere, with culture media on top. The next day, vehicle or TGF-β1 diluted in 1% FBS in DMEM was added on top of gels, which were released from the edge of the well using a sterile needle and imaged at selected time-points using a light microscope (Stemi SV11, Zeiss, Germany). Gel images were analysed using ImageJ software.

2.9. Mini-organotypic gel invasion assay

Transwells (0.4µM pore size, Corning, 3470) were placed in 24-well plates and were coated with type I collagen diluted in PBS (1/100) and incubated at 37^{o}C for 1 hour. Excess collagen in PBS was removed from each Transwell and replaced with a 120µl gel mixture. To produce 1ml organotypic gel mixture, the following volumes were used: 525µl collagen type I, 175µl Matrigel (Corning, 354234), supplemented with 100µl 10x DMEM, 100µl tissue culture media, 100µl filtered FBS and neutralised using 0.1M sodium hydroxide. Gels were left to polymerise at 37^{o}C for 1.5 hours and a 2:1 ratio of fibroblasts (67,000 cells) and tumour cells (33,000 cells) were pre-mixed and plated in a total number of 100,000 cells in 200µl culture media on top of each gel. Next, 600µl tissue culture media containing 10% FBS was pipetted below each Transwell and the plate was incubated at 37^{o}C for 24 hours. The next day, the media above each gel was carefully removed as most cells would have adhered to the gel, while media below each Transwell was replaced with 350µl cell culture media, which

was replaced with fresh media every 2 days. After 7 days, Transwells were fixed in 10% neutral buffered formalin (Cellstor, BAF-0010-25A) for 24 hours and then placed in 70% ethanol for at least 15 minutes. Gels were bisected and embedded in paraffin wax and 4µM thick sections were stained with haematoxylin and eosin by Mr George Elia (Pathology Centre, Barts Cancer Institute) and imaged using the Zeiss Axiophot Microscope (Zeiss, Germany).

2.10. Immunofluorescence

2.10.1. Cells cultured on coverslips

Fibroblasts (1 x 10^4) were plated on to 13mm diameter glass coverslips in 24-well plates. After the treatment period, cells were washed thrice in PBS and a cytoskeletal fixative (10mM 2-(N-morpholino)ethanesulphonic acid (MES) pH6.1, 125mM KCl, 3mM MgCl, 2mM EGTA, 10% sucrose, 4% formaldehyde) was applied for 10 minutes and cells were washed again in PBS. Fibroblasts were permeabilised using 0.1% Triton-x for 5 minutes and blocked with 0.1% sodium azide/0.1% BSA in DMEM for 30 minutes. Primary antibodies were also diluted in blocking buffer and applied for 45 minutes. Species-matched immunoglobulin (IgG) isotype controls were applied as negative controls. Cells were washed thrice with blocking buffer and Alexa Fluor-conjugated secondary antibodies diluted in blocking buffer were applied for 30 minutes while covered with foil. Nuclei were stained with 4',6-diamidino-2-phenylindole (DAPI) diluted in PBS for 10 minutes. Coverslips were gently dipped in distilled water, inverted and mounted on glass slides using Mowiol (Calbiochem, 475904). Stained slides were imaged using a confocal laser-scanning microscope (LSM 710, Carl Zeiss, Germany).

2.10.2. Paraffin-embedded sections

Paraffin-embedded sections were de-waxed in xylene and rehydrated with decreasing concentrations of ethanol. Antigen retrieval constituted heating slides for 8 minutes in 0.01M citrate buffer. Slides were washed in PBS for 10 minutes, permeabilised with 0.2% Triton-x for 5 minutes and blocked in PBSABC (2% BSA, 10% FBS diluted in PBS) for 1 hour at room temperature. Primary antibodies were diluted

in PBSABC and incubated at 4°C overnight. Slides were washed twice for 5 minutes in PBSABC and incubated with Alexa Fluor-conjugated secondary antibodies for 1 hour at room temperature. Slides were washed in PBSABC and PBS alone and incubated with DAPI for 15 minutes. Once re-washed, slides were mounted with glass coverslips and Mowoil.

2.11. Integrin manipulation in fibroblasts

2.11.1. Integrin small-molecule inhibitors

Fibroblasts were cultured in tissue culture flasks and at 50% confluency were treated with either vehicle or TGF-β1 (5ng/ml) in 1% FBS-DMEM for 48 hours. Cells were trypsinised and cell pellets were combined with either DMSO control or each of the three integrin small-molecule inhibitors in an appropriate volume, ready for plating in Transwell invasion assays (Section 2.12) or collagen gel contraction assays (section 2.8).

2.11.2. Integrin siRNA transfection

Fibroblasts were plated in 10cm diameter petri dishes and treated with either vehicle or TGF-β1 (5ng/ml) diluted in 1% FBS-DMEM for 48 hours, reaching approximately 40% confluency. Commercially pooled siRNA (final concentration 15nM, sequences detailed in **Table 2.4**) was mixed with 24µl transfection reagent INTERFERin (PolyPlus, 409-10) in serum-free DMEM, vortexed and incubated for 15 minutes at room temperature. This mixture (1.224ml) was administered to cells covered with a final volume of 8ml fresh 1% FBS-DMEM for 72 hours (in the absence of vehicle and TGF-β1). Non-targeting luciferase siRNA was used as a control for off-target effects. Cells were then trypsinised, counted and 40,000 cells were added to collagen gel contraction assays or after 72 hours' siRNA exposure, dishes were placed on ice and rinsed in ice cold PBS and cells were scraped using a plastic scrapper in RLT lysis buffer to store samples for RNA extraction to confirm integrin knockdown.

2.12. Transwell invasion assay using integrin inhibitors

To measure cell invasion, Matrigel was diluted in serum-free DMEM and 70µl was pipetted to the centre of each Transwell (8µM pore size, Corning, 3422) inserted in a 24-well plate, which was left to polymerise at 37°C for 90 minutes. 50,000 cells were then plated on top of the Matrigel and 500µl of 10% FBS-DMEM was added underneath each Transwell and plates were incubated at 37°C for 48 hours. Invaded cells that had adhered to the bottom well in the 24-well plate were collected with 500µl trypsin-EDTA, which was exposed to cells for 45 minutes and then diluted 1/20 in isotonic buffer (OMNI Life Science, 5651808) for counting using a CASY® counter (Shärfe System GmbH, Germany).

2.13. RNA sequencing

RNA sequencing (RNA-seq) was conducted using total RNA extracted from three strains of primary lung fibroblasts that were treated with vehicle and TGF-β1 (5ng/ml) for 24 hours (RNA extraction: section 2.4). Two biological repeats were performed with lung fibroblast strain 1 and strain 3, and one repeat with strain 2. These RNA samples were the same as those used for time-course stimulation studies.

RNA-seq was conducted by the Oxford Genomics Centre, Welcome Trust Centre for Human Genetics (UK) using the Illumina HiSeq 4000 platform with 2µg total RNA. PolyA selection was performed to detect messenger RNA (mRNA) and 75 base paired-end reads per sample were generated using the TruSeq Stranded mRNA library preparation kit (Illumina, RS-122-2101), with 18 million reads in total.

2.13.1. Data analysis

Bioinformatic analysis was completed by Dr Ai Nagano (Barts Cancer Institute). Sequencing reads were aligned to the human genome build hg38/GRCh38.p5 with the HISAT2 aligner program[163]. Transcript quantification was performed with htseq-count, part of the HTSeq package version 0.6.1p1, using GENCODE vh25 human gene annotation. The read count data was filtered to keep genes that achieved at least one read count per million (cpm) in at least 25% of total number of samples. Reads per kilobase per million mapped reads (RPKM) values were calculated

with the conditional quantile normalization (cqn) counting for gene length and GC content, in the R statistical environment via Bioconductor packages. Differential expression analysis was performed using LIMMA to fit a linear model to the expression data for each gene to detect differentially expressed genes between two groups. Differential expressed genes were gauged using LIMMA empirical Bayes statistics module and the adjusted p-values (false discovery rate) were estimated by the Benjamini and Hochberg procedure[164]. The differentially expressed genes were selected when the raw p-value was less than 0.05 and when the relative fold change was equal to or above 2-fold. Unsupervised hierarchical clustering (method: Ward, distance: Pearson correlation) was performed on the heatmap to assess the reproducibility of the groupings. To generate expression heatmaps, RPKM values were scaled relative to the mean expression of each gene across all samples.

Differentially expressed genes were input into Database for Annotation, Visualisation and Integrated Discovery (DAVID) and Ingenuity Pathway Analysis (IPA) software to detect enriched biological pathways involved in the experimental results.

2.14. FDA-approved drug library screening

2.14.1. Treatment of lung fibroblasts

Primary lung fibroblasts were plated at a density of 1000 cells per well in a volume of 95µl of 1% FBS-DMEM in 96-well plates (Corning, 3599). Dr Sarah Martin (Barts Cancer Institute) kindly provided the FDA-approved drug library (in 2µl aliquots), which was contained in a 96-well plate format (SelleckChem, L1300) and dissolved in 98µl DMEM containing 1% FBS just prior to use. A multi-channel pipette was used to add 5µl compound or DMSO alone to duplicate wells (final concentration 10µM), which was incubated for 48 hours at 37^{o}C. Remaining drug aliquots were stored at 4^{o}C. All media was then removed from the wells by rapidly inverting the plate into a plastic container and 95µl of either vehicle or TGF-β1 (5ng/ml) was added to one of the duplicate wells. 5µl of the same drug (final concentration 10µM) was also added to each well in duplicate, so that wells contained either drug and vehicle or drug and TGF-β1, in addition to DMSO controls. The plate was further incubated for 48 hours

at 37^{o}C. At the end of the treatment period, plates were checked using a light microscope to examine any cell death that may have occurred as a result of drug treatment.

2.14.2. Immunofluorescent staining of 96-well plates

At the end of the treatment period, using a multi-channel pipette plates were twice washed in PBS, fixed using cytoskeletal fixative buffer (see 2.10.1) for 10 minutes and again washed in PBS. Fibroblasts were then permeabilised using 0.1% Triton-x in PBS for 10 minutes and PBS-washed twice. A buffer containing DMEM supplemented with 0.1% BSA and 0.1% sodium azide was applied for 30 minutes and then removed. Primary antibodies for α-SMA (DAKO, anti-mouse, 1/200) and fibronectin (Abcam, ab23750 anti-rabbit, 1/500) were diluted in DMEM (BSA/sodium azide) buffer and added to each well for 1 hour and cells were washed thrice with fresh buffer solution. Species-specific secondary antibodies (Invitrogen, AlexaFluor-488 anti-mouse and AlexaFluor-546 anti-rabbit, 1/125) were diluted in DMEM buffer and applied to every well for 30 minutes. On each plate, duplicate wells containing fibroblasts were treated with secondary antibody only, as a control for background staining. Nuclei was stained using DAPI and whole cells were stained simultaneously in PBS using CellMask (ThermoFisher Scientific, H32721, 1/50,000) for 1 hour. Cells were washed and kept in 100ul PBS at 4^{o}C until imaging.

2.14.3. IN Cell microscope imaging

With the kind help of Mr Luke Gammon (Blizard Institute, QMUL), the IN Cell analyzer 1000 microscope was used automatically image each 96-well plate (10x magnification) with 20 fields collected from each well. Before each batch of 3-4 plates was imaged, one well on each plate was imaged to ensure microscope settings, such as focus and contrast were suitable. Each channel was imaged individually to capture α-SMA, fibronectin, DAPI and CellMask staining. Images were analysed using the Developer Toolbox 2.1 software to ensure α-SMA and fibronectin strands were correctly identified and were associated with whole cells using CellMask/DAPI staining to prevent inclusion of extraneous background staining during data analysis. Various measurements were also selected on the software, including cell counts of

DAPI/CellMask-positive cells, pixel intensity and fibre length. Data was exported as Microsoft Excel files.

2.14.4. Data analysis

Drug screen analysis was conducted using coding programming software RStudio to automate statistical and graphical analysis (with the kind help of Mr William Cross, Barts Cancer Institute). The script used is presented in **Appendix Figure 20**. α-SMA and fibronectin staining was examined in drug + TGF-β1-treated wells compared to DMSO + TGF-β1, while cumulative frequency was used to assess the distribution of staining intensity. Cumulative frequency also used to normalise cell numbers in drug and control wells, as each well may have contained different numbers of cells by the end of the treatment/staining period. The Kolmogorov-Smirnov test was used to analyse the data, which is a statistical test typically used to compare cumulative distribution of a sample (drug) with a control (DMSO) distribution and is non-parametric. A second statistical test (Wilcoxon signed rank test) was used to compare the median staining intensity in drug and DMSO-treated wells. Furthermore, wells that ultimately contained less than 200 cells were excluded from analysis due to potential toxicity from drug treatment.

2.14.5. Validation experiments

To validate the results of the drug screen, 3 compounds from the library were purchased; axitinib (Sigma, PZ0193), anastrozole (Sigma, A2736) and dasatinib (Sigma, 90525). For immunofluorescent staining on coverslips and western blotting, plated fibroblasts were treated with drug or DMSO diluted in 1% FBS-DMEM for 48 hours, this media was removed and replaced with vehicle or TGF-β1 (5ng/ml) diluted in the same media with the same drug or DMSO as a control, for a further 48 hours. Cell lysates were collected according to the method described in Section 2.6 and cells on coverslips were stained for α-SMA and fibronectin according to the method in Section 2.10.

2.15. Statistical analysis

All numerical data are presented as mean or median ± standard deviation (s.d), with respective statistical tests chosen depending on the normality of distribution, the number of groups compared and the chance to avoid type I statistical errors. Standard deviation was selected for representation to demonstrate the variation of the data points and indicate why some differences were considered non-significant.

Significance was defined as $p<0.05$ and software GraphPad Prism 5 (Graphpad, La Jolla, USA) was used for statistical analysis and graphical presentation, unless otherwise stated. The number of independent repeats performed per experiment are listed alongside each figure.

CHAPTER III. RESULTS PART I

Exploring the genetic and functional responses of fibroblasts derived from different tissues to activation with TGF-β1

3.1. Background

In published studies, fibroblast heterogeneity was reported in fibroblasts derived from the same organ, such as skin[165], in addition to fibroblasts from separate organs[64, 134]. TGF-β1 is a key regulator of fibroblast activity, yet the response of different fibroblasts to TGF-β1 has not been extensively studied and compared previously.

The first aim of this study was to characterise the genetic and functional responses of fibroblasts derived from skin, lung and breast tissue, as it was hypothesised that these fibroblasts would display heterogeneity with each other. TGF-β1 is a potent stimulator of fibroblast-to-myofibroblast differentiation and therefore was chosen to stimulate the skin, lung and breast fibroblasts in these experiments. In addition, the term fibroblast 'activation' is used interchangeably with 'differentiation' in this study, as TGF-β1-induced activity of myofibroblasts is synonymous with a differentiated phenotype, while no definitive marker of fibroblast-to-myofibroblast differentiation currently exists.

3.2. Expression of TGF-β1-responsive genes in TGF-β1-stimulated skin, lung and breast fibroblasts

The expression of eight genes that are commonly altered during fibroblast differentiation were investigated to ensure a myofibroblast phenotype was induced and were named 'activation markers' in this study. The eight markers of activation chosen were α-smooth muscle actin (ACTA2/α-SMA)[166], collagen type I (COL1A2)[167, 168], matrix metalloproteinase-1 (MMP-1), tissue inhibitor of metalloproteinase-3 (TIMP-3)[169], fibronectin (FN1)[166], myosin heavy chain-9 (MYH9)[170], connective tissue growth factor (CTGF)[166, 169] and plasminogen activator inhibitor-1 (SERPINE1/PAI-1)[166, 168]. Previously published papers were used as a guide to determine a suitable TGF-β1 concentration, where a range of 1 - 10ng/ml was commonly used to produce a myofibroblast phenotype[166, 171, 172]. Therefore, a preliminary experiment was conducted to test a mid-concentration of 5ng/ml TGF-β1, which was used to stimulate strain 1 and strain 2 skin fibroblasts for

24-hours to assess the expression of the eight activation markers by qPCR. These results revealed genes TIMP3, FN1, CTGF and SERPINE1 were induced by TGF-β1 (**Appendix Figure 1**). However, as genes such as COL1A2 and MMP-1 did not change at the 24-hour time-point in response to TGF-β1, all eight genes were examined at earlier time-points during 24-hours of TGF-β1 stimulation (4-, 8-, 16- and 24-hours) in the next experiment. This was to ensure earlier peaks in gene expression were not missed in skin, lung and breast fibroblasts. To note, qPCR was conducted on all nine fibroblast strains (3 strains per organ), however to facilitate easier comparison for the reader, only one representative strain is shown in the following figures, while the results from the additional strains are displayed in the Appendix.

The qPCR results shown in **Figure 3.1** and **3.2** represent fold-changes of TGF-β1-relative to vehicle-treated fibroblasts and the results of the three tissues are shown on one graph to allow direct comparisons. Please see **Appendix Figures 2-15** for the gene expression by each strain of fibroblast.

The results in **Figure 3.1A** suggests the expression of myofibroblast marker ACTA2 was significantly different between the three tissues, which is particularly evident at the 24-hour time-point, as lung fibroblasts expressed 2.7-fold more ACTA2 than skin ($p<0.001$) and 5.9-fold more than breast ($p<0.001$) respectively, in response to TGF-β1. In contrast, TGF-β1-induced MMP-1 (**Figure 3.1B**) and COL1A2 (**Figure 3.1C**) were not significantly different in fibroblasts from these three tissues. Unfortunately, the MMP-1 data for all three breast fibroblast strains was unusable due to primer contamination in those samples and is therefore not present. **Figure 3.1D** shows FN1 expression patterns were significantly different and appear similar to ACTA2, as TGF-β1-treated lung fibroblasts exhibited approximately 3.7-fold more FN1 than TGF-β1-treated skin or breast fibroblasts at the 24-hour time-point, perhaps indicating a biologically relevant difference in the role of fibronectin in lung tissue. To note, **Appendix Figure 2** and **3** show intra-tissue differences in each of these four genes, signifying differences between donors of the same tissues.

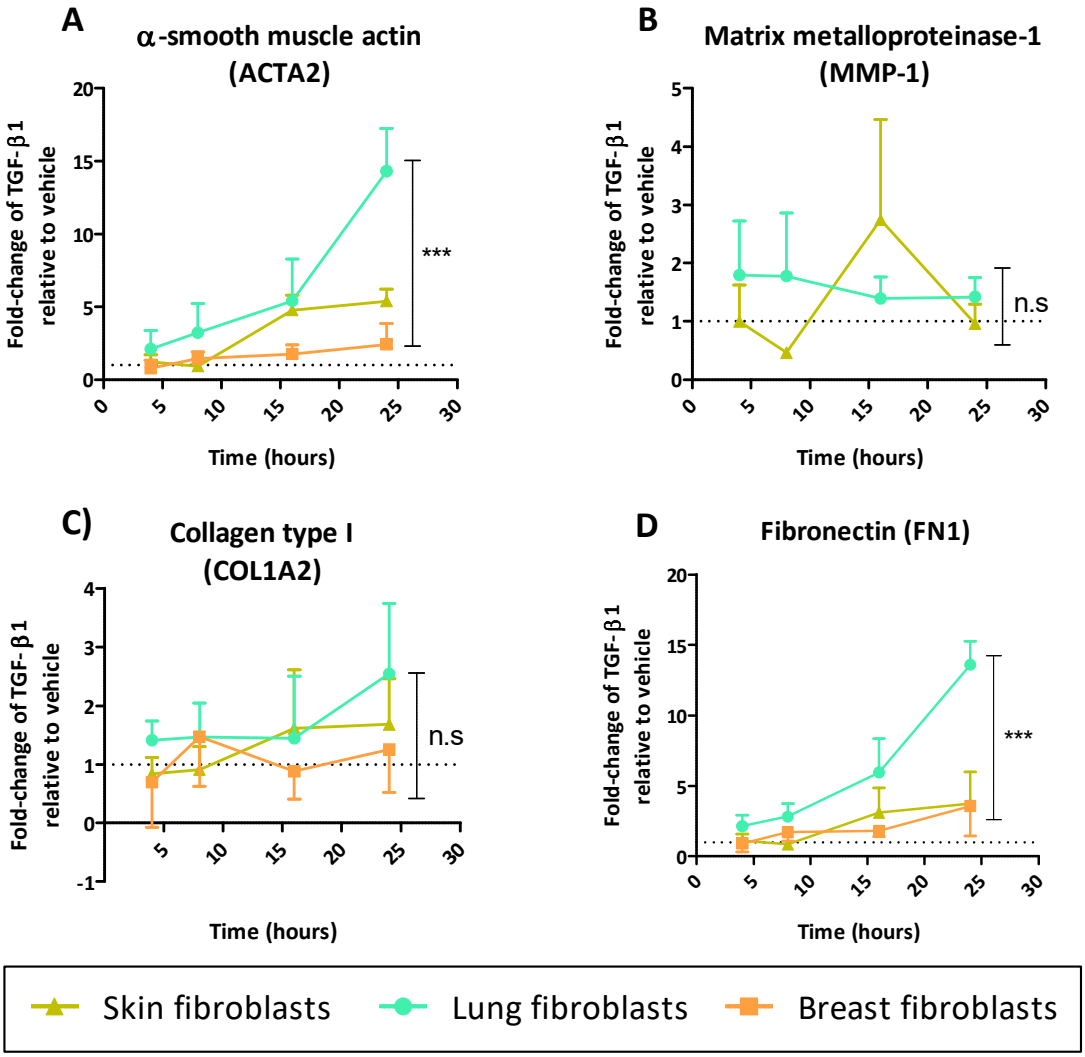

Figure 3. 1. Comparison of 4 myofibroblast-associated genes in TGF-β1-treated skin, lung and breast fibroblasts during 4 - 24-hour exposure.

qPCR used to assess the fold-change of ACTA2 (A), MMP-1 (B), COL1A2 (C) and FN1 (D) mRNA of TGF-β1 (5ng/ml)-treated fibroblasts relative to vehicle-treated cells. One representative fibroblast strain shown out of three per tissue, cell strains shown: skin strain 2, lung strain 2 and breast strain 3. Vehicle-treated cells are represented by dotted line. Data were normalised to 3 housekeeping genes per tissue listed in the Materials and Methods section. ***p<0.001, two-way ANOVA with Bonferroni post-hoc. Data shown represents mean ± s.d of three independent experiments. See **Appendix Figure 2-15** for results of 3 fibroblast strains per tissue and technical repeats for each fibroblast.

Figure 3.2 demonstrates TIMP3, CTGF and PAI-1 also exhibited striking tissue-specific differences in response to TGF-β1. However, this time TIMP3 expression was lowest in skin fibroblasts (**Figure 3.2A**), where TGF-β1 did not significantly affect expression relative to untreated skin fibroblasts. Of note, this was also verified in the three strains of skin fibroblasts derived from separate subjects (**Appendix Figure 4**). TIMP3 was expressed approximately 7-fold and 5-fold more by stimulated lung and breast fibroblasts respectively, than skin fibroblasts at 24-hours. Moreover, lung fibroblasts also displayed higher TIMP3 expression earlier than either skin or breast fibroblasts within eight hours of TGF-β1 addition.

The next gene studied was MYH9, which is a non-muscle, actin-binding protein associated with regulating cell adhesion and contractility[173]. MYH9 results showed high variation in technical repeats and was not differentially expressed by TGF-β1-exposed skin, lung or breast fibroblasts (**Figure 3.2B**). However, MYH9 was significantly upregulated by TGF-β1 only in skin fibroblasts, at the 24-hour time-point ($p<0.05$) relative to vehicle treatment.

As previously mentioned, CTGF was differentially expressed in fibroblasts derived from three different tissues (**Figure 3.2C**), as skin fibroblasts expressed more CTGF mRNA, particularly at the 16-hour time-point compared to lung and breast ($p<0.01$). However, increasing the time of TGF-β1 exposure did not significantly affect CTGF expression in lung and breast fibroblasts, as CTGF largely remained at consistent levels between 4-24 hours. Finally, SERPINE1 mRNA was also differentially expressed, as breast fibroblasts exhibited significantly lower levels compared to skin or lung fibroblasts (**Figure 3.2D**), which was evident within eight hours of TGF-β1 exposure.

Overall, these results demonstrated five out of the eight genes examined displayed differential expression in TGF-β1-treated skin, lung and breast fibroblasts and in cells derived from different donors. Considering all these results, the top four genes chosen to measure myofibroblast activity in later experiments were ACTA2, FN1, CTGF and SERPINE1.

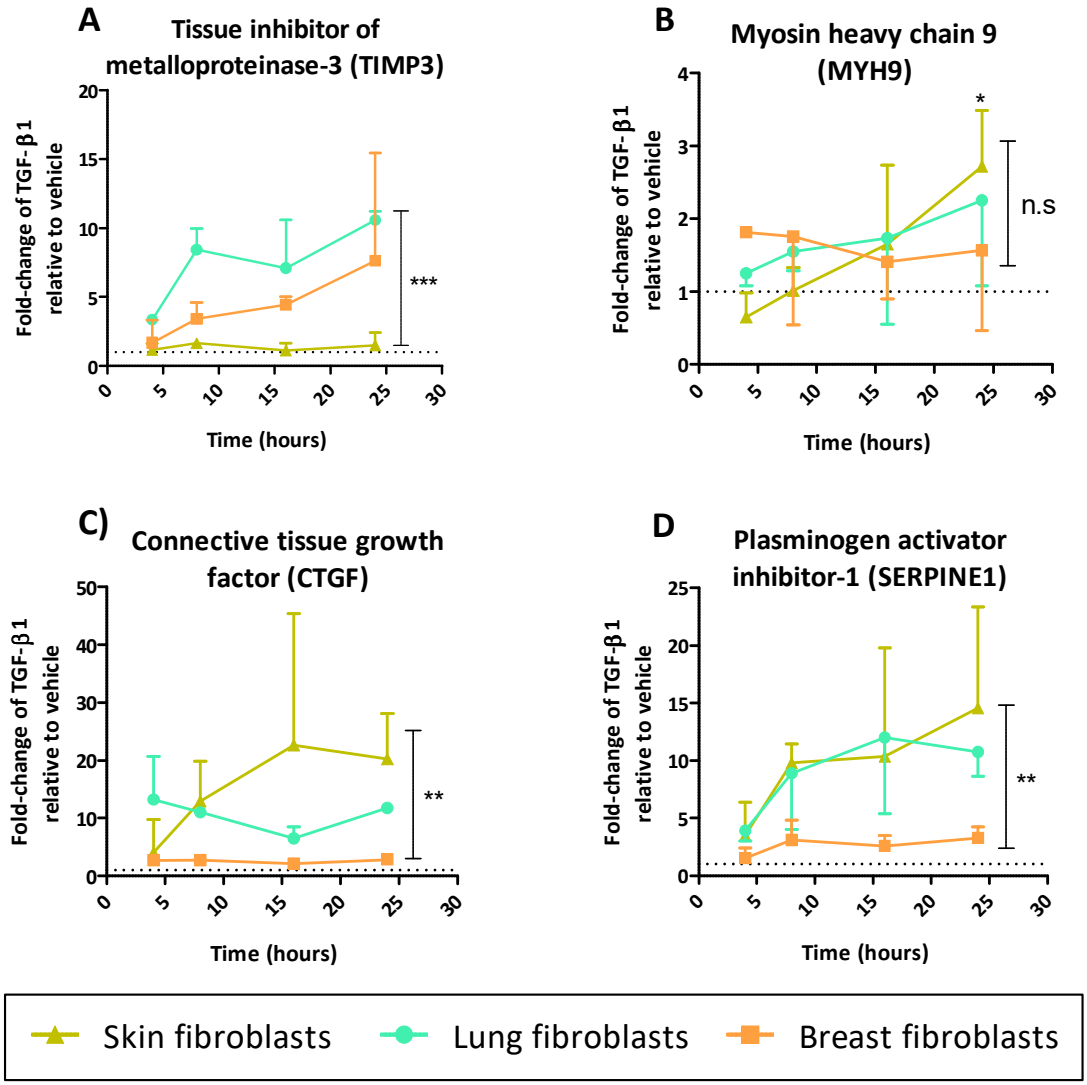

Figure 3. 2. Comparison of 4 myofibroblast-associated genes in TGF-β1-treated skin, lung and breast fibroblasts during 4 - 24-hour exposure.

qPCR used to assess the fold-change of TIMP3 (A), MYH9 (B), CTGF (C) and SERPINE1 (D) mRNA of TGF-β1 (5ng/ml)-treated fibroblasts relative to vehicle-treated cells. One representative fibroblast strain shown out of three per tissue, cell strains shown: skin strain 2, lung strain 2 and breast strain 3. Vehicle-treated cells are represented by dotted line. Data were normalised to 3 housekeeping genes per tissue listed in the Materials and Methods section. ***p<0.001, **p<0.01 two-way ANOVA with Bonferroni post-hoc. Data shown represents mean ± s.d of three independent experiments. See **Appendix Figure 2-15** for results of 3 fibroblast strains per tissue and technical repeats for each fibroblast.

To examine the pattern of expression within each tissue, activation markers were compared at one time-point of peak gene expression. **Figure 3.3A** shows ACTA2 ($p<0.05$), MYH9 ($p<0.05$) and CTGF ($p<0.05$) mRNA were significantly increased in skin fibroblasts in response to 24-hour TGF-β1 treatment, while SERPINE1 was also highly upregulated but was found non-significant, possibly due to technical variations. In contrast, genes COL1A2, MMP-1, TIMP3, FN1 and MYH9 displayed no significant changes in response to TGF-β1.

In 24-hour TGF-β1-treated lung fibroblasts (**Figure 3.3B**), significantly higher ACTA2 ($p<0.05$), TIMP3 ($p<0.01$), FN1 ($p<0.01$), CTGF ($p<0.01$) and SERPINE1 ($p<0.05$) were expressed relative to untreated lung fibroblasts, while COL1A2, MMP-1 and MYH9 showed no change in expression. Surprisingly, this breast fibroblast strain (**Figure 3.3C**) only significantly raised TIMP3 ($p<0.01$) above basal levels, while the residual genes remained unchanged after TGF-β1. Moreover, intra-tissue variation was evident between the three breast fibroblast strains, (**Appendix Figure 16**), while the three skin and three lung strains demonstrated more homogeneity within each tissue, even though each strain was derived from a different donor.

These results demonstrated genes were upregulated to different extents in skin, lung and breast fibroblasts in response to TGF-β1, further highlighting the heterogeneity between these fibroblasts.

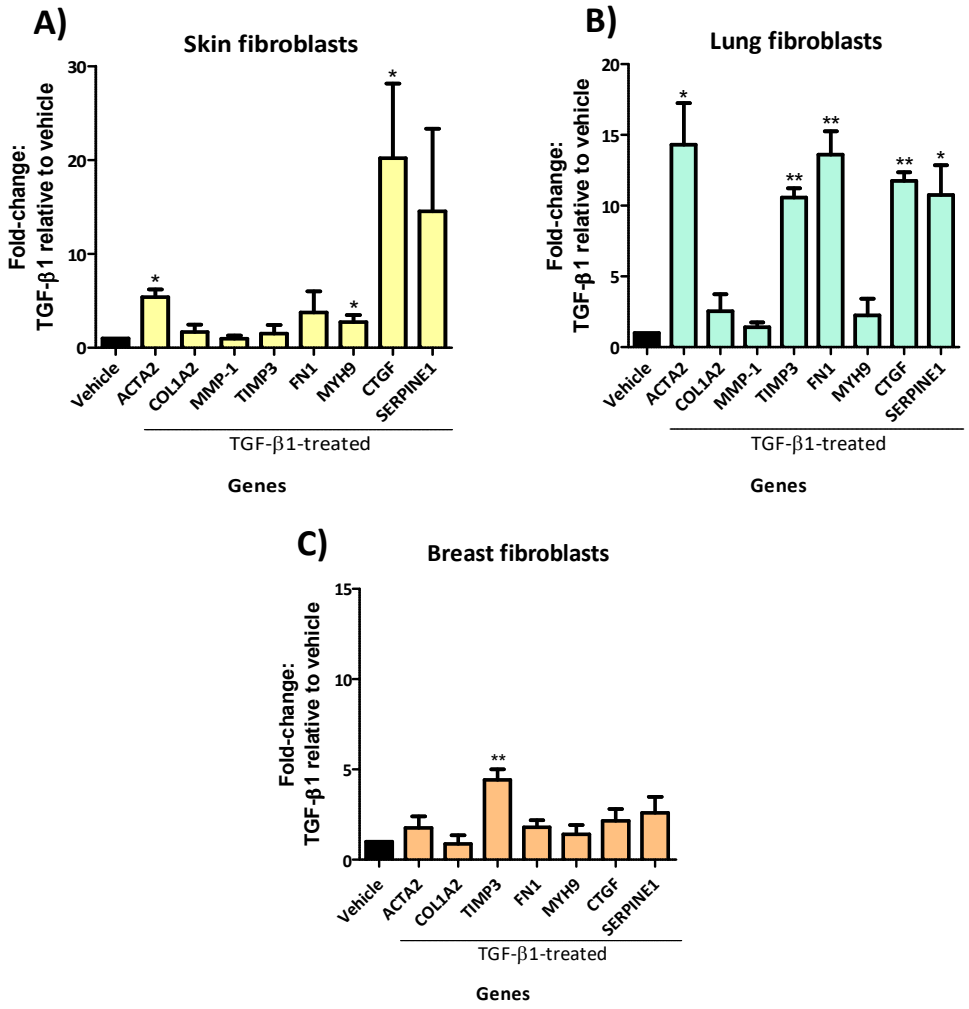

Figure 3. 3. Gene expression of 8 markers of myofibroblast activation after TGF-β1 addition to skin, lung and breast fibroblasts.

The following representative fibroblast strains from skin (A), lung (B) and breast (C) tissue are shown; skin strain 2, lung strain 2 and breast strain 3, which were exposed to TGF-β1 (5ng/ml) for 24 hours. The qPCR data shows fold-change of TGF-β1 relative to vehicle-treated cells and data were normalised to housekeeping genes documented in Materials and Methods. *p<0.05, **p<0.01, Paired Students *t*-test. Data shown represents the mean ± s.d of three independent experiments. See **Appendix Figure 16** for the results of all 9 fibroblast strains.

3.3. Protein expression of key myofibroblast-associated factors in TGF-β1 stimulated skin, lung and breast fibroblasts

Western blotting was conducted to determine the protein expression level of TGF-β1-upregulated genes that were identified using qPCR and to directly compare fibroblasts derived from the three different tissues. This time, all fibroblasts were treated with TGF-β1 for 48-hours to allow time for protein expression to occur. Furthermore, only a subset of differentially expressed genes was examined and were selected according to the previous qPCR results.

Figure 3.4A reveals skin fibroblasts expressed larger quantities of myofibroblast marker α-SMA at the basal level, and as a result, there was no significant change in α-SMA expression after TGF-β1 addition in these cells (**Figure 3.4B**). In contrast, **Figure 3.4B** shows stimulated lung and breast strains upregulated α-SMA up to 2-fold, although the Students *t*-test could not be conducted as only two independent repeats were completed. In addition, TGF-β1-induced CTGF could not be quantified accurately as there were no visible bands in some vehicle samples (lower CTGF band in **Figure 3.4A**), but was clearly upregulated by TGF-β1 in each fibroblast. Plasminogen activator inhibitor-1 (PAI-1) was increased the highest in skin fibroblasts after TGF-β1 (**Figure 3.4B**), though there was approximately a 2-fold increase in PAI-1 expressed by lung and breast fibroblasts.

Figure 3.4C directly compares protein expression between the three tissues. As noted previously, basal α-SMA in skin fibroblasts was significantly higher than basal α-SMA in lung ($p<0.01$) or breast fibroblasts ($p<0.01$), while basal PAI-1 was significantly higher in unstimulated breast fibroblasts ($p<0.01$) compared to skin, though TGF-β1-treated skin fibroblasts expressed more PAI-1 than lung or breast. Conversely, there were no significant differences between skin, lung and breast fibroblasts in the levels of α-SMA and CTGF after TGF-β1 (**Figure 3.4C**), suggesting these proteins were ultimately expressed at similar levels in differentiated fibroblasts, although more repeats and additional strains are needed to confirm this.

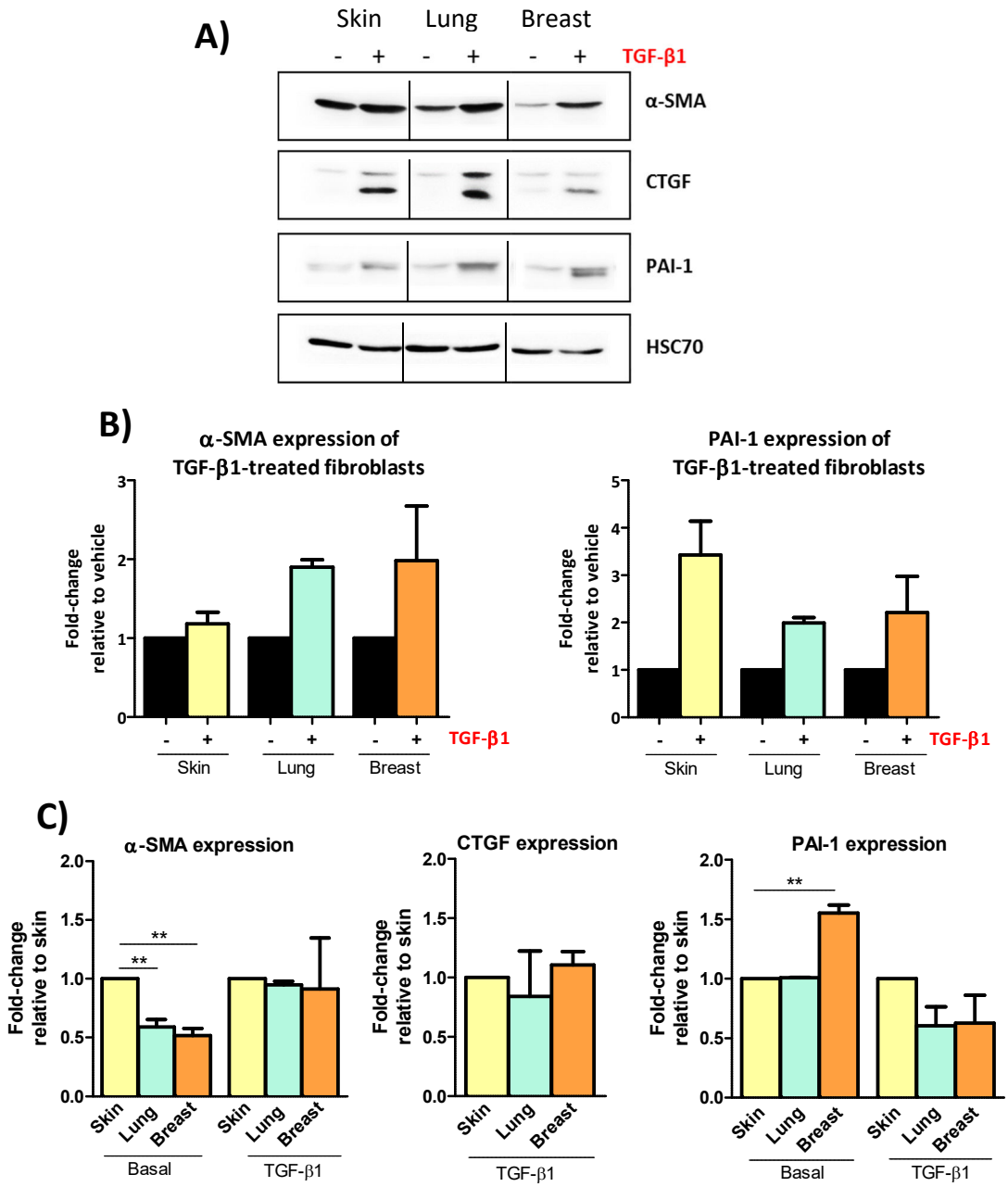

Figure 3. 4. Western blot analysis of myofibroblast-associated proteins in TGF-β1-treated skin, lung and breast fibroblasts.

Fibroblast skin strain 2, lung strain 2 and breast strain 3 were stimulated with either vehicle (-) or TGF-β1 (+) (5ng/ml) for 48-hours. α-SMA, CTGF and PAI-1 protein expression analysed using densitometry to test vehicle vs TGF-β1 (B) and compare the 3 tissues under basal and TGF-β1 conditions (C). Hsc70 serves as loading control. Data shown represents the mean ± s.d of two independent experiments. **p<0.01, one-way ANOVA with Tukey's post-hoc.

3.4. Gene expression of integrin subunits in TGF-β1 stimulated skin, lung and breast fibroblasts

We considered that differential expression or activity of integrins may underlie key differences between skin, lung and breast myofibroblasts. Therefore, to identify which integrins are transcriptionally regulated by TGF-β1 in these fibroblasts, the expression of relevant integrin α- and β-subunits was investigated during 24-hours of TGF-β1 exposure. As expected, integrin subunits α9, β2, β4, β6 and β7, which are not typically expressed by fibroblasts did not produce Ct values for any strain and are therefore excluded in **Figure 3.5**.

The integrin gene expression was examined in all nine strains of fibroblasts, though again, the results of only one representative strain per tissue is displayed. To note, the three strains of lung fibroblasts produced the most consistent patterns in response to stimulation across the three tissue types (see **Appendix Figure 17** for all 9 strains). **Figure 3.5A** shows TGF-β1-treated skin fibroblasts notably increased α1 (5 ± 2.8-fold) and α11 (4 ± 0.7-fold) integrin subunit mRNA, while TGF-β1-exposed lung fibroblasts significantly elevated α11 (19.5 ± 6.2-fold) and β3 (2.4 ± 0.6-fold) (**Figure 3.5B**). To note, α1 was also significantly upregulated in lung strain 1 (2.6 ± 0.5-fold) and strain 2 (2.4 ± 0.2-fold) in response to TGF-β1 treatment (**Appendix Figure 17**). In contrast, TGF-β1-treated breast fibroblasts exhibited more α4 relative to vehicle-treated cells (**Figure 3.5C**), which was consistent between the three breast fibroblast strains. Interestingly, all fibroblasts strains from skin, lung and breast significantly downregulated the β8 subunit in response to TGF-β1.

When comparing the responses to TGF-β1 stimulation, it appears skin fibroblast α1 expression was higher than lung or breast, however more independent repeats are required to confirm this due to large deviations in the replicates. In addition, lung α11 and β3 expression was greater compared to most skin and breast fibroblast strains. Interestingly, only HLF strain 2 significantly upregulated integrin subunit α8, which needs to be repeated at least once more to be statistically relevant (4.0 ± 0.002-fold change, n = 2). This contrasts to breast fibroblasts where no α8 and very little α11 mRNA was detected (**Figure 3.5C**).

These results again demonstrated heterogeneity exists between TGF-β1-treated skin, lung and breast fibroblasts and identified integrin targets of interest within each strain, such as α1 in skin fibroblasts and α11 and β3 in lung.

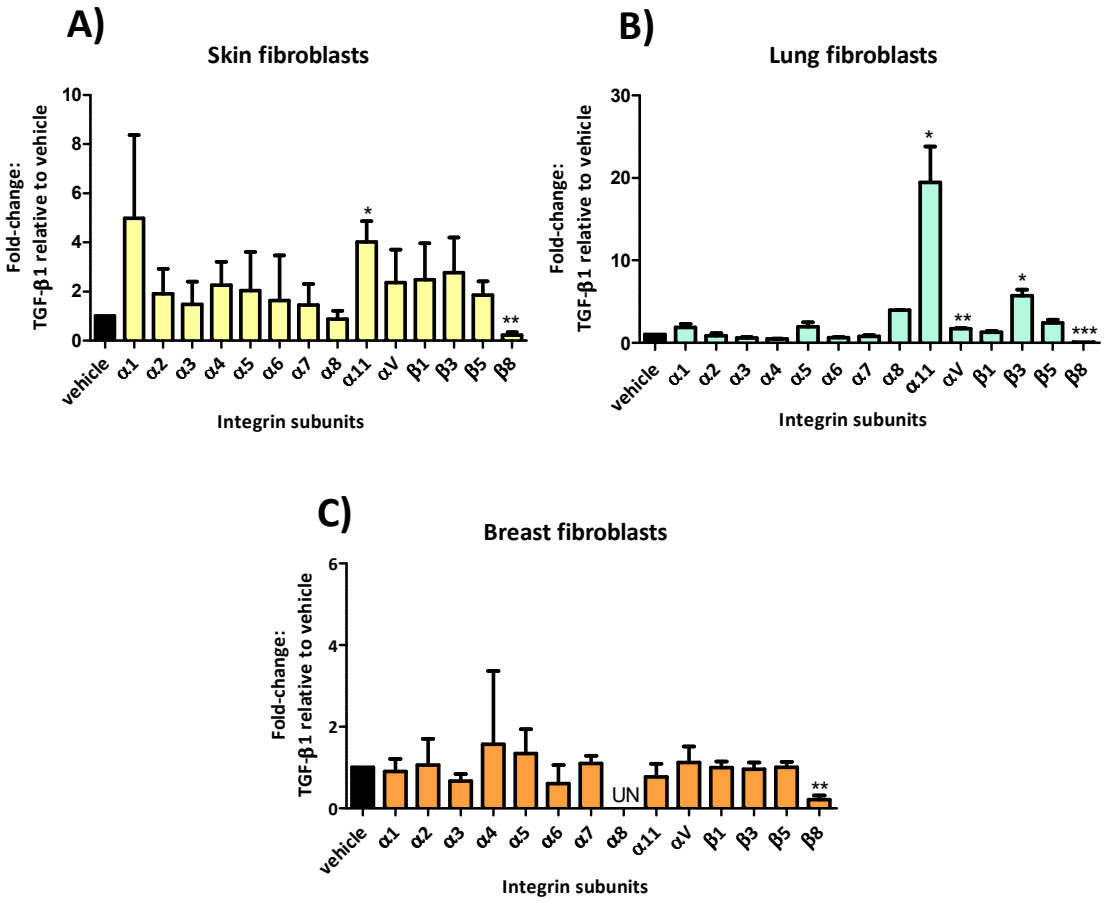

Figure 3. 5. Gene expression of integrin subunits in TGF-β1-treated fibroblasts derived from skin, lung and breast tissue.

The following representative fibroblast strains from skin (A), lung (B) and breast (C) tissue are shown; skin strain 2, lung strain 2 and breast strain 3, which were exposed to TGF-β1 (5ng/ml) for 24 hours. The qPCR data shows fold-change of TGF-β1 relative to vehicle-treated cells and data were normalised to housekeeping genes documented in Materials and Methods. *p<0.05, **p<0.01, ***p<0.001, Paired Students *t*-test. Data shown represents mean ± s.d of three independent experiments, except α8 where only two independent experiments were completed. See **Appendix Figure 17** for the results of all 9 fibroblast strains.

3.5. Protein expression of selected integrins expressed by skin, lung and breast fibroblasts

To determine transmembrane integrin expression and total protein levels, flow cytometry and western blotting were performed, respectively, though, α8 and α11 expression could not be assessed due to poor quality of commercial antibodies.

During flow cytometry experiments, TGF-β1 (5ng/ml) was used to stimulate fibroblasts for 24 hours due to the changes observed in the previous integrin gene expression analysis. However, due to the differential growth rates of fibroblasts it was not possible to examine the three tissues in the same flow cytometry experiment, therefore post-comparisons would be inaccurate.

The flow cytometry results (**Figure 3.6**) suggest TGF-β1 did not induce significant changes in surface integrin expression in either skin or lung fibroblasts. Low cell counts of all three strains breast fibroblasts due to their slow proliferation meant only vehicle-stimulated cells were analysed. Noticeably, most integrins produced mean fluorescence intensities higher than the species-matched isotype control antibody in all fibroblasts (isotype control mean fluorescence intensity was typically between 2.5 - 4), which verified positive surface expression during both basal and stimulated conditions, even though it remained constant in response to TGF-β1.

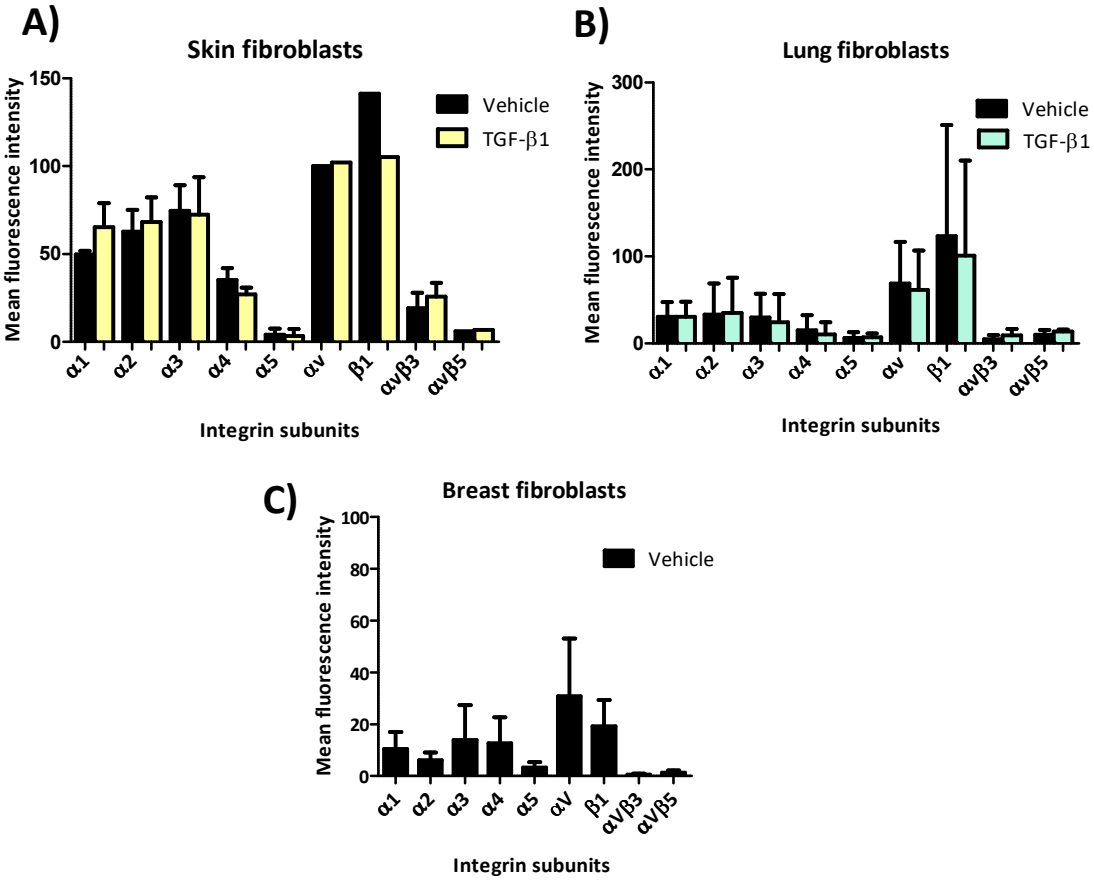

Figure 3. 6. Flow cytometry analysis of integrin expression in TGF-β1-treated skin, lung and breast fibroblasts.

The following representative fibroblast strains from skin (A), lung (B) and breast (C) tissue are shown; skin strain 2, lung strain 2 and breast strain 3, which were exposed to TGF-β1 (5ng/ml) for 24 hours. Note, due to slow growth/low cell number only vehicle treatment was applied to breast fibroblasts. Data shown represents the mean ± s.d of least two-three independent experiments.

As surface integrin expression appeared to remain constant in stimulated fibroblasts, total protein levels were investigated using western blotting, although this time, fibroblasts were treated for 48-hours with TGF-β1, as it was assumed fibroblasts needed longer to generate integrin proteins. Due to the lack of effective integrin antibodies only a few subunits could be examined, as attempted optimisation of various α1 and α11 commercial antibodies suitable for western blotting failed and therefore could not be characterised.

Figure 3.7 shows, in skin fibroblasts total αv (**Figure 3.7B**), β3 (**Figure 3.7E**) and β5 protein (**Figure 3.7H**) were increased 1.5-2-fold after 48-hour TGF-β1 exposure, while lung fibroblasts only upregulated β3 protein (**Figure 3.7E**) after stimulation (3.4 ± 1.2-fold). In contrast, TGF-β1 only slightly raised αv expression in breast fibroblasts, but had no effect on β3 and β5 expression. Although the non-significant changes in total integrin protein after TGF-β1 appear to support the flow cytometry results, I believe more biological repeats are needed for western blotting to confirm this.

Subsequently, to compare between tissues, total protein was examined at either basal levels or after TGF-β1 exposure, where interestingly breast fibroblasts expressed significantly more αv (**Figure 3.7C**), β3 (**Figure 3.7F**) and β5 (**Figure 3.7I**) protein than skin or lung fibroblasts during basal conditions. Whether these results are tissue-specific or not could be established during future studies by examining more strains of fibroblasts from each tissue.

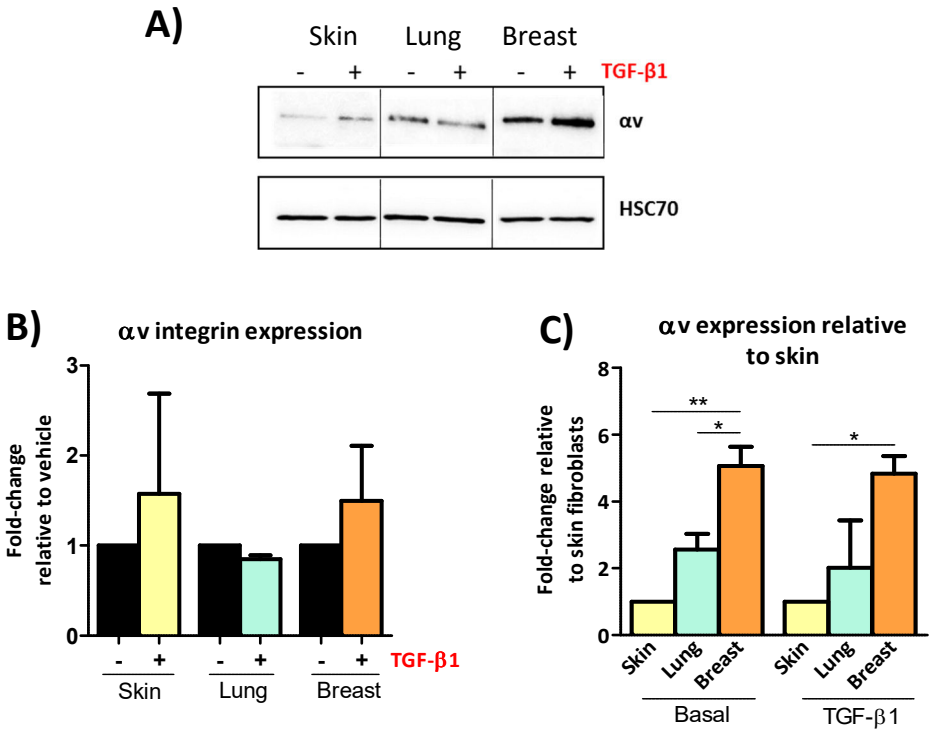

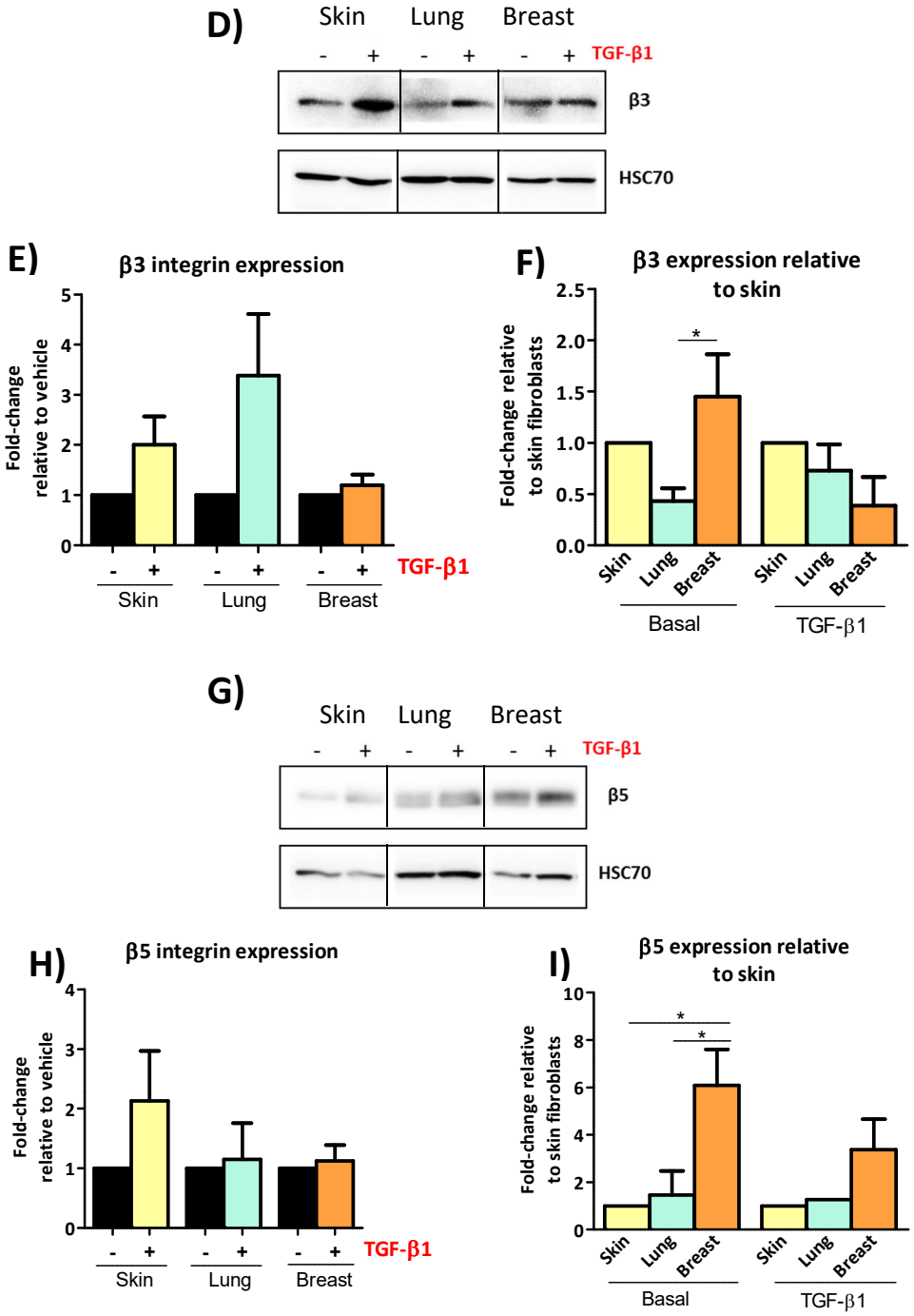

Figure 3. 7. Western blot analysis of αv, β3 and β5 integrin expression in TGF-β1-treated skin, lung and breast fibroblasts.

The following representative fibroblast strains from skin strain 2, lung strain 2 and breast strain 3 were stimulated with either vehicle (-) or TGF-β1 (+) (5ng/ml) for 48-hours. Vehicle vs TGF-β1 (B, E, H) and TGF-β1-stimulated skin vs lung/breast myofibroblasts (C, F, I). HSC70 serves as loading control. Note, the Students *t*-test could not be used to compare vehicle and TGF-β1 in B, E and H as *n*=2. Data shown represents the mean ± s.d. of two independent experiments. *p<0.05, **p<0.01 one-way ANOVA with Tukey's post-hoc.

3.6. The response of skin, lung and breast fibroblasts in functional assays

The contraction of the surrounding ECM by myofibroblasts is a fundamental feature of wound healing[4], while matrix remodelling also facilitates cancer cell invasion[102] and promotes the activation of matrix-bound latent-TGF-β1[39]. Furthermore, *in* vitro co-culture studies demonstrate fibroblasts are necessary to promote tumour cell invasion, as tumour cells plated alone on top of three-dimensional (3D) gels did not invade the underlying matrix[102]. Therefore, to ensure these fibroblasts had differentiated towards the expected functional phenotype, cells were examined in collagen gel contraction and mini-organotypic invasion assays.

3.6.1. Contraction of collagen type I gels by skin, lung and breast fibroblasts

Skin, lung and breast fibroblasts were plated inside collagen type I gels in the absence or presence of TGF-β1 (5ng/ml). The constitution of the gel mixture was adapted from Nystrom and colleagues[174], although Matrigel was left out of the gel contraction mixture due to accelerated fibroblast-mediated contraction in preliminary tests, which became problematic to measure within a 24-hour period. Therefore, the gels used to measure contraction consisted of collagen type I.

When comparing the three fibroblasts during vehicle control treatment (**Figure 3.8A**), the analysis revealed lung fibroblasts contracted collagen gels at the slowest rate compared to skin and breast. Furthermore, the post-hoc test demonstrated that skin and breast fibroblasts contracted gels 30% more than lung fibroblasts by day 9 (skin $p<0.01$, breast $p<0.01$), while skin and breast fibroblasts contracted gels at similar rates.

Furthermore, **Figure 3.8B** shows the addition of TGF-β1 significantly increased skin, lung and breast fibroblast-mediated contraction relative to vehicle-treated cells from day 5 onwards, though there was no significant difference between the three fibroblasts in their response to TGF-β1. **Figure 3.8C** illustrates these results in representative images from selected days during the gel contraction assay.

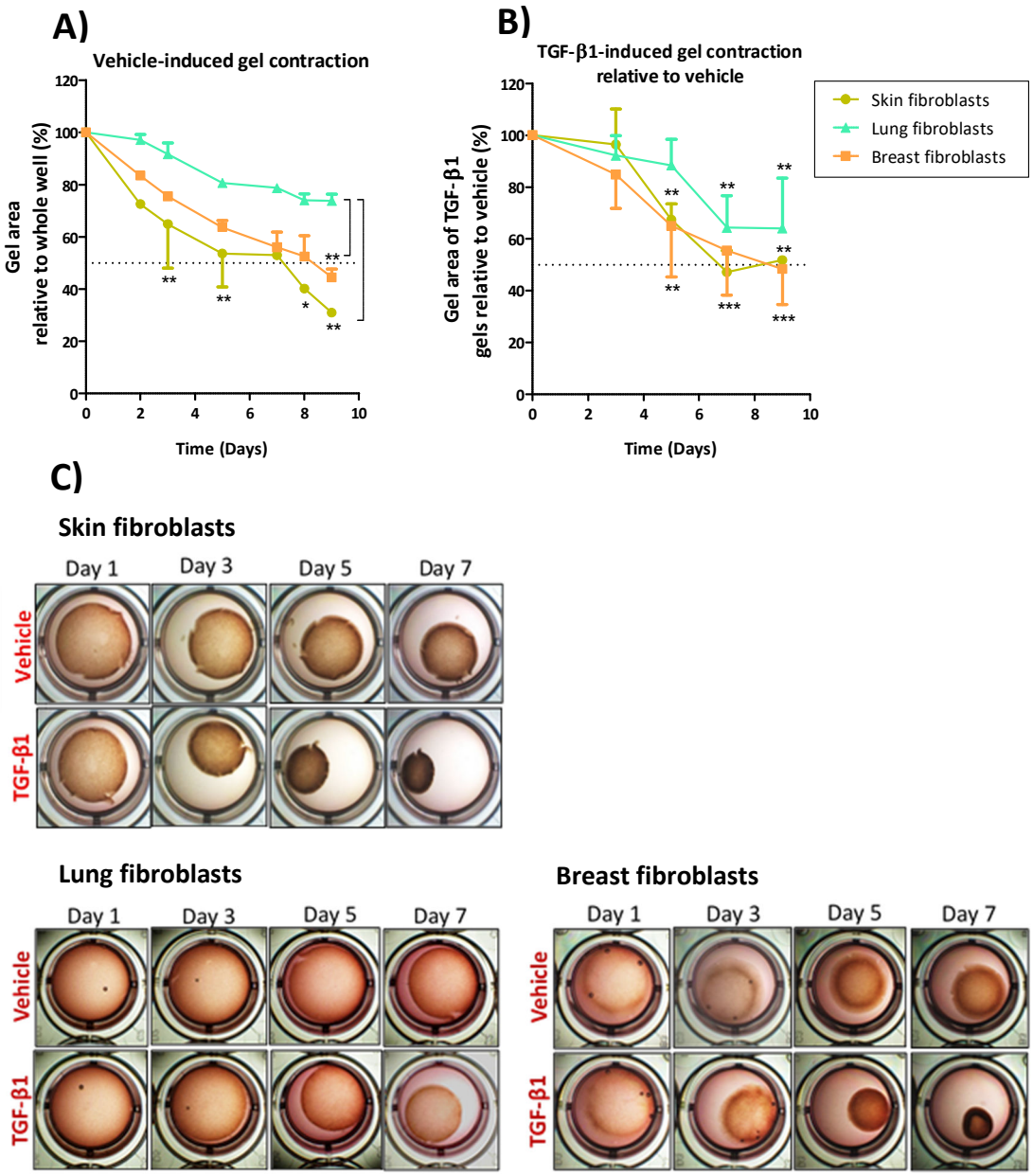

Figure 3. 8. Vehicle and TGF-β1-induced collagen gel contraction by skin, lung and breast fibroblasts.

Fibroblasts plated within collagen type I gels stimulated with either vehicle or TGF-β1 (5ng/ml). One representative fibroblast strain from each tissue shown: skin strain 2, lung strain 2 and breast strain 3. A) The percentage surface area of collagen type I gels relative to a whole well and significance is relative to lung fibroblasts. B) Significance measured by contraction of TGF-β1-treated gels relative to vehicle. C) Representative images of collagen gels on selected days after stimulation. Data shown represents the mean ± s.d from two-three independent experiments. *p<0.05, **p<0.01, ***p<0.001 two-way ANOVA with Bonferroni post-hoc test.

3.6.2. Mini-organotypic invasion assays of tissue-matched cancer cells and corresponding fibroblasts

To investigate whether these non-cancer-associated fibroblasts could promote cancer cell invasion in a 3D setting, a collagen-Matrigel mixture was pipetted into Transwell inserts in a 24-well plate, where tissue-matched cancer cells were cultured with fibroblasts in a 1:2 ratio on top of gels for seven days.

In **Figure 3.9**, cancer cells in the H & E images are distinguished as larger, multi-nucleated cells (red arrow) and fibroblasts are much smaller, appearing as dots with a single nucleus (green arrow). Immunofluorescent staining of organotypic sections was conducted to identify each cell type using cell-specific markers, specifically cytokeratin staining for cancer cells and α-SMA for fibroblasts. Unfortunately, there was only weak α-SMA staining in most sections in **Figure 3.9**. Nevertheless, the images demonstrate cancer cell lines derived from skin (**Figure 3.9A**), lung (**Figure 3.9C**) and breast (**Figure 3.9E**) tissue did not invade into these 3-D gels when plated alone. However, the H and E and immunofluorescent images suggest invasion of both cell types was apparent after seven days when skin (**Figure 3.9B**), lung (**Figure 3.9D**) and breast (**Figure 3.9F**) cancer cells and fibroblasts were admixed and cultured on top of gels. In addition, the immunofluorescent staining of lung tumour cells and fibroblasts (**Figure 3.9D**) shows the majority of cells were positive for α-SMA, perhaps suggesting epithelial-to-mesenchymal (EMT) transition occurred.

In the graphs shown in **Figure 3.9G** and **3.9H**, two fibroblast strains from skin and breast tissue are presented to demonstrate tissue-specific responses, as these same strains were also used in the next set of experiments, presented throughout the forthcoming chapter; Results Part II. Unfortunately, weak cytokeratin staining of lung mini-organotypic gels prevented reliable analysis and is therefore absent from the graphs. In **Figure 3.9G**, the results indicate more oral squamous cell carcinoma cells (OSCC) invaded when plated with skin fibroblasts compared to the number of invading breast cancer cells. Furthermore, co-culture with strain 3 dermal fibroblasts resulted in significantly higher numbers of invading tumour cells than any other combination analysed. Surprisingly, **Figure 3.9H** shows the number of invaded fibroblasts followed an inverse trend to invaded tumour cells, as high numbers of

OSCC cells were associated with low numbers of invaded skin fibroblast strain 3 and lower numbers of breast cancer cells were associated with higher numbers of invading breast fibroblasts (strain 2 and 3). Although whether this was an effect of the fibroblasts themselves or the different cancer cells used is uncertain. In addition, the co-culture of breast cancer cells with breast strain 3 fibroblasts resulted in a thicker layer of cytokeratin-positive tumour cells at the top of the gel (**Figure 3.9F**) compared to skin and lung sections.

Overall, these functional assays demonstrated that these skin, lung and breast fibroblasts exhibited the expected functional responses, as each significantly contracted collagen gels in response to TGF-β1, while fibroblasts markedly promoted tumour cell invasion.

A) VB6 oral squamous cell carcinoma (OSCC) cells alone

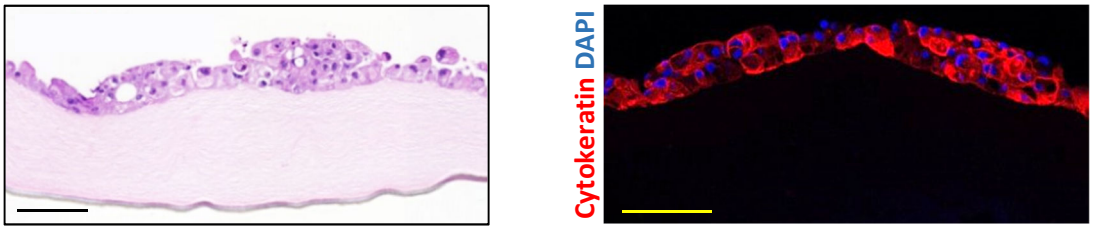

B) VB6 + strain 2 skin fibroblasts (S2)

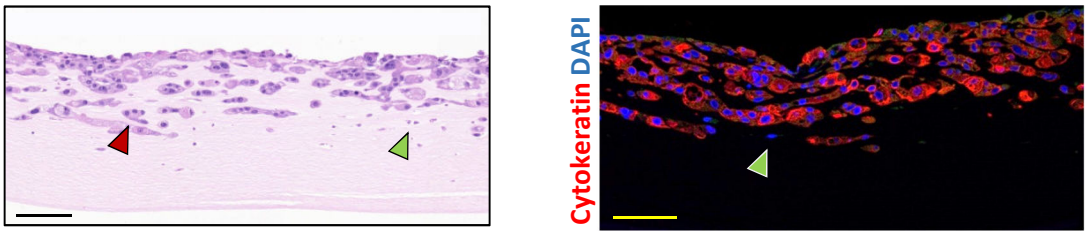

C) H1299 lung cancer cells alone

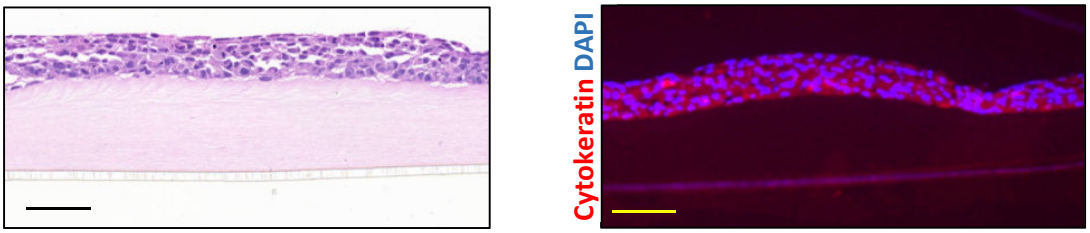

D) H1299 + strain 2 lung fibroblasts

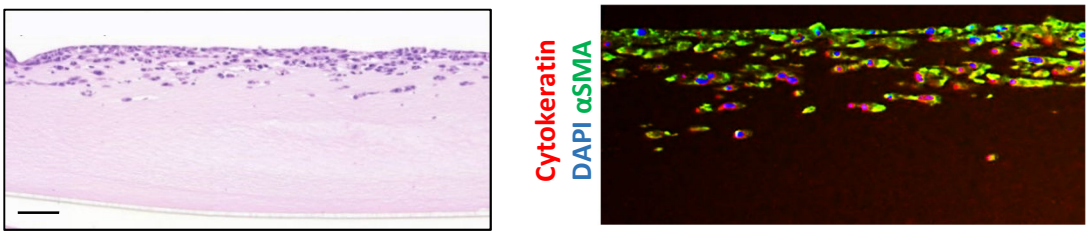

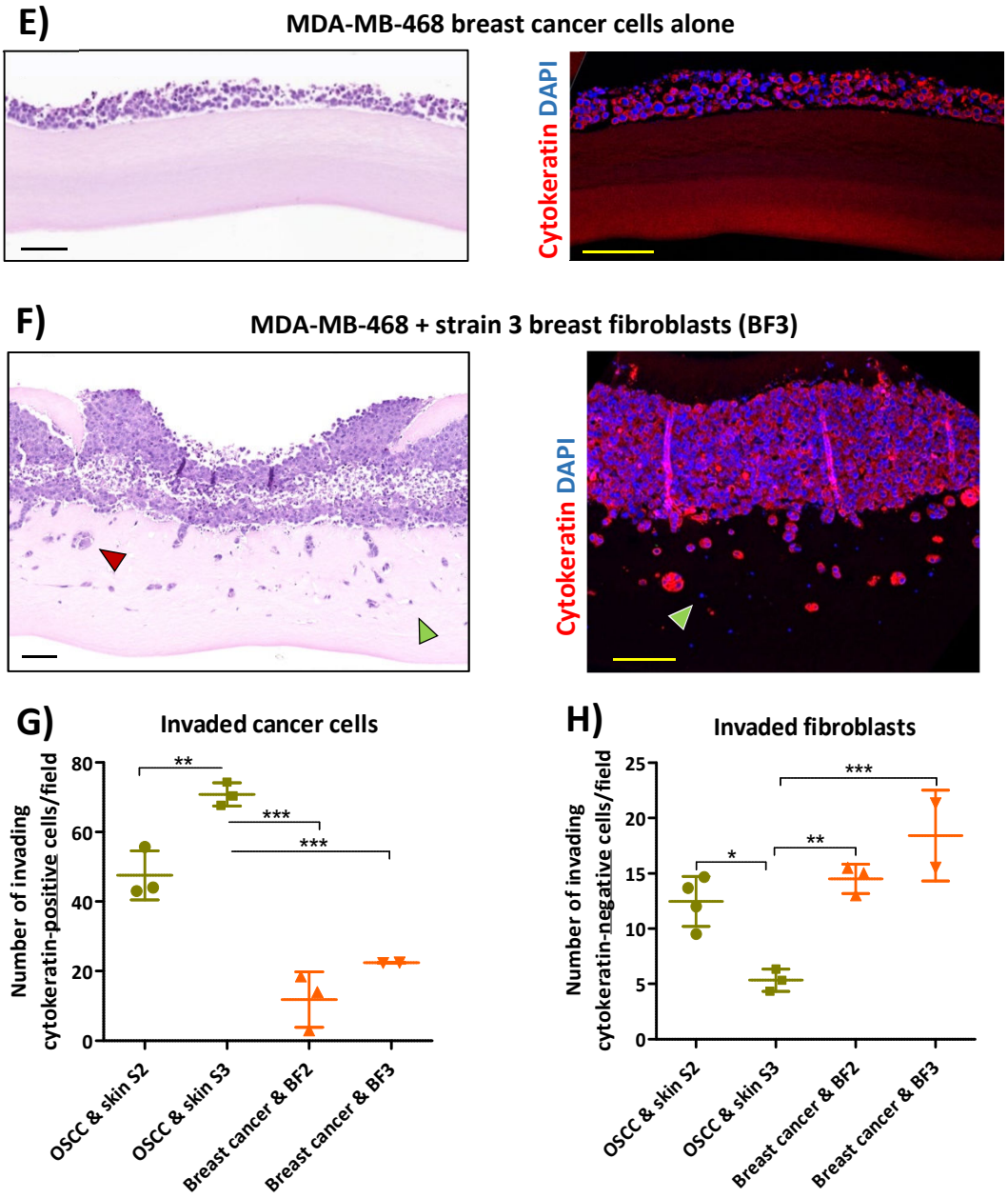

Figure 3. 9. Skin, lung and breast cancer cells co-cultured with fibroblasts in mini-organotypic invasion assays.

H & E and immunofluorescent staining of cancer cells alone (A, C, E) or admixed with fibroblasts (B, D, F) in a 1:2 ratio plated above mini-organotypic gels and cultured for 7 days. Cytokeratin staining (red) identifies tumour cells (red arrow) and cytokeratin-negative/α-SMA-positive cells are fibroblasts (green arrow). Graphs show the average number of invading cancer cells (G) and fibroblasts (I) per field (20x magnification), quantified by counting cytokeratin-positive/negative cells below the epithelial layer, per field in each gel (2-3 fields/gel and 3 gels per condition). Strains: oral squamous cell carcinoma (OSCC), skin fibroblast strain 2 and 3 (skin S2 and S3) and breast fibroblast strain 2 and 3 (BF2 and BF3). Data shown represents mean ± s.d. *P<0.05, **P<0.01, ***P<0.001, one-way ANOVA with Tukey's post-hoc. Representative images from one independent experiment with triplicate wells for each condition. Scale bar: 100µm.

3.7. Discussion

3.7.1. Expression of myofibroblast-associated markers in TGF-β1-treated fibroblasts

This study set out to determine whether the activated form of fibroblasts from separate tissues exhibit different activation markers and biological activities. We used TGF-β1 as an exogenous inducer of the activated phenotype, known as a myofibroblast. Thus we compared normal fibroblasts from skin, lung and breast tissue exposed to TGF-β1 stimulation. After analysis, I can confirm that fibroblasts derived from these tissues exhibit heterogeneity in response to TGF-β1 in context of the various parameters measured. These differences exist in expression patterns of selected 'markers of activation' and integrin expression.

Previous studies investigating fibroblast heterogeneity are limited and involve cells from distinct layers of skin, different organs or compare responses to cytokines, such as TNF-α[134, 165]. Therefore, considering the relevance of TGF-β1 in stimulating fibroblast-to-myofibroblast differentiation during tumour progression and fibrosis, it was surprising that the analysis of fibroblasts' response to TGF-β1 across different tissues had not been studied. However, in 2004, Lygoe and colleagues investigated the response of single strains of fibroblasts from dermal, oral and renal tissues to TGF-β1. Although, these experiments only assessed expression of α-SMA and integrins αv and β1[64]. In contrast, this current study here in has significantly extended those results by comparing three strains of skin, lung and breast fibroblasts and conducting a complete characterisation of the integrin gene expression profile of TGF-β-treated cells. These results now spur further research to test the various integrins identified that were modified by TGF-β1, but were not examined in the later experiments of this study.

The results generated here support other published studies that recognise heterogeneity in different fibroblasts, although the combination of skin, lung and breast fibroblasts has not been directly compared previously. Lindner and colleagues found that fibroblasts from cardiac, dermal and pulmonary tissue produce different levels of MMP-1 and MMP-3 in response to cytokine TNF-α stimulation, parallel to

findings here where skin, lung and breast fibroblasts generate different mRNA levels of ACTA2, FN1, TIMP-3, CTGF and SERPINE1 after TGF-β1 treatment[134]. Therefore, these data support the concept that stimulation of fibroblasts with pro-inflammatory cytokines, such as TNF-α or TGF-β1 affects gene expression differentially according to the tissue origin, but also donor, of the fibroblast.

The role of α-SMA as a consistent marker of fibroblast-myofibroblast differentiation is controversial, as myofibroblasts that display phenotypic characteristics such as stress fibre formation and contraction during wound healing do not necessarily require α-SMA expression[175]. Nevertheless, in this study all fibroblast strains increased α-SMA at either gene or protein levels in response to TGF-β1, indicating differentiation was induced. Notably, α-SMA protein displayed higher basal levels in skin fibroblasts (**Figure 3.4**), possibly suggesting these cells are more sensitive to substrate stiffness than lung or breast fibroblasts and may have already undergone partial differentiation by culture on plastic. Huang and colleagues found that fibroblasts expressed 4-fold more α-SMA when plated on stiff vs soft gel substrates[176], though here, the addition of TGF-β1 to these susceptible skin fibroblasts still produced an active myofibroblast phenotype, as evidenced by increased expression of activation marker and integrin genes and gel contraction in the presence of TGF-β1.

The tissue-specific expression of α-SMA is also supported by other studies. The variances shown in α-SMA time-course data from skin, lung and breast fibroblasts (**Figure 3.1A**) mimics divergences observed in fibroblasts derived from skin, oral mucosa and kidneys, where dermal and oral fibroblasts expressed 3-4-fold more α-SMA after 72-hour TGF-β1 stimulation compared to renal fibroblasts that only increased α-SMA approximately 1.5-fold[64]. However, after TGF-β1 stimulation, α-SMA protein levels (**Figure 3.4**) did not demonstrate significant differences between tissues. It should be acknowledged that this may change if additional repetitions on more strains were performed.

In contrast, MMP-1 and collagen type I gene expression did not significantly change in any fibroblast after TGF-β1 stimulation, although COL1A2 was increased to 2.5 ±

1.2-fold in lung fibroblasts, pointing towards the pro-fibrotic effects of TGF-β by shifting towards collagen deposition and away from proteolysis. These results are supported by studies in which dermal or primary lung fibroblasts were stimulated with TGF-β1 for up to 24 hours, where no change in MMP-1 or decreased expression was evident, respectively [177, 178]. Moreover, Goffin and colleagues suggest MMP-1 and COL1A2 are differentially regulated factors, as TGF-β1 induces transcription factor SP-1 binding to COL1A2 promoter regions, whereas MMP-1 depends on transcription factors, such as c-Jun, independent of TGF-β stimulation[177].

In contrast, TIMP3 revealed tissue-specific expression that was highly induced by TGF-β1 in lung and breast fibroblasts, but not in skin, indicating different mechanisms of regulation of the same gene. Investigation of fibroblast TIMP3 expression in ductal breast tumours showed positive correlation with the presence of distant metastases[179], while TIMP-3 expression was upregulated in the fibroblastic foci of IPF tissues when compared to normal lung sections[180]. These results validate the value of characterising fibroblasts from different sites, which may lead to a better understanding of disease pathophysiology and potentially generate clinical biomarkers.

Overall, the differences noted in myofibroblast genes may result from distinct quantities of TGF-β-receptors expressed by each fibroblast, which should be quantified in future experiments. Chipev and Simon show dermal fibroblasts derived from keloids, normal heel/palm tissue and non-palmar sites exhibit differing levels of TGF-β type II transmembrane receptors. Moreover, in fibroblasts derived from palmar vs non-palmar skin of healthy subjects the levels of TGF-β type II receptor positively correlated with α-SMA and ED-A fibronectin expression[181]. In addition, the secretion of TGF-β1 from fibroblasts may also influence the heterogeneity observed of myofibroblast-associated factors. Therefore, the differences between fibroblasts may also originate from variances in their TGF-β signalling components.

3.7.2. Expression of integrins in TGF-β1-treated skin, lung and breast fibroblasts

Although it seemed TGF-β1 enhanced the expression of some integrin subunits at the gene level (α1, α11, β3), the results at the protein level via western blotting (αv, β3, β5) were non-significant, yet perhaps more biological repeats or longer TGF-β1 exposure may resolve this. In comparison, Lygoe and colleagues assessed αv and β1 subunits using western blotting and flow cytometry by exposing fibroblasts to TGF-β1 for 72 hours. Their results found TGF-β1 significantly increases expression of each subunit by 1.5-fold, with similar changes in dermal, oral and renal fibroblasts[64]. In addition, Heino and colleagues demonstrated that lung fibroblast cell line WI-38 upregulated α1, α2, α3, α5 and β1 subunits to varying degrees in response to TGF-β1, as I also observed, suggesting expression is regulated by independent mechanisms[60].

Flow cytometry data in this study also suggests integrin surface expression is not augmented by TGF-β1 stimulation, although it should be noted fibroblasts were only stimulated for 24 hours. Nevertheless, this suggests that these fibroblasts may not upregulate the number of integrins upon their cell surface to potentially regulate myofibroblast activity. Instead, as integrins can initiate intracellular signalling pathways by clustering on the plasma membrane, perhaps redistribution of transmembrane integrins was sufficient to enhance integrin activation in response to TGF-β1[182]. Preliminary tests (**Figure 3.10**, next page) using an anti-αv integrin to stain vehicle and TGF-β1-treated strain 2 skin fibroblasts showed clustered integrins are present in TGF-β1-exposed cells (**Figure 3.10D-F**), although talin or kindlin co-staining is required to confirm integrin activation. Furthermore, intracellular signalling that begins at the cytosolic portion of the β-integrin tail may have also been amplified to promote myofibroblast functions[28]. However, this will require further characterisation of specific signalling kinases, e.g. FAK, in future studies. In addition, while all fibroblasts were cultured on tissue culture plastic, recent studies demonstrate cardiac fibroblasts differentially express a variety of integrins according to whether cells are grown on collagen, fibronectin or organ-specific decellularised ECM[183]. Therefore, in the future perhaps studying the integrin expression profile

of fibroblasts grown on organ-derived matrices would be more biologically representative.

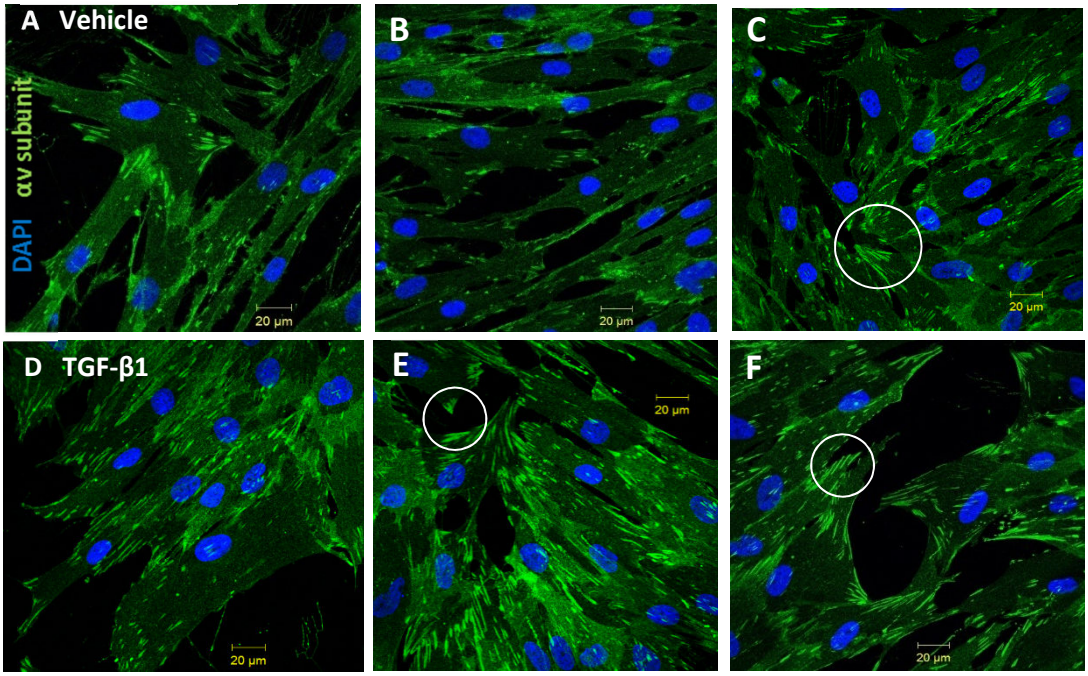

Figure 3. 10. Integrin αv subunit expression in vehicle and TGF-β1 stimulated skin fibroblasts.

Representative images of vehicle (A - C) or TGF-β1 (5ng/ml) (D – F) stimulated strain 2 skin fibroblasts (24 hours), which was fixed with paraformaldehyde and permeabilised. Examples of potentially clustered integrins highlighted inset.

When comparing integrin expression between the 3 tissues, breast fibroblasts appear to express more αv and β5 than skin or lung fibroblasts, evidenced at the protein level. Additional studies are required to determine whether breast fibroblasts have enhanced capacity to activate latent-TGF-β1, as do cardiac fibroblasts *in vitro* via αvβ5-mediated contraction[125]. Moreover, integrin expression should be examined in further strains of breast fibroblasts to establish whether these effects are tissue- or strain-specific.

The expression of integrin α11 by myofibroblasts is also of particular interest as published literature contains large gaps in understanding of its contribution to tumour progression and fibrosis. Data here showed TGF-β1 significantly increased α11 in skin and lung fibroblasts, though α11 mRNA in breast fibroblasts displayed no change in response to stimulation. However, investigating the protein levels in each

of these fibroblasts would validate these results. Previous published studies have focused on the role of α11 in skin and lung myofibroblasts and show knockdown of integrin α11 in mouse embryonic fibroblasts co-implanted with lung adenocarcinoma cells significantly delayed tumour growth compared with wild-type fibroblasts. In addition, knockdown of α11 was linked to markedly lower insulin-like growth factor-2 expression in fibroblasts, impacting tumour growth[104], demonstrating the potential impact of myofibroblast integrin expression in cancer tissues.

Integrin subunit β8 also revealed striking results, as this gene was downregulated in all skin, lung and breast fibroblasts in response to TGF-β1 stimulation. Moreover, this effect was also similar in each strain of fibroblast from each tissue. Published findings demonstrate this integrin is expressed in cerebral astrocytes, where αvβ8 appears to regulate MMP-14-dependent activation of latent TGF-β1[22] and hence, its expression was associated with the invasiveness of glioblastoma cells[184]. In addition, though there are few studies investigating the role of β8 in fibroblasts, Kitamura and colleagues found this integrin is upregulated on human chronic obstructive pulmonary disease fibroblasts by IL-1β, where it activated latent TGF-β1, which in turn increased the expression of TGF-β1-responsive ECM genes in fibroblasts, such as COL1A2 and SERPINE1[185]. However, my results indicate β8 downregulation may constitute a negative feedback loop to perhaps prevent further activation of latent TGF-β1 by skin, lung and breast fibroblasts.

3.7.3. Functional activity of skin, lung and breast fibroblasts: collagen gel contraction and invasion

According to the results, vehicle-treated lung fibroblasts contracted collagen type I gels significantly less than skin or breast-derived cells (**Figure 3.8**). However, these observations cannot be explained by differences in α-SMA or integrin expression, as skin and breast fibroblasts contracted gels at similar rates, even though breast fibroblasts expressed less basal α-SMA than skin. Moreover, recent investigations into the role of α-SMA expression in fibroblasts revealed α-SMA correlates with contractile activity, but is not essential for contraction to occur. Hinz and colleagues showed lung fibroblasts with higher α-SMA levels contracted collagen gels more than rat subcutaneous fibroblasts that expressed less α-SMA[186], though Tomasek and

colleagues demonstrated there was no notable difference in dermal fibroblasts from α-SMA-null and wild-type mice, as both contracted collagen gels to a similar extent in response to TGF-β1. They found this was possible as other actin isoforms had replaced α-SMA function in null fibroblasts[175]. Furthermore, in ACTA2$^{-/-}$ and heterozygous mice, wound healing is significantly slower than controls, yet contraction still occurs indicating α-SMA enhances contraction but is not essential[187]. The data in this current study provides support to the notion that α-SMA expression does not directly correlate with the contractile activity of fibroblasts. However, after skin, lung or breast fibroblasts were plated inside collagen gels the expression of α-SMA was not examined, which may help to clarify this conclusion. In addition, previous studies suggest fibroblast exhibit a more proliferative phenotype when plated on collagen[188], therefore perhaps differences in proliferation rates would also contribute to the differential rates of gel contraction observed.

Myofibroblasts are also known to invade into the surrounding ECM and promote tumour cell invasion. Therefore, mini-organotypic invasion assays provided a translational model to examine tumour-stroma interactions. The importance of close proximity of fibroblasts to cancer cells to promote invasion has been demonstrated previously by this laboratory. Nystrom and colleagues reported that tumour cell invasion through collagen-Matrigel gels required the presence of fibroblasts[174]. Gaggioli and colleagues also demonstrated fibroblasts created physical tracks within the ECM that squamous cell carcinoma cells (SCCs) exploited to follow behind the leading fibroblast. In addition, these authors reported that SCC cells did not invade underlying gels in the absence of matrix remodelling by fibroblasts, in agreement with my results here (**Figure 3.9**). Furthermore, Gaggioli et al. reported that integrin α3β1 and α5β1 expression was linked to this force-mediated remodelling by fibroblasts, as knockdown of these integrins resulted in a lack of holes in the organotypic gel, ultimately reducing the level of collective SCC cell invasion[102].

Tumour-fibroblast interactions are dynamic; thus tumour cells release factors such as TGF-β1 that stimulate fibroblasts to secrete ECM-degrading proteases and TGF-β1 secreted from CAFs, in turn can promote EMT of local tumour cells, enhancing the ability of tumour cells to invade through a 3D matrix, demonstrating the symbiotic

relationship of tumour cells and fibroblasts[91, 189]. Quantifying the levels of TGF-β1 secreted by both tumour cells and fibroblasts would shed further light on the results obtained from these invasion assays.

My data suggests some breast fibroblasts appear to promote more cancer cell proliferation, owing to the thicker cytokeratin-positive layer observed during mini-organotypic assays. This effect was specific to this breast fibroblast strain (strain 3), as when an alternative breast fibroblast strain (strain 2) was combined with the same MDA-MB-468 breast cancer cells, the epithelial layer was noticeably thinner in comparison (**Appendix Figure 18A**). Incidentally, breast fibroblast strain 3 expressed more basal αv and β5 integrin protein than breast strain 2 (**Appendix Figure 18B**), therefore perhaps breast strain 3 had a higher capacity to activate latent-TGF-β than other fibroblasts. This would result in the presence of additional active TGF-β1, thereby potentially establishing autocrine TGF-β signalling in breast myofibroblasts[190], which may have continuously secreted factors that promoted tumour growth.

Overall, my findings demonstrate skin, lung and breast fibroblasts exhibited heterogeneity in response to TGF-β1, predominantly by their activation marker gene expression and integrin expression, though strain-specific responses were also evident. In addition, lung fibroblasts contracted collagen gels at the slowest rate, but the levels of contraction by skin, lung and breast fibroblasts in response to TGF-β1 were similar. Furthermore, each strain of fibroblast, which were derived from healthy tissues promoted the invasion and growth of tumour cells in a 3D environment. These results also identified which integrins were to be further investigated, as shown in Chapter IV.

CHAPTER IV. RESULTS PART II

The role of specific integrins in the functional behaviour of activated skin, lung and breast fibroblasts.

4.1. Background

Having examined which integrins were expressed by skin, lung and breast fibroblasts and which were regulated by TGF-β1, I next used a combination of pharmalogical (small-molecule integrin inhibitors from my sponsor, GlaxoSmithKline) and genetic (siRNA) tools to investigate the role of key integrins in both the activation state of myofibroblasts and their functional activity. Previous experiments by Lygoe and colleagues using pan-αv, αvβ3 and αvβ5 blocking antibodies on dermal, oral mucosa and renal fibroblasts in the presence of TGF-β1, suggested different integrins regulated fibroblast activation and activity depending on which tissue the fibroblast was derived from[64]. Therefore, it was hypothesised that different integrins in skin, lung and breast fibroblasts would be responsible for regulating myofibroblast invasion, contraction and gene expression.

4.2. The inhibition of integrins in TGF-β1-treated skin, lung and breast fibroblasts

4.2.1. Cell viability of fibroblasts treated with small-molecule inhibitors

The three integrin inhibitors provided by GSK were a pan-αv integrin inhibitor, cilengitide (targeting αvβ3/αvβ5) and an αvβ1-selective compound. As detailed in the Materials and Methods section, the pan-αv inhibitor[159] and cilengitide[160] are RGD-mimetics, while each of the three inhibitors bind to the ligand-binding regions of integrins. To determine a suitable concentration to use with fibroblasts, a MTT assay was performed to examine cell viability during exposure to each drug at 10-fold dilutions (0.1-10μM) for 72 hours. The same 2 fibroblast strains per tissue tested in the previous mini-organotypic invasion assays are also presented here, although note, each result represents one independent experiment.

Overall, **Figure 4.1** shows pan-αv inhibition significantly reduced the viability of skin strain 2 fibroblasts by 15-35% (**Figure 4.1A**), although there was no clear correlation between cell viability and inhibitor concentration, and no significant effect on the viability of skin strain 3 (**Figure 4.1B**). In addition, in lung (**Figure 4.1C-D**) and breast fibroblast strains (**Figure 4.1E-F**), the highest concentration of 10μM pan-αv reduced the viability of each strain by approximately 25-50%.

In contrast, whereas cilengitide had no significant effect on skin or lung fibroblast viability, the viability of both strains of breast fibroblasts was significantly affected by cilengitide at each of the concentrations tested, particularly using the highest 10μM dose (**Figure 4.1E-F**).

The αvβ1-selective compound only slightly reduced the viability of skin and breast fibroblasts at lower concentrations between 0.1-1μM, while 5μM doubled the viability of breast strain 3 fibroblasts (**Figure 4.1F**). In addition, it appears lung fibroblast viability was unaffected by αvβ1 blockade. Overall, as most fibroblasts exhibited at least 60% viability using 1μM of each drug, this concentration was deemed the most suitable for further experiments.

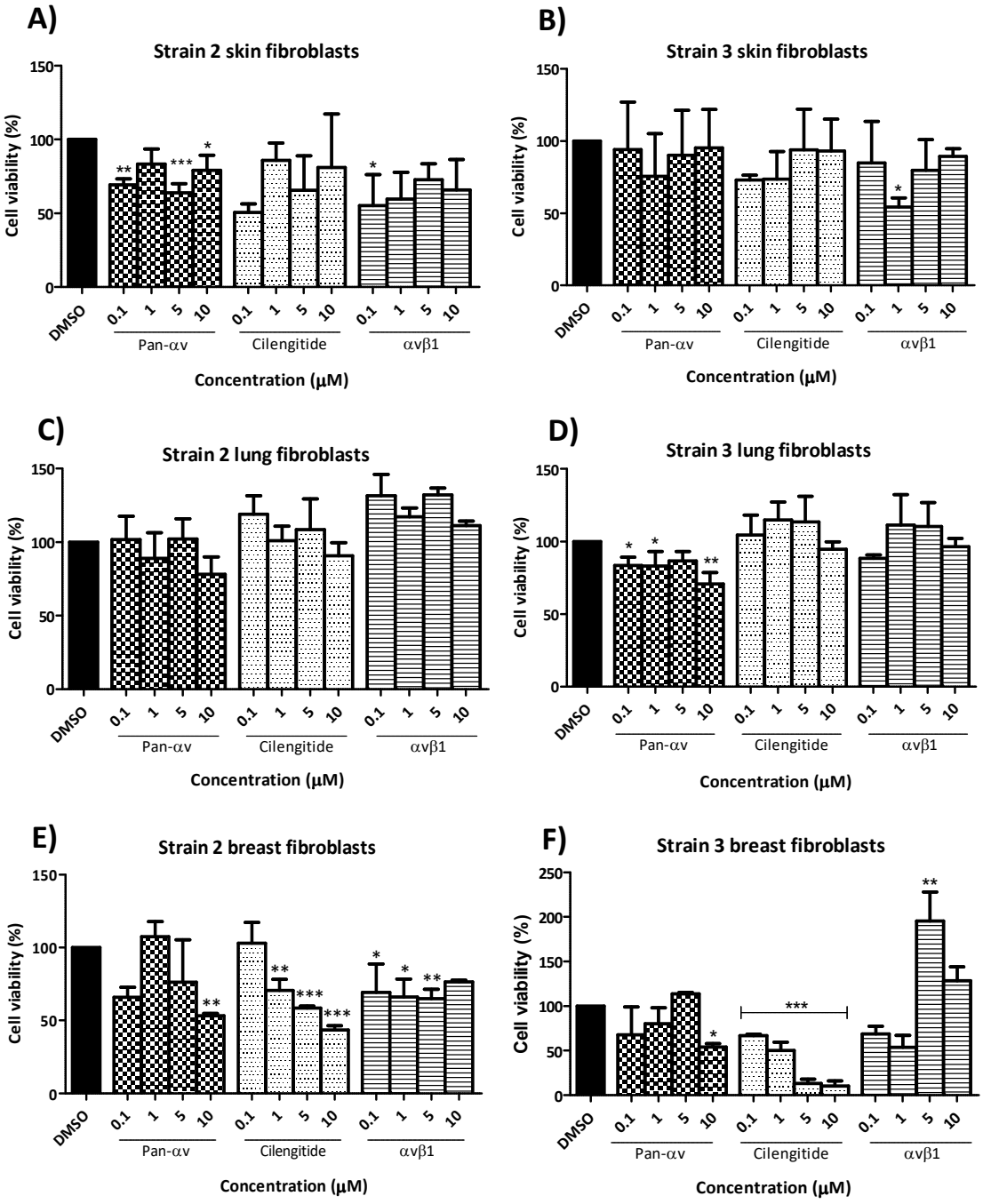

Figure 4. 1. The effect of integrin inhibitors on fibroblast cell viability.

The cell viability of two strains of skin (A, B), lung (C, D) and breast (E, F) fibroblasts was assessed using a MTT assay after 72 hours culture in 10-fold dilutions of DMSO control or integrin small-molecule inhibitors; pan-αv, cilengitide (targeting β3/β5) and αvβ1-selective. *p<0.05, **p<0.01, ***p<0.001, one-way ANOVA with Dunnet's post-hoc to compare each concentration to DMSO control. Data represented by mean ± s.d of one independent experiment with triplicate wells.

4.2.2. The effect of small-molecule integrin inhibitors on skin, lung and breast myofibroblast invasion

An *in* vitro Transwell invasion assay was conducted to test the effect of integrin blockade on the ability of skin, lung and breast fibroblasts to invade Matrigel. In preliminary tests, I used three different concentrations of compounds with non-TGF-β1 stimulated skin and lung fibroblasts. **Figure 4.2A** shows the pan-αv inhibitor at 10μM ($p<0.01$) and 1μm cilengitide ($p<0.05$) both significantly inhibited invasion of skin fibroblasts after 48 hours, although it appears 0.1μM of the αvβ1-selective inhibitor promoted invasion relative to the DMSO control. In addition, each of these integrin inhibitors also significantly promoted the invasion of lung fibroblasts at either 0.1μM or 1μM concentrations (**Figure 4.2B**). Furthermore, in general the data for each drug followed a dose-response pattern. For practical and cost reasons, only one concentration could be selected for additional functional studies; 1μM was chosen as an intermediate concentration with generally acceptable toxicity.

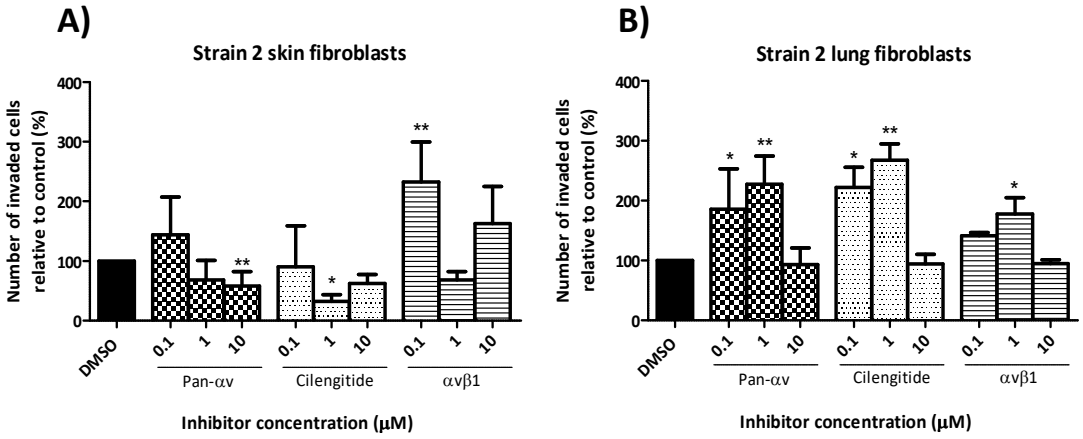

Figure 4. 2. Preliminary test of the effect of integrin inhibitors on skin and lung fibroblast invasion.

Skin (A) and lung (B) fibroblasts were exposed to either matched DMSO volumes (control) or 0.1μM, 1μM or 10μM integrin inhibitors; pan-αv, cilengitide (targeting β3/β5) and αvβ1-selective before addition to Matrigel-coated Transwells for a 48-hour invasion assay. *$p<0.05$, **$p<0.01$ one-way ANOVA with Dunnet's post hoc to compare each column to DMSO. Data represented by mean ± s.d (skin *n*=1, lung *n*=2) with at least 4 technical replicates per concentration.

To examine the effect of each compound on skin, lung and breast myofibroblast invasive propensity, cells were pre-treated with TGF-β1 for 48-hours and then combined with inhibitors (1μM) shortly before plating on top of Matrigel-coated Transwells and left to invade for 48 hours. The rationale behind pre-treating fibroblasts with TGF-β1 was to test how integrin inhibitors would affect the phenotype of activated fibroblasts. This result would also be more clinically relevant as fibroblasts in the tumour microenvironment are likely to already be exposed to TGF-β1 before a possible integrin-targeting therapeutic would be administered.

Figure 4.3 shows the invasion of only skin strain 2 and lung strain 3 fibroblasts were significantly increased by TGF-β1 pre-treatment. The invasion of other skin, lung and breast strains were unaffected by TGF-β1.

Figure 4.4 demonstrates that myofibroblasts displayed a highly variable response to small molecule integrin inhibitors, which appeared in a tissue-specific pattern. Firstly, targeting αv-containing integrins using the pan-αv compound inhibited invasion by skin strain 2 fibroblasts by 63% ($p<0.001$), but did not affect skin strain 3. Cilengitide significantly reduced the invasion of skin fibroblast strain 2 by 60 ± 16% (**Figure 4.4A**) and skin strain 3 by 46 ± 22% (**Figure 4.4B**), while the administration of the αvβ1-selective inhibitor also significantly decreased invasion of skin strain 2 by 41 ± 14% and skin strain 3 by 38 ± 16%.

In contrast, pan-αv and αvβ1 inhibition had no significant effect in lung (**Figure 4.4C-D**) and breast (**Figure 4.4E-F)** fibroblast invasion. Strikingly, cilengitide had the opposite effect on lung and breast fibroblasts as it significantly promoted at least 50% more invasion in lung strain 2 (**Figure 4.4C**) and breast strain 3 fibroblasts (both $p<0.01$, **Figure 4.4F**), with a similar trend in the remaining lung and breast strains.

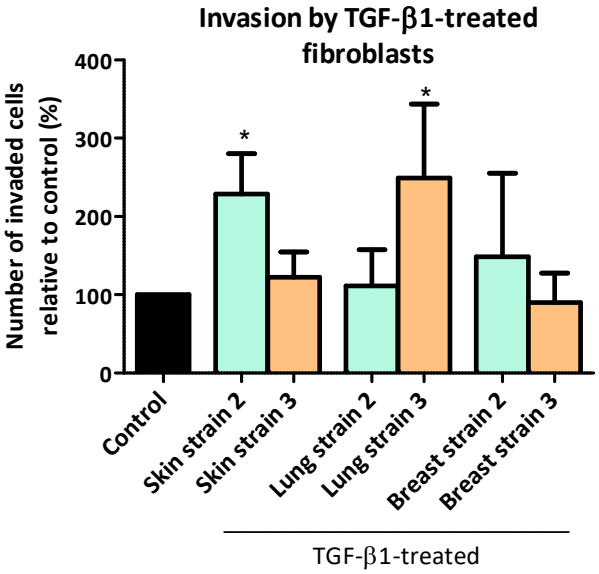

Figure 4. 3. The effect of TGF-β1 on skin, lung and breast fibroblast invasion.

Skin, lung and breast fibroblasts were pre-treated with vehicle or TGF-β1 (5ng/ml) in tissue culture flasks for 48 hours and then trypsinised and plated on top of Matrigel-coated Transwells. Cells were incubated for a further 48 hours and only cells underneath Transwells were counted. *$p<0.05$, one-way ANOVA with Dunnet's post hoc to compare each column to DMSO. Data represented by mean ± s.d of three independent experiments with at least 3 technical replicates per cell strain.

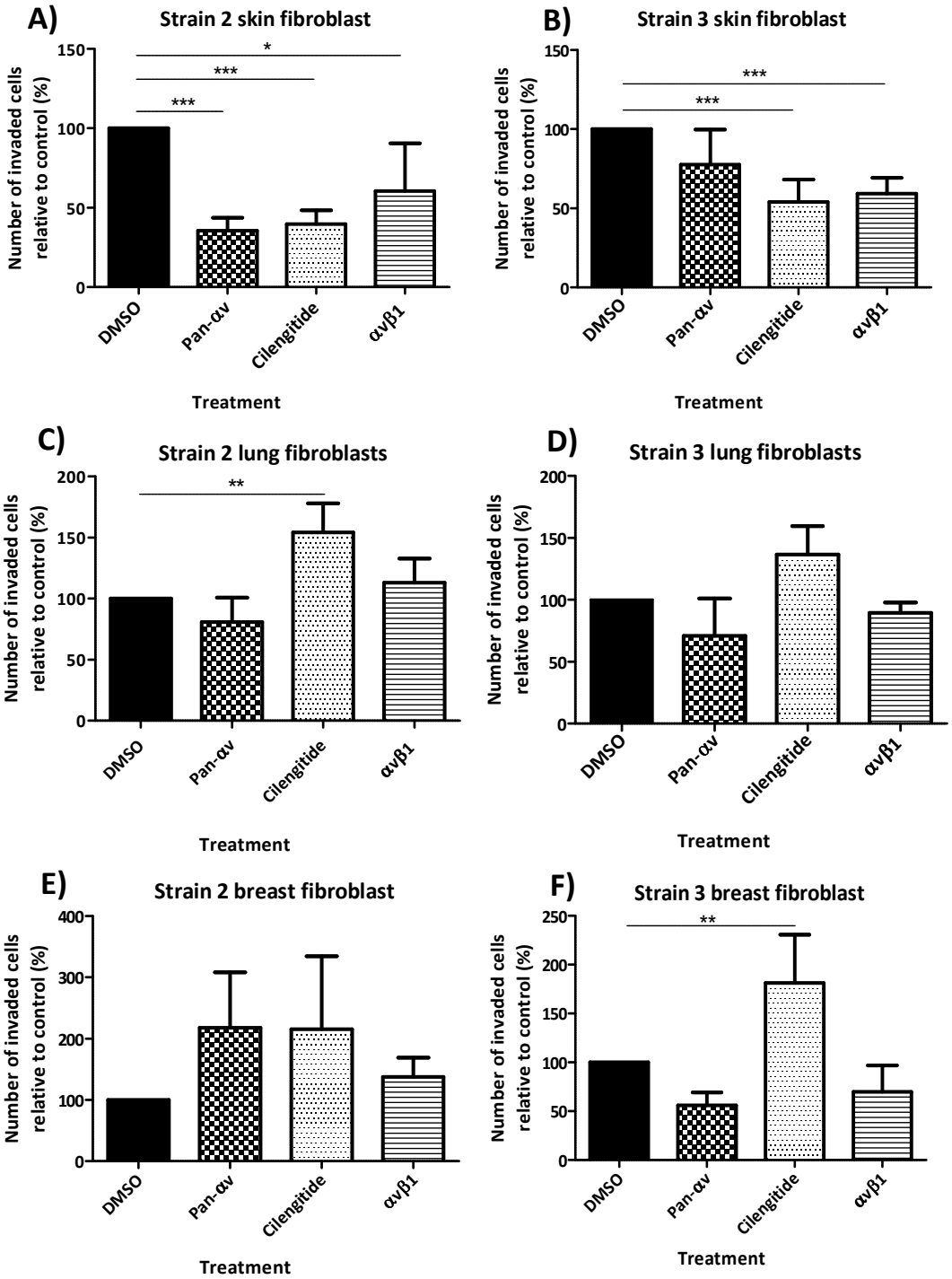

Figure 4. 4. Invasion assay using integrin inhibitors with TGF-β1 treated skin, lung and breast fibroblasts.

Skin (A, B), lung (C, D) and breast (E, F) fibroblasts were pre-treated with TGF-β1 (48-hours), trypsinised and then combined with a matched volume of DMSO (control) or 1μM integrin inhibitors; pan-αv, cilengitide (targeting β3/β5) and αvβ1-selective and plated on Matrigel-coated Transwells for a 48-hour invasion assay. Only cells underneath the Transwell were counted. *p<0.05, **p<0.01 ***p<0.001 one-way ANOVA with Dunnet's post hoc to compare each column to DMSO. Data shown represents mean ± s.d of three independent experiments with 3-5 Transwells per treatment.

4.2.3. The effect of small-molecule integrin inhibitors on skin, lung and breast myofibroblast-mediated collagen gel contraction

All fibroblasts were again pre-treated with TGF-β1 (5ng/ml) for 48-hours before being plated inside collagen type I gels. TGF-β1-treated fibroblasts were trypsinised and resuspended in collagen gels containing 1μM concentrations of each integrin inhibitor. The next day, media containing TGF-β1 (5ng/ml) was added on top of gels, which were imaged on every 2-3 days.

Figure 4.5 shows gel contraction on selected days, where none of the three integrin inhibitors significantly affected gel contraction by 2 strains of skin (**Figure 4.5A-B**), lung (**Figure 4.5C-D**) or breast (**Figure 4.5E-F**) fibroblasts compared to control gels (TGF-β1 + DMSO). However, in strain 2 breast fibroblasts pan-αv blockade significantly increased gel contraction by an average of 36% ($p<0.01$). In addition, breast fibroblasts took longer to contract gels overall, with or without inhibitors, therefore their images and graphs in **Figure 4.5** are from later time-points (Day 14 and Day 25) compared to skin or lung (Day 4-7). To ensure efficacy of the inhibitors was maintained during the assay, gels were re-drugged with inhibitors at 1μM concentrations in TGF-β1-containing media every 3 days, although this also had no effect on the rate of gel contraction.

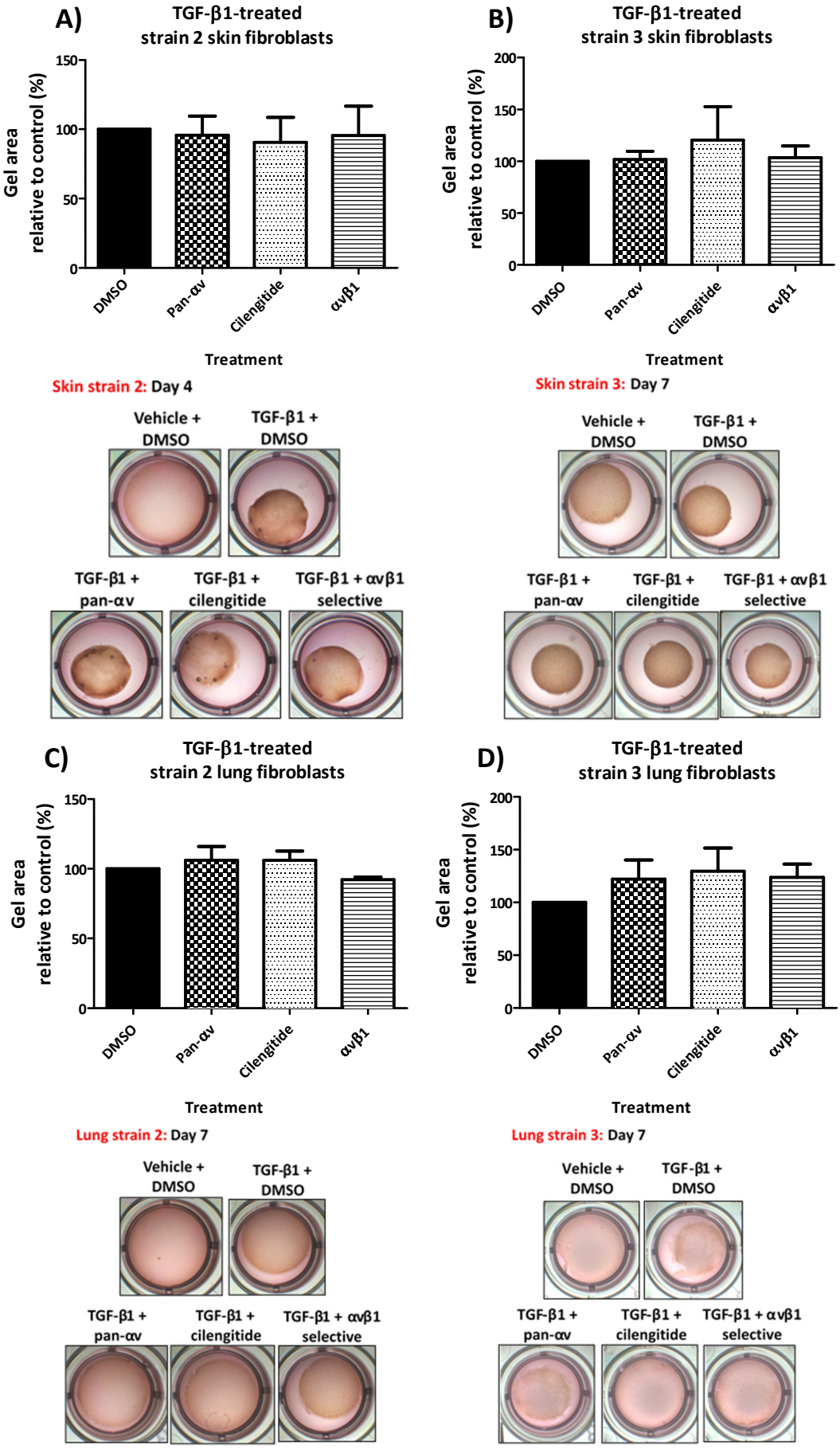
A)
TGF-β1-treated
strain 2 skin fibroblasts
Gel area
relative to control (%)
150
100
50
0
DMSO
Pan-αv
Cilengitide
αvβ1
Treatment
B)
TGF-β1-treated
strain 3 skin fibroblasts
Gel area
relative to control (%)
200
150
100
50
0
DMSO
Pan-αv
Cilengitide
αvβ1
Treatment
Skin strain 2: Day 4
Vehicle +
DMSO
TGF-β1 +
DMSO
TGF-β1 +
pan-αv
TGF-β1 +
cilengitide
TGF-β1 + αvβ1
selective
Skin strain 3: Day 7
Vehicle +
DMSO
TGF-β1 +
DMSO
TGF-β1 +
pan-αv
TGF-β1 +
cilengitide
TGF-β1 + αvβ1
selective
C)
TGF-β1-treated
strain 2 lung fibroblasts
Gel area
relative to control (%)
150
100
50
0
DMSO
Pan-αv
Cilengitide
αvβ1
Treatment
D)
TGF-β1-treated
strain 3 lung fibroblasts
Gel area
relative to control (%)
200
150
100
50
0
DMSO
Pan-αv
Cilengitide
αvβ1
Treatment
Lung strain 2: Day 7
Vehicle +
DMSO
TGF-β1 +
DMSO
TGF-β1 +
pan-αv
TGF-β1 +
cilengitide
TGF-β1 + αvβ1
selective
Lung strain 3: Day 7
Vehicle +
DMSO
TGF-β1 +
DMSO
TGF-β1 +
pan-αv
TGF-β1 +
cilengitide
TGF-β1 + αvβ1
selective

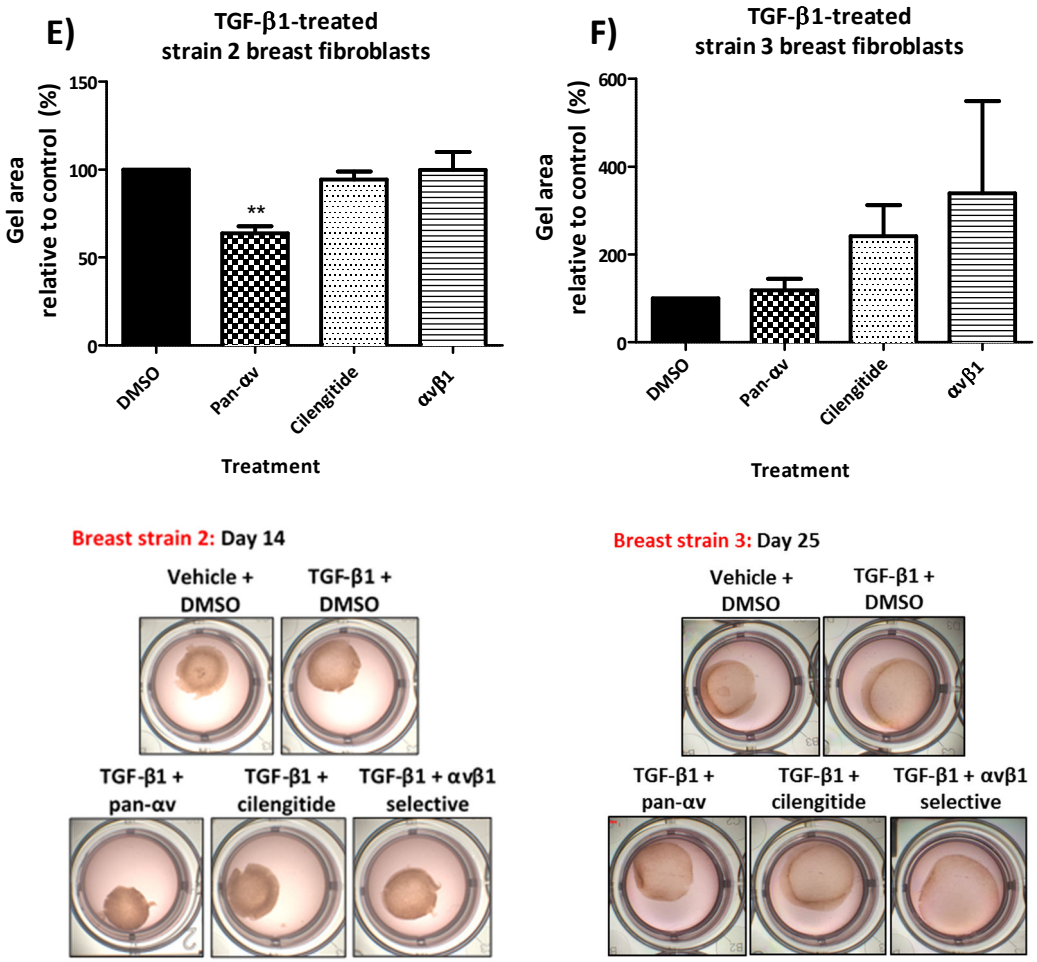

Figure 4. 5. Effect of integrin inhibitors on skin, lung or breast myofibroblast-mediated gel contraction.

Skin (A, B), lung (C, D) and breast (E, F) fibroblasts were pre-treated with TGF-β1 (5ng/ml) for 48 hours and then combined with matched volumes of DMSO (control) or 1μM integrin inhibitors; pan-αv, cilengitide (targeting β3/β5) and αvβ1-selective and plated inside collagen type I gels. TGF-β1 (5ng/ml) was added to gels the following day, which were released from the edge of each well. Graphs show selected days of gel contraction as listed in the images below each graph. **p<0.01 one-way ANOVA with Dunnet's post-hoc. Data shown represents mean ± s.d of three independent experiment with triplicate gels.

4.2.4. Collagen gel contraction after integrin silencing in skin, lung and breast myofibroblasts

As the integrin inhibitors used bind only transiently to the extracellular ligand-binding regions of heterodimers, it's possible not all integrin functional activity was inhibited. Therefore, siRNA was utilised to silence the expression of selected subunits and further understand the role of integrins. Ideally, every integrin subunit should be knocked down and investigated, but to make the range of experiments more feasible only α1, α11, β3 and β5 were targeted in this study. Integrin subunits αv or β1 could not be targeted, as this would affect multiple heterodimers. Collagen-binding subunit α1 was chosen due to evident TGF-β1-induced transcription in skin fibroblasts and high mean fluorescence intensity values during flow cytometry. Although much less is known about α11, published studies suggest it has a role in regulating dermal fibroblast α-SMA expression and contraction [61, 74], therefore α11 exists as a potential therapeutic target. Lastly, TGF-β1-induced β3 and β5 expression was validated at both the gene and protein level, while previous studies have also demonstrated their role in myofibroblast regulation and latent-TGF-β activation *in vitro* [64, 191, 192], though this combination of fibroblasts (skin, lung and breast) has not been examined previously.

Figure 4.6 and 4.7 show α11 and β5 integrin knockdown significantly inhibited skin fibroblast-induced collagen contraction, which was a consistent observation between the two different skin fibroblast strains tested. In strain 2 skin fibroblasts (**Figure 4.6**), α11 silencing produced gels 180% larger than control gels (non-targeting siRNA-treated fibroblasts), even in the presence of TGF-β1 ($p<0.001$). While in skin strain 3 (**Figure 4.7**), β5 integrin subunit knockdown was most effective in reducing gel contraction as gels were on average 130% larger than controls. Note that, qPCR results in **Figure 4.6C** and **4.7C** confirmed the expression of each integrin subunit was effectively silenced.

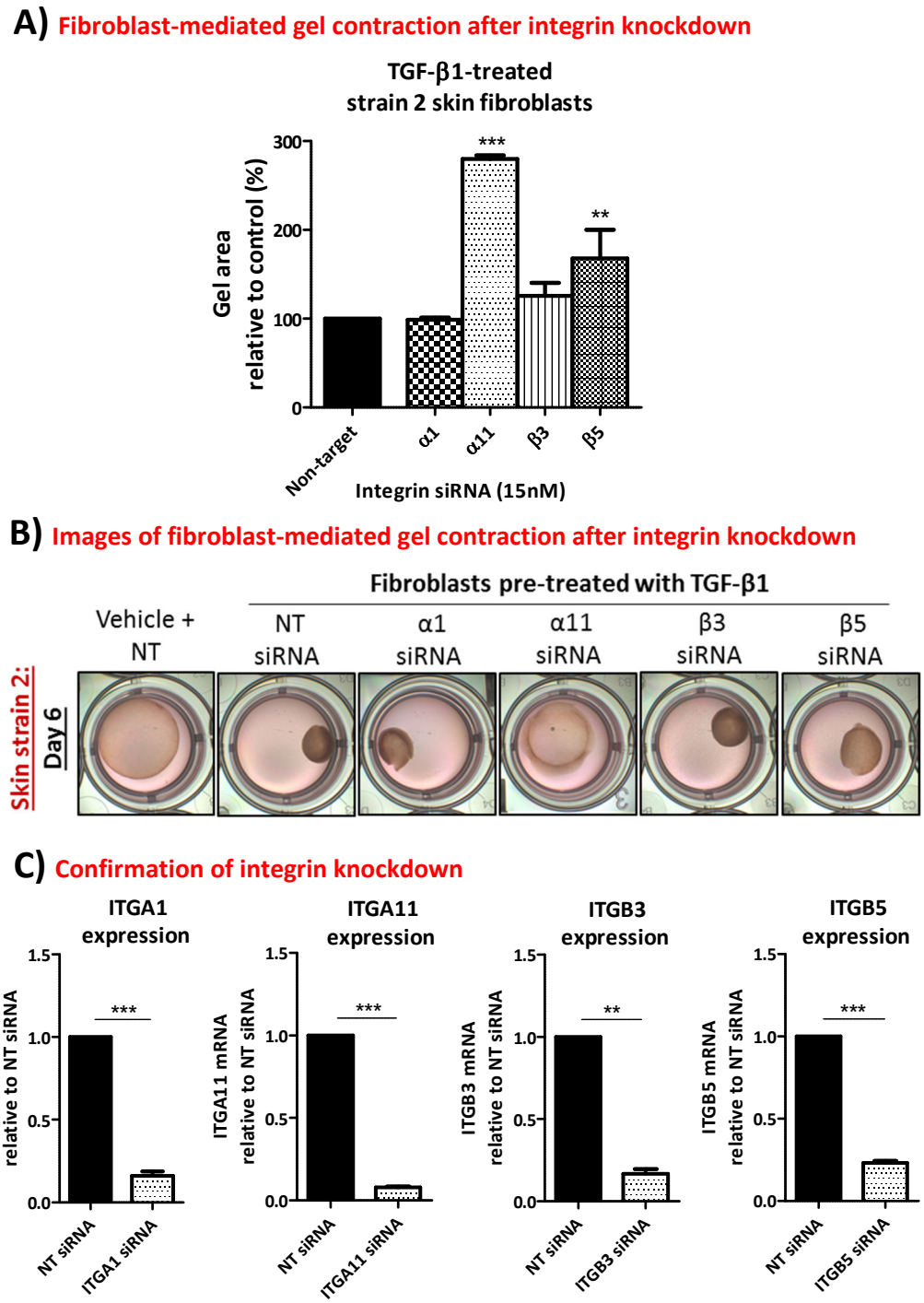

Figure 4. 6. Effect of integrin-targeted siRNA on skin strain 2 myofibroblast-mediated collagen contraction.

Fibroblasts were pre-treated with TGF-β1 (5ng/ml) for 48 hours and then integrin siRNA (15nM) for 72 hours. Fibroblasts were then plated inside collagen gels with RNA collected from the remaining cells. Vehicle or TGF-β1 was added to each gel. A) Graph and images (B) show representative results on day 6. **p<0.01, ***p<0.001 one-way ANOVA with Dunnet's post-hoc to compare each column to NT (non-target siRNA). C) Effective integrin knockdown confirmed using qPCR. **p<0.01, ***p<0.001, paired Student's *t*-test. Data shown represents mean ± s.d of two independent experiments with triplicate gels.

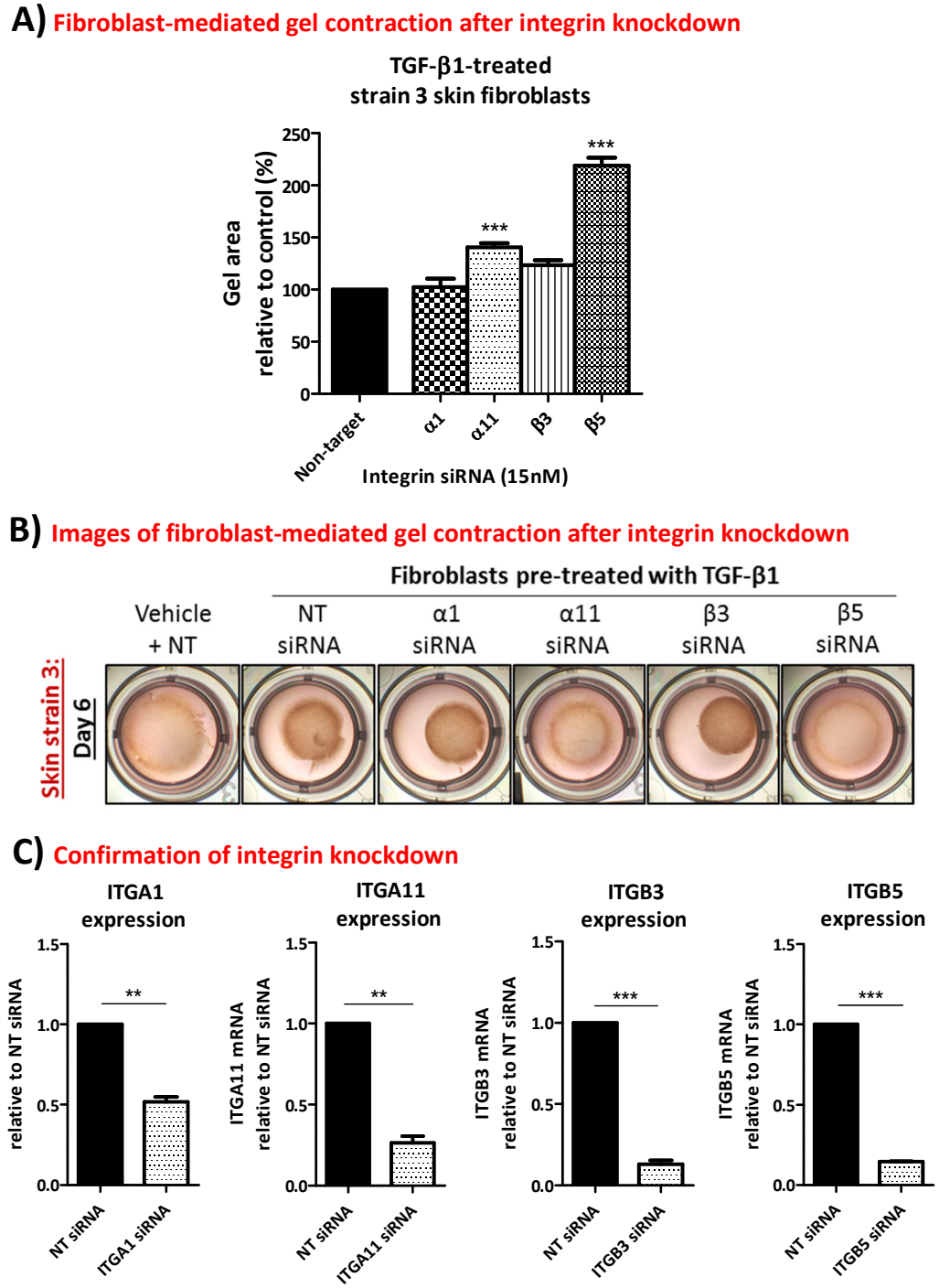

Figure 4. 7. Effect of integrin-targeted siRNA on skin strain 3 myofibroblast-mediated collagen contraction.

Fibroblasts were pre-treated with TGF-β1 (5ng/ml) for 48 hours and then integrin siRNA (15nM) for 72 hours. Fibroblasts were then plated inside collagen gels with RNA collected from the remaining cells. Vehicle or TGF-β1 was added to each gel. A) Graph and images (B) show representative results on day 6. ***p<0.001 one-way ANOVA with Dunnet's post-hoc to compare each column to NT (non-target siRNA). C) Effective integrin knockdown confirmed using qPCR, **p<0.01, ***p<0.001 Students paired *t*-test. Data shown represents mean ± s.d of two independent experiments with triplicate gels.

Figure 4.8 and **4.9** display the results of lung strain 2 and breast strain 3-mediated contraction, respectively. Unfortunately, an additional second strain from lung and breast tissue was not completed. Nevertheless, collagen gels containing lung fibroblasts where α11 or β5 expression was abolished were 50% larger than control gels (non-targeting siRNA) and did not display any contraction by day 8 (**Figure 4.8B**). Although striking, it should be noted this is only a result from one independent experiment and again, integrin knockdown was confirmed using qPCR (**Figure 4.8C**).

Lastly, **Figure 4.9A** demonstrates α1 knockdown had striking effects on breast fibroblasts, as gel contraction was significantly prevented in the presence of TGF-β1, although only 20% ITGA1 gene knockdown was achieved (**Figure 4.9C**). In addition, α11 and β3 knockdown produced similar results as both sets of gels were approximately 33% larger than control gels, while silencing of β5 in breast fibroblasts also significantly reduced contraction and resulted in collagen gels 58% larger than controls on average. **Figure 4.9C** demonstrates at least 50% gene silencing was induced for α11, β3 and β5 subunits, although this needs to be improved in future replicate assays.

Overall, these results suggest different integrins are responsible for mediating collagen contraction in TGF-β1-stimulated skin, lung and breast fibroblasts.

A) Fibroblast-mediated gel contraction after integrin knockdown

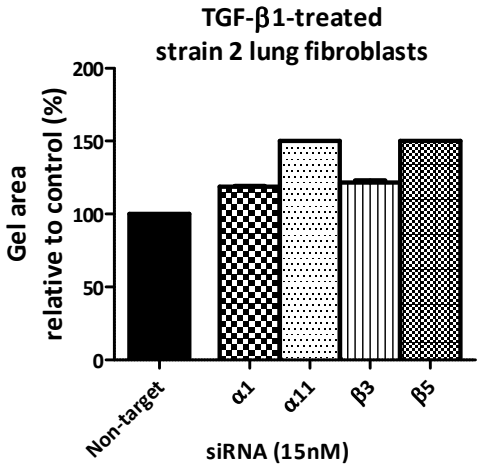

B) Images of fibroblast-mediated gel contraction after integrin knockdown

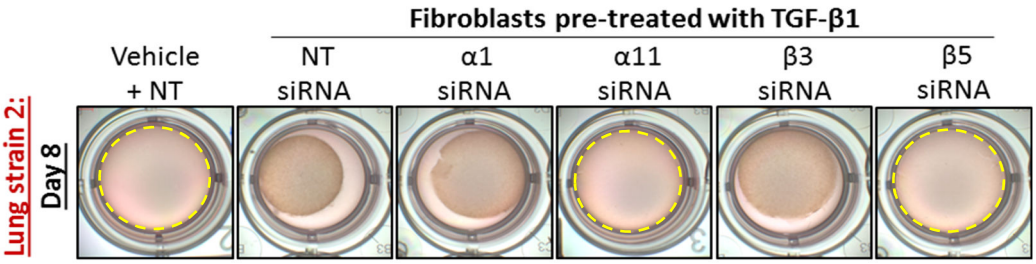

C) Confirmation of integrin knockdown

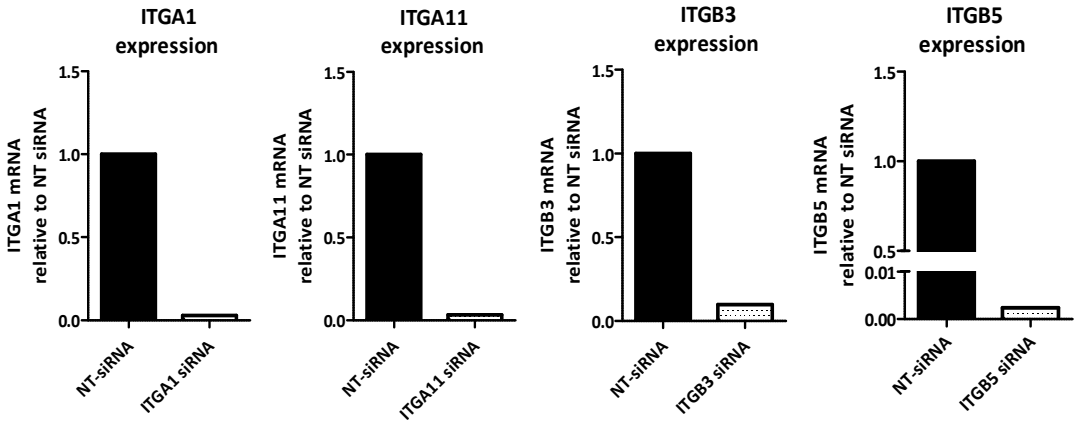

Figure 4. 8. Effect of integrin-targeted siRNA on lung strain 2 myofibroblast-mediated collagen contraction.

Fibroblasts were pre-treated with TGF-β1 (5ng/ml) for 48 hours and then integrin siRNA (15nM) for 72 hours. Fibroblasts were then plated inside collagen gels with RNA collected from the remaining cells. Vehicle or TGF-β1 was added to each gel. A) Graph and images (B) show representative results on day 8 gel contraction. Dashed lines outline non-contracted gels. C) Effective integrin knockdown confirmed using qPCR (NT=non-target siRNA). Data shown represents mean ± s.d of one independent experiment with triplicate gels.

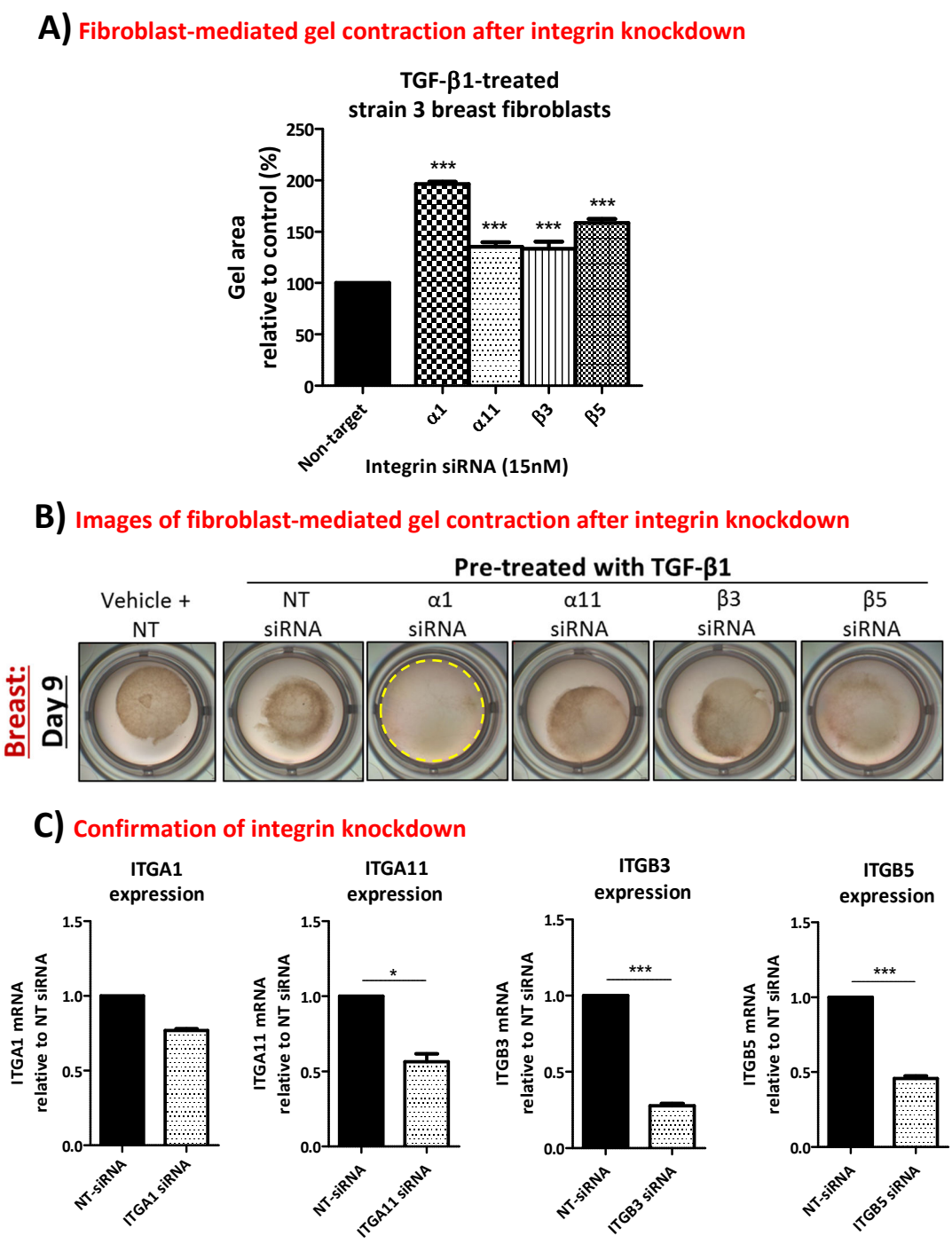

Figure 4. 9. Effect of integrin-targeted siRNA on breast strain 3 myofibroblast-mediated collagen contraction.

Fibroblasts were pre-treated with TGF-β1 (5ng/ml) for 48 hours and then integrin siRNA (15nM) for 72 hours. Fibroblasts were then plated inside collagen gels with RNA collected from the remaining cells. Vehicle or TGF-β1 was added to each gel. A) Graph and images (B) show representative results on day 8. ***p<0.001 one-way ANOVA with Dunnet's post-hoc. Dashed line outlines non-contracted gel. C) Integrin knockdown examined using qPCR (NT = non-target siRNA); *p<0.05, ***p<0.001 Students paired *t*-test. Data shown represents mean ± s.d of three independent experiments with triplicate gels, although α1: *n*=2.

4.2.5. Expression of myofibroblast-associated genes after integrin silencing in skin, lung and breast myofibroblasts

As the previous results demonstrated integrin blockade affects fibroblast invasion and integrin knockdown prevents gel contraction, the expression of ACTA2, FN1, CTGF and SERPINE1 was re-examined after α1, α11, β3 or β5 gene ablation to determine whether integrins also regulate the gene expression of 'markers of fibroblast activation'.

Again, fibroblasts were pre-treated with TGF-β1 (5ng/ml) for 48 hours, washed and then exposed to either non-targeting or integrin-targeted siRNA (15nM) for 72 hours in media without supplemented TGF-β1 and RNA was collected at this point to examine gene expression. **Figure 4.10A** demonstrates that TGF-β1-treated skin strain 2 fibroblasts maintained ACTA2, FN1, CTGF and SERPINE1 expression up to 72 hours after the removal of TGF-β1 and therefore, remained activated. **Figure 4.10B** shows the effects of integrin-targeted siRNA on skin strain 2 genes. Overall, α1, α11, β3 and β5 knockdown significantly decreased the expression of ACTA2, FN1, CTGF and SERPINE1, although to slightly different extents, i.e. α1 knockdown was the most potent, as knockdown reduced the expression of each gene by at least 50%. Surprisingly, silencing of the β3 subunit significantly increased ACTA2 by 1.2-fold.

Figure 4.11 demonstrates similar experiments using strain 3 skin fibroblasts to determine whether the effects are strain- or organ-specific. Again, **Figure 4.11A** confirms the expression of each myofibroblast-associated gene is upheld when TGF-β1 is removed from culture media. However, **Figure 4.11B** indicates integrin regulation is strain-specific as integrin silencing significantly increased myofibroblast-associated genes, particularly CTGF. Although it appears SERPINE1 was significantly lowered after α1, α11, β3 and β5 siRNA is applied to cells, suggesting this gene is regulated by multiple integrins.

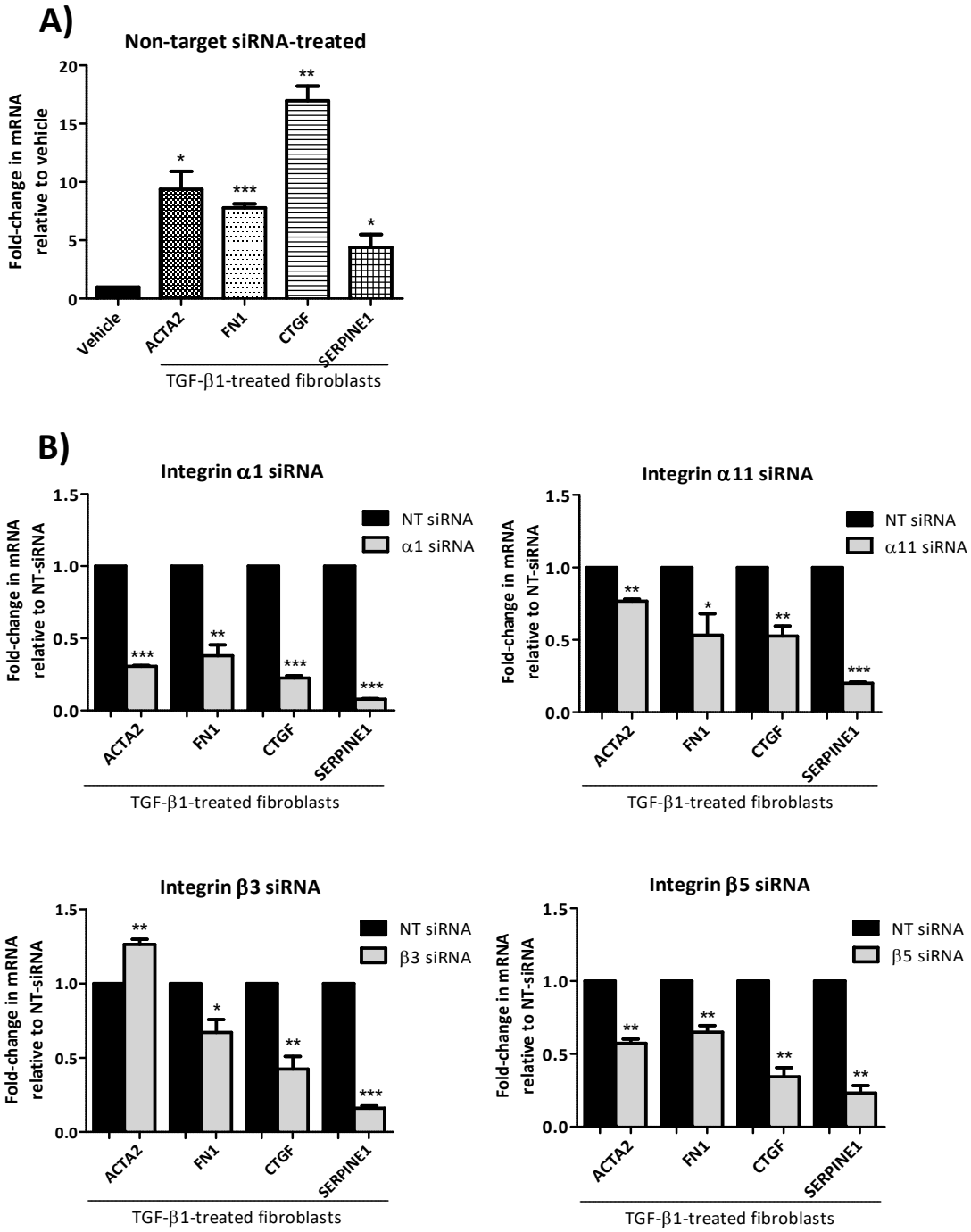

Figure 4. 10. Effect of integrin siRNA on skin strain 2 myofibroblast genes.

Fibroblasts were pre-treated with vehicle or TGF-β1 (5ng/ml) for 48 hours and then non-target (NT) or integrin siRNA (15nM) for 72 hours. Integrin knockdown was confirmed, as shown in **Figure 4.6C**. A) TGF-β1-induced expression of selected genes relative to vehicle-treated fibroblasts, exposed to NT siRNA. B) The expression of selected genes in integrin siRNA-treated cells relative to non-targeting-siRNA. *p<0.05, **p<0.01, ***p<0.001, paired Student's *t*-test. Data shown represents mean ± s.d of two independent experiments with triplicate samples.

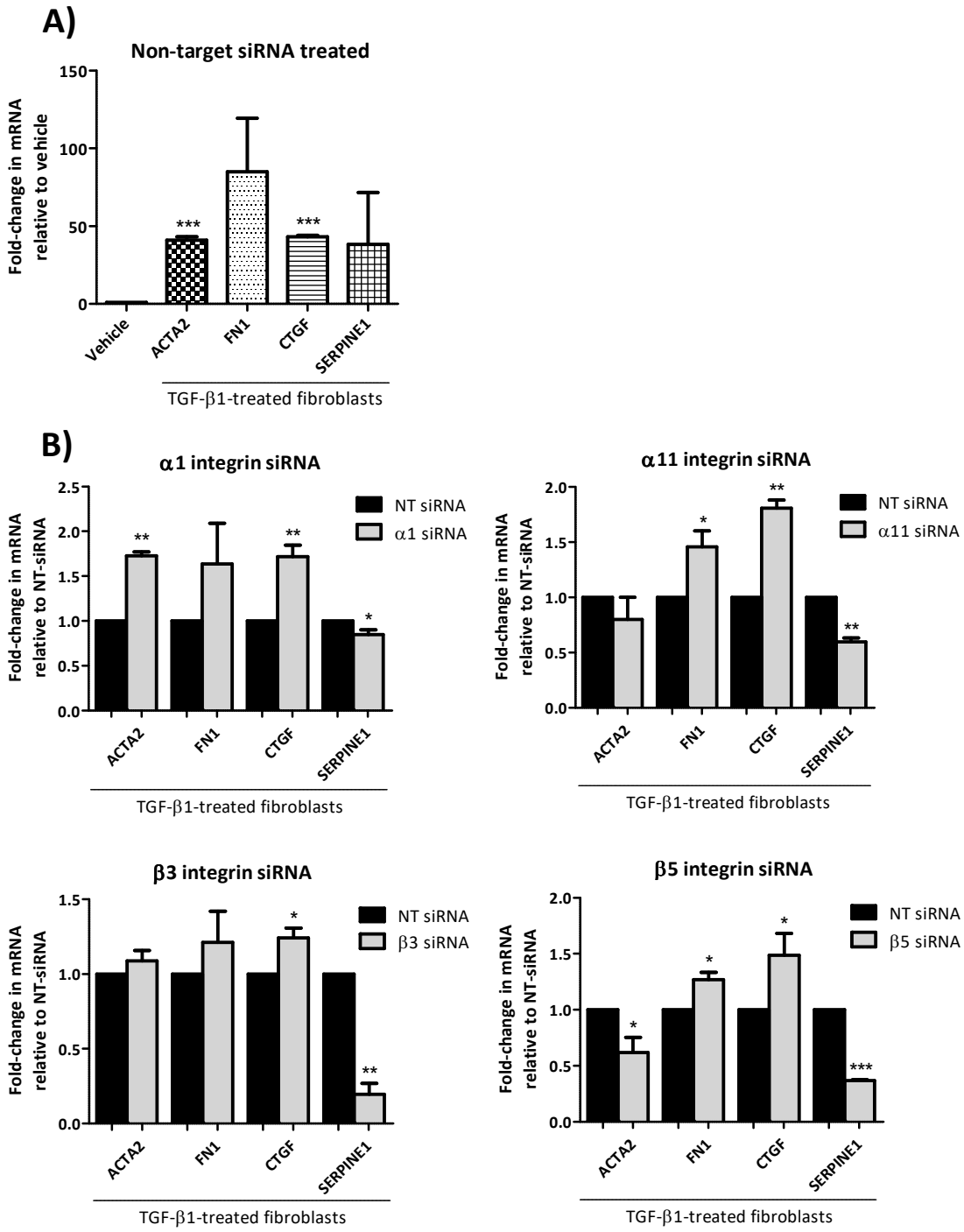

Figure 4. 11. Effect of integrin siRNA on skin strain 3 myofibroblast genes.

Fibroblasts were pre-treated with vehicle or TGF-β1 (5ng/ml) for 48 hours and then non-target (NT) or integrin siRNA (15nM) for 72 hours without TGF-β1. Integrin knockdown was confirmed, as shown in **Figure 4.7C**. A) TGF-β1-induced expression of selected genes relative to vehicle-treated fibroblasts, exposed to NT siRNA. B) The expression of selected genes in integrin siRNA-treated cells relative to non-targeting-siRNA. *p<0.05, **p<0.01, ***p<0.001, paired Student's *t*-test. Data shown represents mean ± s.d of two independent experiments with triplicate samples.

Figure 4.12A and **4.13A** shows both lung fibroblast strains continued to express significantly high mRNA levels of ACTA2, FN1, CTGF and SERPINE1 after pre-treatment with TGF-β1. **Figure 4.12B** displays differential effects of integrin knockdown on lung strain 2 fibroblasts, as α1 significantly downregulated the expression of each of the four genes, conversely α11, β3 and β5 knockdown significantly increased fibronectin expression. Furthermore, as previously noted in skin fibroblasts, knockdown of α1, α11 and β3 in lung fibroblasts also significantly reduced SERPINE1 expression.

Figure 4.13B exhibits the effects of integrin silencing on lung strain 3 fibroblasts. Again results appear as strain-specific, as each marker decreased in response to integrin knockdown, contrary to lung strain 2 fibroblasts. In addition, β3 and β5 targeting was particularly effective, as ACTA2, FN1, CTGF and SERPINE1 were all reduced more than 50% relative to genes expressed by non-targeting siRNA-treated fibroblasts. However, it should be noted that these results represent one independent experiment.

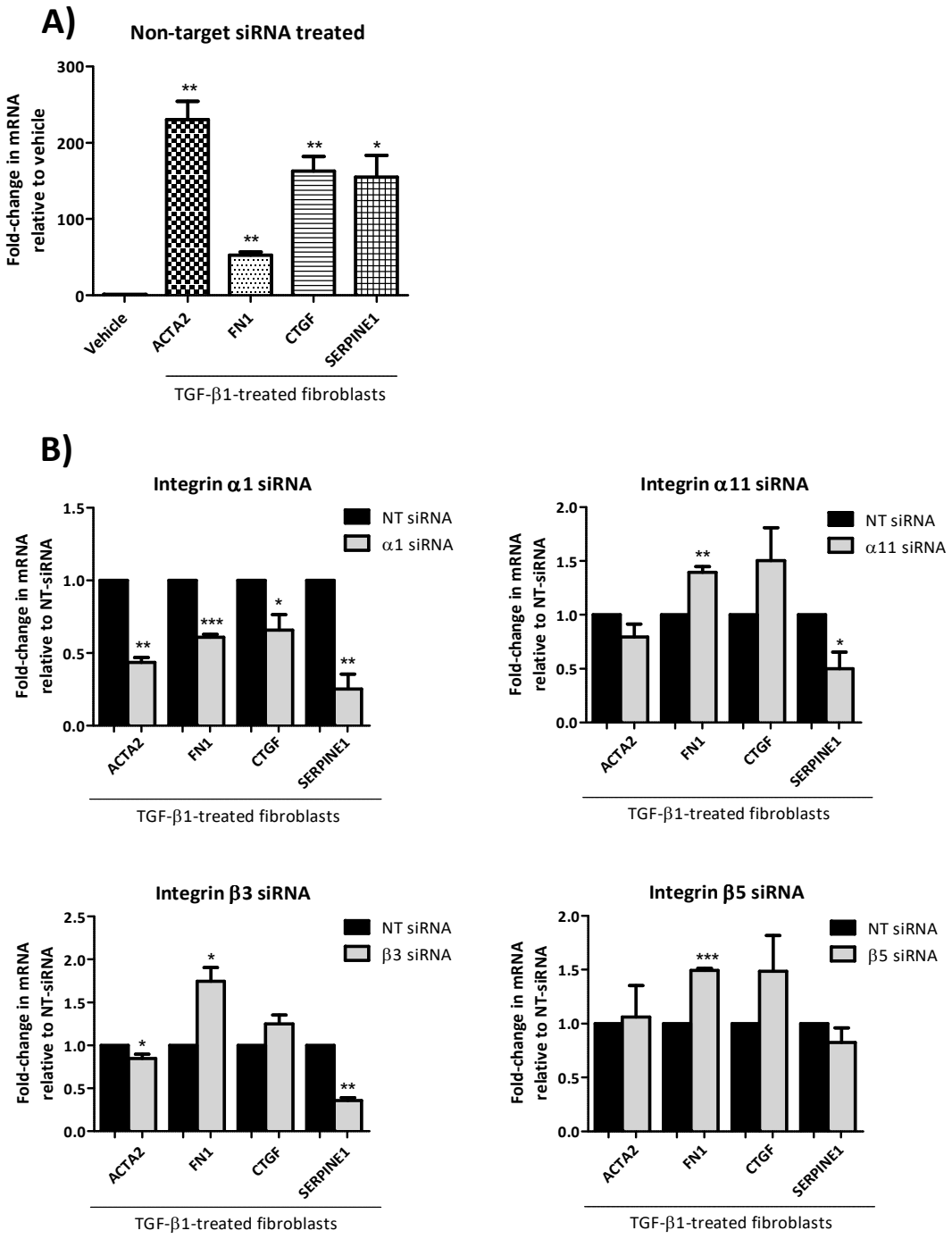

Figure 4. 12. Effect of integrin siRNA on lung strain 2 myofibroblast genes.

Fibroblasts were pre-treated with vehicle or TGF-β1 (5ng/ml) for 48 hours and then non-target (NT) or integrin siRNA (15nM) for 72 hours without TGF-β1. Integrin knockdown was confirmed, as shown in **Figure 4.8C**. A) TGF-β1-induced expression of selected genes relative to vehicle-treated fibroblasts, exposed to NT siRNA. B) The expression of selected genes in integrin siRNA-treated cells relative to non-targeting-siRNA. *p<0.05, **p<0.01, ***p<0.001, paired Student's *t*-test. Data shown represents mean ± s.d of two independent experiments with triplicate samples.

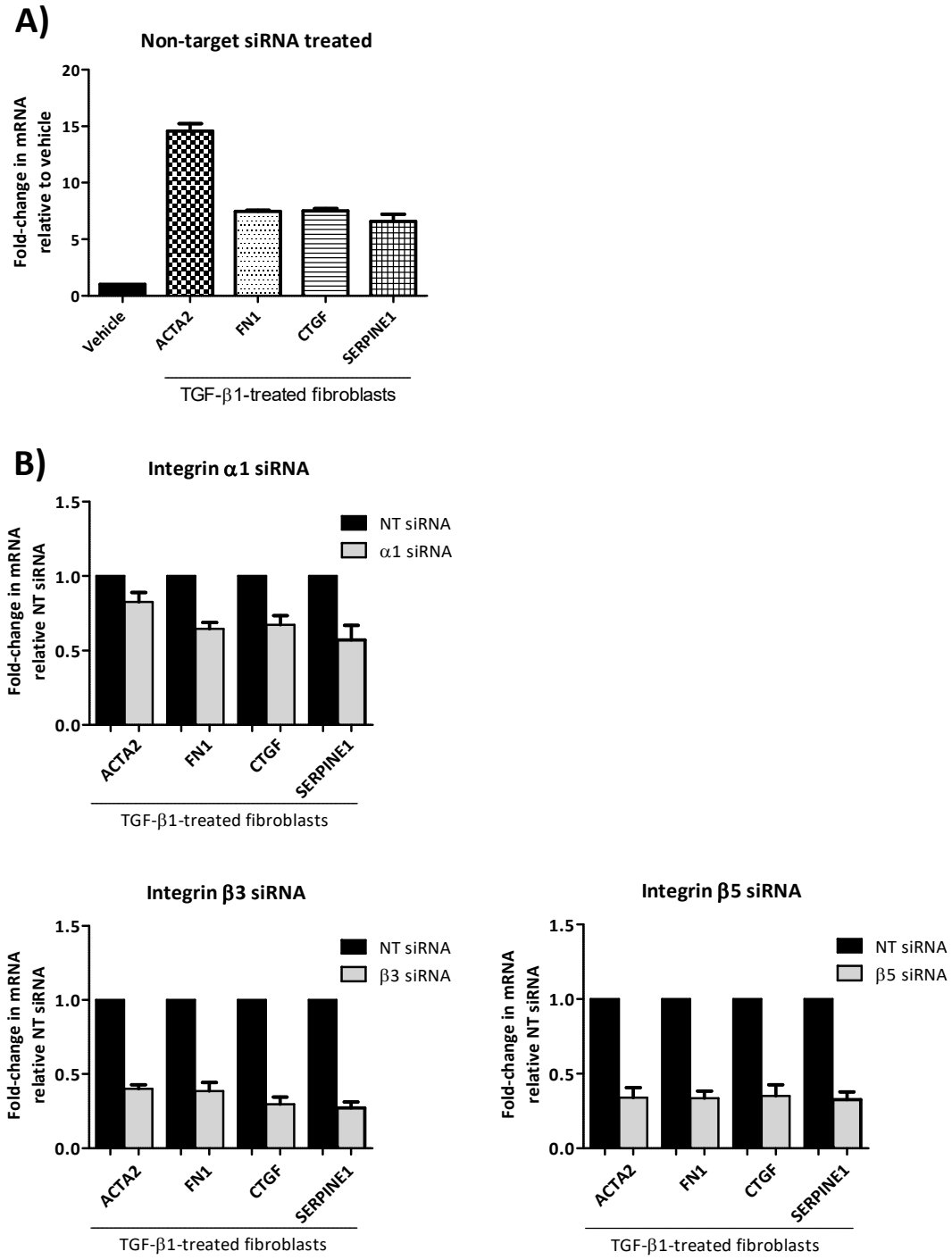

Figure 4. 13. Effect of integrin siRNA on lung strain 3 myofibroblast genes.

Fibroblasts were pre-treated with vehicle or TGF-β1 (5ng/ml) for 48 hours and then non-target (NT) or integrin siRNA (15nM) for 72 hours without TGF-β1. Integrin knockdown was confirmed, as shown in **Appendix Figure 19**. A) TGF-β1-induced expression of selected genes relative to vehicle-treated fibroblasts, exposed to NT siRNA. B) The expression of selected genes in integrin siRNA-treated cells relative to non-targeting-siRNA. Data shown represents mean ± s.d of one experiment with triplicate samples.

Next, the effect of integrin knockdown was examined using 2 strains of breast fibroblasts.

Figure 4.14 displays breast fibroblasts strain 2, where unfortunately silencing of only β3 and β5 was sufficient (**Figure 4.14B**), though this should be improved in future repeats as integrin expression was only reduced by 30-40%. Regardless, this was enough to impact the expression of myofibroblast genes, all four of which were evidently lowered in response to β3 or β5 knockdown (**Figure 4.14C**), with ACTA2 and SERPINE1 decreased the most relative to non-target treated fibroblasts.

Lastly, in **Figure 4.15** similar results were achieved using breast strain 3 fibroblasts, whereby α1, α11, β3 and β5 silencing markedly downregulated the expression of these myofibroblast-associated genes. Moreover, these results support the findings from breast strain 2, as ACTA2 and SERPINE1 are notably lower when comparing all four genes. Again, it should be noted both these strains each represent one independent experiment.

Overall, these experiments demonstrate that integrins modulate TGF-β1-induced fibroblast activation and activity, as measured by invasion, collagen contraction and 'activation marker' gene expression. In addition, integrin-regulated functions such as invasion and contraction appear to be tissue-specific, although there is variation between strains derived from different people. Furthermore, it is evident that α1, α11, β3 and β5 integrins regulate the TGF-β1-induced expression of SERPINE1 regardless of which organ fibroblasts are derived from.

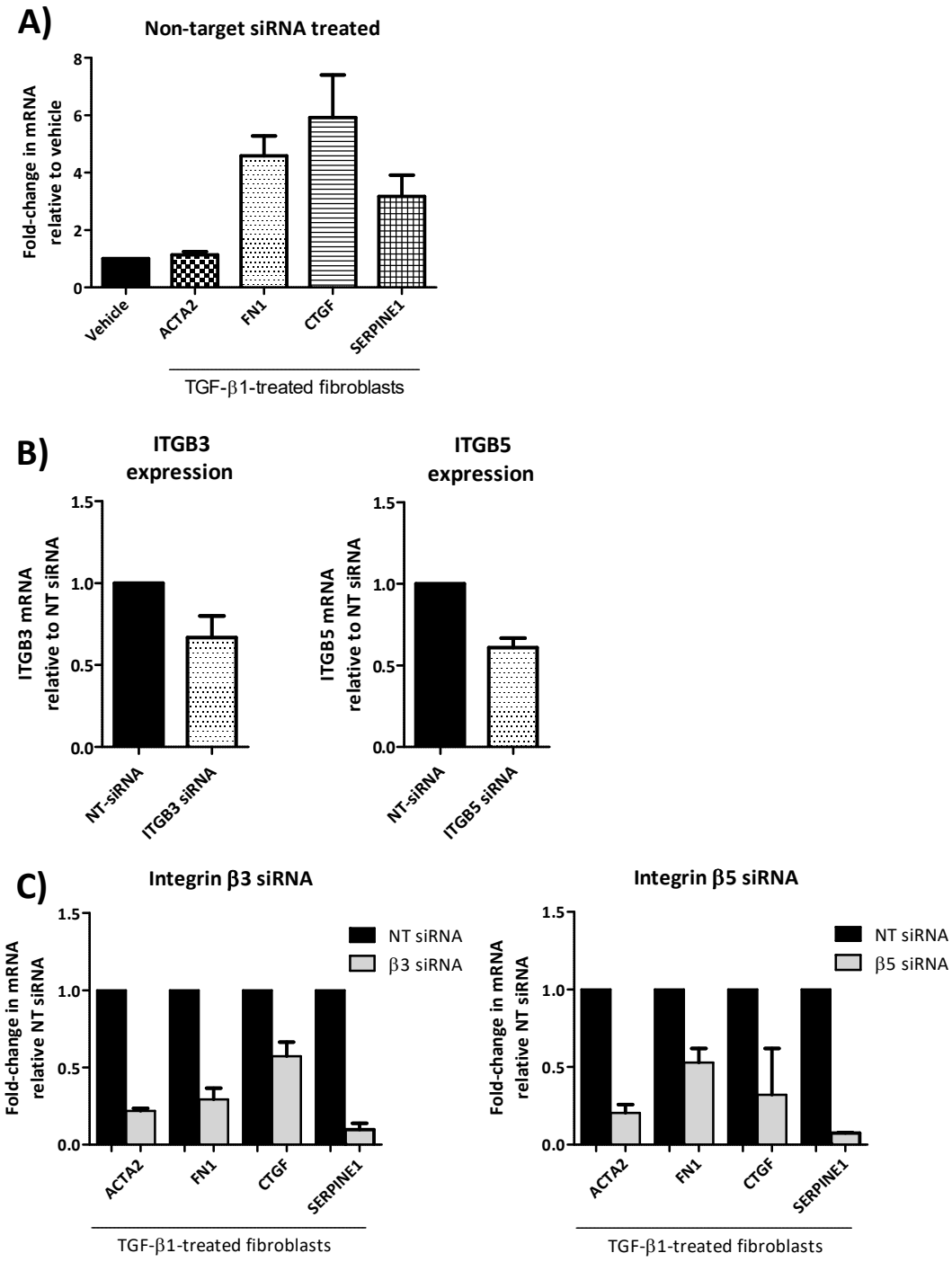

Figure 4. 14. Effect of integrin β3 and β5 siRNA on breast strain 2 myofibroblast genes.

Fibroblasts were pre-treated with vehicle or TGF-β1 (5ng/ml) for 48 hours and then non-target (NT) or integrin siRNA (15nM) for 72 hours without TGF-β1. A) TGF-β1-induced expression of selected genes relative to vehicle-treated fibroblasts, exposed to NT siRNA. B) Partial β3 and β5 integrin knockdown was confirmed. C) The expression of selected genes in integrin siRNA-treated cells relative to non-targeting-siRNA. Data shown represents mean ± s.d of one experiment with triplicate samples.

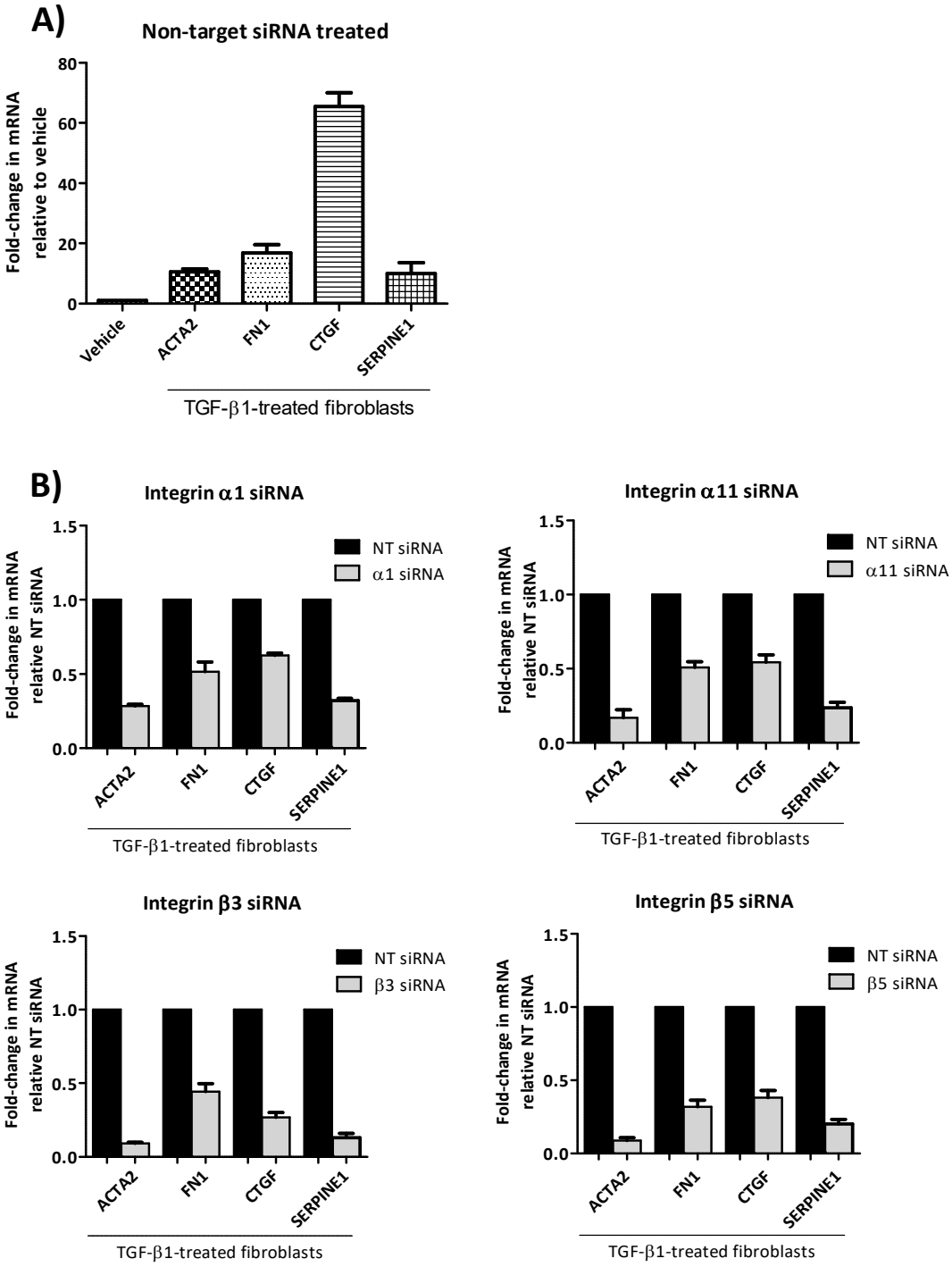

Figure 4. 15. Effect of integrin siRNA on breast strain 3 myofibroblast genes.

Fibroblasts were pre-treated with vehicle or TGF-β1 (5ng/ml) for 48 hours and then non-target (NT) or integrin siRNA (15nM) for 72 hours without TGF-β1. Integrin knockdown was confirmed, as shown in **Figure 4.9C**. A) TGF-β1-induced expression of selected genes relative to vehicle-treated fibroblasts, exposed to NT siRNA. B) The expression of selected genes in integrin siRNA-treated cells relative to non-targeting-siRNA. Data shown represents mean ± s.d of one experiment with triplicate samples.

4.3. Discussion

Previous studies have demonstrated that there is increased integrin expression during fibroblast-myofibroblast differentiation[191] and have identified various roles that particular integrins play during typical fibroblast functions, such as adhesion, contraction and migration. In addition, the presence of α-SMA-positive myofibroblasts correlates with a poor prognosis in various cancers, such as breast[92] and oral squamous cell carcinomas[94], while *in vitro* studies also suggest that αvβ3 and αvβ5 integrins expressed by fibroblasts regulate α-SMA expression and contraction[64]. More recently, *in vivo* studies demonstrate the targeting of αv-containing integrins expressed by lung and liver fibroblastic cells reduces organ fibrosis in mice[130]. Therefore, this study here in hypothesised that integrins are capable of regulating myofibroblast functions, such as contraction and invasion, in tissues which have not been compared previously. Furthermore, the integrins examined in this study were chosen by monitoring fibroblast activation and have also not been previously investigated simultaneously. Using small-molecule integrin inhibitors and integrin-targeted siRNA, I have shown that αv-containing integrins regulate myofibroblast invasion and α1, α11, β3 and β5 modulate TGF-β1 induced collagen gel contraction, as well as the expression of 'markers' of fibroblast activation. Moreover, the targeting of integrins in this study also identified organ- and strain-specific responses.

4.3.1. The effect of integrin small-molecule inhibitors on regulating the invasion of skin, lung and breast myofibroblasts

Firstly, fibroblasts pre-treated with TGF-β1 demonstrated strain-specific responses when plated in Matrigel-coated Transwells, as only the invasion of skin myofibroblast strain 2 and lung strain 3 was significantly enhanced when compared to fibroblasts pre-treated with vehicle, while the invasion of additional skin, lung and breast myofibroblast strains were unaffected by TGF-β1 (**Figure 4.3**). Previous studies have reported TGF-β1 did not affect the migration of renal fibroblasts on collagen, but increased adhesion[193]. In addition, Denys and colleagues found that TGF-β1 increased stress fibre formation in immortalised dermal fibroblasts, but significantly reduced invasion, which was associated with low Rac1 expression, known to

positively regulate cell invasion[68]. Overall, these findings suggest TGF-β1 does not support fibroblast invasion.

Organ-specific functions were apparent using integrin small-molecule inhibitors, whereby skin fibroblast invasion was significantly impaired by cilengitide and an αvβ1-selective compound. Encouragingly, these effects were validated in two strains of skin fibroblasts, which were derived from separate donors. The specificity and efficacy of this αvβ1 compound was first published in 2015 by Reed and colleagues, who demonstrated that αvβ1 blockade reduced liver and lung fibrosis *in vivo*, as αvβ1 has a key role in activating TGF-β by binding to its latency-associated peptide[38]. However, the study of αvβ1 biology had been previously hampered due to the lack of specific suitable reagents to identify this heterodimer; thus no heterodimer-specific antibodies exist, and as both αv and β1 partner with many other subunits, antibodies to either subunit cannot be used to specifically identify αvβ1. Therefore, the authors acknowledged that unidentified functions of αvβ1 may still exist[38].

αvβ1 expression has previously been linked to tumour cell migration and invasion. Before use of this small-molecule inhibitor, αvβ1 expression was manipulated by intracellular antibody blockade of the αv subunit, as it was hypothesised that αvβ1 is formed in the presence of an excess of both αv and β1 subunits. After confirming knockdown of αvβ1 by immunoprecipitating αv and then blotting for subunits including β1, Koistinen and Heino found that αvβ1 mediates the migration of melanoma cells on fibronectin coated wells[194]. More recently, fibroblast-specific deletion of β1 integrin in conditional-knockout mice displayed delayed wound closure and less α-SMA-positive myofibroblasts. Furthermore, explant growth of dermal fibroblasts from knockout mice showed reduced adhesion to fibronectin, migration and activation of latent-TGF-β1, although it was not confirmed whether the heterodimer mediating these effects was αvβ1[195]. In addition, Hu and colleagues showed that αvβ1 regulates glioma cell invasion *in vitro* by enhancing MMP-2 expression after activating the FAK-ERK1/2 pathway[196]. Aside from this, it is clear that further research into the role of αvβ1 in fibroblasts is much needed and this new αvβ1-selective inhibitor, makes this now possible.

It is possible that skin fibroblasts express distinct amounts of αvβ1 and aside from TGF-β activation, utilise this integrin to regulate unknown mechanisms relevant during fibroblast invasion, such as protease expression. In contrast, lung and breast fibroblast invasion was unaffected by αvβ1 blockade, suggesting redundancy of this integrin in these cells. However, only one concentration was tested in these assays (1μM), therefore perhaps multiple lower concentrations should be tested to examine dose-response effects, as Reed and colleagues reported, as little as 1nM was sufficient to prevent αvβ1 binding to LAP *in vitro* [38].

The use of cilengitide also produced differential effects during invasion through Matrigel-coated Transwells, as skin fibroblast invasion was significantly prevented while lung and breast fibroblast invasion was enhanced, again a phenomenon observed in two strains per tissue derived from different donors. The effect on skin fibroblasts is supported by Fu and colleagues, who also discovered that cilengitide inhibited the migration of dermal fibroblasts on fibrinogen matrices. After addition of cilengitide they also found that fibroblasts exhibited significantly lower α-SMA and phospho-Smad3 protein, suggesting integrin inhibition directly interfered with TGF-β signalling, although the mechanism of interaction was not investigated. The authors proposed that binding of fibrinogen to αvβ3 integrin may have triggered clustering with TGF-β receptors on the cell surface, enhancing the activation of TGF-β1-induced Smad signalling. Therefore, binding of cilengitide may have obstructed αvβ3-ligand binding, reducing clustering and signal transduction[188]. Moreover, previous reports suggested the expression of protease MMP-9 is partially Smad3-dependent[189], which is important for fibroblast invasion[197]. Alternatively, cilengitide may prevent latent-TGF-β activation. Sarrazy and colleagues discovered the use of cilengitide (1μM) on cardiac fibroblasts prevented contraction-mediated activation of latent-TGF-β1 and subsequent α-SMA expression *in vitro*[125], with similar findings using cilengitide on intestinal smooth muscle cells[198]. As a reminder, TGF-β1 was not supplemented during my own invasion assays. Skin, lung and breast fibroblasts were pre-treated with TGF-β1 and then plated on top of Transwells in media without TGF-β1, although the cytokine was present in its latent form in the Matrigel coating of the Transwells and perhaps in the serum below. It is

also possible that latent TGF-β1 was secreted by skin fibroblasts, which required activation via β3 or β5 integrins.

The tissue-specific responses and increased invasion by lung and breast fibroblasts in response to cilengitide cannot be explained by differing levels of integrins, as breast strain 3 fibroblasts exhibited higher amounts of αv and β5 subunits than skin or lung, although β1 levels were not characterised and cilengitide also inhibits αvβ1, albeit weakly[199]. Lung and breast fibroblasts may over-compensate for integrin blockade by raising the expression of other integrins and integrin-associated proteases. Sarrazy and colleagues found the overexpression of β3 integrins in cardiac fibroblasts *in vitro* significantly reduced the expression of β5 and *vice versa*. Conversely, short hairpin RNA-mediated silencing of either subunit also increased expression of the other subunit[125]. It would be interesting to determine whether cilengitide has similar effects on other integrin subunits, particularly in lung and breast fibroblasts. Furthermore, Caswell and colleagues reported that administration of 1μM cilengitide promoted migration of ovarian tumour cells into Matrigel by promoting α5β1 recycling and the formation of pseudopod extensions[200], while a similar mechanism of α5β1 internalisation was also necessary to promote the migration of a human foreskin fibroblast cell line on fibronectin[201]. These studies provide a potential mechanism by which cilengitide could promote fibroblast invasion.

It appears my data adds to the previously reported differential effects of cilengitide and further experiments using cilengitide on skin, lung and breast fibroblasts would likely reveal more on the diverse mechanisms of αvβ3 and αvβ5 integrins utilised during invasion. In the wider context, cilengitide previously reached phase III clinical trials for glioblastoma and randomized controlled Phase II studies for non-small-cell lung cancer and squamous cell carcinoma of the head and neck, although proved unsuccessful[202]. Consequently, determining the mechanism of action of cilengitide on stromal cells growing in the tumour microenvironment would also guide the therapeutic efficacy of this compound.

Lastly, due to lack of time, the effect of integrin silencing during fibroblast invasion was not investigated. Future completion of these experiments may validate the

findings from using integrin inhibitors and the use of 3D organotypic invasion assays would assess repercussions on tumour cell growth and invasion when the expression of particular integrins in fibroblasts are abolished using siRNA.

4.3.2. The role of integrins in regulating TGF-β1-induced skin, lung and breast fibroblast gel contraction

The ability of adult fibroblasts to contract the ECM is a central role during wound healing to induce closure of injured tissues. However, in more pathogenic settings such as the tumour microenvironment, activated fibroblasts secrete collagens, collagen cross-linking proteins and contract the matrix, stiffening the area immediately surrounding tumours, resulting in the promotion of tumour growth via stiffness-induced signalling[203]. Furthermore, fibrosis itself is enough to compromise the normal function of organs[204]. Therefore, reducing the capacity of fibroblasts to contract and stiffen tissue is an important therapeutic goal.

In this study, siRNA-mediated knockdown of α11 and β5 subunits impaired collagen contraction by the skin and lung fibroblast strains tested, suggesting these integrins are key regulators of contractile activity in these fibroblasts. These results are supported by Barczyk and colleagues, who demonstrated α11 knockdown in periodontal ligament fibroblasts reduced gel contraction by 20-30% after 8 days[74]. Moreover, in 2015, Navab and colleagues used α11-knockout mice to show stromal α11β1 integrin mediated the reorganisation of collagen fibres in tumour xenografts, where measurements of tissue stiffness were lower in α11-knockout mice compared to wild-type. Furthermore, knockout of stromal-localised α11 in these mouse models also significantly reduced tumour growth and the metastatic potential of lung cancer cells, suggesting α11β1-mediated tissue stiffness may contribute to tumorigenicity and metastasis[205]. In support of the findings generated by β5 knockdown, administration of integrin-neutralising antibody, P1F6 (αvβ5) to dermal and oral mucosal fibroblasts inhibited contraction, as gels were 100% larger than TGF-β-treated control gels[64]. It may be worth noting that siRNA to α11 was particularly effective in regulating strain 2 foreskin fibroblasts derived from a young donor, whereas siRNA to β5 displayed a more prominent role during gel contraction

mediated by adult dermal fibroblasts. It would be interesting to determine whether these effects are dependent on the age of donors.

As a reminder, integrin inhibitors (pan-αv, cilengitide and αvβ1-selective compounds) did not affect gel contraction overall. In this study, active TGF-β1 was supplemented at the beginning of gel contraction assays, therefore if the mechanism of integrin inhibitors is to prevent latent TGF-β1 activation, this function becomes redundant in the presence of active TGF-β1. Furthermore, it is likely that small-molecule inhibitors that bind to the extracellular ligand-binding region of integrins may not interfere with the ability of integrins to activate intracellular signalling pathways and proteins involved in contraction. In contrast, although integrin knockdown was not validated at the protein level, qPCR results confirmed silencing at least at the mRNA level, suggesting that siRNA may have also impacted integrin expression at the plasma membrane, preventing activation of integrin signalling pathways. This is supported by findings here that siRNA-mediated knockdown of integrins also modified the expression of TGF-β-responsive genes, such as ACTA2, which is partially responsible for the level of contractile activity exhibited by myofibroblasts[175]. Of course, the effect of integrin inhibitors on ACTA2 expression should also be investigated to validate this. If time permitted, the effect of antibody-mediated blockade of integrins during collagen contraction would have also been investigated, as previous studies have demonstrated this prevented fibroblast-induced contraction[64]. In addition, perhaps proteomic analysis of fibroblasts after integrin silencing would identify the regulation of other proteins that may contribute to contraction.

Furthermore, integrins are also known to form complexes with growth factor receptors on the cell surface, which couples their intracellular signalling pathways. For example, proximity ligation assays identified β1 integrin interaction with VEGF receptor-2 on the surface of endothelial cells, which was necessary for downstream VEGF signalling[206]. In addition, β1 integrin is known to associate with EGFR in breast cancer cells, which together activates FAK and the MAPK pathway and when either of these transmembrane components were neutralised with specific antibodies, the expression of both proteins decreased[207]. More importantly, Asano and colleagues found that β5 subunits are associated with TGF-β receptor I and

receptor II proteins in clathrin-coated membranes in dermal fibroblasts, potentially establishing an autocrine signalling network[191]. Therefore, perhaps the addition of siRNA in this study removed integrins from potential complexes involving growth factor receptors, which small-molecule integrin inhibitors did not affect, thereby permitting lateral integrin interactions and allowing fibroblasts to contract gels as usual.

My results support the concept that integrins expressed by myofibroblasts regulate collagen contraction; one potential mechanism is by perhaps mediating TGF-β1-activated non-canonical signalling pathways. Though some previous studies suggest canonical Smad3[208] and Smad7[209] signalling regulate fibroblast-mediated contraction, recent studies show non-canonical proteins, such as Jun N-terminal kinase mediate α11 integrin-induced collagen remodelling[210]. In future studies, the expression and activity of proteins involved in typical signalling pathways, such as Smads, FAK, integrin-linked kinase, ERK1/2 and p38 MAPK should be characterised after integrin knockdown in the presence of TGF-β1 to investigate this hypothesis.

Tissue-specific effects were also observed during gel contraction experiments, particularly with the effect of silencing α1. α1β1 integrin is a collagen receptor and significantly prevented gel contraction in breast fibroblasts alone. Furthermore, as noted in Results Part I, the expression of an alternative collagen receptor subunit, α11 integrin, is significantly increased in skin and lung after TGF-β1 treatment but not in breast fibroblasts, perhaps indicating skin and lung fibroblasts rely on α11β1 for collagen remodelling, while breast fibroblasts principally utilise α1β1. The key role of α11 in dermal fibroblasts has been reported by Schulz and colleagues, who compared the effects of collagen receptor subunits α2 and α11 by silencing either subunit or both in knockout mice during wound healing, and found only α11 was responsible for impairing wound closure, suggesting this is the predominant collagen receptor regulating the function of dermal fibroblasts, although they did not compare α1 integrin function[210].

The impact of integrin knockdown on the expression of other integrins in the same cell is unknown. Other studies identify compensatory increases in integrins, such as

silencing of β1 integrin in dermal fibroblasts upregulated β3 protein[195], therefore the expression of other integrins, such as α2β1, which is also known to contribute to collagen gel contraction should be characterised in each fibroblast after knockdown as this may explain the observed phenotypes[211]. In addition, while I did not notice significant changes in cell morphology in response to siRNA treatment when fibroblasts were adhered to collagen, measurement of fibroblast cell viability, adhesion, proliferation and apoptosis after integrin siRNA treatment would rule out these factors as influencing gel contraction.

4.3.3. The role of integrins in regulating TGF-β1-induced skin, lung and breast myofibroblast gene expression

My study also confirmed integrins can modulate the expression of myofibroblast gene markers during TGF-β1 treatment of fibroblasts. However, intra-strain variation meant the two skin and lung fibroblast strains examined displayed differential responses, though these experiments need to be repeated to reach three independent experiments per strain. Nevertheless, the qPCR results clearly indicate that integrins potently regulated SERPINE1 regardless of tissue type, as its expression was reduced by at least 80% in some fibroblasts. PAI-1 is an indirect protease inhibitor by preventing function of the enzyme 'plasminogen activator', which converts plasminogen to protease plasmin, hence the expression of PAI-1 results in reduced breakdown of ECM proteins, enhancing fibrosis. PAI-1 expression is also a common measure in TGF-β1 signalling assays[35] and previous studies have linked PAI-1 activity to regulating the expression of αvβ3 in corneal[212] and cardiac fibroblasts[213]. Previously, Pedroja and colleagues had shown that PAI-1 binding to its receptor promoted the internalisation of αvβ3[214] and this study has shown β3 regulates PAI-1 expression, suggesting the presence of a regulatory feedback loop. Furthermore, this study provides evidence that αvβ3 is not the only integrin to regulate PAI-1 expression, but α1, α11 and β5 each contribute to regulating disease-promoting genes, including PAI-1. Again, mini-organotypic assays and fibroblast-tumour cell co-culture experiments would demonstrate the knock-on effects on tumour cells, when expression of these and other potentially tumour-promoting genes are minimised.

In summary, my findings indicate integrins modulate myofibroblast invasion in a tissue-specific manner. In addition, integrins α1, α11, β3 and β5 regulated TGF-β1-induced collagen contraction and gene expression, particularly in a strain-specific manner. Integrin α1 appeared to only regulate TGF-β1-induced contraction by breast fibroblasts, however additional repeats and strains need to be tested. Overall, these results indicate particular integrins are potential therapeutic targets to dampen the activation and activity of myofibroblasts in diseased tissues.

CHAPTER V. RESULTS PART III

RNA sequencing of TGF-β1-stimulated human lung fibroblasts

5.1. Background

Previous microarray studies using TGF-β1-treated lung fibroblasts have demonstrated that TGF-β1 can induce the expression of a variety of genes, including those involved in cytoskeletal reorganisation, signalling, matrix formation, cell proliferation and metabolism[168, 169], which facilitated the characterisation of genes that were commonly upregulated in myofibroblasts. The profiling of CAFs has also provided invaluable information that has shown to predict clinical outcomes in breast cancers[215], therefore characterising gene expression in TGF-β1-activated fibroblasts and CAFs has immense prognostic value[85].

In Chapter III (Results Part I), one primary task was to select a manageable subset of eight TGF-β1-induced genes to characterise in skin, lung and breast fibroblasts using qPCR. However, to obtain a broader picture of the genetic response of fibroblasts to TGF-β1 and a better understanding of lung fibroblast biology, RNA sequencing (RNA-seq) was conducted on three normal strains of primary lung fibroblasts (named HLF1, HLF2 and HLF3). To note, the same RNA samples from 24-hour vehicle and TGF-β1-treated lung fibroblasts that were used during the qPCR experiments presented in Results Part I were sent for RNA sequencing. Ideally, RNA-seq would have been performed on TGF-β1-treated skin, lung and breast fibroblasts to compare differentially expressed genes and further identify heterogeneity, however, due to cost, only one tissue type could be selected. Lung fibroblasts were utilised due to the availability of remaining RNA from previous qPCR experiments and to provide contextual information on any successful drug hits identified during the upcoming drug library screen, which was also performed on lung fibroblasts derived from the same donors (Chapter VI, Results Part IV). In addition, my sponsor, GSK Fibrosis and Lung Injury unit, have a specific interest in lung biology.

RNA-seq was conducted on HLF1, HLF2 and HLF3 to identify which genes are up- or downregulated after 24 hours of TGF-β1 (5ng/ml) stimulation relative to vehicle treatment. The subsequent data was input into knowledgebase software ‘Database

for annotation, visualisation and integrated discovery' (DAVID) and 'Ingenuity pathway analysis' (IPA) that independently accrues published data to identify biological networks that these differentially expressed genes are likely to map to.

5.2. RNA sequencing of TGF-β1-stimulated human lung fibroblasts

The raw data generated from RNA sequencing was analysed by Bioinformatician Dr Ai Nagano (Barts Cancer Institute), whereby gene expression in vehicle-treated lung fibroblasts was compared with TGF-β1-treated cells. Only genes that were significantly differentially expressed and up- or downregulated by at least 2-fold were included for further analysis.

Figure 5.1 shows the global expression changes of 1,643 genes that were differentially expressed in the three strains of vehicle and TGF-β1-treated lung fibroblasts. The results indicate numerous genes were both up- (762 genes) and downregulated (881 genes) by TGF-β1, while each of the three strains of lung fibroblasts derived from different donors displayed similar responses to treatment overall, although some variability was visible between biological repeats and strains.

The datasets of differentially expressed genes were first investigated using software DAVID to identify possible biological networks that these genes are involved in; the top networks and their associated genes are listed in **Table 5.1**. The top networks identified were 'TGF-β signalling', 'pathways in cancer', 'cytokine-cytokine receptor interaction', 'ECM-receptor interaction' and 'focal adhesion'. The genes associated to the network 'TGF-beta signalling pathway' includes TGF-β1 (TGFB1) and TGF-β2 (TGFB2), which were significantly upregulated by an average of 2.5-fold and 2.1-fold in all three TGF-β1-treated strains, respectively. Furthermore, key components that typically enhance TGF-β1 signalling, including SMAD3 and type II receptor TGFBR2 were both significantly downregulated after 24-hour exposure to TGF-β1, whereas the expression of pathway inhibitor SMAD7 was significantly raised 4.3-fold in TGF-β1-activated HLFs.

In addition, the same genes were also linked to the 'pathways in cancer' network, which included several genes, such as fibroblast growth factors (FGFs), e.g. FGF2,

which was upregulated by an average of 3.9-fold in all three HLFs in response to TGF-β1, and vascular endothelial growth factor-A (VEGFA), which was raised 2.8-fold, while each molecule is known to promote fibrosis[86] and angiogenesis[216], respectively. In addition, RNA-seq revealed the hedgehog signalling pathway was activated in lung myofibroblasts, as indicated by upregulated ligands HHIP and WNT5A, transmembrane receptor FZD8 and transcription factors GLI1 and GLI2.

Table 5.1 also shows the network 'cytokine-cytokine receptor interaction' was enriched, which encompasses various pro-inflammatory molecules produced by myofibroblasts; an area that was not investigated in my own previous qPCR experiments. Many genes in this network were downregulated, though cytokines such as interleukin-6 (IL6), which is implicated in cancer progression, was significantly elevated 2.9-fold in TGF-β1-treated HLFs, in addition to the interleukin-21 receptor (IL21R), which was increased 5-fold. Most notably, several receptor subtypes constituting the tumour necrosis factor (TNF) superfamily, a major inflammatory cytokine, were downregulated by TGF-β1 exposure (TNFRSF1B, TNFRSF11B, TNFRSF14, TNFRSF19, TNFRSF21).

Reassuringly, a variety of integrin subunits were also upregulated by TGF-β1 stimulated lung fibroblasts, including α1 (ITGA1), α11 (ITGA11) and β3 (ITGB3), validating the integrin qPCR results using lung fibroblasts in Results Part I. The individual fold-changes for each integrin are listed in **Table 5.2**, showing α11 exhibited the highest significant increase of 17.5-fold in TGF-β1-treated HLFs relative to vehicle and β8 was significantly downregulated after 24-hour TGF-β1 exposure by an average of 8.3-fold in the three strains of HLFs. The integrin genes comprised the networks 'ECM-receptor interaction' and 'focal adhesion' (**Table 5.1**), encompassing the fundamental feature of fibroblasts to transmit extracellular signals internally via ECM-integrin interaction. Furthermore, genes identified by RNA-seq could spur future studies, such as actin-binding protein filamin B (FLNB), which is associated with mouse embryonic fibroblast invasion[217] and was increased approximately 4-fold in HLFs and yet, the function of filamin B in lung fibroblasts has not been previously established. Furthermore, it is also clear that the expression of several types of collagens were enhanced by TGF-β1, including COL4A1, COL4A2 and COL5A1, as well

as COL7A1 (not listed in **Table 5.1**). Of note, collagen cross-linking genes lysyl oxidase (LOX) and lysyl oxidase-like 2 (LOXL2) were also significantly upregulated 3.8-fold and 2.3-fold by TGF-β1, respectively.

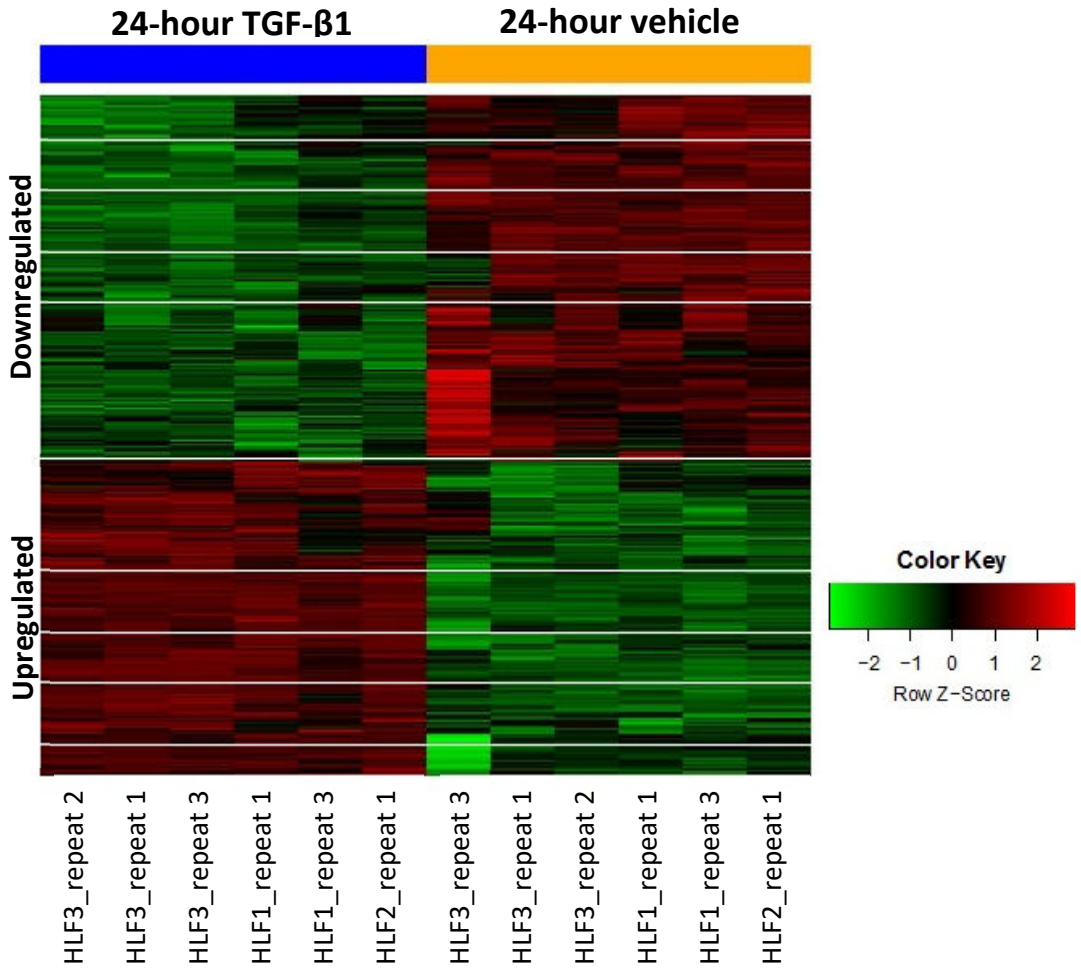

Figure 5. 1. Global profile of lung fibroblasts genes regulated by TGF-β1.

Figure shows fold-changes in gene expression in 3 strains of 24-hour TGF-β1-treated human lung fibroblasts (HLF1, 2, 3) compared to vehicle-treatment. Each row displays expression data for a single gene (1643 genes in total) and each column represents pairwise comparisons of TGF-β1 or vehicle treatment in each biological repeat. HLF1 (*n* = 2), HLF2 (*n* = 1), HLF3 (*n* = 3). Changes in gene expression are based on log-transformed values of fold ratios, where brighter shades of red and green represent greater gene upregulation and downregulation, respectively.

Table 5. 1. Top biological networks linked to differentially expressed genes regulated by TGF-β1 in human lung fibroblasts.
Networks were generated in software Database for annotation, visualisation and integrated discovery ('DAVID') using RNA sequencing data from 3 strains of 24-hour vehicle and TGF-β1-treated (5ng/ml) lung fibroblasts. All genes listed were up- (**red**) or downregulated (**green**) at least 2-fold relative to vehicle-treated fibroblasts. Genes mentioned in the text are underlined in the table.

Network	Genes associated	Fold enrichment	Benjamini adjusted p-value
TGF-β signalling pathway	BMP4, BMP2, SMAD9, ACVRL1, SMAD7, SMAD6, GDF6, TGFBR2, RBL1, GDF5, SMAD3, DCN, TGFB1, TGFB2, INHBA, CDKN2B, INHBE, COMP, ID3, THBS2, BMP6, PITX2	2.730068087	0.004937307
Pathways in cancer	E2F1, E2F2, FGF5, FGF7, PTGS2, PDGFA, STAT5A, PPARG, MITF, FGF10, GLI2, TGFB1, GLI1, TGFB2, CCNE2, CDKN2B, SLC2A1, RARA, RARB, HHIP, FGF2, AR, DAPK1, VEGFC, VEGFA, PDGFRA, LAMC2, WNT5A, WNT16, APC2, KITLG, KIT, RAC2, LAMB1, EGF, FIGF, TRAF5, BMP4, FZD8, COL4A2, IL6, BMP2, COL4A1, EPAS1, TGFBR2, SMAD3, IGF1, HGF, BIRC3, WNT2B, LAMA4, RASSF5, LAMA3	1.744504428	0.00453466
Cytokine-cytokine receptor interaction	TNFRSF21, IL1R1, CCL2, ACVRL1, PDGFA, CSF1, IL21R, GDF5, KITLG, KIT, TNFSF12, IL7R, TGFB1, IL11, TGFB2, LIF, TNFRSF1B, TNFRSF11B, TNFRSF19, IL15RA, EGF, FIGF, GHR, IL18R1, BMP2, IL6, TNFSF4, IL7, TGFBR2, LIFR, TNFRSF14, HGF, IL6R, INHBA, VEGFC, TNFSF13B, RELT, INHBE, CXCL16, VEGFA, PDGFRA, IL12A	1.730685078	0.015410653
ECM-receptor interaction	COL4A2, COL4A1, TNXB, ITGA1, ITGA11, ITGB3, SDC4, COL5A1, SDC2, CD47, VWF, ITGA9, LAMA4, LAMA3, CD44, ITGA5, ITGB8, COMP, LAMC2, LAMB1, THBS2	2.699044586	0.003151116
Focal adhesion	CAV1, PDGFA, ITGA11, ITGB3, RAC2, PAK3, ITGB8, COMP, PDGFD, LAMB1, EGF, FIGF, THBS2, COL4A2, COL4A1, TNXB, ITGA1, ACTN1, IGF1, HGF, BIRC3, FLNB, COL5A1, VASP, ITGA9, VWF, VEGFC, LAMA4, LAMA3, CCND2, ITGA5, VEGFA, PDGFRA, LAMC2	1.826219222	0.016952332

Table 5. 2. Gene expression of integrin subunits in TGF-β1-treated lung fibroblasts.

RNA sequencing was conducted on three strains of vehicle- and TGF-β1-treated (5ng/ml) human lung fibroblasts. The average fold-change between the 3 strains of TGF-β1 relative to vehicle treatment is presented.

Gene	Description	Fold-change	p-value
ITGA1	integrin subunit alpha 1	2.76	0.007973475
ITGA5	integrin subunit alpha 5	2.22	0.000580488
ITGA11	integrin subunit alpha 11	17.49	4.82E-05
ITGB3	integrin subunit beta 3	6.25	0.000165655
ITGB8	integrin subunit beta 8	0.12	3.33E-05

The RNA-seq dataset was also input into IPA software for further analysis to determine which TGF-β1-induced genes corresponded to proteins that would be localised to the plasma membrane. This was to identify transmembrane proteins that may be highly upregulated only on activated fibroblasts and that could potentially regulate the lung myofibroblast phenotype if targeted therapeutically in future studies. **Table 5.3** shows the top TGF-β1-induced genes, which are known to be expressed as proteins localised to the plasma membrane. The most highly increased genes included potassium voltage-gated channel subfamily H (KCNH1), which was upregulated by an average of 60-fold by TGF-β1 across the three strains of HLFs and gene frizzled class receptor 8 (FZD8), which was elevated 47.5-fold after stimulation. In addition, integrin subunits α9, α11 and β3 were also among this dataset, while though not shown, many genes corresponding to cell surface proteins were also downregulated in response to TGF-β1 exposure.

Table 5. 3. Top plasma membrane-associated genes upregulated by TGF-β1 in lung fibroblasts relative to vehicle.

Symbol	Entrez Gene Name	Fold-change	Type(s)
KCNH1	potassium voltage-gated channel subfamily H member 1	60.09	ion channel
FZD8	frizzled class receptor 8	47.50	G-protein coupled receptor
PMEPA1	prostate transmembrane protein, androgen induced 1	31.43	Other
AMIGO2	adhesion molecule with Ig like domain 2	24.17	Other
ITGA11	integrin subunit alpha 11	17.50	Other
CNTN1	contactin 1	13.23	Enzyme
SGCG	sarcoglycan gamma	12.94	Other
ADAM12	ADAM metallopeptidase domain 12	12.08	Peptidase
NALCN	sodium leak channel, non-selective	11.62	ion channel
LRRC15	leucine rich repeat containing 15	11.59	Other
ITGA9	integrin subunit alpha 9	11.46	Other
DSP	Desmoplakin	9.34	Other
HHIP	hedgehog interacting protein	8.81	Other
PCDH1	protocadherin 1	8.37	Other
KCNG1	potassium voltage-gated channel modifier	7.62	ion channel
ADAM19	ADAM metallopeptidase domain 19	7.56	Peptidase
KIAA1324	KIAA1324	6.97	Other
NPR3	natriuretic peptide receptor 3	6.71	G-protein coupled receptor
SEMA7A	semaphorin 7A (John Milton Hagen blood group)	6.53	transmembrane receptor
CLTCL1	clathrin heavy chain like 1	6.52	other
RTKN2	rhotekin 2	6.46	other
ITGB3	integrin subunit beta 3	6.25	transmembrane receptor
CDH2	cadherin 2	6.17	other
AOC3	amine oxidase, copper containing 3	6.13	enzyme
KCNMB1	potassium calcium-activated channel subfamily	6.12	ion channel
CELSR1	cadherin EGF LAG seven-pass G-type receptor 1	6.09	G-protein coupled receptor
TSPAN13	tetraspanin 13	5.91	other
SCUBE3	signal peptide, CUB domain and EGF like domain	5.90	other
PCDH9	protocadherin 9	5.72	other
SLC19A2	solute carrier family 19 member 2	5.54	transporter
DYSF	Dysferlin	5.49	other
AKAP5	A-kinase anchoring protein 5	5.37	other
PKP1	plakophilin 1	5.19	other

IPA software is also able to relate datasets with biological networks by tracking the fold-changes of each gene and comparing this with published data, generating an 'overlap p-value'. Using this method of analysis, IPA independently recognised that TGF-β1 was a principal upstream regulator in this dataset and several of its target genes, as established by IPA, are listed in **Figure 5.2A**. To note, this list included genes that were verified previously using qPCR in Results Part I, such as ACTA2, CTGF and SERPINE1.

In addition, IPA suggested the top cellular processes induced by TGF-β1 stimulation of HLFs were 'mitogenesis of fibroblasts', 'cell cycle progression' and 'adhesion of connective tissue cells'. Each of these networks and the genes associated are displayed in **Figure 5.2B** and **5.2C**.

In addition, as various inflammatory factors were up- and down-regulated by TGF-β1 in HLFs, IPA software was used to determine potential signalling pathways involved in regulating these genes. **Figure 5.3** shows many cytokine cell surface receptors, such as IL-6R, IL-1R, TNFR and ET-BR (endothelin receptor type B) were downregulated in activated HLFs, though ligands, IL-6 and ET-1 were significantly increased. In addition, transcription factor NF-κB (nuclear factor-κB) appeared to directly mediate the transcription of several cytokines, many of which were also downregulated in response to TGF-β1.

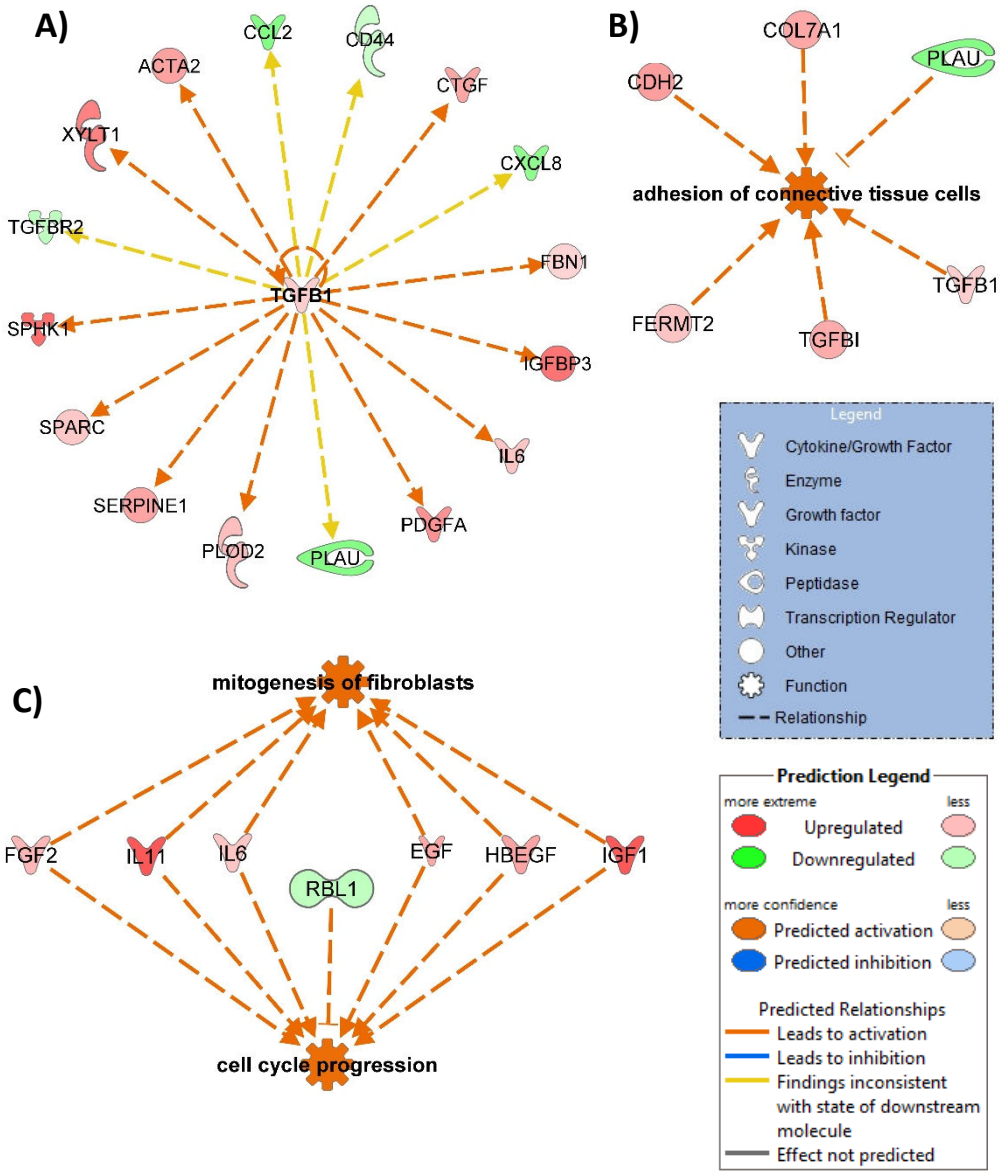

Figure 5. 2. Biological network of TGF-β1 downstream target genes and top cellular processes.

Ingenuity pathway analysis of RNA sequencing data from three strains of 24-hour TGF-β1-treated lung fibroblasts relative to vehicle-treated cells. Darker shades of green indicate higher gene downregulation compared to vehicle and darker shades of red indicate higher gene upregulation in TGF-β1 vs vehicle-treated cells. Dashed lines signify indirect relationships between molecules (N.B. physical contact is required between two factors to represent direct interaction). A) Significant downstream targets of TGF-β1. Top activated cellular processes were identified by IPA and the genes involved in; adhesion of connective tissue cells (B) and mitogenesis of fibroblasts and cell cycle progression (C).

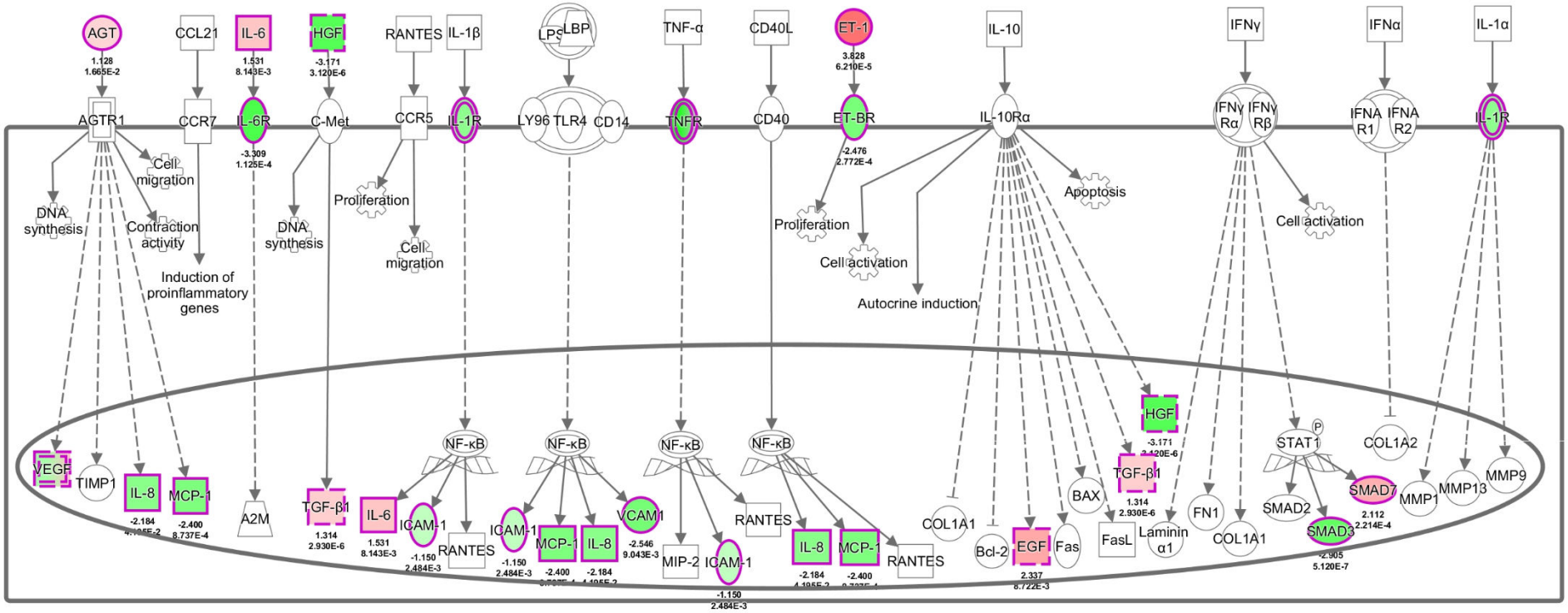

Figure 5. 3. Signalling pathways that regulate TGF-β1-induced genes in human lung fibroblasts.

Ingenuity pathway analysis (IPA) software was used to determine which inflammation-associated pathways were active in TGF-β1 stimulated lung fibroblasts. Upregulated genes (red), downregulated genes (green) and unchanged genes (non-coloured) derive from the RNA sequencing analysis of three strains of lung fibroblasts. Darker shades of colour represent higher fold-change, log fold change and p-values are stated beneath each molecule. Lines connecting molecules are either dashed (indirect relationships) or solid (direct relationships). Inner circle represents the nucleus and outer square represents the cell plasma membrane. Image generated by IPA.

Although the analyses presented so far was performed on the combined dataset generated by HLF1, -2 and -3, overlapping genes were also common between the different lung strains. **Figure 5.4** shows the same 99 differentially expressed genes were identified in both HLF1 and HLF3. Note, HLF2 was unusable for this analysis as only one biological repeat was completed, whereas at least two independent experiments were performed using strains HLF1 and HLF3. Although there was a disparity between the total numbers of differentially expressed genes found in each strain; 138 genes in HLF1 and 1162 in HLF3, these results show that lung fibroblasts derived from two separate donors share similarities in their responses to TGF-β1.

Figure 5. 4. Overlap of differentially expressed genes in TGF-β1-treated lung fibroblasts.

Differentially expressed (DE) genes were identified in TGF-β1 relative to vehicle-treated lung fibroblasts. Ninety-nine common differentially expressed genes were identified in 2 strains of lung fibroblasts; strain 1 (HLF1) and strain 3 (HLF3).

Overall, RNA sequencing results demonstrated that only 24 hours of TGF-β1 exposure of healthy lung fibroblasts was sufficient to produce a gene signature reminiscent of a reactive stroma, with the potential to promote detrimental actions including angiogenesis, fibrosis and invasion.

5.3. Discussion

RNA-seq was conducted on TGF-β1-stimulated lung fibroblasts to examine which genes are significantly regulated by TGF-β1, in addition to those genes studied in my own qPCR experiments. Firstly, the results of the RNA-seq support the findings obtained by previous qPCRs, as genes such as ACTA2, CTGF, SERPINE1 and several integrin genes demonstrated similar levels of expression in response to TGF-β1. Ideally, RNA-seq would also be performed on skin and breast fibroblasts to determine the level of overlap of differentially expressed genes and heterogeneity that exists between fibroblasts derived from all three organs. From **Figure 5.4**, we can already confirm that some intra-tissue heterogeneity was present when comparing differentially expressed genes in lung strains HLF1 and HLF3, although 72% of TGF-β1-regulated genes in HLF1 were also common to HLF3.

RNA-seq was also performed to understand which biological networks TGF-β1-regulated genes map to using various knowledgebase programs. Unsurprisingly, the 'TGF-β signalling pathway' was a significantly regulated network and identified as a key upstream regulator, although TGF-β1-stimulated lung fibroblasts appear to involve negative feedback loops, as key TGF-β signalling components such as SMAD3 and TGF-β1 receptor gene TGFBR2 were downregulated after 24 hours of TGF-β1 exposure. However, determining the protein and phospho-protein levels of these genes would be required to confirm whether these results translate into biological effects. In addition, according to the analyses, TGF-β1 and TGF-β2 genes were significantly increased, suggesting if the encoded protein was secreted these molecules could act in a paracrine mechanism instead of autocrinally as their co-receptor TGF-βRII was downregulated. It would be interesting to determine whether these feedback mechanisms in normal fibroblasts are also functioning in lung cancer-associated fibroblasts, as several studies indicate TGFBR2 is a tumour suppressor[218].

Recently, Busch and colleagues revealed that fibroblast-specific TGFBR2 expression is a biomarker for breast cancer prognosis, as expression positively correlated with recurrence-free survival[219], while loss of TGFBR2 in colon CAFs increased lymph

node metastases[220]. Moreover, xenograft tumours in mice where TGFBR2 was silenced in CAFs resulted in larger breast tumours. A potential mechanism for these effects was reported by Cheng and colleagues, who found that TGF-βRII knockdown in mammary fibroblasts resulted in increased secretion of TGF-α, HGF and macrophage-stimulating protein (MSP). In addition, the corresponding receptors of these factors, expressed by tumour cells, displayed enhanced phosphorylation, while pharmacologic inhibition of each pathway reduced tumour cell proliferation and motility in the presence of conditioned medium from TGF-βRII-knockout fibroblasts[221]. Furthermore, the authors noted when TGFBR2 was knocked down in normal unstimulated fibroblasts, there was no influence on the clonogenicity of co-cultured breast cancer cells, in contrast to the effects by TGFBR2-knockout CAFs, which promoted tumour cell survival *in vitro*[219]. This study highlighted the distinct differences between undifferentiated fibroblasts and CAFs, whilst in my own results, the downregulation of TGFBR2 indicates that TGF-β1-treated fibroblasts express a potentially tumour-promoting gene signature, similar to CAFs. Future studies involving RNA sequencing of primary lung fibroblasts from additional donors would validate these findings and perhaps also highlight TGFBR2 and other genes as clinical biomarkers in fibroblast-related lung pathologies.

The 'pathways in cancer' network was also enriched in TGF-β1-treated lung fibroblasts. Surprisingly, HGF, a key fibroblast-secreted molecule known to promote tumour cell invasion[222] and chemoresistance[110] was downregulated in response to TGF-β1 in lung fibroblasts, though perhaps longer periods of TGF-β1 exposure would induce additional sets of genes. In addition, many extracellular matrix proteins, such as several collagens and collagen-crosslinking protein LOX were significantly increased. The genes regulated by TGF-β1 are reminiscent of those that contribute to wound repair[223], while excessive secretion of collagens and lysyl oxidases produces a fibrotic extracellular matrix, which is associated with promoting cancer cell growth and invasion[203]. Furthermore, lysyl oxidase-like 2 (LOXL2) was significantly upregulated by TGF-β1 in HLF3 by 2.3-fold. Immunohistochemical staining of several types of human tumour biopsies revealed LOXL2 localised to the tumour stroma, as opposed to healthy tissues. In addition, antibody-blockade of

LOXL2 significantly reduced the production of cross-linked collagen, breast tumour volume, the percentage of α-SMA-positive myofibroblasts and phospho-Smad2 expression in fibroblasts. Moreover, the same monoclonal antibody diminished levels of cross-linked fibrillar collagen in a bleomycin-induced model of lung fibrosis[224]. Therefore, it appears these TGF-β1-activated lung fibroblasts could prime local fibroblasts for activation and encourage cancer progression by increasing the stiffness of the local microenvironment.

The hedgehog signalling pathway also appeared to be activated in TGF-β1-treated HLFs. This pathway is known to mediate tumour-stroma interactions by paracrine activation, resulting in the expression of the hedgehog pathway transcription factor Gli1, collagen type I and fibronectin by fibroblasts, contributing to a desmoplastic stroma[225]. In addition, WNT5a, which was also upregulated in HLFs, is known to promote fibronectin expression, fibroblast proliferation and resistance to apoptosis, while WNT5a also displays higher expression in HLFs derived from fibrotic lung tissues[226], indicating TGF-β1 enhances hedgehog signalling, which together promote fibrosis.

CAFs are also known to express pro-inflammatory gene signatures[227] and RNA-seq revealed that TGF-β1 also induced inflammation-associated genes, such as cytokine receptor IL21R, which was reported to enhance protease MMP expression by intestinal fibroblasts[228]. Although, whether this receptor serves the same function in lung fibroblasts is unknown. In addition, IL-6, which was also elevated, correlates with poor prognoses in prostate and ovarian cancers[229, 230], and promotes monocyte to macrophage differentiation[231]. Furthermore, when comparing fibroblasts from common sites of breast tumour metastases, such as the lung, bone and skin, levels of IL-6 secreted by fibroblasts directly correlated with tumour growth and invasion, which was mediated by activation of the STAT3 pathway in breast tumour cells[137]. As mentioned previously, the TGF-β1 gene was also increased in lung myofibroblasts, and it is well-documented that this cytokine is a paracrine stimulant of EMT in tumour tissues[91] and contributes to the population of activated fibroblasts in fibrotic organs[232]. These results suggest activated lung fibroblasts have the potential to promote an invasive tumour phenotype. In addition,

the role of many genes identified by RNA-seq have not been previously examined in the context of cancers, therefore their functions in fibroblasts are unknown.

RNA-seq revealed subtypes of the TNF receptor superfamily were downregulated in response to TGF-β1 stimulation. The ligand for the type 1 receptor subtype is pro-inflammatory cytokine TNF-α, which is associated with promoting tumour metastases[233]. Furthermore, mapping of signalling pathways involving inflammatory genes (**Figure 5.3**), showed key downstream transcription factor NF-κB exhibited no change in mRNA expression level, though NF-κB-regulated genes, such as IL-8 and MCP-1 displayed reduced expression, perhaps indicating they are negatively regulated by other transcription factors or by post-translational modifications of NF-κB[234]. Moreover, these effects also comply with role of fibroblasts during wound healing, where cytokines such as macrophage-secreted TNF-α is necessary to promote inflammation during the early stages of wound healing and negatively regulates myofibroblast activity. Abraham and colleagues have reported that TNF-α inhibits the expression of pro-fibrotic CTGF in TGF-β1-activated skin fibroblasts. Hence, when wound healing transitions from the inflammatory phase into the remodelling phase, myofibroblast activity is required to stabilise the matrix, therefore perhaps the downregulation of TNF receptors removes the negative regulatory effect of this cytokine to permit the secretion of matrix proteins[235]. In addition, **Figure 5.3** indicates additional receptor genes, including IL-6R and ET-BR (endothelin receptor type B) were each decreased by TGF-β1 treatment, though their respective ligands (IL-6 and ET-1) were elevated, suggesting negative feedback may have resulted in receptor downregulation.

It would also be interesting to determine whether integrins expressed by myofibroblasts regulate the expression of pro-inflammatory genes. Previous research suggests αvβ8 regulates chemokine CCL2 secretion from IL-1β-treated lung fibroblasts[185]. However, in this study β8 and CCL2 were each downregulated in response to TGF-β1, though perhaps other integrins are responsible for regulating pro-inflammatory genes in these cells.

IPA was used to identify TGF-β1-induced genes that would correspond to proteins localised to the plasma membrane of lung fibroblasts, as indicated by published reports. This analysis was performed to generate a top list of hits that if time permitted, could be further investigated to determine whether any of the proteins could regulate the myofibroblast phenotype. Integrin subunits α11 and β3 were included in this list, which were already examined in Results Part II. To note, RNA-seq also revealed the FERMT2 (kindlin-2) gene was upregulated by TGF-β1 in HLFs (**Figure 5.2B**), which is known to mediate integrin activation[47].

As RNA sequencing was conducted towards the end of the project, novel membrane-associated hits could not be investigated. Nevertheless, published reports have shown genes, such as frizzled class receptor 8 (FZD8), which was increased 47.50-fold by TGF-β1 in my own experiments, was also upregulated in healthy and COPD lung fibroblasts by TGF-β1. FZD8 comprises the WNT/β-catenin pathway and is associated with fibroblast activation during organ fibrosis and tissue repair[236] and recent findings suggest this receptor may regulate the secretion of inflammatory mediators[237], though its role in lung myofibroblast biology is still undefined. Another highly upregulated gene, prostate transmembrane protein, androgen induced 1 (PMEPA1) was reported to display significantly higher expression in OSCC CAFs compared to healthy fibroblasts and correlated with reduced disease-free survival in cases of head and neck SCC[238]. In addition, the top gene elevated by TGF-β1 in HLFs was potassium voltage-gated channel subfamily H member 1 (KCNH1); while its expression is associated with tumour cell growth and drug resistance, its role in fibroblasts has yet to be defined. Overall, the hits identified give rise to a new set of experiments to determine how they contribute to myofibroblast biology, and whether they exhibit any therapeutic potential.

IPA software was also used to assess the top cellular processes associated with the dataset, and genes involved in fibroblast proliferation and cell cycle progression were overall, upregulated after stimulation. These included genes such as IL-11[239] and FGF-2, which previous reports show act in a paracrine manner, where ERK1/2 activation by each of these factors promoted fibroblast proliferation. Furthermore, increased numbers of fibroblasts has been noted in diseases such as pulmonary

fibrosis[240]. Analysis by software IPA suggested the factors identified in **Figure 5.2** are not physically involved in proliferation and cell cycle functions (noted by the dashed lines in **Figure 5.2**), but are secreted mediators, indicating activated fibroblasts may promote growth in an autocrine manner, as described by Strutz[241], or perhaps support the proliferation of resident fibroblasts, amplifying their response.

As mentioned throughout this section, the characterisation of TGF-β1-activated fibroblasts has the potential to identify genes associated with predicting the clinical outcome in cancer, which has previously been demonstrated using breast tumours[242]. Similarly, Chang and colleagues examined the transcriptional responses of breast, lung and gastric fibroblasts to foetal bovine serum to identify common genes expressed by fibroblasts from different anatomical sites. They identified 512 genes and named the wound-like signature the 'core serum response' and used published clinical and molecular data from breast carcinomas to examine overlapping genes. They found that tumour cells with the activated core serum response were more likely to progress to metastasis and patient death in the 5-year follow-up period. Furthermore, they validated microarray data by sub-selecting four genes linked to ECM remodelling and cell-cell interaction and confirmed their expression in fibroblasts using tissue microarrays containing hundreds of breast carcinoma tissues. The four molecules chosen were collagen cross-linking enzymes PLOD2 and LOXL2, urokinase-type plasminogen activator receptor PLAUR and SDFR1, a transmembrane protein belonging to the immunoglobulin superfamily[215]. These results are noteworthy because PLOD2, LOXL2 and PLAUR genes were also significantly upregulated in HLFs, per my own RNA-seq analysis. PLOD2 and ligand PLAU are displayed in **Figure 5.2A**, while the receptor PLAUR was increased by 1.8-fold in HLFs, as was previously mentioned LOXL2. These results demonstrate that similar studies characterising TGF-β1-treated lung fibroblasts may also identify a core signature linked to prognosis and perhaps guide effective treatment plans in cancer and fibrosis.

In summary, the global gene expression profiling of TGF-β1 activated lung fibroblasts has indicated these cells represent a gene signature similar to CAFs, as noted by the

downregulation of tumour suppressor TGFBR2 and the upregulation of genes encoding matrix proteins, collagen crosslinking proteins, integrins and pro-inflammatory mediators. In addition, the results further highlight the potential benefits of interfering with TGF-β1 signalling in fibroblasts, which could reduce the expression of each of these factors, in addition to fibroblast proliferation. Furthermore, enriched cell surface-associated genes may represent novel regulators of the myofibroblast phenotype, which could be examined in future studies.

CHAPTER VI. RESULTS PART IV

FDA-approved drug library screen using TGF-β1-treated human lung fibroblasts

6.1. Background

The overall aims investigated in Results Part I and Part II revolved around understanding the role of integrins in regulating myofibroblast activity and whether integrins exist as potential therapeutic targets to reduce the severity of cancer and fibrosis by inhibiting myofibroblast functions. In this section, the aim was to identify integrin-independent compounds and novel pathways that regulate TGF-β1-induced activation of lung fibroblasts, to gain a better understanding of fibroblast biology and generate additional potential therapeutic targets expressed by myofibroblasts.

To do this I used a FDA-approved drug library containing 1,177 compounds with known mechanisms of action that are already used to treat a variety of diseases. The detailed method is described in Chapter II: Materials and Methods, but briefly, the concept was to test which, if any, drugs could prevent TGF-β1-induced differentiation of fibroblasts into myofibroblasts. To increase selectively I chose to examine the regulation of two, rather than one, myofibroblast activation marker. Thus, each compound of the FDA-approved drug library (10μM) was applied to lung fibroblasts plated in 96-well plates for 48 hours. Fibroblasts were then stimulated with TGF-β1 (5ng/ml) in combination with the same drugs (10μM) for a further 48-hours. Subsequently, each well was fixed and stained for α-SMA and fibronectin using immunofluorescence and imaged on an IN Cell 1000 to enable high-throughput screening. The intensity of the fluorescence in drug + TGF-β1 treatment wells versus DMSO + TGF-β1 control was measured and compared. Drugs that reduced the expression of α-SMA and fibronectin, both key myofibroblast-associated proteins, were identified.

Due to the high number of compounds, this assay could only be conducted on one strain of fibroblast. Lung fibroblasts were chosen over skin and breast, as the lung fibroblasts were provided by co-funding supporters GlaxoSmithKline, therefore the

identification of any hits could be further investigated with their high throughput resources and generate greater scope for the development of therapeutics.

6.2. The optimisation of a 96-well plate phenotypic screen using immunofluorescent staining of TGF-β1-stimulated lung fibroblasts

Before the screen was conducted in 96-well plates, preliminary tests were performed on coverslips using vehicle and TGF-β1-stimulated lung fibroblasts (5ng/ml) to select 2 reliable primary antibodies for immunofluorescent staining. Markers were chosen according to the previous lung fibroblast qPCR results presented in **Appendix Figure 16** and the availability of antibodies in the group. The proteins examined were α-SMA, fibronectin (FN1), myosin heavy chain 9 (MYH9) and connective tissue growth factor (CTGF) at three different primary antibody dilutions (1:100, 1:300, 1:500). **Figure 6.1** shows the immunofluorescent staining of each marker in lung fibroblasts at one optimal primary antibody concentration. Note that, CTGF images are not presented due to poor staining, possibly as a result of the antibody used.

Figure 6.1A-D shows the intensity of α-SMA and FN1 staining was clearly higher in TGF-β1-stimulated lung fibroblasts compared to vehicle-treated cells. In addition, **Figure 6.1E** and **6.1F** shows MYH9 staining was present in both vehicle- and TGF-β1-exposed fibroblasts, although interestingly MYH9 appeared to form fibres and align with F-actin in TGF-β1-activated cells. As a result of this assay, α-SMA and fibronectin were selected as the two markers to be used in the drug screen due to the clear differences in staining intensity in vehicle and TGF-β1-treated cells.

Next, one strain of lung fibroblast needed to be chosen out of the three strains. Therefore, all three strains were first tested in preliminary runs of the screen by plating and stimulating each strain with TGF-β1 in 96-well plates. These preliminary experiments also enabled validation of α-SMA and fibronectin staining, as the protocol was adapted from staining on coverslips in 24-well plates and facilitated the optimisation of the number of fibroblasts to be seeded in each well (1000 cells). After repeat experiments, lung fibroblast strain 3 was selected as its performance was more reliable; the fibroblasts remained more adherent than strains 1 and 2 after the various wash steps were conducted during the staining procedure (data not shown).

Furthermore, the three lung strains exhibited similar responses to TGF-β1, as each strain significantly increased α-SMA (**Figure 6.2A**) and fibronectin (**Figure 6.2B**) expression compared to vehicle-treated cells, as expected. These results validated the immunofluorescent staining of cells using the protocol adapted to 96-well plates.

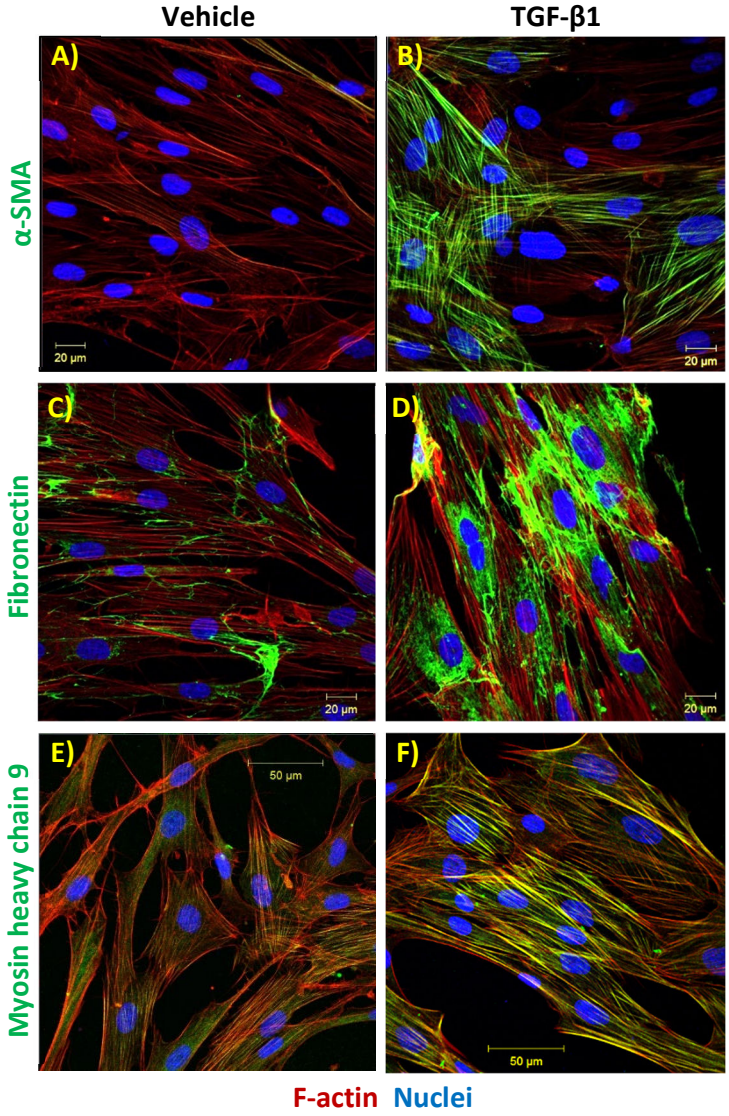

Figure 6. 1. Immunofluorescent staining of α-SMA, fibronectin and myosin heavy chain 9 in vehicle and TGF-β1-treated lung fibroblasts.

Representative images from lung strain 1 fibroblasts plated on coverslips in a 24-well plate and stimulated with vehicle or TGF-β1 (5ng/ml) for 48-hours and stained using anti-α-SMA (**A**, **B**), anti-fibronectin (**C**, **D**) or anti-myosin heavy chain 9 (**E**, **F**) antibodies (green), F-actin (red) and nuclei (blue).

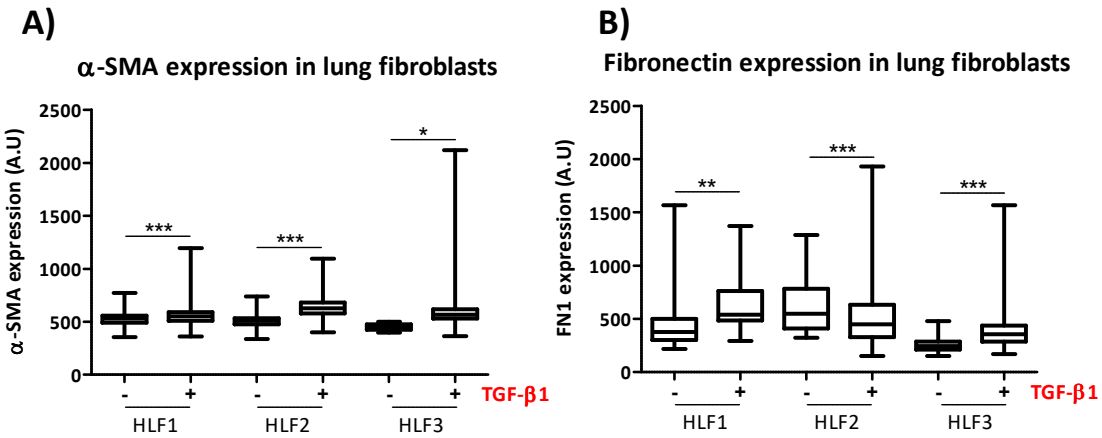

Figure 6. 2. Expression of α-SMA and fibronectin in 3 strains of vehicle and TGF-β1-treated lung fibroblast stained in a 96-well plate.

Three strains of lung fibroblasts (HLF1, HLF2, HLF3) were plated in a 96-well plate and stimulated with vehicle or TGF-β1 (5ng/ml) for 48-hours and stained using anti-α-SMA or anti-fibronectin antibodies, plus DAPI to identify nuclei. The mean immunofluorescence intensity of individual cells (≤7500) in each well was quantified (arbitrary units: A.U). *p<0.05, **p<0.01, ***p<0.001, Wilcoxon signed rank test. Data shown represents the median ± interquartile range of one independent experiment.

Figure 6.3 demonstrates how the analysis of α-SMA and fibronectin staining was quantified after imaging was completed. **Figure 6.3A** displays a representative image of merged α-SMA and fibronectin staining of TGF-β1-treated lung strain 3 fibroblasts plated in a 96-well plate and imaged using the IN Cell 1000. **Figure 6.3B** shows the same cells as **Figure 6.3A**, stained using whole-cell dye 'CellMask', which is a membrane-labelled fluorochrome used in phenotypic screening to visualise individual cells. The post-analysis was conducted using Developer Toolbox 2.3 software, whereby a series of filters were applied to ensure the software only recognised α-SMA and fibronectin staining that was associated with both CellMask and DAPI. This was to prevent the software measuring background staining or extraneous clumps of α-SMA and fibronectin that were not associated with a whole adhered fibroblast. **Figure 6.3C** exhibits the use of a software-generated filter applied to roughly segment each cell using CellMask to identify the edges of each cell. Using this segmentation, the level of α-SMA (**Figure 6.3D**) and fibronectin (**Figure 6.3E**) staining in each cell could be quantified. Furthermore, additional filters were applied to ensure the software separated background staining within cells from true α-SMA

and fibronectin expression. Hence, staining that presented under a certain threshold was labelled as background staining and the staining of individual α-SMA fibres (**Figure 6.3F**) and fibronectin strands (**Figure 6.3G**) per cell was measured, providing more accurate quantification. An example of excluded staining is shown inset in **Figure 6.3F** as red pixels.

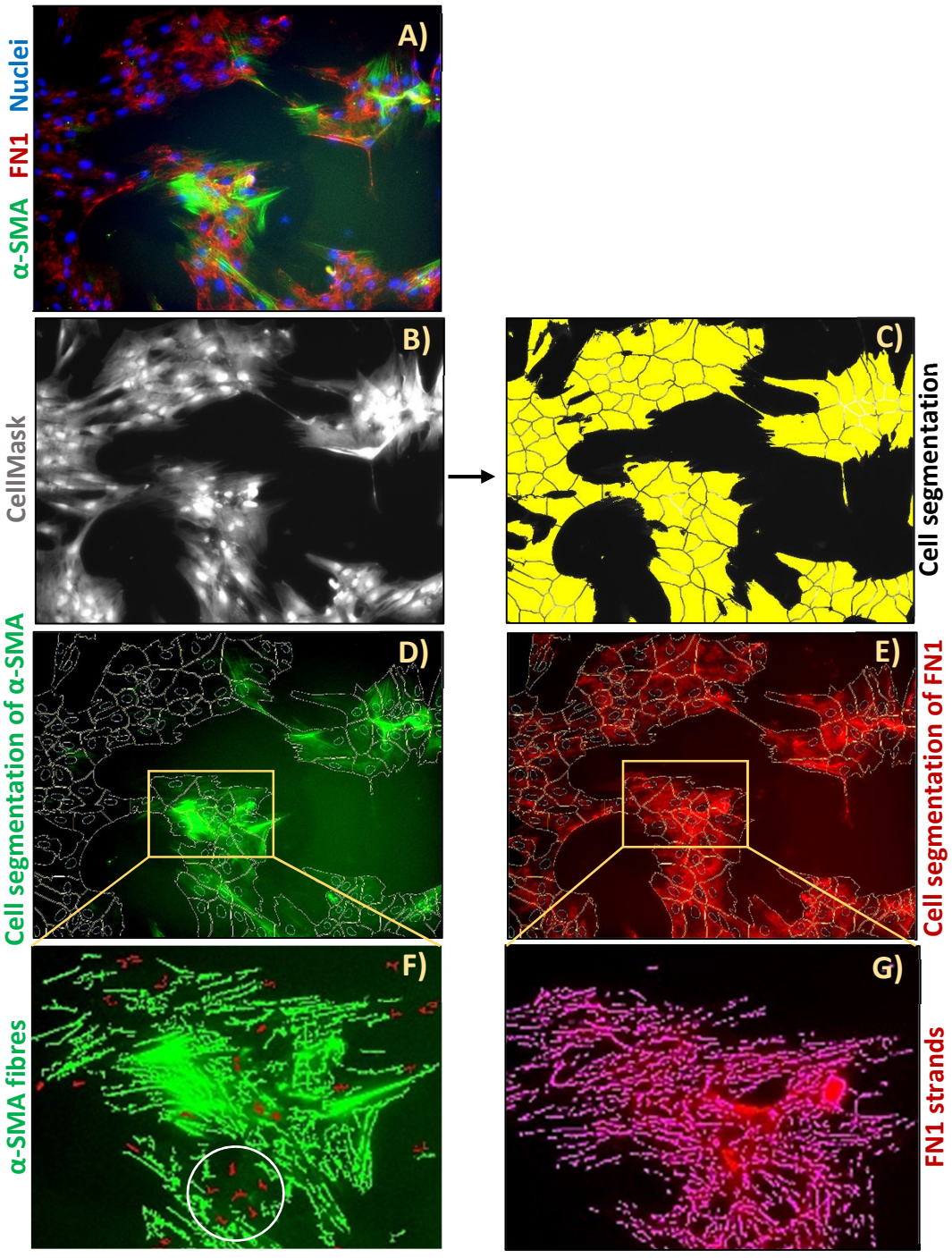

Figure 6. 3. Method of IN Cell image analysis of α-SMA and fibronectin (FN1) staining during the lung fibroblast drug screen.

Every well was stained with DAPI, CellMask, anti-α-SMA and anti-FN1. The IN Cell microscope imaged each relevant channel in each well in a 96-well plate and the staining was analysed by software Developer Toolbox 2.3. A) Representative image of merged DAPI (nuclei), α-SMA and FN1 staining of TGF-β1-treated lung fibroblasts. B) An image of the same field as A of cells dyed with CellMask to identify each cell. C) A software-generated filter was applied to segment cells using CellMask. Using this cell segmentation, the staining of α-SMA (D) and FN1 (E) in each cell could be quantified. On top of this, additional filters were applied to precisely identify α-SMA fibres (F) and FN1 strands (G) to avoid the inclusion of background staining and extraneous clumps (this can be observed as red filters inset (F), which were excluded from quantification).

6.3. The effect of FDA-approved drugs on TGF-β1-induced lung fibroblast activation

After the treatment, staining and imaging of lung fibroblasts was complete, various measurements of α-SMA and fibronectin staining were assessed in the first plate of the drug screen, including staining intensity, average fibre length, number of fibres and maximum fibre length per cell to compare in the absence and presence of each compound. **Figure 6.4** shows TGF-β1-induced fibronectin expression was significantly reduced after the addition of drug axitinib compared to DMSO-treated cells when comparing staining intensity (**Figure 6.4A**), average strand length (**Figure 6.4B**) and the number of strands (**Figure 6.4C**). In contrast, the maximum fibronectin strand length did not significantly change between DMSO and axitinib-treated lung fibroblasts in the presence of TGF-β1 (**Figure 6.4D**). The measurement for staining intensity (**Figure 6.4A**) demonstrated the clearest reduction compared to the DMSO control, which was visible by the lower median and smaller upper quartile range. Similar results were also found using other compounds (data not shown), therefore fluorescence intensity was selected as the primary α-SMA and fibronectin measurement for the remainder of the drug screen.

Computer programming software R-Studio was used to automate statistical and graphical analysis for the complete drug screen (the coding for the script was kindly conducted by bioinformatics PhD student William Cross at Barts Cancer Institute). As,

cell numbers may have varied between some drug-treated wells and controls, a rule was incorporated into the script, whereby if less than 200 cells remained per well at the end of the screen (1000 cells were initially plated), then the results of these wells were disregarded. Cumulative frequency was used to determine the distributions of α-SMA and fibronectin in drug + TGF-β1-treated cells relative to DMSO + TGF-β1 by displaying the number of cells within each range of fluorescence intensity (**Figure 6.5**, x-axis). The Kolmogorov-Smirnov test was used to analyse the data as it is typically performed for cumulative frequency and is non-parametric. Note that the optimisation of the analysis using software R-Studio took approximately 5 months.

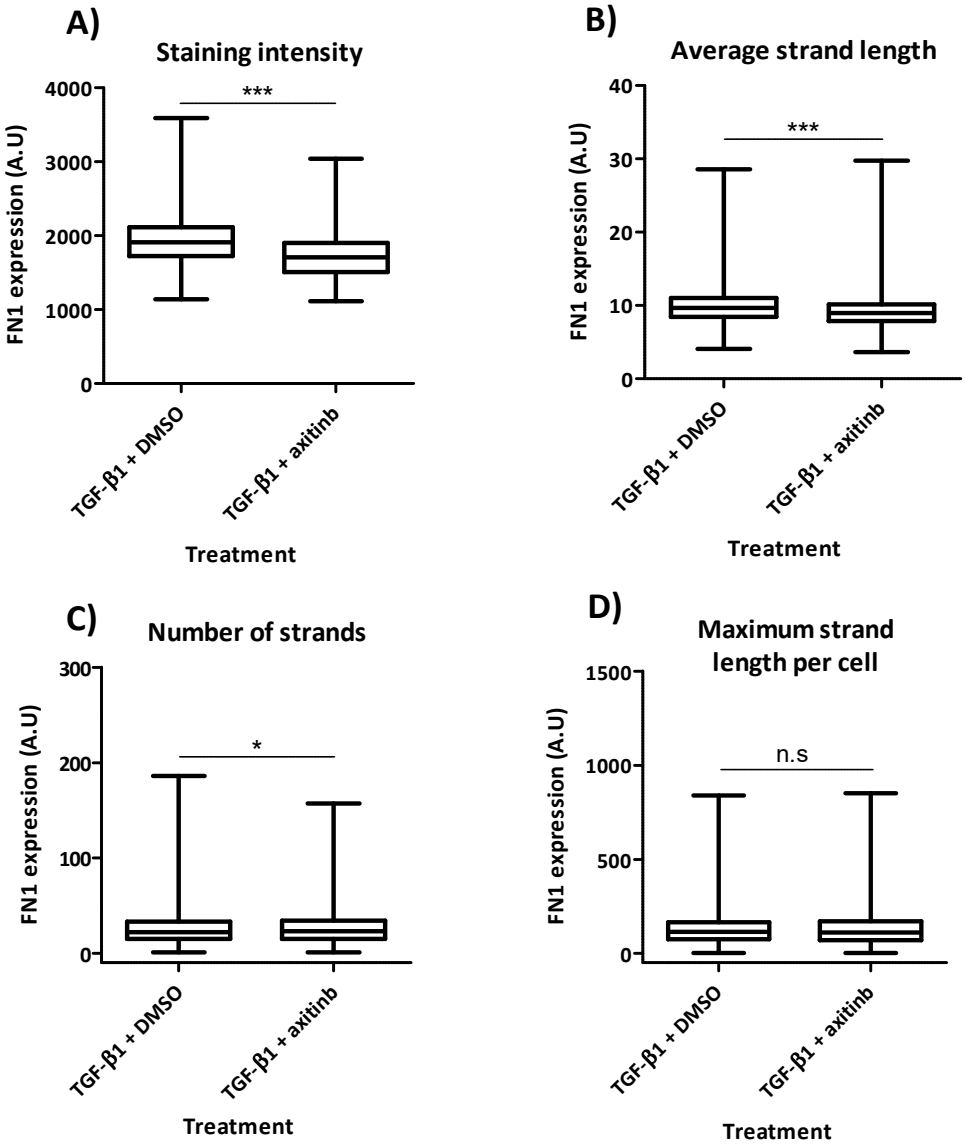

Figure 6. 4. Four measurements of fibronectin expression in TGF-β1-treated lung fibroblasts in the presence of drug axitinib.

Lung fibroblasts (strain 3) were plated in a 96-well plate and treated with DMSO or drug axitinib (10µM) for 48 hours and then TGF-β1 (5ng/ml) combined with either DMSO or drug axitinib (10µM) for a further 48 hours. Cells were stained for fibronectin and the immunofluorescent intensity (A), average strand length (B), number of strands (C) and maximum strand length (D) in individual cells (≤2000) was quantified (arbitrary units: A.U). ***p<0.001, Wilcoxon signed rank test. n.s = non-significant. Data shown represents the median ± interquartile range of one independent experiment.

To confirm which drugs significantly reduced the expression of α-SMA and fibronectin compared to DMSO in the presence of TGF-β1, R-studio was programmed so that drugs which significantly decreased marker expression reveal their true p-value and drugs that increased marker expression were automatically assigned a value of 1, to easily distinguish between the different outcomes on the MS Excel output generated by R-studio. This method was applied as my primary aim was to only identify drugs that reduced the expression of α-SMA and/or fibronectin. One example of cumulative frequency analysis is shown in **Figure 6.5** using α-SMA, whereby drug alfacalcidol significantly reduced α-SMA expression compared to DMSO and the p-value is 5.08E-33 (**Figure 6.5A**), whereas the drug bisoprolol increased α-SMA, hence the value generated was 1 (**Figure 6.5B**). This analysis was followed by the Wilcoxon signed rank test to compare the medians of fluorescence intensity of drug and DMSO-treated cells, demonstrating stringent statistical analyses were performed on the drug screen data.

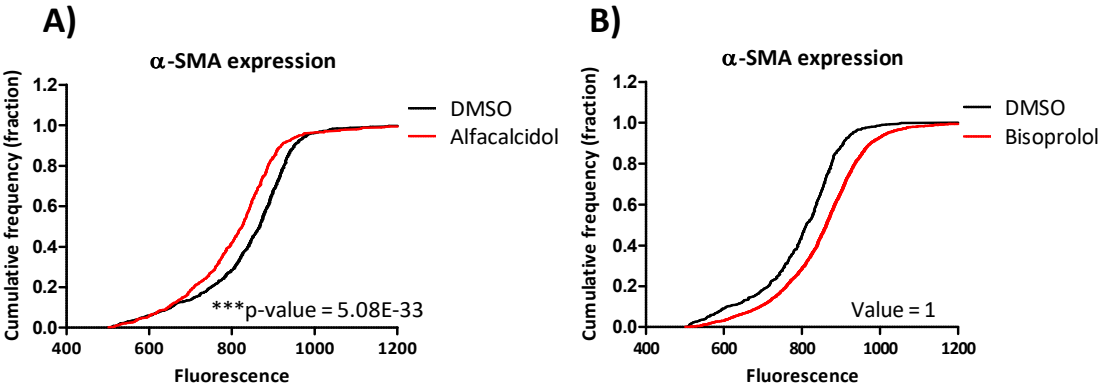

Figure 6. 5. Comparison of cumulative frequency results of α-SMA expressed by drug-treated lung fibroblasts.

Lung fibroblasts (strain 3) were plated in a 96-well plate and treated with DMSO or drug Alfacalcidol (A) or Bisoprolol (B) (10µM) for 48 hours and then TGF-β1 (5ng/ml) combined with either DMSO or drug (10µM) for a further 48 hours. Cells were stained using anti-α-SMA antibodies and the immunofluorescent intensity in individual cells was quantified. The cumulative frequency fraction (y-axis) represents the number of cells per fluorescence interval as a fraction of the total number of cells in the well. ***p<0.001, Kolmogorov-Smirnov test. Data shown represents mean fluorescence intensity per cell of one independent experiment.

The results of the complete drug screen are shown in **Table 6.1**, whereby drugs that significantly inhibited both α-SMA and fibronectin intensity in the presence of TGF-β1 compared to DMSO + TGF-β1-treated fibroblasts are presented. Only one set of p-values for each of these compounds are listed in **Appendix Table 1**, as calculated by the Kolmogorov-Smirnov test used for cumulative frequency, as it would be unfeasible to publish each graph and the second set of p-values measured by the Wilcoxon signed rank test. The drug library screen results shown represent one independent experiment, however a subset of drugs were tested in a second biological repeat and achieved the same results as the first experiment; these compounds are highlighted in **Table 6.1** with an asterisk.

As shown in **Table 6.1**, 46 FDA-approved compounds with various mechanisms significantly inhibited the expression of both α-SMA and fibronectin in TGF-β1-activated lung fibroblasts. The classes of drugs were broad and included anti-infective agents (i.e. antibiotics, antimycotics), tyrosine kinase inhibitors, ion channel blockers, phosphodiesterase inhibitors, non-steroidal anti-inflammatory drugs and hormones. In addition, the total number of cells in drug wells relative to DMSO are listed in **Table 6.1**, whereby most of the drugs did not exhibit toxicity, but increased cell numbers, indicating that reduced α-SMA and fibronectin was not a consequence of decreased numbers of cells in drug wells.

In addition, as part of a collaboration with Dr Angus Cameron (Barts Cancer Institute), who studies the role of the GTPase Rho signalling pathway in fibroblasts, I received 6 inhibitors of this pathway and included them in the same screen, though the Rho inhibitory drugs are non-FDA approved. **Table 6.2** shows the inhibitors of RhoA and Rho-kinase (ROCK) also significantly inhibited α-SMA and fibronectin expression in TGF-β1-treated lung fibroblasts.

A number of drugs also inhibited either α-SMA or fibronectin expression only. The overall results of the drug screen are summarised in **Figure 6.6**, which shows 184 compounds reduced α-SMA expression only in TGF-β1-treated lung fibroblasts and 132 compounds that significantly downregulated fibronectin expression relative to DMSO-TGF-β1-treated cells.

Table 6.1. FDA-approved drugs that significantly reduced α-SMA and fibronectin expression in TGF-β1-treated lung fibroblasts during high throughput screening. Drug screen: one independent experiment, *two independent repeats. The percentage (%) of cells represents the number of cells in drug wells relative to DMSO.

Drug name	Mechanism of action/Targets	Indication	% Cells
Anti-infectives			
Ofloxacin*	Antimicrobial, i.e. topoisomerase inhibitor	Infection	114
Marbofloxacin*	Antibiotic, i.e. topoisomerase inhibitor	Infection	120
Norfloxacin	Antibiotic, i.e. topoisomerase inhibitor	Infection	272
Chloramphenicol	Antimicrobial, binds the 50S ribosomal subunit	Infection	144
Cefaclor	Antibiotic	Infection	252
Flucytosine*	Antimycotic, pyrimide analog	Infection	254
Piperacillin sodium	Antibiotic, binds penicillin-binding proteins	Infection	183
Toltrazuril	Antiprotozoal agent	Infection	148
Sulfacetamide sodium	Antibiotic; inhibitor of bacterial para-aminobenzoic acid	Cardiovascular	237
Atazanavir sulfate*	HIV-1 protease inhibitor	Infection	139
Ritonavir	HIV-1 protease inhibitor	Infection	123
Tyrosine kinase inhibitors			
Axitinib	Tyrosine kinase inhibitor, i.e. VEGFR-2 and -3, PDGFR	Cancer	70
Erlotinib HCl	Receptor tyrosine kinase inhibitor, i.e. EGFR	Cancer	44
Gefitinib*	Selective tyrosine kinase EGFR inhibitor	Cancer	104
Ion channel blockers			
Carbamazepine	Sodium channel blocker	Neurological	155
Nicardipine HCl	Calcium-channel blocking agent	Neurological	125
Isradipine	Calcium channel blocker	Neurological	98
Chlorpropamide	Sulfonylurea; bind to ATP-sensitive potassium channels	Endocrinology	140
Tolperisone HCl	Ion channel blocker	Neurological	188
Phosphodiesterase inhibitors			
Tadalafil	Phosphodiesterase inhibitor	Cardiovascular	242
Pimobendan	Calcium sensitizer and phosphodiesterase inhibitor	Cardiovascular	118

Nonsteroidal anti-inflammatory drugs (NSAID)			
Benzydamine HCl	Inhibits prostaglandin biosynthesis	Inflammation	149
Sasapyrine	Inactivates COX-1 and COX-2	Inflammation	170
Hormones			
Estrone	Estrogenic hormone	Endocrinology	120
Tiratricol	Thyroid hormone analogue	Endocrinology	170
Various mechanisms			
Mesalamine	Mechanism not fully understood, but may block cyclooxygenase	Inflammation	115
Trichlormethiazide*	Diuretic, inhibits the sodium-chloride ion symporter	Cardiovascular	127
Rizatriptan benzoate	Serotonin receptor agonist	Neurological	234
Zolmitriptan*	Selective serotonin receptor agonist	Neurological	109
Enalaprilat dihydrate	Dicarboxylate-containing ACE inhibitor	Cardiovascular	167
Pilocarpine HCl	Nonselective muscarinic acetylcholine receptor agonist	Neurological	200
Biperiden HCl	Cholinergic receptor antagonist	Neurological	109
Lamivudine	Nucleoside analog reverse transcriptase inhibitor	Infection	124
Fludarabine	Inhibits DNA synthesis, purine analog	Cancer	125
1-Hexadecanol	A fatty alcohol used in drug preparations	-	194
Sevelamer HCl	Phosphate binding drug, prevents absorption	Cardiovascular	153
Pomalidomide	Inhibits production of TNF-α, inhibits ubiquitin ligase activity	Cancer	219
Abiraterone	Steroidal CYP17 inhibitor, i.e. cytochrome P450.	Cancer	136
Ramelteon	Selective melatonin receptor agonist	Neurological	198
Deoxyarbutin	Reversible inhibitor of tyrosinase activity	Cardiovascular	207
Teriflunomide	Prevents pyrimidine synthesis by inhibiting the mitochondrial enzyme dihydroorotate dehydrogenase	Immunology	186
Amoxapine	Inhibits glycine transporter 2 (GLYT2a) activity	Neurological	176
Misoprostol	Synthetic analog of prostaglandin E1	Endocrinology	125
Plerixafor	CXCR4 chemokine receptor antagonist	Immunology	226

Table 6.1; The drug library compounds, their mechanisms and indications were provided by SelleckChem (L1300). Abbreviations: VEGFR; vascular endothelial growth factor receptor, CYP17; cytochrome P450 17α-hydroxylase, HCl; hydrochloride, EGFR; epidermal growth factor receptor, HIV; human immunodeficiency virus, TNF-α; tumour necrosis factor-α, 5-HT; *5*-hydroxytryptamine, ACE; angiotensin-converting-enzyme, COX; cyclooxygenase.

Table 6. 2. RhoA pathway inhibitors that significantly reduced α-SMA and fibronectin expression in TGF-β1-treated lung fibroblasts during high throughput screening.

Results shown represent one independent experiment. The percentage (%) of cells represents the number of cells in drug + TGF-β1 wells relative to DMSO + TGF-β1.

Drug name	Mechanism of action/Targets	Indication	% Cells
Fasudil	Rho kinase inhibitor	Cardiovascular	160
Y27632	Rho kinase inhibitor	-	154

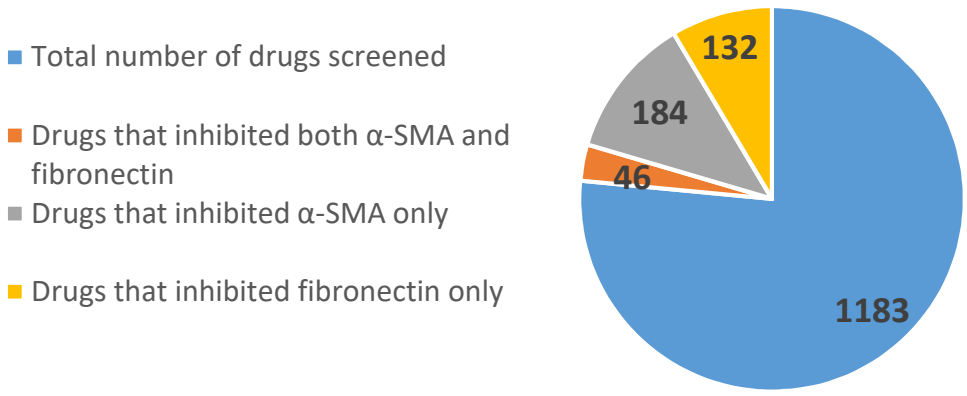

Figure 6. 6. Summary of the total number of drugs screened and the effect on α-SMA and fibronectin expression in TGF-β1-treated lung fibroblasts.

The expression of α-SMA and fibronectin was measured during a high throughput screen using 1,177 FDA-approved drugs and 6 additional Rho signalling pathway inhibitors in TGF-β1-treated lung fibroblasts.

Figure 6.7A-B shows many of the drugs that reduced α-SMA or fibronectin expression alone are known as anti-infective drugs, as they target bacterial/viral proteins. In addition, various receptors (e.g. serotonin, histamine, cholinergic), enzymes, (e.g. tyrosine kinases, COX-1/COX-2) and ion channels (potassium, sodium) were also among the common targets that reduced each marker.

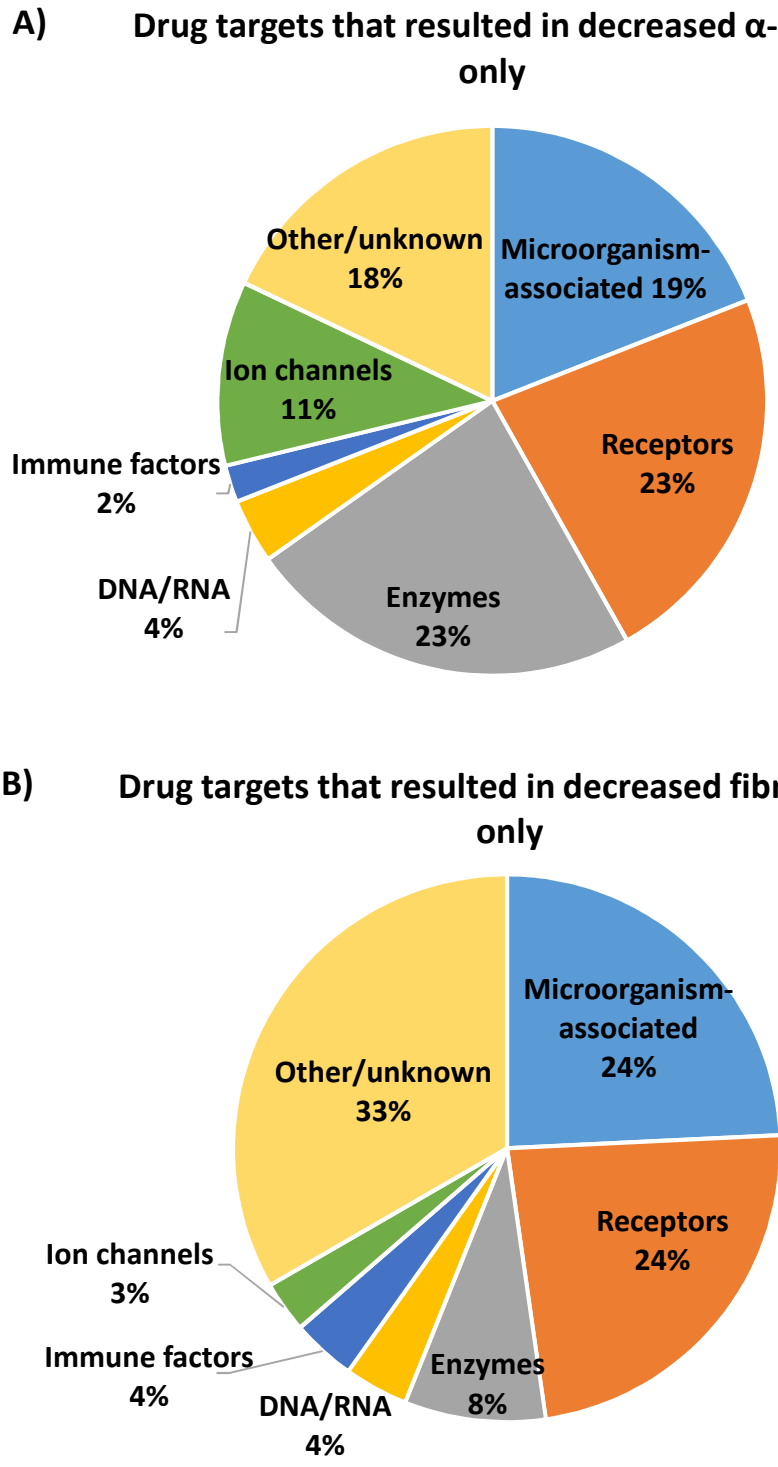

Figure 6. 7. FDA-approved drugs and their targets that only reduced α-SMA (A) or fibronectin (B) expression in TGF-β1-treated lung fibroblasts relative to DMSO + TGF-β1 treatment.

To note, microorganism-related targets are due to anti-infective agents, e.g. antibiotics, antifungal, antiviral drugs.

6.4. The validation of individual FDA-approved drugs on lung fibroblasts

While I was establishing the best method to analyse the whole screen, I chose to re-test hits from the first plate. According to a preliminary analysis assessing frequency distribution, three hits were identified; dasatinib, a BCR/ABL and Src kinase inhibitor, anastrozole; an aromatase inhibitor, and axitinib (listed in **Table 6.1**), which inhibits tyrosine kinase receptors VEGFR-1, -2 and -3[243]. (To note, more robust analysis of the drug screen completed after the following validation studies revealed dasatinib and anastrozole did not significantly reduce α-SMA and fibronectin). To validate and examine the potential of the hits identified, these three drugs were tested in experiments of cell viability, immunofluorescence, western blotting and collagen gel contraction.

6.4.1. The cell viability of lung fibroblasts treated with dasatinib, anastrozole and axitinib

The cell viability of unstimulated lung strain 3 fibroblasts in the presence of each drug (1-20μM) was assessed for 72 hours using a MTT assay. **Figure 6.8A** shows dasatinib significantly decreased cell viability below 50% at every concentration tested ($p<0.001$), which supported the results obtained during the drug screen, where dasatinib + TGF-β1 had similar effects at 10μM. As a result of dasatinib's toxic effect on cell numbers during both the drug screen and then the MTT assay, it was not used in further experiments.

In contrast, anastrozole increased viability relative to DMSO at 5μM and 20μM doses (**Figure 6.8B**), corresponding with the drug screen, as 10μM also increased cell number.

In addition, axitinib significantly reduced fibroblast viability, particularly at 10μM (48 ± 17%) and 20μM doses (**Figure 6.8C**), which was to a higher degree compared with the screen results, where cell number was reduced to 70% compared with DMSO-treated cells (**Table 6.1**).

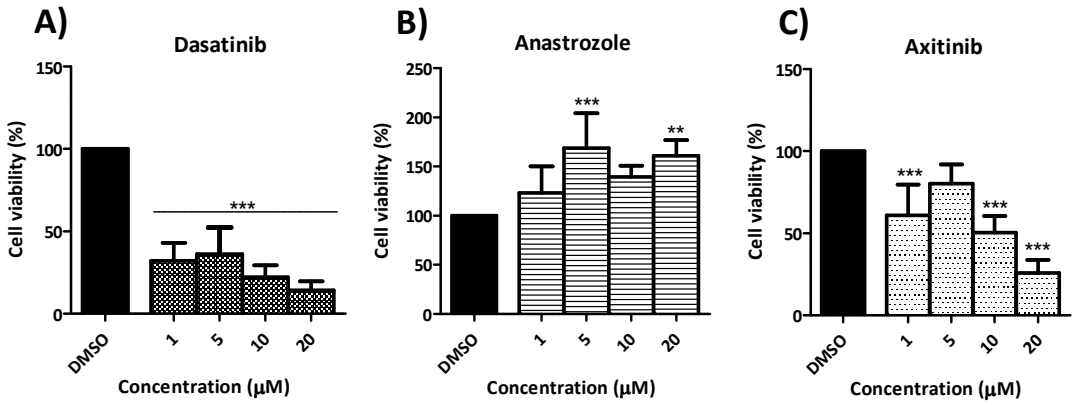

Figure 6. 8. The effect of dasatinib, anastrozole and axitinib on lung fibroblast viability.

Lung strain 3 fibroblast viability was assessed using a MTT assay after 72 hours culture in dilutions (μM) of DMSO, dasatinib (**A**), anastrozole (**B**) or axitinib (**C**). **p<0.01, ***p<0.001, one-way ANOVA with Dunnet's post-hoc to compare each concentration to DMSO control. Data shown represents the mean ± s.d of two independent experiments.

6.4.2. The expression of α-SMA and fibronectin protein by lung fibroblasts treated with anastrozole and axitinib

To validate the results of the drug screen, the changes in α-SMA and fibronectin protein expressed by lung fibroblasts were validated using immunofluorescent staining on coverslips in a 24-well plate and western blotting. To emulate the drug screen, fibroblasts were also treated with anastrozole or axitinib (10μM) first for 48 hours and then in combination with TGF-β1 (5ng/ml) for a further 48 hours.

Figure 6.9 shows the analysis of the average mean fluorescence intensity per lung fibroblast, which was seeded on coverslips and stained with the same anti-α-SMA and anti-fibronectin antibodies used during the drug screen. According to the more robust analysis of the drug screen data, anastrozole did not significantly affect the expression of either marker, which was also supported by the coverslip staining of α-SMA (**Figure 6.9A**) and fibronectin (**Figure 6.9B**) compared to DMSO + TGF-β1. Surprisingly, axitinib significantly reduced α-SMA, but not fibronectin (**Figure 6.9A-B**). This was also illustrated in representative images from this experiment (**Figure 6.9C**) of drug + TGF-β1-treated lung fibroblasts.

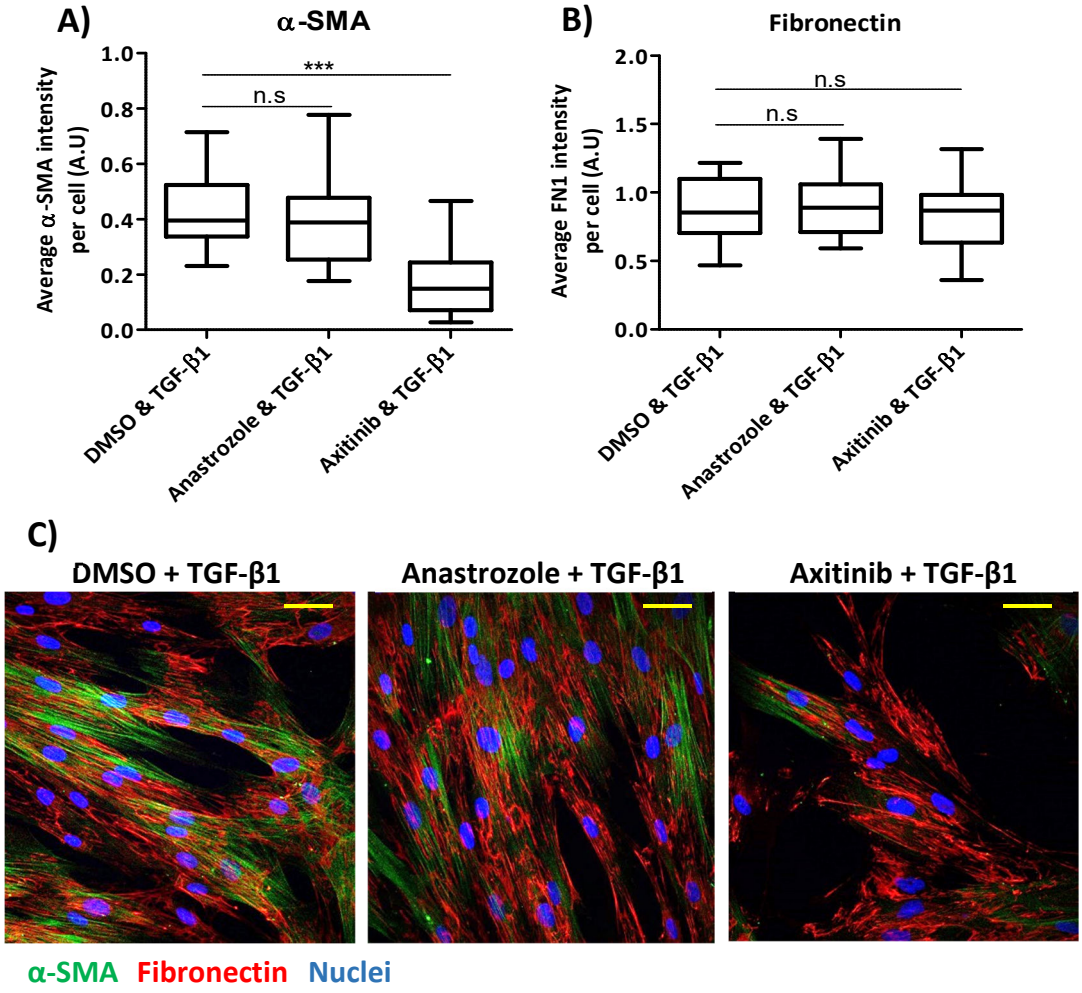

Figure 6. 9. Immunofluorescent staining of α-SMA and fibronectin in anastrozole or axitinib-treated lung fibroblasts in the presence of TGF-β1.

Lung fibroblasts (strain 3) were plated on coverslips and treated with DMSO, anastrozole or axitinib (10μM) for 48-hours and then TGF-β1 (5ng/ml) combined with either DMSO or drug (10μM) for a further 48-hours. Cells were stained using anti-α-SMA (green) or anti-fibronectin (red) antibodies and the mean fluorescence intensity in each field was quantified (**A, B**) (arbitrary units: A.U) and imaged (**C**), approximately 20 fields were imaged per condition. **p<0.01, ***p<0.001, Wilcoxon signed rank test. n.s: non-significant. Data shown represents the median ± interquartile range of one independent experiment. Scale bar: 50μM.

Next, α-SMA protein expression was investigated using western blotting (**Figure 6.10A**). The same experimental design of the drug screen was again performed here, but cell lysates were subsequently collected. In addition, two concentrations of drug were tested (1μM and 10μM) to examine whether a lower concentration of 1μM would also reduce the expression of myofibroblast marker α-SMA.

Densitometry in **Figure 6.10B** shows α-SMA expression in DMSO + TGF-β1-treated fibroblasts increased 5.7-fold compared to DMSO + vehicle treatment. The addition of 1μM anastrozole + TGF-β1 resulted in 3.3-fold α-SMA above vehicle, while the addition of 1μM axitinib upregulated only 1.6-fold α-SMA in response to TGF-β1. **Figure 6.10C** shows the use of 10μM treatment, where again axitinib produced less α-SMA in response to TGF-β1 than DMSO + TGF-β1. The 10μM anastrozole + vehicle sample could not be quantified here as the very faint band present would lead to inaccurate quantification and is therefore missing from the graph in **Figure 6.10C**. The levels of α-SMA were then directly compared in vehicle-treated samples only (**Figure 6.10D**) to determine whether the compounds stimulated baseline expression of α-SMA above the DMSO control. As shown in **Figure 6.10D**, anastrozole had no notable effect on α-SMA, while 1μM axitinib raised basal α-SMA expression, whereas 10μM did not produce a change. Next, in **Figure 6.10E** α-SMA was directly compared in only TGF-β1 stimulated cells to validate the previous immunofluorescent staining results obtained in the drug screen and the coverslip staining. **Figure 6.10E** shows anastrozole reduced α-SMA at both 1μM and 10μM concentrations by 23% and 11%, respectively, while axitinib was only effective at the 10μM dose, which reduced α-SMA expression by 34% in the presence of TGF-β1. Regrettably, I did not have time to perform western blotting for fibronectin on these samples.

Taken together with previous immunofluorescent staining analysis, these results show that 10μM anastrozole did not affect α-SMA or fibronectin expression significantly, yet 1μM appeared to reduce α-SMA, though western blotting requires additional biological repeats. In addition, axitinib reduced α-SMA during staining and western blotting experiments, while there was no effect on fibronectin expression in TGF-β1-stimulated lung fibroblasts. To determine whether these effects had functional implications, both drugs were studied in collagen gel contraction assays.

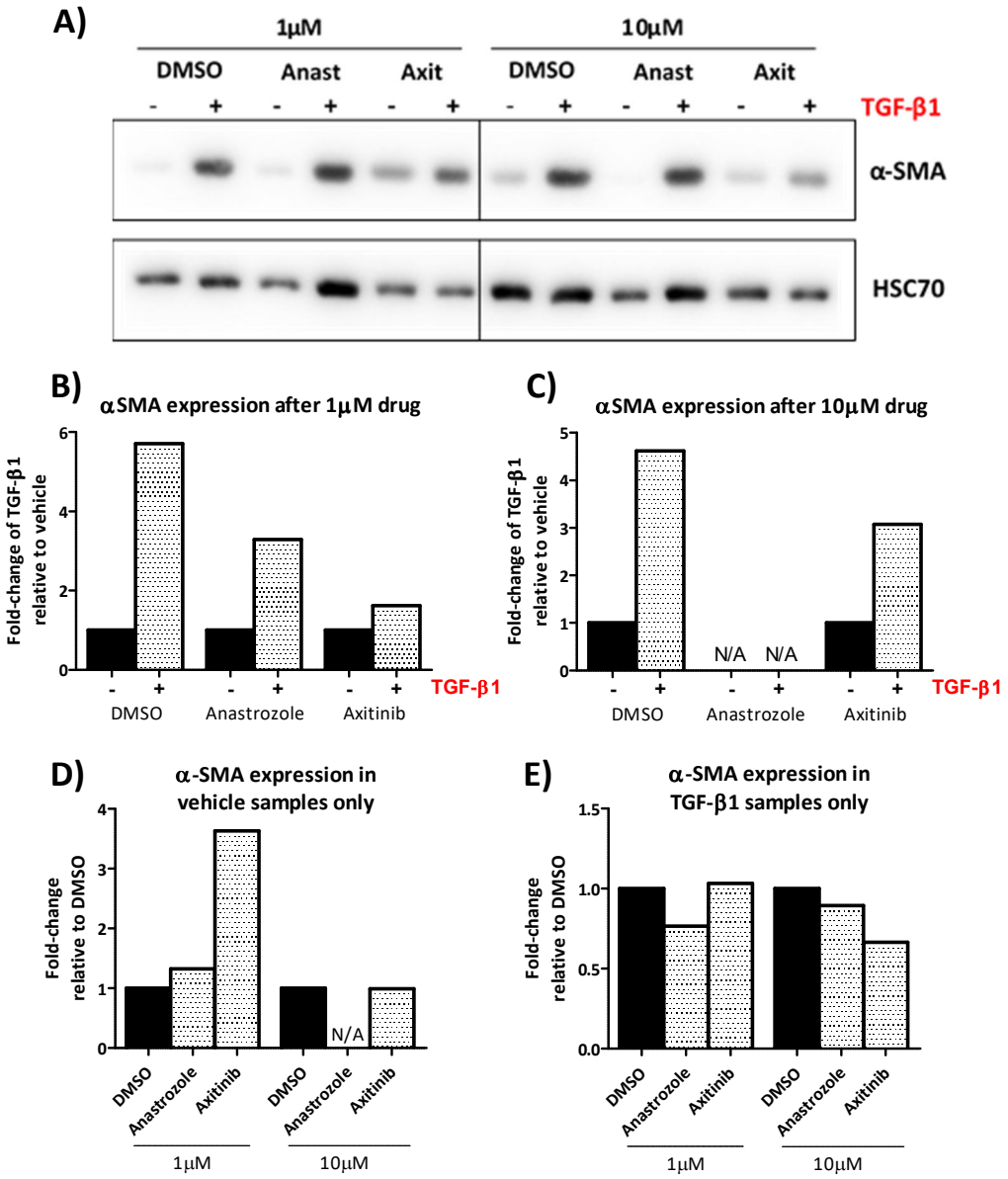

Figure 6. 10. Western blot analysis of α-SMA expression in drug-treated lung fibroblasts with and without TGF-β1.

Lung fibroblasts (strain 3) were treated with DMSO, anastrozole (anast) or axitinib (axit) at 2 different concentrations (1μM and 10μM) for 48-hours and then stimulated with vehicle or TGF-β1 (5ng/ml) combined with either DMSO or drug for a further 48-hours and lysates collected and immunoblotted for α-SMA (**A**). The analyses are presented as vehicle vs TGF-β1 for each concentration (**B**, **C**) and DMSO vs drug in only vehicle (**D**) or TGF-β1 samples (**E**). As there is no band for vehicle + anastrozole (10μM), densitometry could not be conducted (N/A). HSC70 serves as loading control. Data shown represents the mean of one independent experiment.

6.4.3. Collagen gel contraction by lung fibroblasts treated with anastrozole and axitinib

To examine whether anastrozole and axitinib affected myofibroblast activity, collagen gel contraction was studied. Lung strain 3 fibroblasts were first treated with 10μM drug or DMSO for 48 hours in petri dishes and then plated inside collagen type I gels with fresh drug. The next day, gels were detached from the edge using a needle and vehicle or TGF-β1 (5ng/ml) was added on top of the gels. **Figure 6.11A-C** shows representative images taken of gels in each condition 10 days after the addition of vehicle/TGF-β1. The analysis in **Figure 6.11D** compares the surface area of only vehicle-treated gels and shows both anastrozole (**Figure 6.11B**) and axitinib (**Figure 6.11C**) contracted gels 50% and 20% more than DMSO (**Figure 6.11A**), respectively.

When examining the response of each drug-treated fibroblast to TGF-β1 (**Figure 6.11E**), DMSO gels contracted by 60% in response to TGF-β1, visible in **Figure 6.11A**, while anastrozole contracted gels to a similar size in the absence and presence of TGF-β1 and did not inhibit gel contraction relative to DMSO + TGF-β1 gels. Interestingly, axitinib + TGF-β1-treated fibroblasts exhibited notably reduced gel contraction compared to DMSO + TGF-β1, hence the gels were much larger (**Figure 6.11C**) and there was no difference in gel sizes between axitinib + vehicle and TGF-β1-treated gels (**Figure 6.11E**).

Overall, this drug library screen has generated 46 compounds of interest that inhibited two key markers of fibroblast activation, which now need to be examined further. In addition, this preliminary drug validation of dasatinib, anastrozole and axitinib demonstrated the reliability of the screen (marker expression studies summarised in **Table 6.3**), while tyrosine kinase inhibitor axitinib displayed promising results in its capacity to perturb myofibroblast activity.

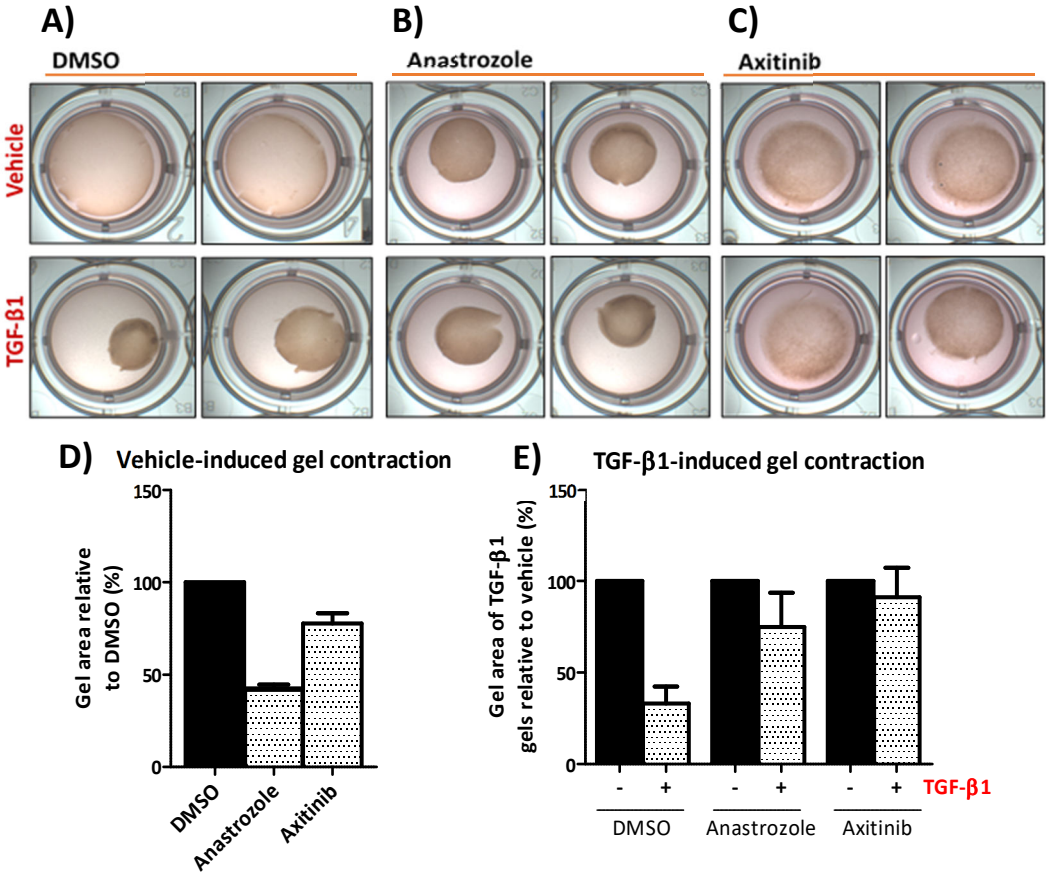

Figure 6. 11. Collagen gel contraction by anastrozole and axitinib-treated lung fibroblasts.

Strain 3 lung fibroblasts were treated with DMSO, anastrozole or axitinib (10µM) for 48 hours in petri dishes and then trypsinised and plated inside collagen type I gels with fresh drug (10µM) and stimulated the next day with vehicle or TGF-β1 (5ng/ml). Representative images of collagen gel contraction were taken at day 10 after either vehicle of TGF-β1 addition (**A-C**). Analysis shown as gel area of drug + vehicle relative to DMSO + vehicle (**D**) and vehicle vs TGF-β1 per drug (**E**). Data shown represents the mean ± s.d of one independent experiment with triplicate wells.

Table 6. 3. Summary of anastrozole and axitinib effects on marker expression during drug screen, immunofluorescent staining (IMF) and western blotting (WB).

		α-SMA	Fibronectin
Anastrozole	**Drug screen**	No change	No change
	IMF	No change	No change
	WB	Reduced	--
Axitinib	**Drug screen**	Reduced	Reduced
	IMF	Reduced	No change
	WB	Reduced	--

6.5. Discussion

The aim of this study was to identify novel pathways that regulate lung fibroblast activation by applying a library of 1,177 FDA-approved drugs and Rho signalling pathway inhibitors on to lung fibroblasts in the presence of TGF-β1. As a result, several drugs of varying mechanisms were identified that significantly reduced the expression of both α-SMA and fibronectin in TGF-β1-activated fibroblasts. These results suggested several unknown molecular pathways that may regulate TGF-β1-induced myofibroblast activity.

Further experiments for validation included MTT assays, which confirmed the cytotoxic effects of dasatinib and supported the results of anastrozole and axitinib also. Analysis of total cell numbers during the drug screen revealed many drug hits that significantly inhibited α-SMA and fibronectin expression, actually increased fibroblast numbers compared with DMSO + TGF-β1-treated wells. Although, it is unknown what effect these fibroblasts would have in diseased tissues if this translated *in vivo*. Repeated proliferation assays using the hits identified from the screen are first needed to confirm whether these drugs truly increase fibroblast numbers. Instead, it is possible that during the drug screen DMSO + TGF-β1-treated wells had consistently lower cell numbers than other wells, as these wells were at the edge of the 96-well plate, where higher levels of evaporation can occur, which may contribute to 'edge effects'.

In addition, protein expression studies validated the actions of anastrozole, which did not alter the expression of α-SMA or fibronectin in either the drug screen or post-immunofluorescent staining experiments. Although, additional biological repeats of western blotting are needed to further validate these results. Treatment with axitinib also supported the results of the drug screen, as post-immunofluorescent staining and western blotting displayed decreased α-SMA in lung fibroblasts. However, fibronectin showed no significant change after the addition of axitinib in post-immunofluorescent staining experiments, although perhaps more data points are required as axitinib also reduced fibroblasts numbers compared to DMSO controls, visible in **Figure 6.9C**.

To examine whether the selected drugs could affect the functional capacity of the TGF-β1-stimulated fibroblasts, gel contraction assays were conducted whereby only axitinib notably inhibited contraction. Axitinib was approved by the FDA in 2012[244] and is also currently used in the UK as second-line treatment for advanced renal cell carcinomas[245]. Axitinib primarily functions by inhibiting the autophosphorylation of VEGF receptors -1, -2 and -3 and has shown to reduce the phosphorylation of Akt and ERK1/2 in endothelial cells *in vitro*, although axitinib has also been described to target PDGF receptors[243]. The effects of axitinib on fibroblasts are supported by Lin and colleagues, who pre-treated hepatic stellate cells with TGF-β1 and then administered 50nM axitinib and found gel contraction was significantly prevented. This demonstrates axitinib had similar effects on cells pre-exposed to TGF-β1, which is an important feature of drugs that may be used to clinically treat fibroblasts already activated by TGF-β1 in the tumour microenvironment. Furthermore, Lin et al. also reported that axitinib-treated stellate cells secreted significantly less VEGF into culture medium and expressed less phosphorylated VEGFR-2 in the presence of TGF-β1, while the addition of VEGF increased gel contraction. This suggests that axitinib inhibited contraction as a result of VEGF receptor blockade and not by inducing alternative effects, such as cell death[246].

Huang and colleagues recently demonstrated that axitinib reduced dermal fibroblast migration and proliferation during scratch wound assays. They also compared the effects of tyrosine kinase inhibitor nintedanib, which inhibits multiple key pathways, including PDGF, VEGF and FGF receptor signalling, and had more potent effects on fibroblast migration and TGF-β1-induced α-SMA and fibronectin expression than the selective inhibition of each pathway. Nintedanib is currently in Phase III clinical trials for cancer treatment and has been approved for the treatment of idiopathic pulmonary fibrosis[247], indicating the benefits of a multifaceted approach to drug targeting. Axitinib is also currently under-investigation for combination treatment in advanced non-small cell lung carcinoma[248], thyroid[249] and pancreatic cancers[250], demonstrating the therapeutic potential of tyrosine kinase inhibitors.

Surprisingly, several effective drugs were classed as ‘anti-infective agents’, as their primary roles were described as targeting the DNA/RNA or protein components of

particular microorganisms. Although initially it was reported that many of these drugs target bacterial DNA gyrase to prevent DNA replication and thereby inhibit rapid bacterial proliferation, later studies demonstrated their mechanism of action includes inhibiting similar mammalian enzymes, such as topoisomerases I and II, therefore these drugs can also inhibit mammalian cell proliferation[251]. In consequence, these compounds have also been investigated for their anti-tumour activity. The anti-proliferative effect of norfloxacin was previously noted on a non-small cell lung carcinoma cell line *in vitro*[252] and ofloxacin in bladder carcinoma cells[253], both of which also significantly downregulated α-SMA and fibronectin expression in HLFs. Moreover, norfloxacin has also shown to induce mitochondrial damage in dermal fibroblasts[254], however these drugs did not lower cell number during the drug screen, as detected by joint DAPI and CellMask staining, indicating they acted by an alternative, unknown mechanism in lung fibroblasts.

ROCK inhibitors Fasudil and Y27632 also significantly inhibited α-SMA and fibronectin expression in HLFs. The Rho family of small GTPases transmits mechanical forces through the actin cytoskeleton by regulating actin reorganisation after RhoA activates downstream kinases, including ROCK and myosin light chain kinase, therefore this signalling pathway is important during cell motility and contraction[255]. In return, the Rho-activated pathway also responds to the detection of stiff matrices, as RhoA mediates stretch induced α-SMA expression and actin filament assembly in cardiac fibroblasts, via co-transcription factor MRTF-A, demonstrating the mechano-responsive nature of the Rho signalling pathway[256]. In addition, previous reports show TGF-β1 stimulation increases RhoA activation[257] and in human embryonic lung fibroblasts, Y27632 significantly reduced the expression of α-SMA protein and fibronectin detected in cell supernatents in the presence of TGF-β1, supporting the results of the drug screen.

The Rho pathway may also mediate feedback loops, as RhoA, RhoC and Smad2 exhibited reduced gene expression after inhibition of downstream ROCK, which indicates targeting this pathway may prevent continued myofibroblast activity[258]. It also appears Rho-ROCK signalling is required for fibronectin assembly in TGF-β1-treated lung fibroblasts, as recent data suggests contractile activity may facilitate the

assembly of fibronectin. This is supported by siRNA-mediated knockdown of α-SMA, which attenuates fibronectin matrix formation, although this mechanism requires further investigation[259].

RhoA appears to regulate myofibroblast differentiation via the generation of NADPH oxidase-derived reactive oxygen species (ROS), which conduct intracellular signals and promote TGF-β1-induced fibroblast differentiation in lung[260], cardiac[261] and prostate[262] tissues. The link between the Rho pathway and NADPH oxidase NOX4 was investigated in renal fibroblasts, where TGF-β1 increased NOX4 protein, NOX4 regulator Poldip2 and intracellular ROS levels. Each of these factors was abrogated by RhoA siRNA and ROCK inhibitor Y27632, indicating Poldip2-NOX4 functions downstream of RhoA. Furthermore, inhibition of ROCK significantly decreased TGF-β1-induced α-SMA and fibronectin isoform EIIIA expression, which was rescued by the overexpression of Poldip2[263]. This indicates that Rho mediates fibroblast-myofibroblast differentiation via a RhoA-ROCK-Poldip2-NOX4 axis. Furthermore, in my own RNAseq experiments, NOX4 was upregulated by an average of 24-fold in TGF-β1-treated lung fibroblasts relative to vehicle, indicating the same pathway could exist in these cells.

The potential therapeutic efficacy of ROCK inhibitor fasudil was demonstrated in a bleomycin-induced model of pulmonary fibrosis[264]. RhoA/ROCK signalling is activated in fibrotic tissues[265], while the *in vivo* administration of fasudil reduced collagen crosslinking, as measured by hydroxyproline content. Furthermore, the expression of TGF-β1-regulated genes implicated in pulmonary fibrosis were also examined in these fibrotic tissues. As expected, bleomycin increased TGF-β1, CTGF, PAI-1 and α-SMA mRNA and protein levels, while fasudil significantly downregulated the expression of each marker[264]. However, further studies are needed to determine the transcription factors activated downstream of ROCK, which may be involved in regulating these genes.

The drug screen analysis also demonstrated overlap with the RNA sequencing results. The drug screen indicated several potassium and sodium ion channel blockers regulated α-SMA and fibronectin expression by HLFs. Coincidently, RNA sequencing

analysis of membrane-associated factors (**Table 5.3**) showed TGF-β1 significantly upregulated several types of potassium (up to 60-fold) and sodium ion channel genes (up to 12-fold) in HLFs derived from the same donor, as those used in the drug screen. Although it has previously been reported that potassium channels that were upregulated in HLFs (genes KCNN4, KCNH1) are also expressed by tumour cells and promote proliferation and migration, their role in lung fibroblasts is undefined[266]. In addition, non-steroidal anti-inflammatory drugs that target COX-1/COX-2 proteins, such as benzydamine and sasapyrine also prevented the expression of the two HLF activation markers, while RNA-seq showed the COX-2 gene (PTGS2) was increased 2.5-fold in response to TGF-β1 stimulation.

Previous reports suggest particular phosphodiesterase subtypes (PDE4B and PDE4D) regulate TGF-β1-induced lung fibroblast to myofibroblast conversion and collagen contraction[267, 268], while my own RNA-seq data revealed PDE4D was elevated 2.9-fold after stimulation. Furthermore, PDE5 inhibitors prevented HLF activation during the drug screen, although whether they also target the PDE4 subtype is unknown. Overall, these results have identified targets that may be enriched in activated lung fibroblasts and concurrently, may have the potential to regulate their activity, though there is much still to discover about their mechanisms of action.

During the drug screen analysis, it also became clear there were a number of drugs that specifically inhibited α-SMA expression, but not fibronectin, and vice versa. Although recent studies suggest fibroblast contractile activity is needed for fibronectin assembly[259], the results of the drug screen indicates separate mechanisms exist to regulate the contractile and ECM-secreting phenotype of myofibroblasts. Transcription factors myocardin and serum response factor promote α-SMA gene expression[269], therefore perhaps fibronectin-specific transcription factors also exist, which account for the drug-induced inhibition of fibronectin and not α-SMA. Unpicking the mechanisms by which these drugs act would provide a more detailed understanding of contractile and matrix-secreting fibroblasts and potentially allow manipulation of fibroblasts towards either phenotype.

Overall, these results have demonstrated that examining α-SMA and fibronectin expression by high throughput phenotypic screening is an effective method for identifying drugs that modulate TGF-β1-induced fibroblast activation. The reliability of the assay was also validated in later experiments, albeit using three selected drugs. To further identify potential drug targets, hits should be sub-selected by examining their effects during functional assays, such as fibroblast gel contraction and 3D invasion. To establish the mechanism by which these drug hits are acting, likely target molecules as indicated in online drug databases and key signalling molecules should be studied using siRNA-mediated knockdown and western blotting to define the downstream pathways activated in lung fibroblasts. This is in the hope that select pathways, which effectively regulate the myofibroblast phenotype can provide novel targets for the treatment of cancer and lung fibrosis.

CHAPTER VII. CONCLUSION

TGF-β1 has a key role in activating fibroblasts during tissue injury to promote wound repair via the secretion of matrix proteins and growth factors, in addition to fibroblast-mediated contraction to induce wound closure[270]. However, in the presence of tumours that secrete excessive amounts of TGF-β1, fibroblasts can become chronically activated and promote tumour progression by the exploitation of their wound healing properties[215]. Therefore, although previous studies have documented fibroblast intra- and inter-tissue heterogeneity[134, 165], it was surprising that few studies had compared the responses of fibroblasts from different tissues to TGF-β1 stimulation. This study has shown fibroblasts derived from skin, lung and breast tissues exhibited differences in gene expression when activated with TGF-β1. Common genes, such as ACTA2, TIMP3, FN1 and CTGF were differentially expressed between fibroblasts from the three tissues, though fibroblasts derived from the same tissue, but different donors also displayed some heterogeneity. Future studies involving fibroblasts from additional donors would determine if these differences are characteristic of skin, lung and breast tissues and perhaps aid the identification of tissue-specific markers of fibroblast activation. The evidence of differential responses by fibroblasts to TGF-β1 is supported by Lygoe and colleagues, who also found α-SMA was differentially expressed in three tissue fibroblasts in response to TGF-β1[64]. This study has extended these findings by comparing eight markers of fibroblast activation in cells derived from additional tissues.

Although previous studies described individual integrin subunits that are upregulated by TGF-β1[60, 191], few studies had characterised the complete TGF-β1-induced integrin expression profile in fibroblasts. This study provides evidence of differential integrin expression in skin, lung and breast fibroblasts, particularly at the mRNA level of subunits including, α1, α4 and α11. However, I am aware that further experimentation is required to determine the levels of integrin protein, particularly using flow cytometry before and after TGF-β1 stimulation. This new information would indicate whether heterogeneity of myofibroblasts extends to integrins expressed on the cell surface. Additionally, experiments involving the characterisation of phosphorylated signalling proteins downstream of activated

integrins, such as FAK, Src and ERK1/2 would determine whether changes in integrin activity occur alongside or instead of increases in integrin expression.

Myofibroblasts appear to maintain their own autocrine signalling after initial activation. A recent study by Eberlein and colleagues demonstrated that although αvβ6-dependent activation of TGF-β1 by lung tumour cells was necessary to induce a myofibroblast phenotype, once fibroblasts were activated only direct TGF-β receptor inhibition of myofibroblasts reduced α-SMA expression[87]. This suggested that targeting myofibroblasts directly in established tumours may be an effective therapeutic strategy to reduce progression, while previous studies suggest particular fibroblast integrins are capable of mediating the TGF-β1-induced phenotype[64]. In this study, the use of small-molecule integrin inhibitors and siRNA-mediated knockdown indicates different integrins are involved in regulating the same myofibroblast functions depending on the tissue of origin. In particular, the invasion assays performed with pan-αv, cilengitide and αvβ1 integrin inhibitors significantly reduced skin myofibroblast invasion, whereas cilengitide promoted the invasion of lung and breast myofibroblasts, perhaps suggesting αvβ3 and αvβ5 integrins have distinct mechanisms of action in these cells. In addition, these inhibitors were unable to modulate myofibroblast-induced collagen contraction, in contrast to siRNA-mediated silencing of, particularly, the β5 subunit which prevented collagen contraction by skin, lung and breast myofibroblasts. Although knockdown of integrin protein at the cell surface was not confirmed, these results suggest that integrins may regulate contraction by intracellular signalling or physical contact with the actomyosin network, as blockade of the extracellular ligand binding site was ineffective. In addition, integrin inhibition was limited to the peptide inhibitors supplied by my sponsor GSK. With additional time and money, I would like to have also used integrin-blocking antibodies.

Collagen contraction also was regulated by different integrins in skin, lung and breast myofibroblasts. Collagen receptor α1β1 integrin appeared to be a potent regulator of breast fibroblast-mediated contraction in the presence of TGF-β1, but not in skin or lung. Although α1β1 has previously demonstrated a role in cardiac fibroblast-

mediated collagen contraction[271], additional biological repeats are essential to determine whether these are strain- or tissue-specific responses.

Modulation of integrin subunits α11, β3 and β5 also exhibited roles in regulating TGF-β1-induced gel contraction and gene expression. These results are supported by additional research suggesting α11β1 regulates corneal myofibroblast differentiation[61] and collagen contraction *in vitro*[74], and tissue stiffness *in vivo*, which was associated with promotion of lung tumour growth and invasion. Previous studies of αvβ3 and αvβ5 integrins revealed contraction mediated by these integrins in cardiac[125] and lung fibroblasts[272] was necessary for the activation of latent TGF-β1. In addition, in my own studies it is unknown whether integrin silencing of collagen receptors α1 and α11 prevented adhesion of fibroblasts to collagen during contraction assays (**Figure 4.6-4.9**), which could be resolved using adhesion assay experiments by plating fibroblasts on collagen-coated Transwells in combination with integrin inhibitors and siRNA.

In addition, though my findings indicate β3 and β5 integrins modulate TGF-β1 signalling in skin, lung and breast fibroblasts, Henderson and colleagues demonstrated that fibroblast-specific knockout of β3 and β5 integrins in hepatic stellate cells did not affect collagen expression and collagen cross-linking in mouse models of liver fibrosis[130]. In 2015, Sheppard and colleagues revealed that αvβ1 may have been the integrin responsible for significantly reducing organ fibrosis in the Henderson study[38], potentially demonstrating heterogeneity between fibroblasts of different tissue types. In addition, in my own experiments using the same small-molecule αvβ1 inhibitor used by Sheppard, skin fibroblast invasion was significantly reduced in two strains of skin fibroblasts. Therefore, additional functional assays using skin fibroblasts are warranted where the effects of αvβ1 blockade are further explored to understand the function of this integrin, as much is still unknown about its biology, as there are no αvβ1-specific antibodies to interrogate cells and tissue samples.

Due to lack of time, the mechanism by which integrins regulated the myofibroblast phenotype in these TGF-β1-activated skin, lung and breast fibroblasts was not

investigated. According to previous research, potential molecules that may mediate both TGF-β1 and integrin signalling includes focal adhesion kinase[28] and integrin-linked kinase[67], although additional mechanisms may exist, including the physical association of TGF-β receptors and integrins and interaction via novel intermediary proteins. Further research into this area is required to establish this mechanism and to determine whether fibroblasts from different tissues utilise the same pathways.

The ability of integrins to regulate TGF-β1-induced functions, as found in this study provides the foundation to continue the investigation into the role of integrins in myofibroblast activation and activity. Better reagents to integrins such as α11 and β8 are required to facilitate their characterisation in both untreated and TGF-β1-exposed fibroblasts. The findings revealed in this study also support the hypothesis that α11β1 integrin may regulate myofibroblast activity[210], particularly in those derived from skin and lung tissue, though development of a blocking antibody or small-molecule inhibitor targeting α11 is needed to better evaluate its role in myofibroblast biology. This is in the hope that this research could progress to the use of *in vivo* models of fibroblast-specific α11 and β5 knockout (which also modulated collagen contraction), where their potential as therapeutic targets in cancer and organ fibrosis could be further assessed, as these studies are lacking in the current literature.

In addition, the invasion assays conducted using integrin inhibitors involved Transwells coated with a thin layer of Matrigel. The next step to develop this data would involve the use of mini-organotypic invasion assays (as displayed in **Figure 3.9**), to examine the effects on co-cultured tumour cells, when targeting fibroblasts in a 3D environment that better models tumour-stromal cell interactions. Furthermore, the effects of fibroblast culture on softer matrices, such as an organ-derived ECM could be examined, as the cells used in the experiments performed were all cultured on plastic. It is known that fibroblasts are responsive to the tension held in matrices they are adhered to[176], therefore it is possible that culture on plastic primed these skin, lung and breast fibroblasts towards activation, as noted by the α-SMA protein expressed in untreated skin strain 2 fibroblasts. Therefore, *in vitro* systems that

better mimic the normal tissue and tumour microenvironment would better represent TGF-β1-induced changes in fibroblast biology.

RNA sequencing of TGF-β1-stimulated lung fibroblasts revealed a variety of genes were up- and downregulated by this cytokine, many of which were similar to those identified in wound healing signatures of fibroblasts[223], which could be exploited in the presence of transformed epithelial cells[215]. Perhaps then unsurprisingly, these activated lung fibroblasts expressed genes associated with cancer-related networks, including various collagens and collagen cross-linking genes that were upregulated by TGF-β1. These factors are also relevant to organ fibrosis, whereby fibroblast activation is mediated by integrin-dependent activation of latent-TGF-β1[124]. This suggests that the availability of active TGF-β1 in these tissues may dictate the level of fibrosis that occurs, while the stiffened matrix may further promote integrin expression and myofibroblast-mediated ECM contraction, thereby activating additional TGF-β1, resulting in a continuous cycle of uncontrolled TGF-β1 activation[16]. Therefore, perhaps dampening myofibroblast activity could reduce features such as matrix stiffness and subsequent tumour progression/organ fibrosis[95].

Previous studies demonstrate CAFs express pro-inflammatory genes, which are associated with promoting cancer cell invasion. RNA sequencing revealed TGF-β1 exposed fibroblasts also upregulated several pro-inflammatory genes, such as IL6[137] and TGFB1[89], which are reported to promote cancer cell growth and EMT. Additionally, previous research suggests αvβ8 regulates chemokine CCL2 secretion from IL-1β-treated lung fibroblasts[185]. However, in this study β8 and CCL2 were each downregulated in response to TGF-β1, though it is unknown whether alternative integrins regulate inflammation-associated genes in TGF-β1-treated fibroblasts.

In addition, although RNA-seq revealed the TGFB1 gene was increased after stimulation, TGF-β1 signalling genes, including TGFBR2 and SMAD3 were downregulated, suggesting a negative feedback loop. These results coincide with cancer-associated fibroblasts[219] and fibroblasts derived from chronic

wounds[273], which also exhibit downregulated type II TGF-β receptors, demonstrating TGF-β1 stimulation of healthy fibroblasts mimics the phenotype of fibroblasts in the presence of tumours. Moreover, it is currently unknown whether TGF-β receptor downregulation is compensated for by the activation of non-canonical signalling pathways, which would render the use of TGF-β receptor targeted inhibitors ineffective.

In the context of tumour tissues, fibroblasts are genetically more stable cells compared with cancer cells, as they are less likely to mutate[274], making them better drug targets. Overall, this study has begun the groundwork needed to move this investigation into further translational research. In addition to the identified integrins capable of regulating the myofibroblast phenotype, RNA sequencing identified membrane-associated factors upregulated in myofibroblasts, while the drug screen conducted on lung fibroblasts demonstrated several distinct mechanisms may converge with the TGF-β1 signalling pathway to mediate a contractile and/or matrix-secreting phenotype. Of interest are the several anti-microbial drugs identified, as the mechanism by which they regulate TGF-β1 activation has yet to be defined. Moreover, various tyrosine kinase and phosphodiesterase inhibitors were effective in reducing α-SMA and fibronectin expression; drugs that have also been shown to regulate activated fibroblasts in published studies[247, 275], validating some of the potential hits identified. In addition, successful clinical trials using the pan-tyrosine kinase inhibitor nintedanib, which was recently approved for the treatment of IPF, demonstrates the potential translational benefits of targeting myofibroblasts, in addition to epithelial cells. Further investigation into the mechanisms of these already FDA-approved drugs may reveal novel druggable targets and expand the current strategies under investigation to regulate the activity of activated fibroblasts.

Although many studies have established myofibroblasts promote tumour progression[86], recent findings using pancreatic cancer models where fibroblasts were depleted showed that although fibrosis was reduced, the cancer condition was aggravated, as observed by immune suppression (decreased effector T cells and increased regulatory T cells), enhanced EMT and reduced survival of mice[276].

Furthermore, inhibited hedgehog signalling in stromal pancreatic cells led to reduced numbers of α-SMA-positive myofibroblasts, which also led to accelerated pancreatic tumour progression[277]. However, the data are conflicting, as other studies demonstrate inducing quiescence in activated pancreatic stellate cells overcomes chemotherapeutic drug resistance, reduces tumour volume and increases survival[278]. These studies may show differences due to the *in vivo* models used, but highlight the potential detrimental effects of completely removing fibroblasts from the tumour stroma and indicate pathways, such as stromal hedgehog signalling may prove to be tumour-suppressive. Nevertheless, these implications perhaps demonstrate the need to characterise tissue-specific effects of fibroblasts, in addition to their functions, in 3D microenvironments that mimic the cancer.

To add to the complexity of cancer biology, it is reported that CAFs may not only derive from resident fibroblasts, but from vascular smooth muscle cells, pericytes[279], adipocytes[280], bone marrow[281] and tumour cells via EMT[282], though, it is unclear how many of these subtypes exist within specific tumour types at one time. In addition, Costea and colleagues examined the functional significance of two different subpopulations of OSCC CAFs and found they exhibited different levels of motility and utilised distinct mechanisms to promote tumour cell invasion. Though, whether these subsets derived from different sources was unclear[238]. While the origin of fibroblasts constituting the tumour stroma is still under contention, studies characterising the functional heterogeneity of fibroblasts populations within single tumours are required to determine how to effectively target CAFs within each patient.

In summary, I have shown that fibroblasts derived from skin, lung and breast tissue display heterogeneity in their response to TGF-β1, while different integrins appear to modulate TGF-β1 signalling, as measured by markers of fibroblast activation, invasion and collagen gel contraction. In addition, enhanced characterisation of fibroblasts from each tissue may improve therapeutic efficacy by identifying tissue fibroblast-specific biomarkers and drug targets. Further studies are required to investigate the mechanisms by which integrins, such as α11 and the FDA-approved drugs identified in this study influence TGF-β1 signalling, in the hope that these data can propel these

studies into translational *in vivo* research to evaluate potential therapeutic targets. These studies are particularly needed to expand the approach for targeting stromal fibroblasts, which are currently very limited. Lastly, RNA sequencing of healthy lung fibroblasts suggested TGF-β1 activation increases the expression of genes which seem to ultimately support a tumour-promoting microenvironment. Therefore, reversing the myofibroblast phenotype in particular tissues by means of small-molecule inhibitors and antibodies to key membrane markers of the myofibroblast phenotype, is likely to reduce the severity of cancer and organ fibrosis and improve patient prognoses.

Appendix

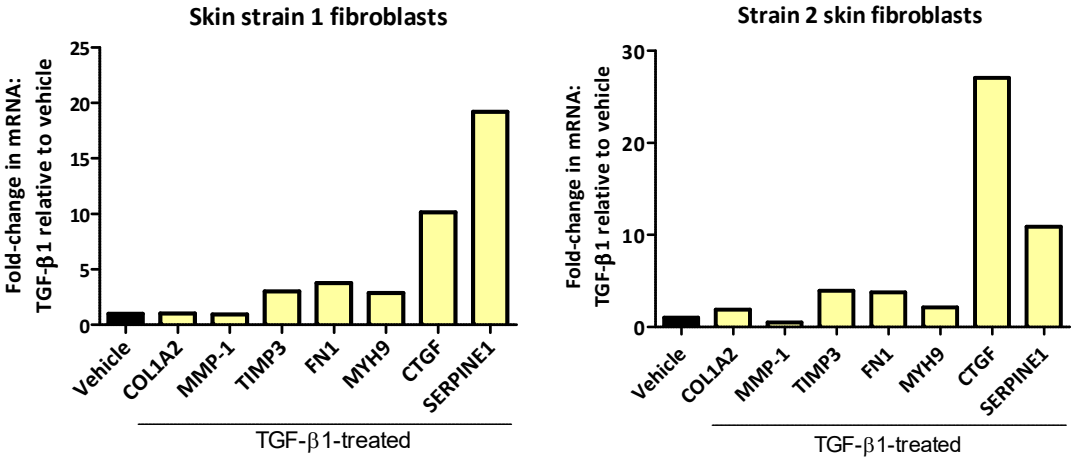

Appendix Figure 1. Gene expression of markers of myofibroblast activation after TGF-β1 addition to skin strain 1 and strain 2 fibroblasts. A preliminary experiment where skin strain 1 and 2 fibroblasts were exposed to TGF-β1 (5ng/ml) for 24 hours. ACTA2 is missing due to primer contamination. The qPCR data shows fold-change of TGF-β1 relative to vehicle-treated cells and data was normalised to housekeeping gene beta-2 microglobulin. Data shown represents the mean of one independent experiment.

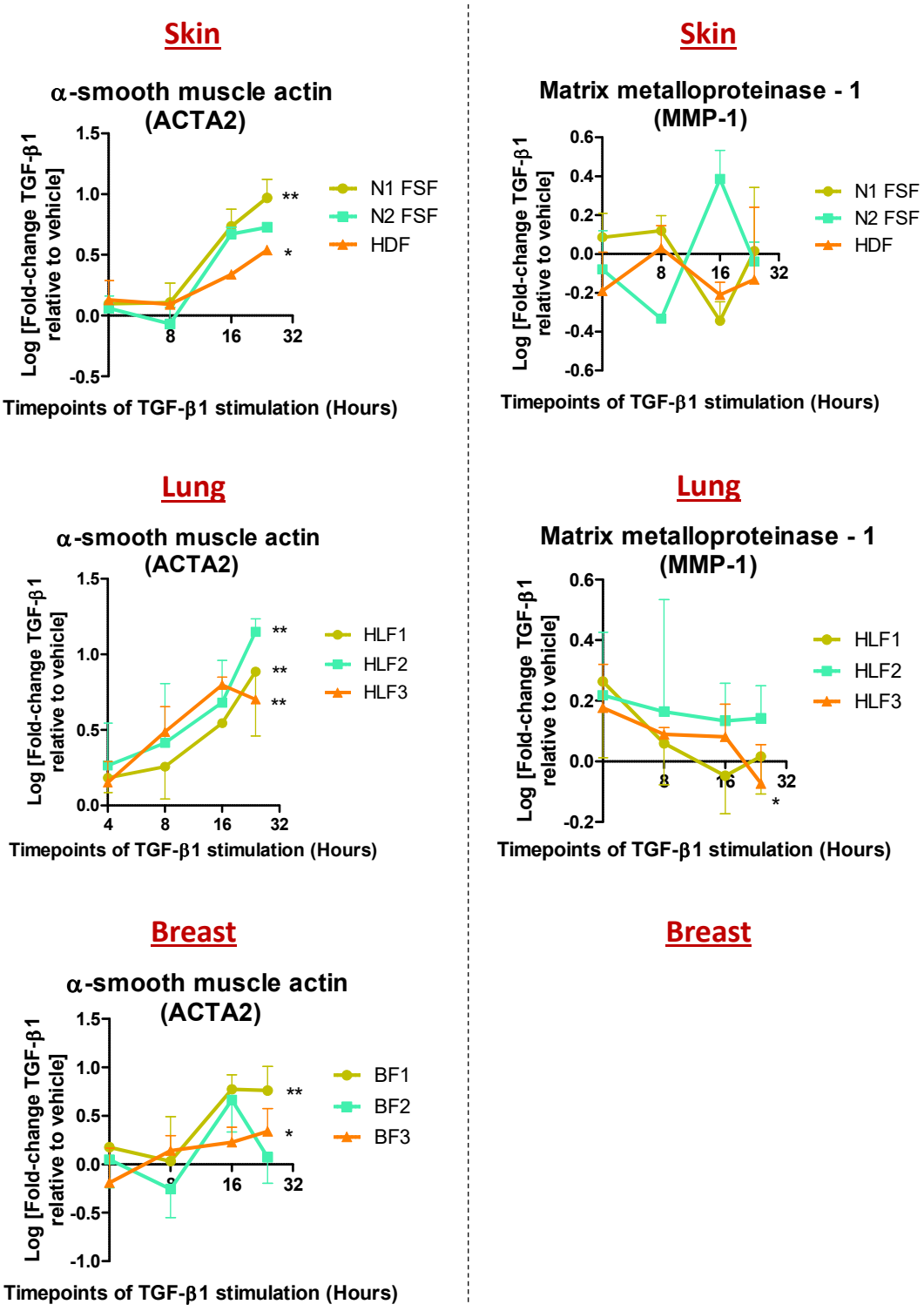

Appendix Figure 2. qPCR analysis comparison of α-SMA and MMP-1 during 4-24-hour TGF-β1 (5ng/ml) exposure in 3 skin, lung and breast fibroblast strains. Graphs show skin strain 1 (N1 FSF), strain 2 (N2 FSF) and strain 3 (HDF), lung strain (HLF) 1, 2, 3 and breast fibroblast strain (BF) 1, 2 and 3. Data of TGF-β1 relative to vehicle-treated cells and normalised to housekeeping genes. Linear regression analysis, significance measured as deviance of slope from 0. *p<0.05, **p<0.01. *n = 3*. See **Appendix Figure 6-15** for individual biological repeats per strain.

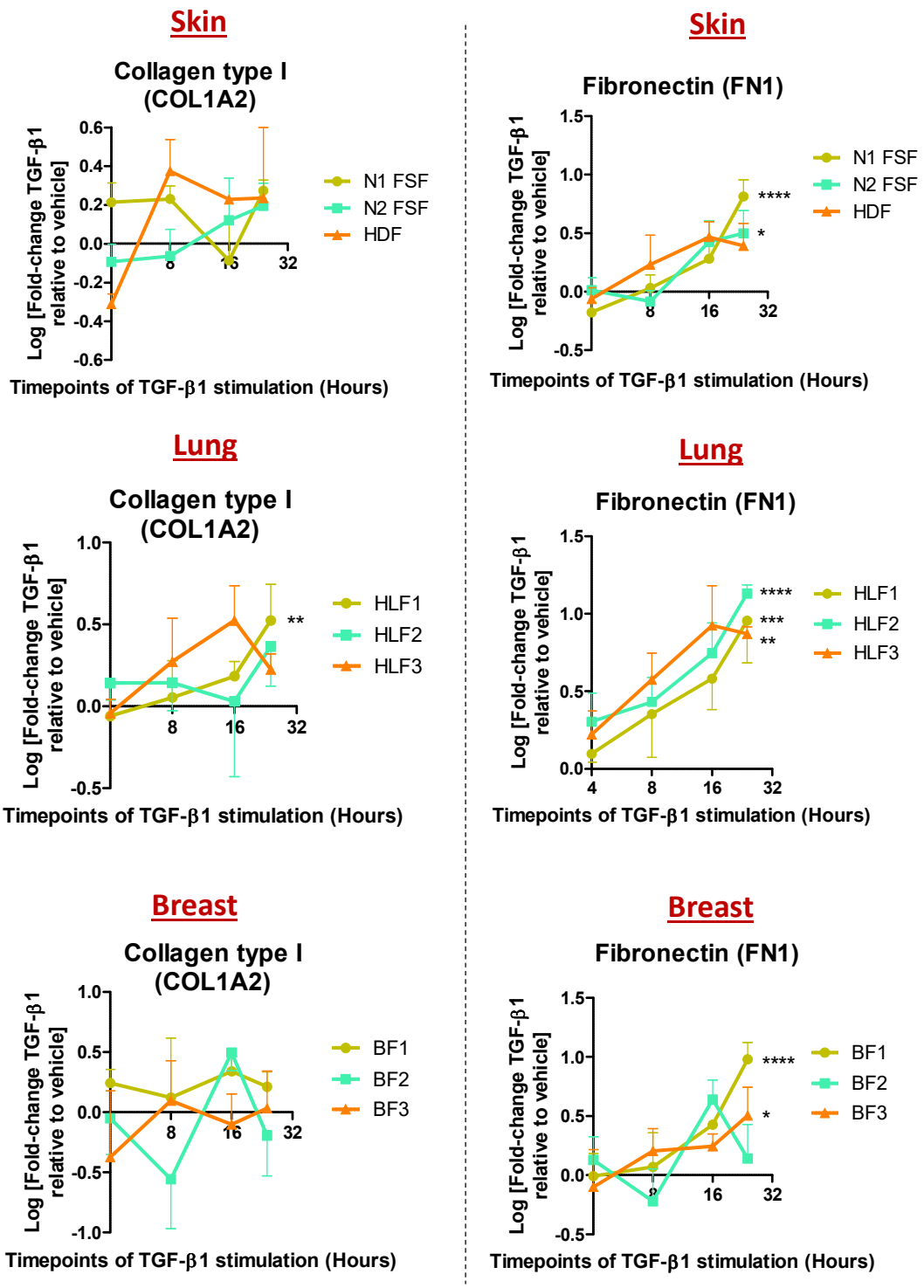

Appendix Figure 3. qPCR analysis comparison of COL1A2 and FN1 during 4-24-hour TGF-β1 (5ng/ml) exposure in 3 skin, lung and breast fibroblast strains. Graphs show skin strain 1 (N1 FSF), strain 2 (N2 FSF) and strain 3 (HDF), lung strain (HLF) 1, 2, 3 and breast fibroblast strain (BF) 1, 2 and 3. Data of TGF-β1 relative to vehicle-treated cells and normalised to housekeeping genes. Linear regression analysis, significance measured as deviance of slope from 0. *p<0.05, **p<0.01. *n = 3*. See **Appendix Figure 6-15** for individual biological repeats.

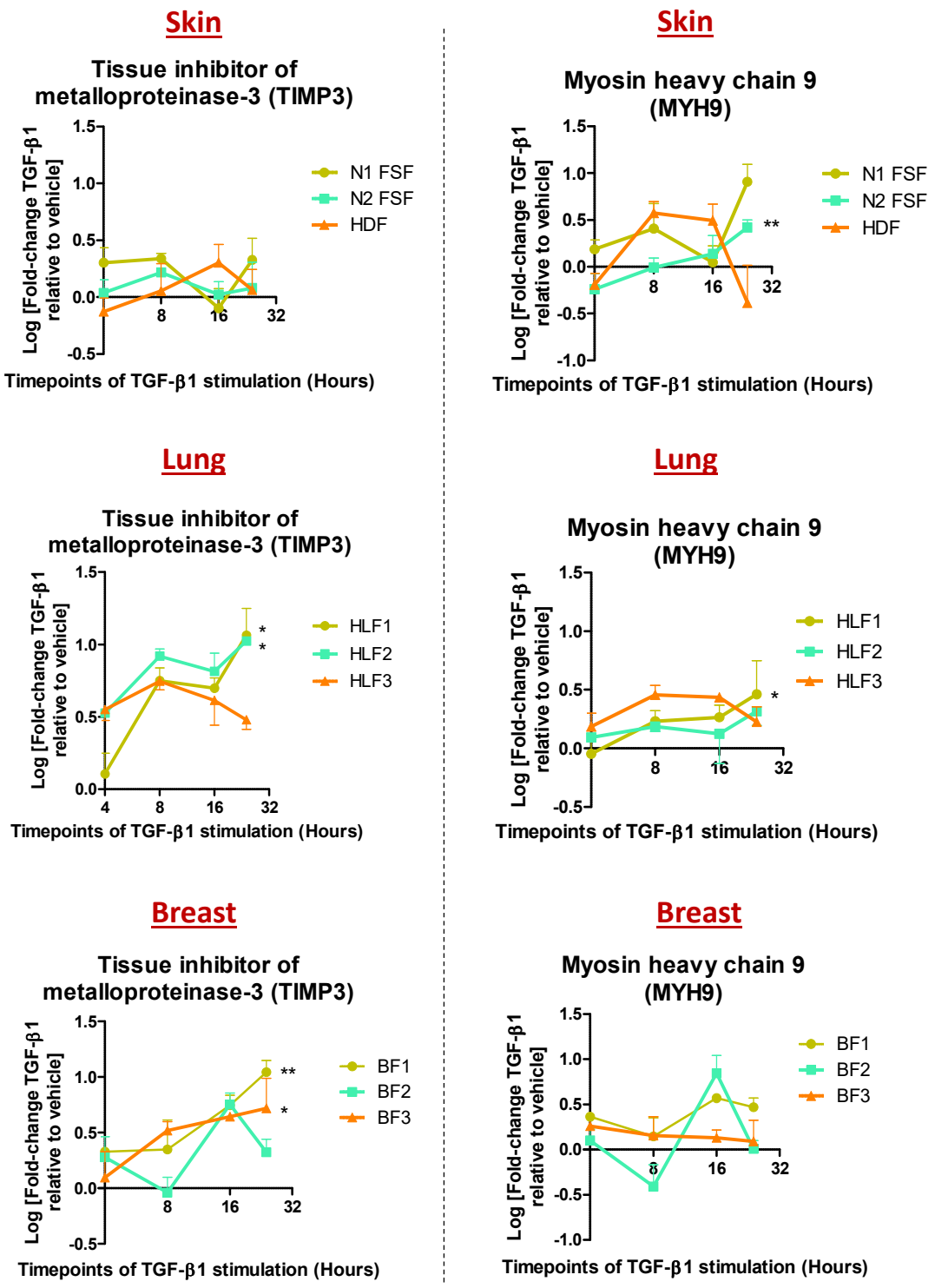

Appendix Figure 4. qPCR analysis comparison of TIMP3 and MYH9 during 4-24-hour TGF-β1 (5ng/ml) exposure in 3 skin, lung and breast fibroblast strains. Graphs show skin strain 1 (N1 FSF), strain 2 (N2 FSF) and strain 3 (HDF), lung strain (HLF) 1, 2, 3 and breast fibroblast strain (BF) 1, 2 and 3. Data of TGF-β1 relative to vehicle-treated cells and normalised to housekeeping genes. Linear regression analysis, significance measured as deviance of slope from 0. *p<0.05, **p<0.01. *n = 3*. See **Appendix Figure 6-15** for individual biological repeats per strain.

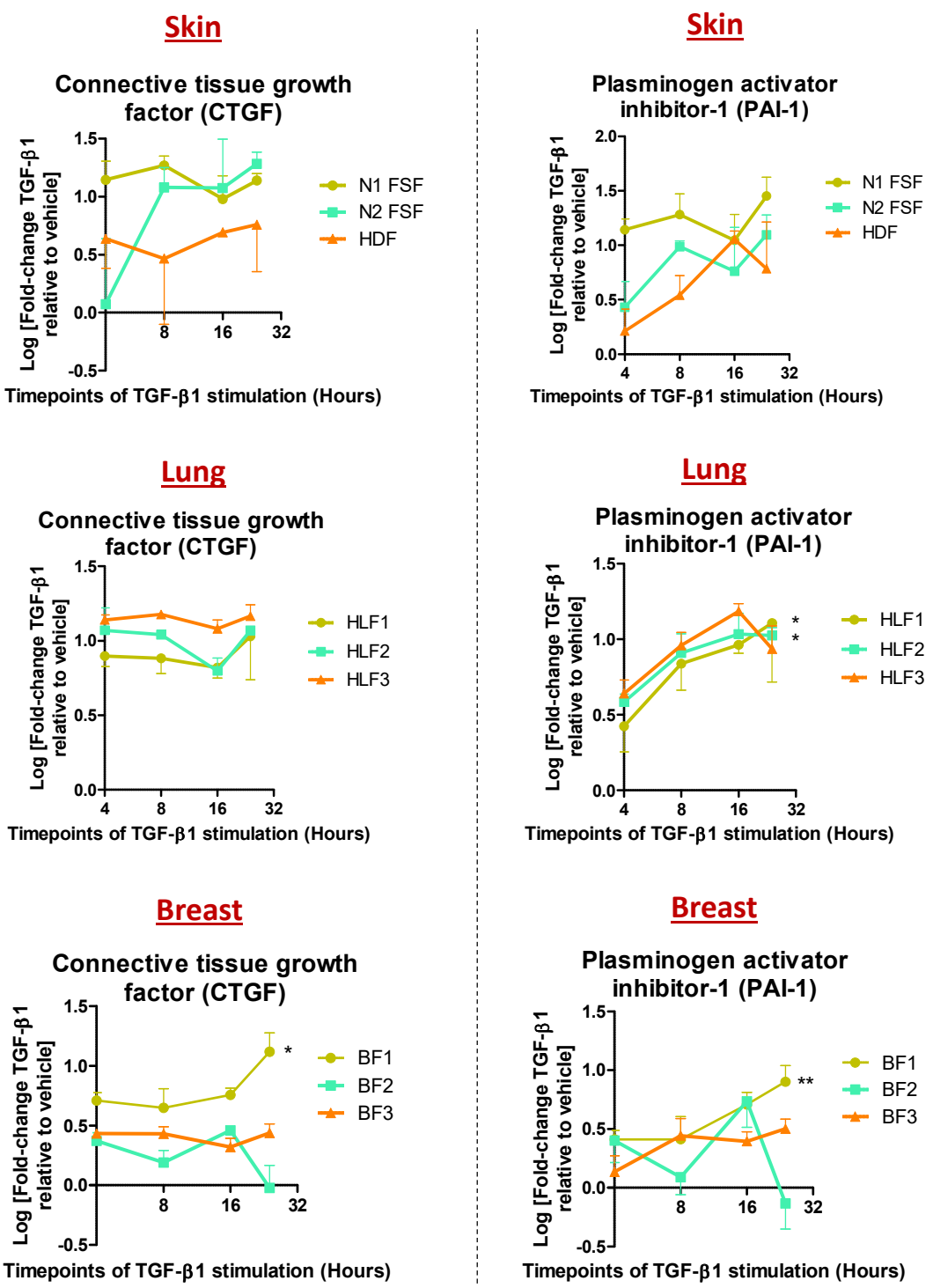

Appendix Figure 5. qPCR analysis comparison of CTGF and PAI-1 during 4-24-hour TGF-β1 (5ng/ml) exposure in 3 skin, lung and breast fibroblast strains. Graphs show skin strain 1 (N1 FSF), strain 2 (N2 FSF) and strain 3 (HDF), lung strain (HLF) 1, 2, 3 and breast fibroblast strain (BF) 1, 2 and 3. Data of TGF-β1 relative to vehicle-treated cells and normalised to housekeeping genes. Linear regression analysis, significance measured as deviance of slope from 0. *p<0.05, **p<0.01. *n = 3*. See **Appendix Figure 6-15** for individual biological repeats per strain.

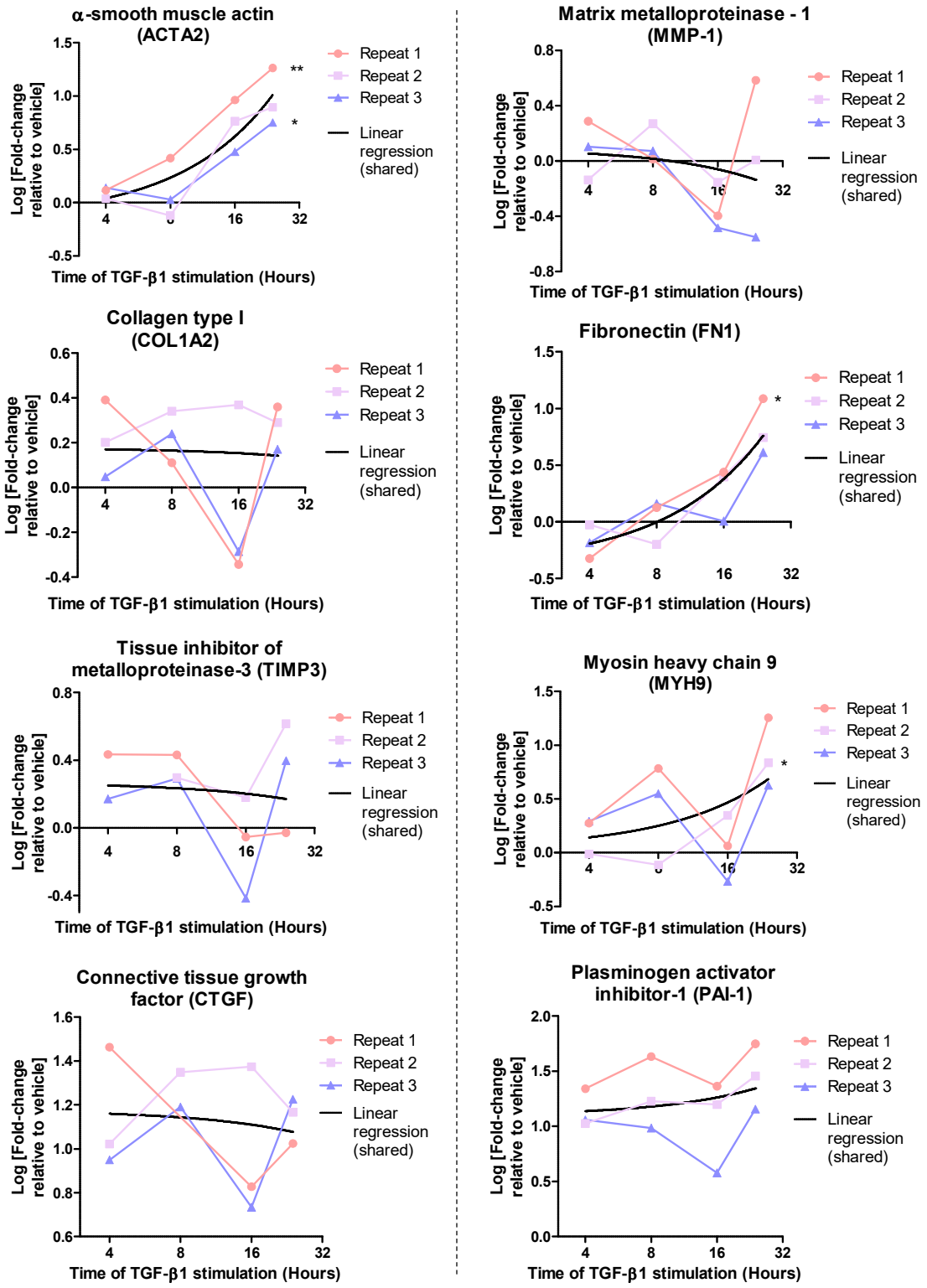

Appendix Figure 6. Gene expression in TGF-β1-treated strain 1 skin fibroblasts. qPCR analysis of 8 myofibroblast-associated genes during 4-24-hour TGF-β1 (5ng/ml) exposure**.** Data of TGF-β1 relative to vehicle-treated cells and normalised to B2M, GAPDH and PPIA housekeeping genes. *p<0.05, **p<0.01 Linear regression analysis, significance measured as deviance of slope from 0.

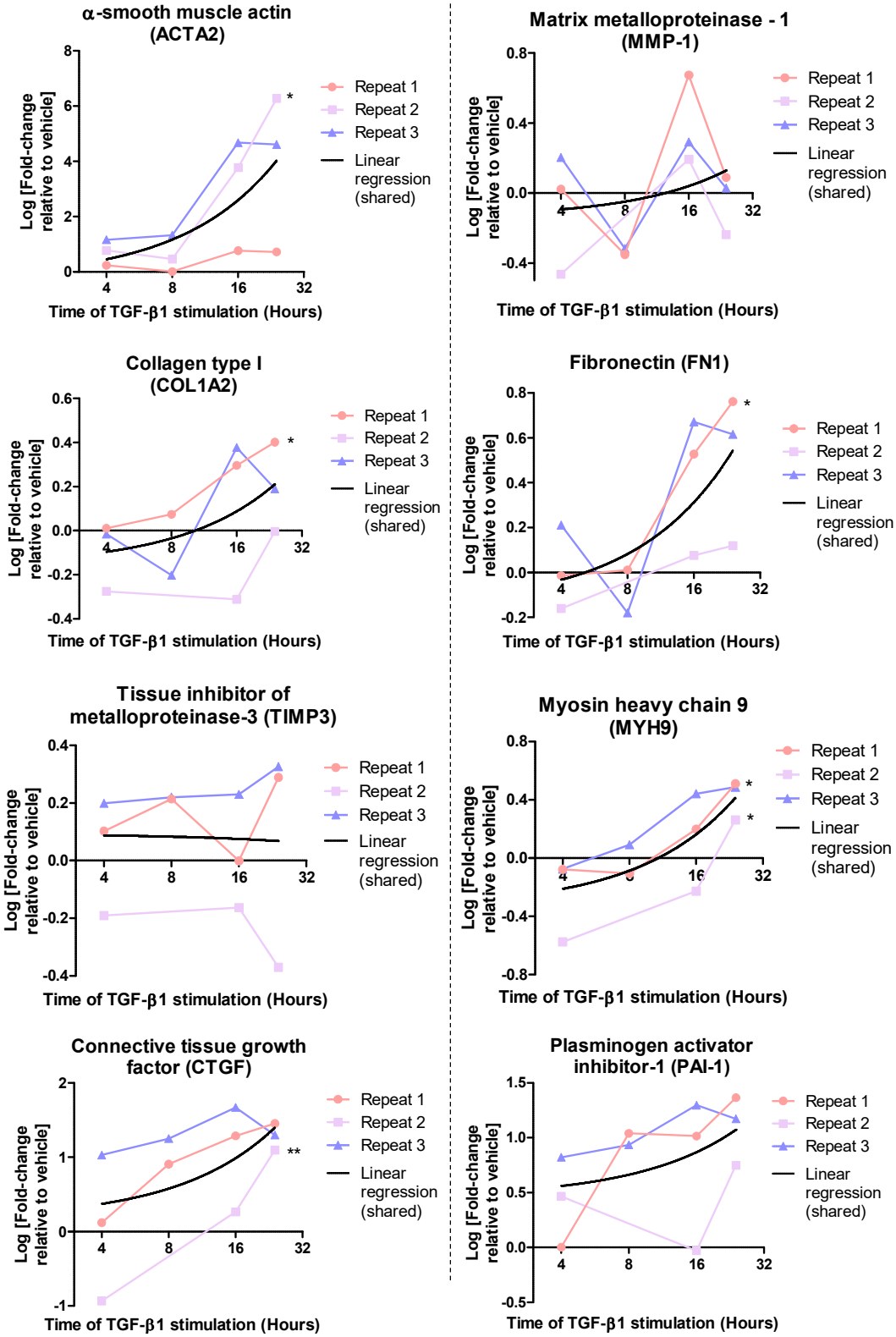

Appendix Figure 7. Gene expression in TGF-β1-treated strain 2 skin fibroblasts. qPCR analysis of 8 myofibroblast-associated genes during 4-24-hour TGF-β1 (5ng/ml) exposure**.** Data of TGF-β1 relative to vehicle-treated cells and normalised to B2M, GAPDH and PPIA housekeeping genes. *p<0.05, **p<0.01 Linear regression analysis, significance measured as deviance of slope from 0.

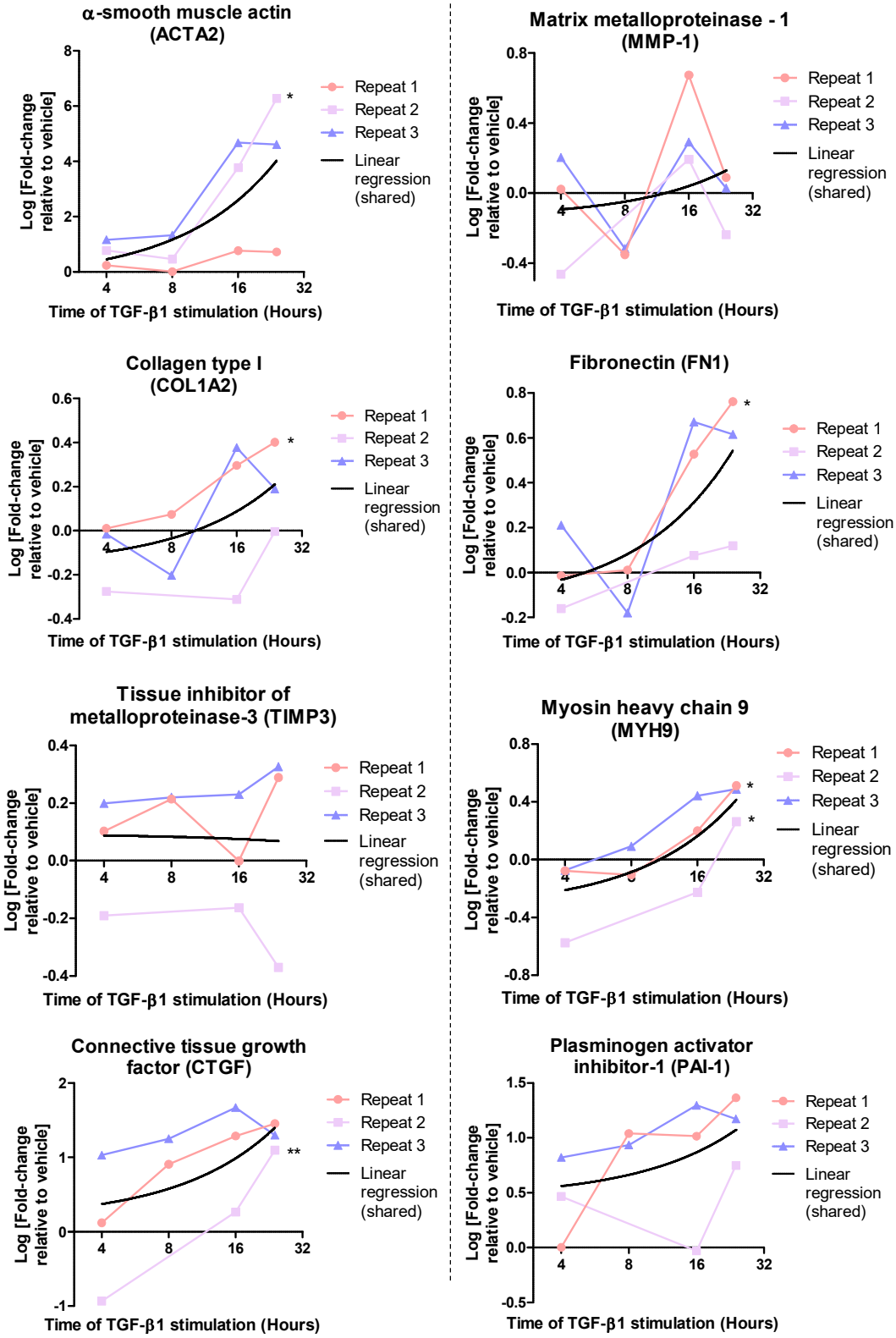

Appendix Figure 8. Gene expression in TGF-β1-treated strain 2 skin fibroblasts. qPCR analysis of 8 myofibroblast-associated genes during 4-24-hour TGF-β1 (5ng/ml) exposure**.** Data of TGF-β1 relative to vehicle-treated cells and normalised to B2M, GAPDH and PPIA housekeeping genes. *p<0.05, **p<0.01 Linear regression analysis, significance measured as deviance of slope from 0.

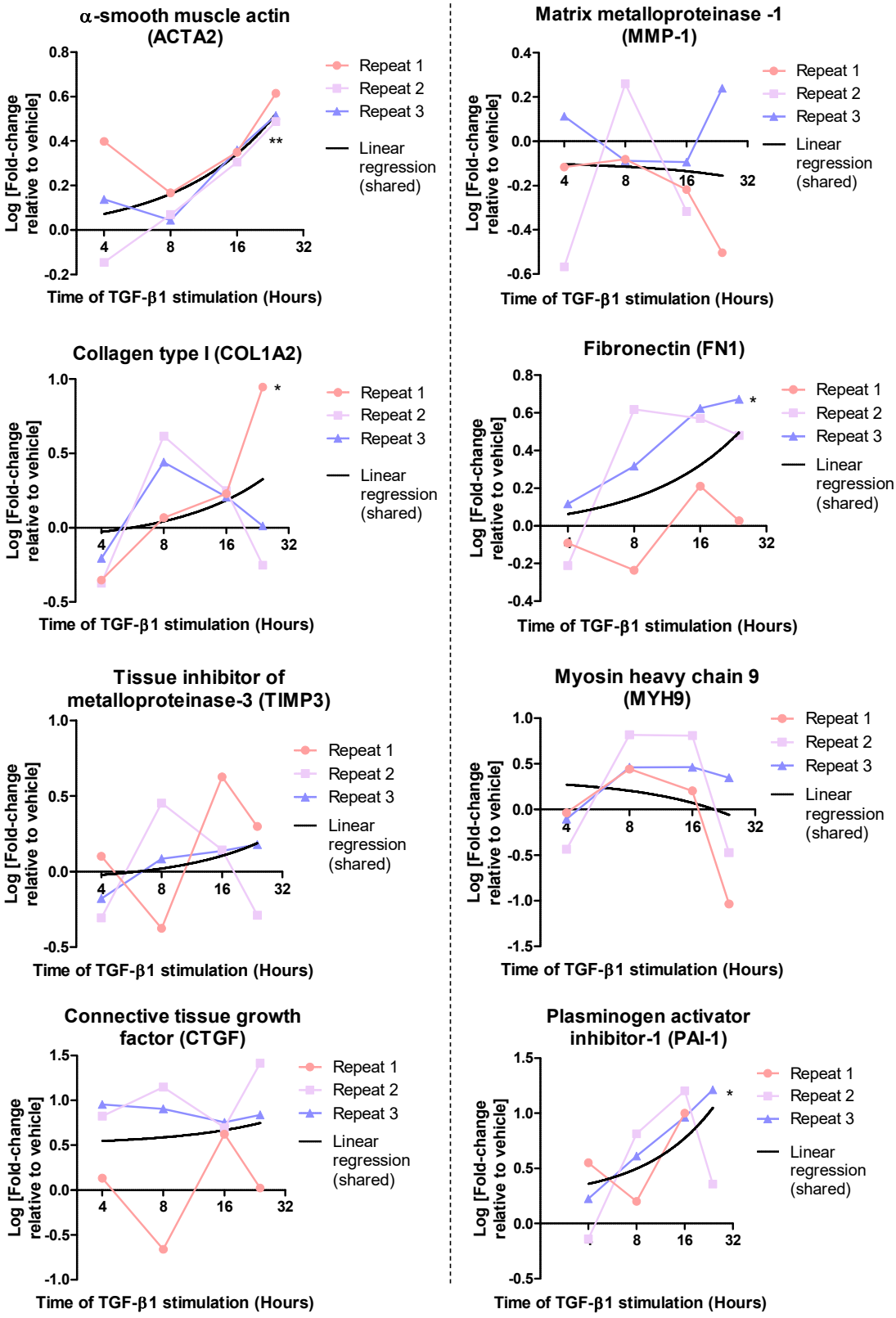

Appendix Figure 9. Gene expression in TGF-β1-treated strain 3 skin fibroblasts. qPCR analysis of 8 myofibroblast-associated genes during 4-24-hour TGF-β1 (5ng/ml) exposure. Data of TGF-β1 relative to vehicle-treated cells and normalised to B2M, GAPDH and HPRT-1 housekeeping genes. *p<0.05, **p<0.01 Linear regression analysis, significance measured as deviance of slope from 0.

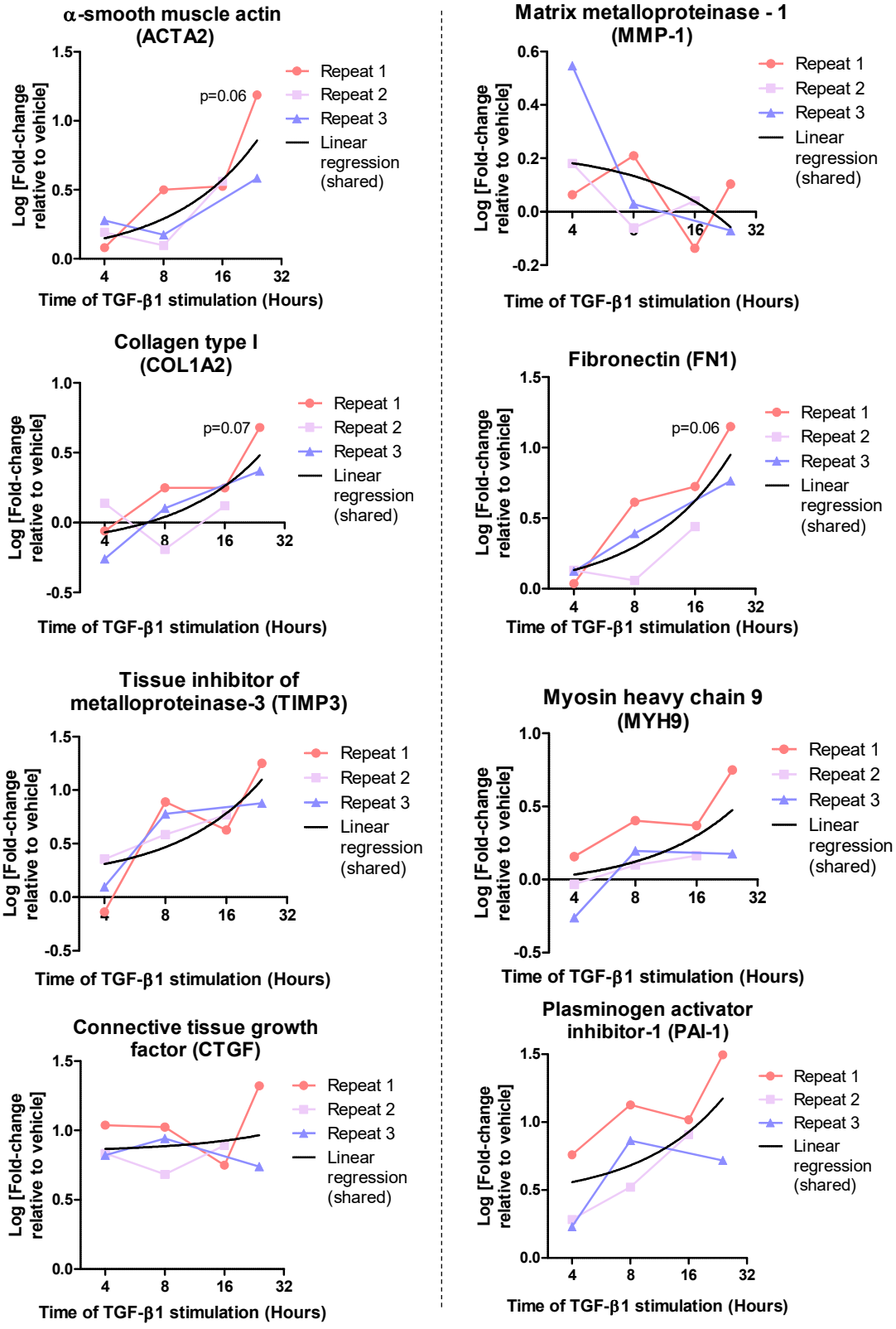

Appendix Figure 10. Gene expression in TGF-β1-treated strain 1 lung fibroblasts. qPCR analysis of 8 myofibroblast-associated genes during 4-24-hour TGF-β1 (5ng/ml) exposure. Data of TGF-β1 relative to vehicle-treated cells and normalised to B2M, GAPDH & TRIM27 housekeeping genes. *p<0.05, **p<0.01 Linear regression analysis, significance measured as deviance of slope from 0.

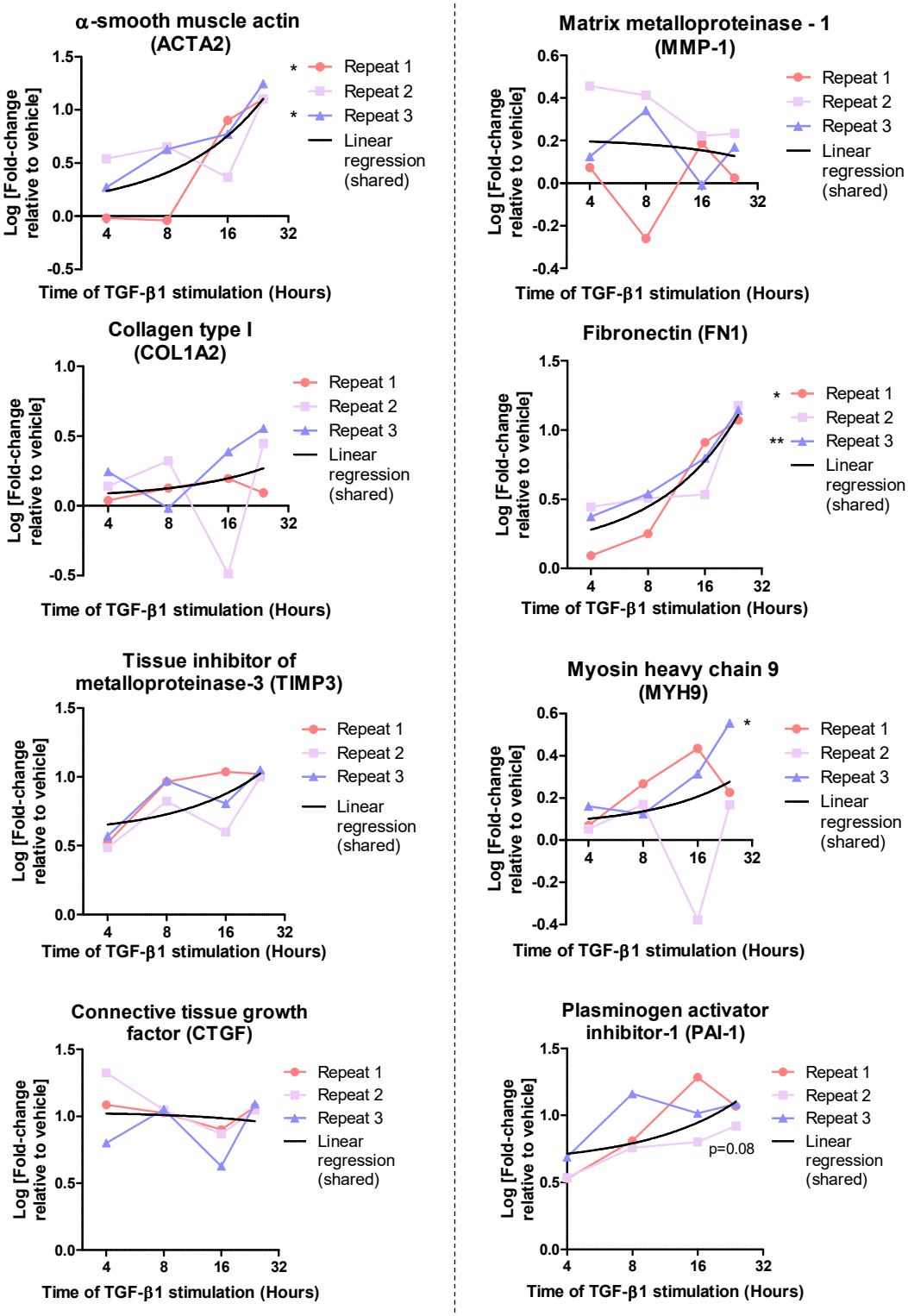

Appendix Figure 11. Gene expression in TGF-β1-treated strain 2 lung fibroblasts. qPCR analysis of 8 myofibroblast-associated genes during 4-24-hour TGF-β1 (5ng/ml) exposure. Data of TGF-β1 relative to vehicle-treated cells and normalised to B2M, GAPDH & TRIM27 housekeeping genes. *p<0.05, **p<0.01 Linear regression analysis, significance measured as deviance of slope from 0. (Asterisks next to legend to identify which repeat is significant).

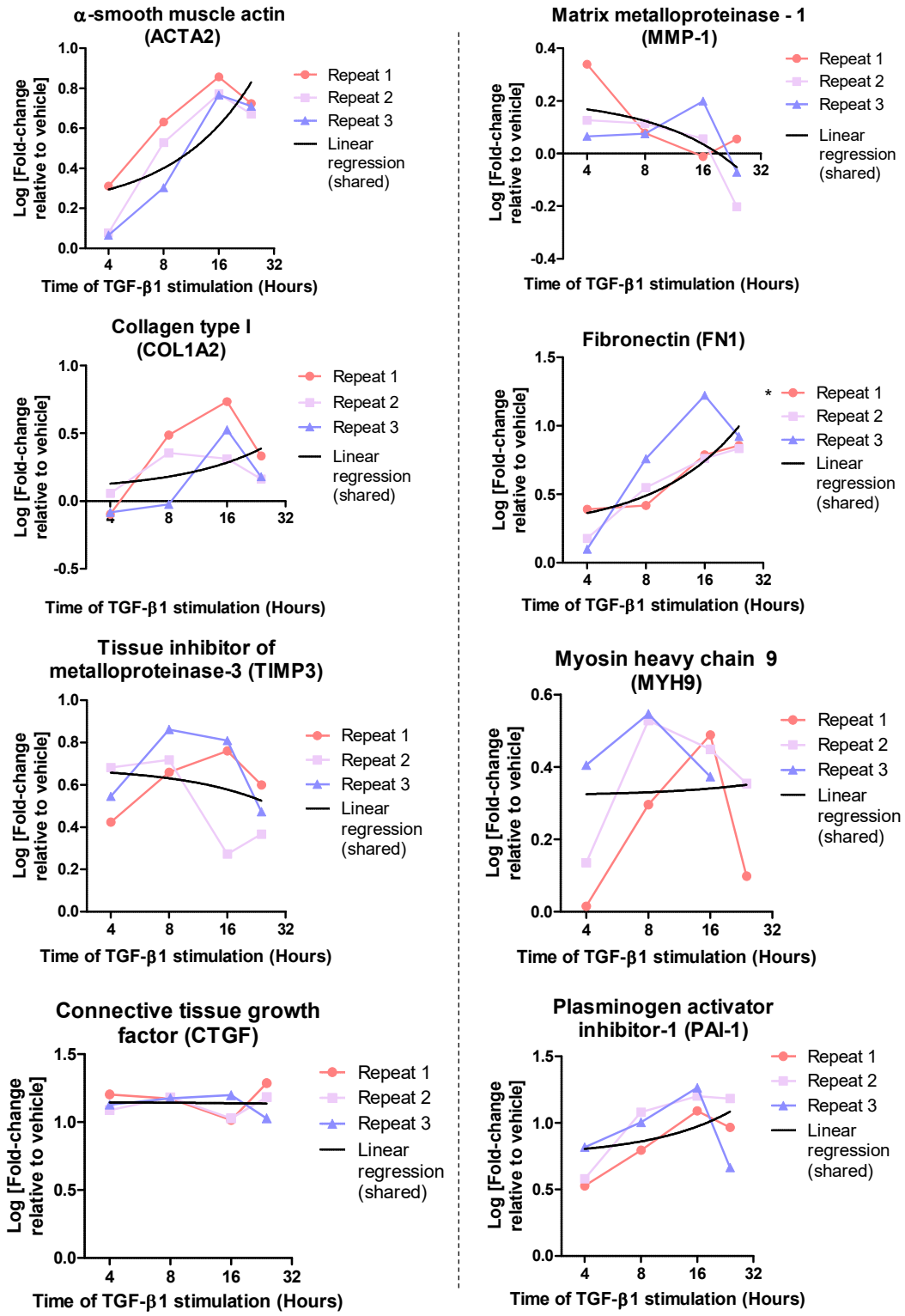

Appendix Figure 12. Gene expression in TGF-β1-treated strain 3 lung fibroblasts. qPCR analysis of 8 myofibroblast-associated genes during 4-24-hour TGF-β1 (5ng/ml) exposure. Data of TGF-β1 relative to vehicle-treated cells and normalised to B2M, GAPDH & TRIM27 housekeeping genes. *p<0.05 Linear regression analysis, significance measured as deviance of slope from 0. (Asterisks next to legend to identify which repeat is significant).

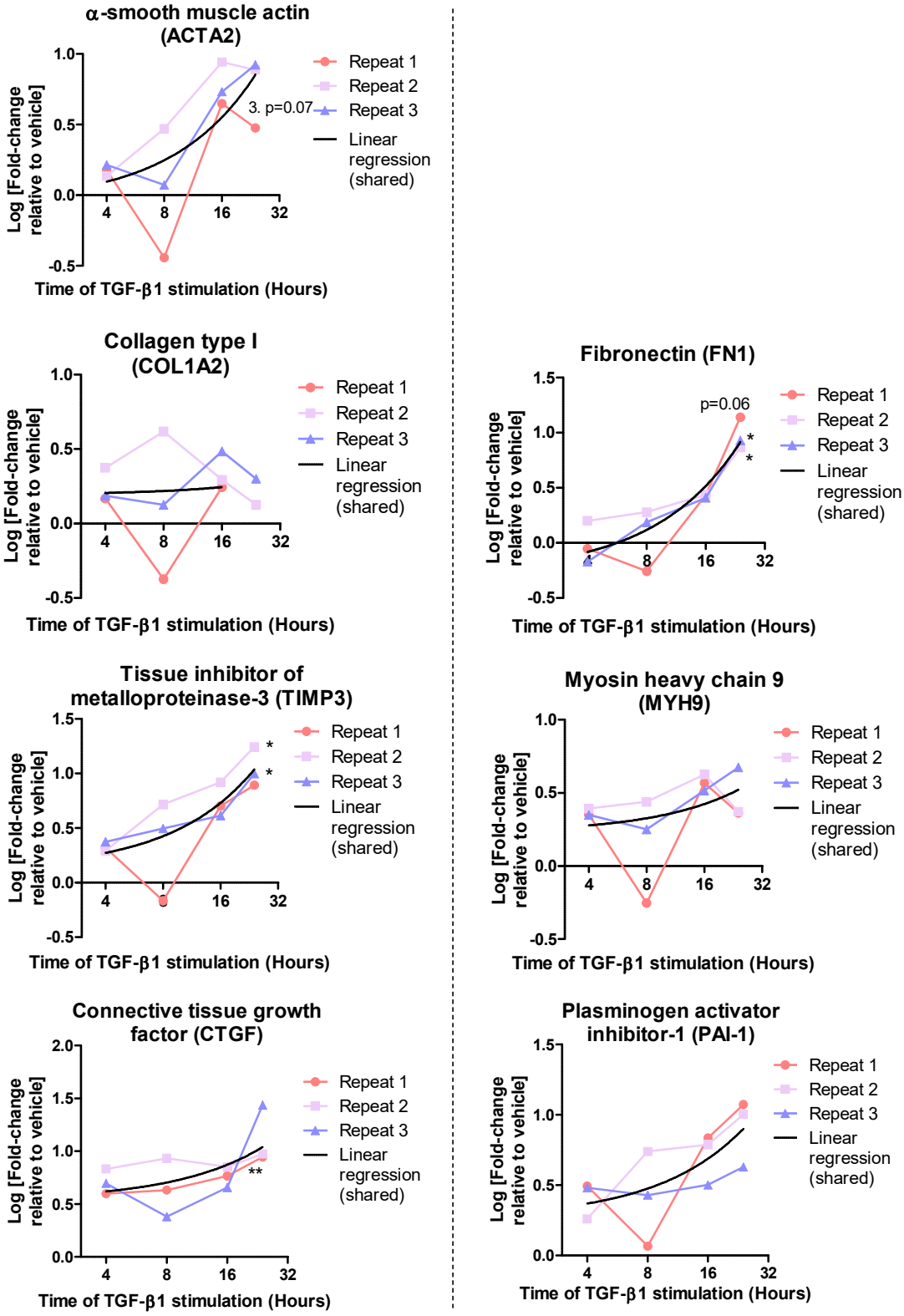

Appendix Figure 13. Gene expression in TGF-β1-treated strain 1 breast fibroblasts. qPCR analysis of 8 myofibroblast-associated genes during 4-24-hour TGF-β1 (5ng/ml) exposure. Data of TGF-β1 relative to vehicle-treated cells and normalised to HPRT-1, B2M & PPIA housekeeping genes. *p<0.05, **p<0.01 Linear regression analysis, significance measured as deviance of slope from 0. MMP-1 uncompleted.

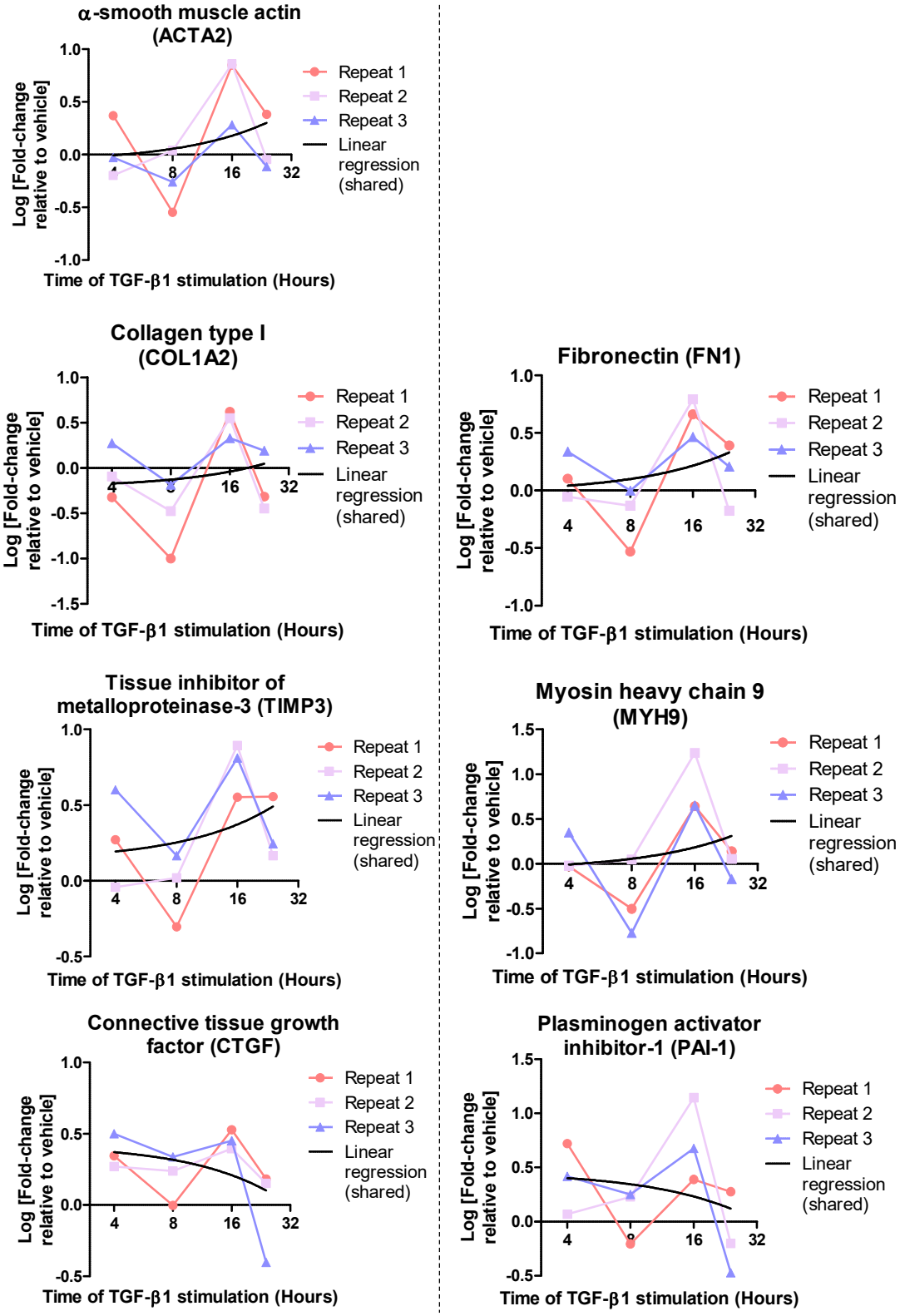

Appendix Figure 14. Gene expression in TGF-β1-treated strain 2 breast fibroblasts. qPCR analysis of 8 myofibroblast-associated genes during 4-24-hour TGF-β1 (5ng/ml) exposure. Data of TGF-β1 relative to vehicle-treated cells and normalised to HPRT-1, B2M & TRIM27 housekeeping genes. Linear regression analysis, significance measured as deviance of slope from 0. MMP-1 uncompleted.

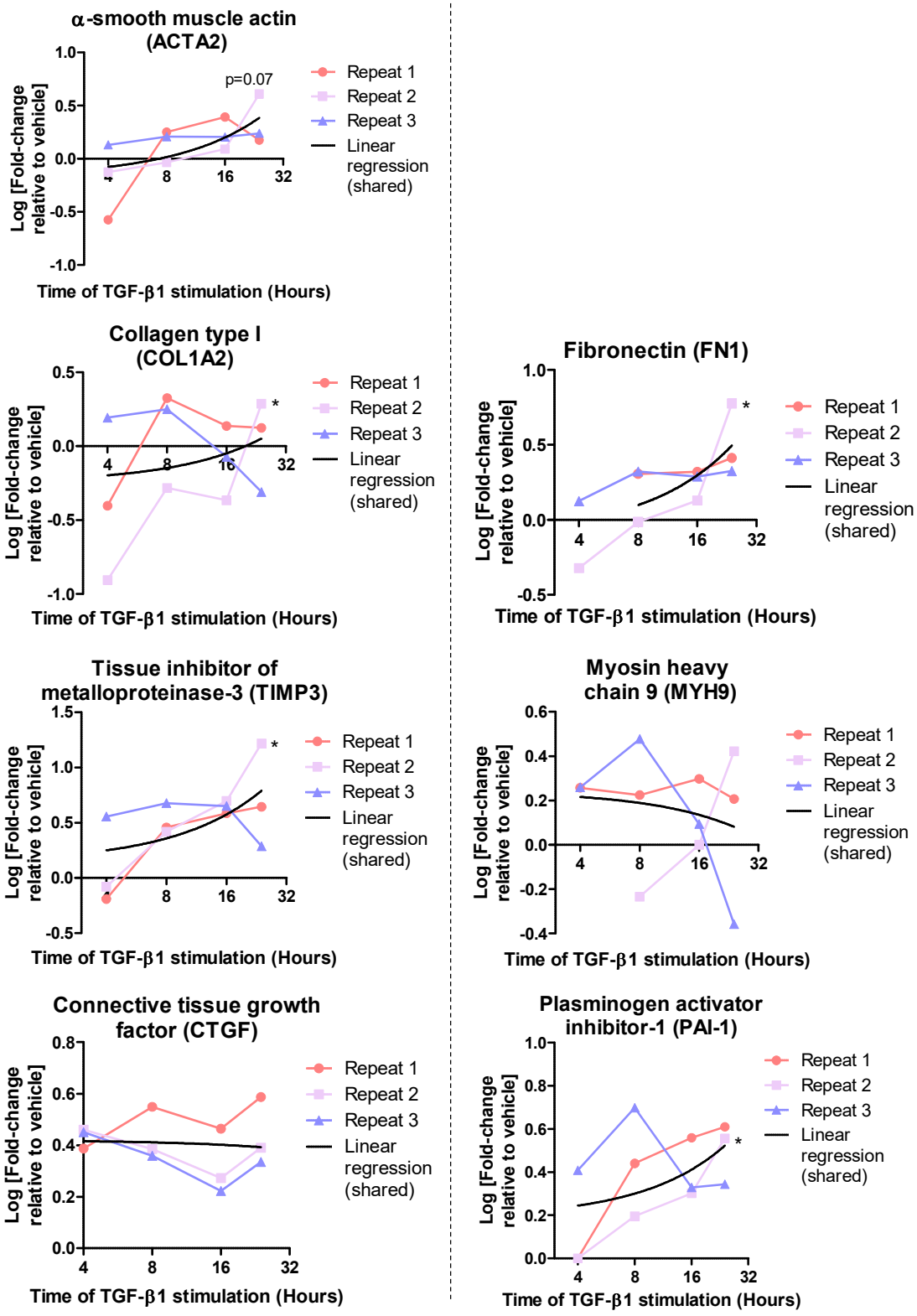

Appendix Figure 15. Gene expression in TGF-β1-treated strain 3 breast fibroblasts. qPCR analysis of 8 myofibroblast-associated genes during 4-24-hour TGF-β1 (5ng/ml) exposure. Data of TGF-β1 relative to vehicle-treated cells and normalised to HPRT-1, B2M & PPIA housekeeping genes. *p<0.05, Linear regression analysis, significance measured as deviance of slope from 0. MMP-1 uncompleted.

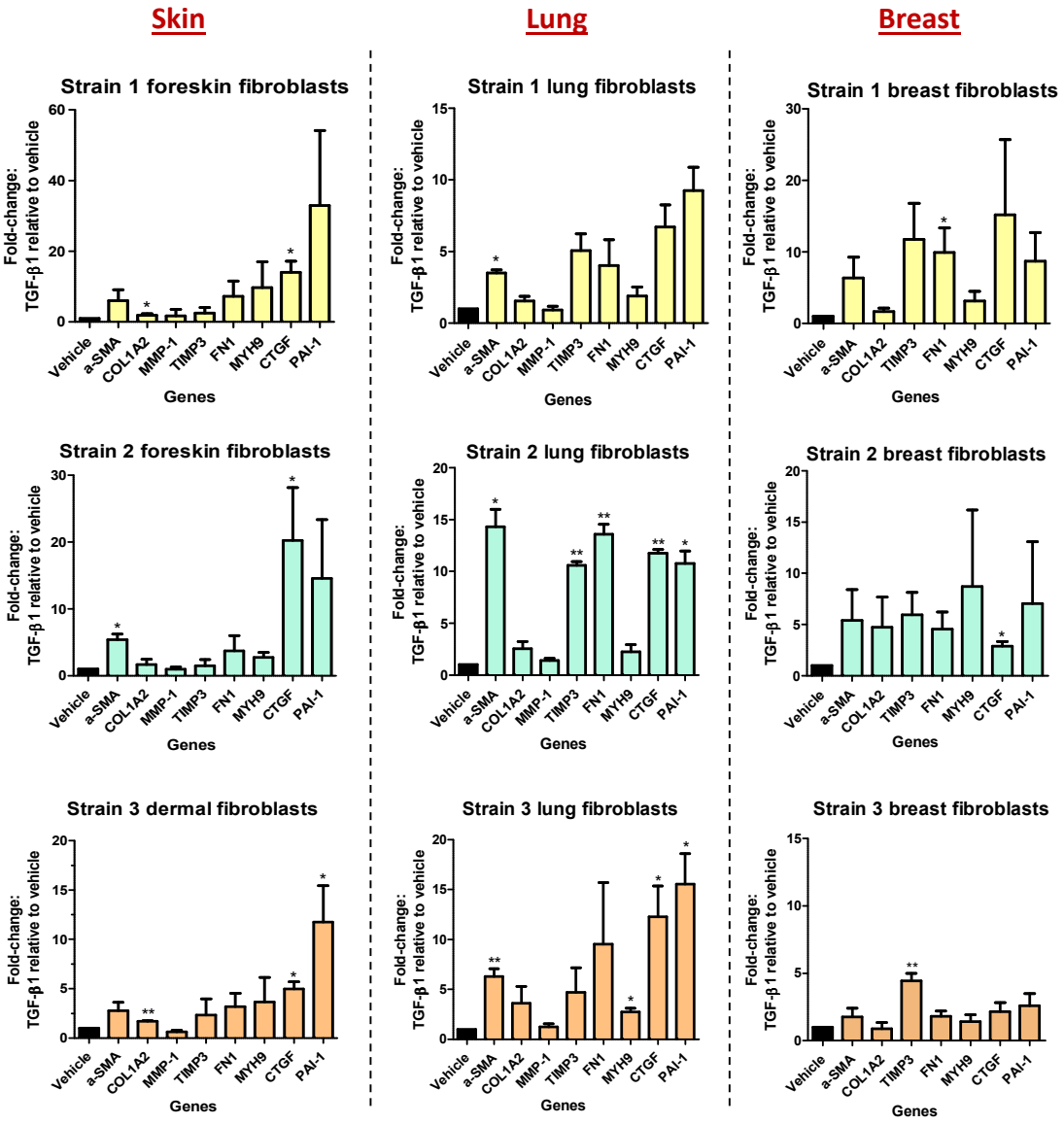

Appendix Figure 16. Gene expression of 8 markers of myofibroblast activation after TGF-β1 addition to 3 strains of skin, lung and breast fibroblasts. Data is presented from the 16-hour or 24-hour time-point of TGF-β1 (5ng/ml) stimulation, according to which time-point induced peak gene expression. This was to establish which markers were most highly upregulated by TGF-β1 to facilitate the selection of markers to be analysed by western blot. Skin fibroblast strains 1 & 2 (24-hours) and strain 3 (16-hours). Lung fibroblast strain 1 and 3 (16-hours) and lung strain 2 (24-hours). Breast fibroblasts strain 1 and 3 (24-hours) and strain 2 (16-hours). Housekeeping genes listed in Materials and Methods. Graphs show TGF-β1-induced genes significantly upregulated relative to vehicle-cell stimulation. *p<0.05, **p<0.01, Paired students *t*-test. Data shown represents the mean ± standard deviation of three independent experiments.

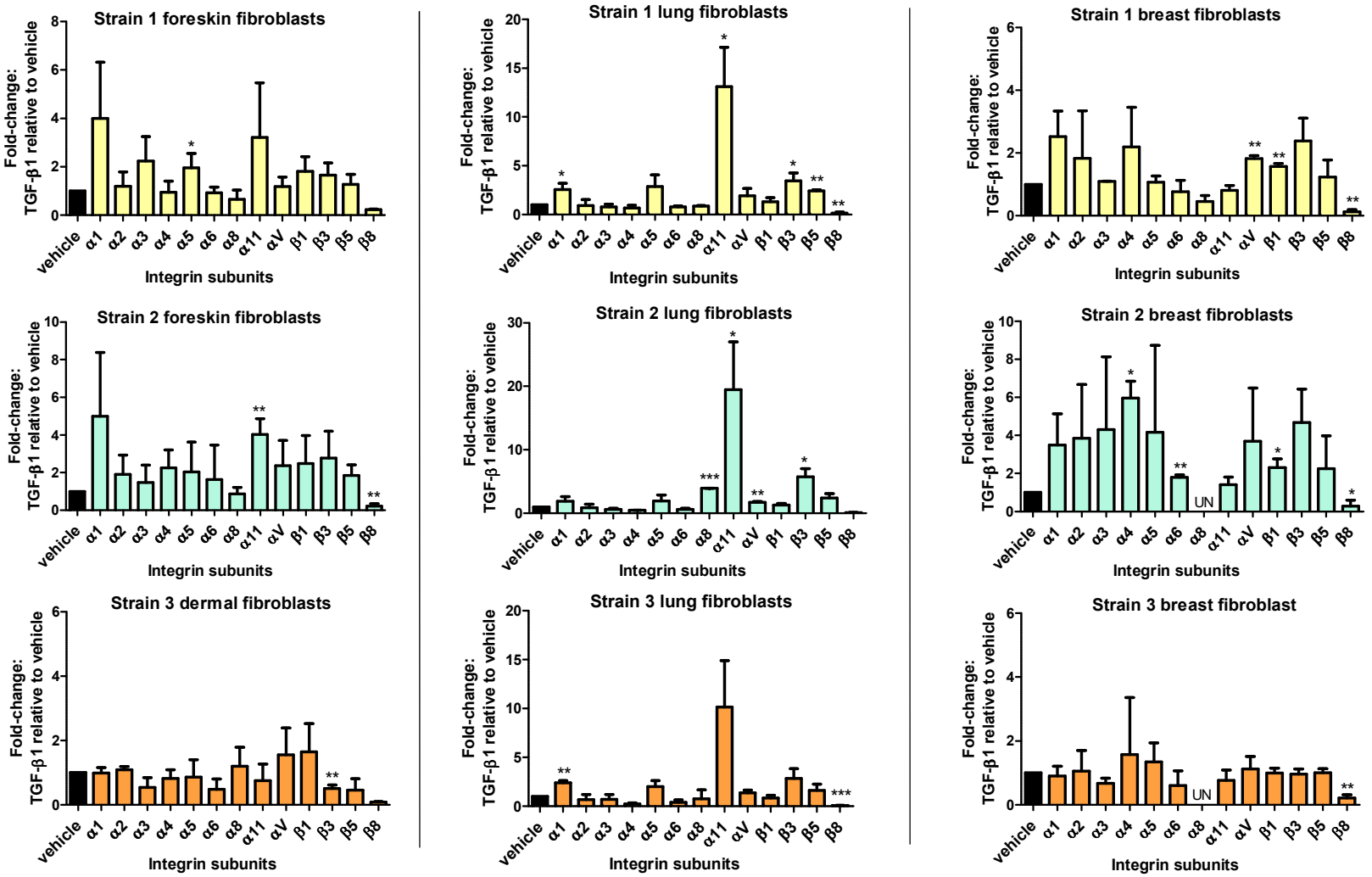

Appendix Figure 17. Comparison of integrin subunit genes after TGF-β1 addition in skin, lung and breast fibroblasts. Fibroblasts were exposed to TGF-β1 (5ng/ml) at varying times due according to peak expression during time course. Foreskin fibroblast strains 1 & 2 (24-hours), strain 3 HDF (16-hours). HLF1, HLF3 (16-hours) and strain 2 (24-hours). Breast fibroblasts strain 1 and 3 (24 hours), strain 2 was treated for 16-hours. Housekeeping genes listed in Materials and Methods. Fold-change of TGF-β1-treated relative to vehicle stimulation. *p<0.05, **p<0.01, Paired students *t*-test. Data represented as mean ± s.d.

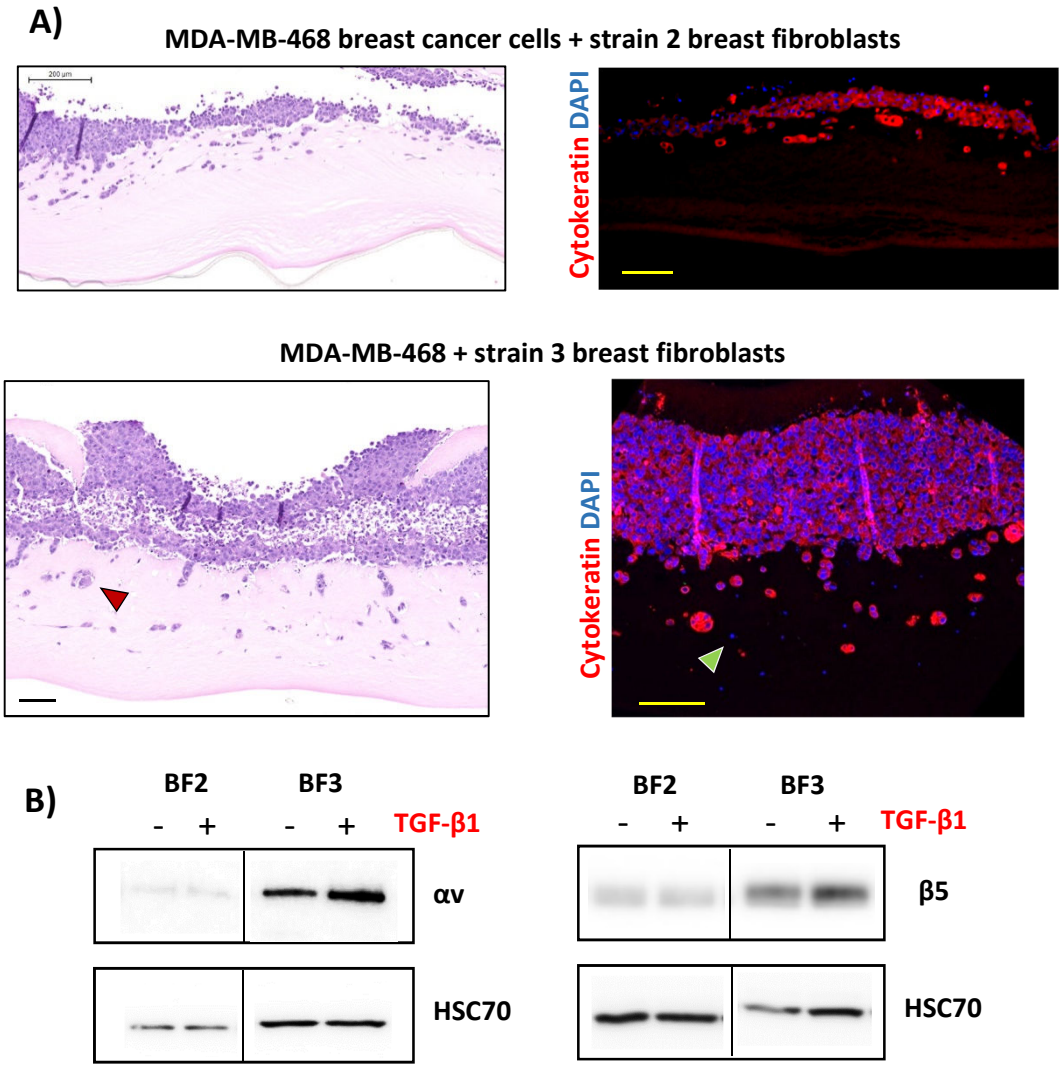

Appendix Figure 18. Mini-organotypic invasion assay and western blot of αv and β5 integrin expression in TGF-β1-treated breast fibroblasts. A) H & E and immunofluorescent staining of breast cancer cells admixed with breast fibroblasts in a 1:2 ratio plated above organotypic gels in transwell inserts and cultured for 7 days. The cancer cell layer was thinner when plated with breast fibroblast strain 2 (BF2) compared to breast cancer cells plated with strain 3 (BF3). B) Western blots: BF2 and BF3 were stimulated with either vehicle (-) or TGF-β1 (+) (5ng/ml) for 48-hours. Strain 3 fibroblasts expressed more αv and β5 than strain 2. HSC70 serves as loading control.

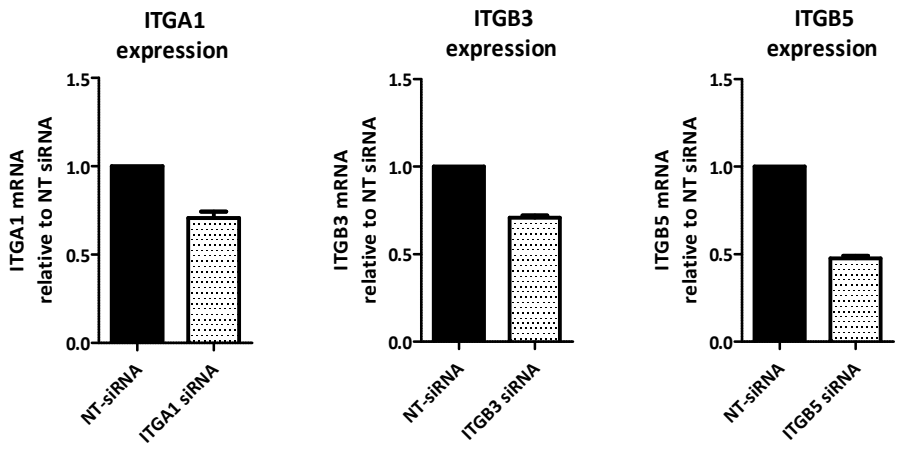

Appendix Figure 19. qPCR confirming integrin knockdown using integrin siRNA in lung strain 3 fibroblasts. Fibroblasts were pre-treated with TGF-β1 (5ng/ml) for 48 hours and then 15nM integrin siRNA for 72 hours. Only 30% knockdown was achieved of α1 and β3 integrin and 50% knockdown of β5. Data shown represents mean ± s.d of one experiment with triplicate samples.

Drug name	α-SMA p-value	Fibronectin p-value
Axitinib	7.85E-08	1.26E-09
Abiraterone	5.77E-43	9.54E-51
Erlotinib HCl	7.57E-07	6.39E-16
Gefitinib	3.33E-05	1.29E-26
Atazanavir sulfate	1.66E-250	1.19E-221
Ofloxacin	2.65E-239	3.66E-59
Marbofloxacin	4.06E-209	1.95E-22
Zolmitriptan	1.76E-162	1.39E-12
Flurdarabine	3.65E-210	1.55E-163
Cefaclor	5.43E-87	5.50E-24
Flucytosine	3.24E-122	0.000685314
Trichlormethiazide	2.83E-171	1.34E-05
Norfloxacin	1.10E-185	8.84E-229
Tadalafil	8.81E-156	7.92E-25
Pimobendan	1.86E-130	1.87E-124
Pomalidomide	7.58E-95	2.04E-12
Rizatriptan benzoate	5.23E-113	1.14E-11
Lamivudine	1.17E-11	6.96E-17
Enalaprilat dihydrate	1.02E-78	6.08E-07
Isradipine	6.47E-52	2.95E-16
Estrone	2.65E-63	4.89E-110
Chloramphenicol	1.08E-50	1.45E-14
Mesalamine	1.09E-47	1.63E-12
Carbamazepine	4.77E-61	1.05E-37

1-Hexadecanol	8.84E-05	1.85E-06
Tiratricol	4.26E-08	4.22E-35
Sevelamer HCl	9.03E-06	6.93E-11
Toltrazuril	8.88E-05	0.000428613
Sulfacetamide sodium	0.000269903	5.66E-16
Ritonavir	0.000183239	0.000123
Chlorpropamide	4.08E-06	0.001947822
Plerixafor	0.000132417	1.32E-38
Misoprostol	2.89E-06	1.32E-12
Teriflunomide	7.59E-06	0.001765107
Deoxyarbutin	0.00012313	8.51E-08
Ramelteon	0.000428992	1.85E-99
Biperiden HCl	6.02E-86	0.000458
Amoxapine	1.28E-05	0.000103919
Tolperisone HCl	1.20E-07	4.03E-06
Piperacillin sodium	4.84E-08	5.21E-15
Benzydamine HCl	1.00E-26	1.06E-05
Nicardipine HCl	1.79E-05	2.96E-06
Sasapyrine	7.59E-11	1.76E-05
Pilocarpine HCl	2.27E-17	2.24E-24
Fasudil	1.23E-05	1.77E-16
Y27632	0.000286166	3.31E-24

Appendix Table 1. FDA-approved drugs that significantly reduced α-SMA and fibronectin expression in TGF-β1-treated lung fibroblasts. Statistical test Kolmogorov-Smirnov was used to compare cumulative frequency of drug & TGF-β1-treated lung fibroblasts relative to DMSO & TGF-β1-treated cells.

Appendix Figure 20. RStudio script used to analyse IN Cell drug screen data. The script presented below was used to assess fibronectin (FN) staining intensity of lung fibroblasts in drug + TGF-β1 compared to DMSO + TGF-β1 treated wells. For α-SMA analysis, 'FN' was substituted for 'SMA' to access the correct data file.

```
#To show plate list:

plateList <-
read.table(file="C:\\Users\\Zareen\\Desktop\\drugTestingStats\\plateList.txt",
sep="\t", header = FALSE, stringsAsFactors = FALSE)

#wells containing drug data

drugsWells <- expand.grid(seq(2,10,2), c("A", "B", "C", "D", "E", "F", "G", "H"))

#loop though each plate and perform statistics,

for(currPlate in 1:nrow(plateList)){

#make results table

mainFNTab <- data.frame(matrix(NA, ncol=7, nrow=40))

names(mainFNTab) <- c("well", "type", "NorCells", "DrugCells", "meanNorm",
"meanDrug", "p.value")

mainFNTab[1:40, 2] <- "FN"

#plate locations

SMAplateTemp <- paste("C:\\Users\\Zareen\\Desktop\\drugTestingStats\\",
as.character(plateList[currPlate,1]), "\\", as.character(plateList[currPlate,1]),
".SMA.A.csv", sep="")

FNplateTempA <- paste("C:\\Users\\Zareen\\Desktop\\drugTestingStats\\",
as.character(plateList[currPlate,1]), "\\", as.character(plateList[currPlate,1]),
".FN.A.csv", sep="")

FNplateTempB <- paste("C:\\Users\\Zareen\\Desktop\\drugTestingStats\\",
as.character(plateList[currPlate,1]), "\\", as.character(plateList[currPlate,1]),
".FN.B.csv", sep="")

#make output directory

#system(command = paste("mkdir ",
"C:\\Users\\Zareen\\Desktop\\drugTestingStats\\",
as.character(plateList[currPlate,1]), sep=""))

#### FN analysis ####
```

#read in tables

```
FNtab <- read.csv(file=FNplateTempA, stringsAsFactors = FALSE)
```

#remove NA rows

```
FNtab <- FNtab[FNtab[[1]] != "", ]
```

#remove unwanted spaces from cell names

```
 for(currStr in 1:nrow(FNtab)){FNtab[currStr,1] <-
paste(strsplit(as.character(FNtab[currStr,1]), split = " ")[[1]][1],
strsplit(as.character(FNtab[currStr,1]), split = " ")[[1]][3], sep = "")
  }
```

#separate control from plate

```
normalFN <- FNtab[FNtab[[1]]=="A12" | FNtab[[1]]=="B12", ]
meanNormal <- mean(normalFN[["Levels.FN_NM.Cells"]])
```

#plot graphs as grid

```
graphName <-
paste("C:\\Users\\Zareen\\Desktop\\drugTestingStats\\",as.character(plateList[cur
rPlate,1]), "\\", as.character(plateList[currPlate,1]), ".FN.pdf", sep="")
pdf(file=graphName, height = 40, width = 20)
par(mfrow=c(10, 4), mar=c(2,2,2,2))
```

#status message during running of the script

```
for(currTest in 1:nrow(drugsWells)){
currentWell <- paste(drugsWells[currTest, 2], drugsWells[currTest, 1], sep="")
print(paste("#### analyzing plate", currPlate, "drug well", currentWell, "####"))
```

#save current well name to main table

```
mainFNTab[currTest, "well"] <- currentWell
mainFNTab[currTest, "NorCells"] <- nrow(normalFN)
mainFNTab[currTest, "meanNorm"]<- meanNormal
```

#show current drug data

```
currDrugData <- FNtab[FNtab[["Section"]]==currentWell, ]
```

#test to see if current well has drug

```
if(nrow(currDrugData) < 200){
```

#do not perform statistical test

mainFNTab[currTest, "DrugCells"] <- nrow(currDrugData) next

}

#perform a Kolmogorov Smirnov test or Wilcoxon signed rank test ('wilcox.test')

tempStats <- ks.test(x = normalFN[["Levels.FN_NM.Cells"]], y = currDrugData[["Levels.FN_NM.Cells"]], alternative = "less")

#save the statistics to a main table (MS Excel)

mainFNTab[currTest, "meanDrug"] <- mean(currDrugData[["Levels.FN_NM.Cells"]])

mainFNTab[currTest, "p.value"] <- tempStats["p.value"]

mainFNTab[currTest, "DrugCells"] <- nrow(currDrugData)

#plot cumulative frequency graph to compare distribution*

plot(ecdf(x=normalFN[["Levels.FN_NM.Cells"]]), cex=0.5, col=rgb(0,0,1,0.5), main=paste(as.character(plateList[currPlate,1]), " ", currentWell))

plot(ecdf(x=currDrugData[["Levels.FN_NM.Cells"]]), cex=0.5, col=rgb(1,0,0,0.5), add=TRUE)

legend("bottomright", legend = c("drug", "normal"), col=c(rgb(1,0,0,0.5), rgb(0,0,1,0.5)), lty=1, lwd=5, cex=1.5)

text(x=600, y=0.8, labels = paste("p =", round(as.numeric(tempStats["p.value"], digits = 10))), cex=3) }

dev.off()

#save main table to chosen directory location

outFNfile <- paste("C:\\Users\\Zareen\\Desktop\\drugTestingStats\\", as.character(plateList[currPlate,1]), "\\", as.character(plateList[currPlate,1]), ".FN.cumulfreq.csv", sep="")

write.table(mainFNTab, file=outFNfile, sep=",", row.names = FALSE, quote = FALSE)}

***#or instead to a plot a box and whiskers plot to compare medians**

graphName <- paste("C:\\Users\\Zareen\\Desktop\\drugTestingStats\\FN\\", as.character(plateList[currPlate,1]), "\\", as.character(plateList[currPlate,1]), ".boxplot.", currentWell, ".pdf", sep="") pdf(file=graphName, height = 5, width = 5) boxplot(normalFN[["Levels.FN_NM.Cells"]], currDrugData[["Levels.FN_NM.Cells"]], main=paste(as.character(plateList[currPlate,1]), currentWell), ylab="Fluorescence", names = c("Normal", "Drug"))

dev.off() }

References

[1] B. Hinz *et al.*, "Recent developments in myofibroblast biology: paradigms for connective tissue remodeling," *The American journal of pathology,* vol. 180, no. 4, pp. 1340-1355, 2012.

[2] F. Grinnell, "Fibroblast biology in three-dimensional collagen matrices," *Trends in cell biology,* vol. 13, no. 5, pp. 264-269, 2003.

[3] G. Gabbiani, G. B. Ryan, and G. Majno, "Presence of modified fibroblasts in granulation tissue and their possible role in wound contraction," *Experientia,* vol. 27, no. 5, pp. 549-550, 1971.

[4] L. Germain, A. Jean, F. A. Auger, and D. R. Garrel, "Human wound healing fibroblasts have greater contractile properties than dermal fibroblasts," *Journal of Surgical Research,* vol. 57, no. 2, pp. 268-273, 1994.

[5] I. Darby, O. Skalli, and G. Gabbiani, "a-Smooth muscle actin is transiently expressed by myofibroblasts during experimental wound healing," *Lab Invest,* vol. 63, no. 1, pp. 21-29, 1990.

[6] I. A. Darby, B. Laverdet, F. Bonté, and A. Desmoulière, "Fibroblasts and myofibroblasts in wound healing," *Clinical, cosmetic and investigational dermatology,* vol. 7, p. 301, 2014.

[7] C. F. Singer, E. Marbaix, P. Lemoine, P. J. Courtoy, and Y. Eeckhout, "Local cytokines induce differential expression of matrix metalloproteinases but not their tissue inhibitors in human endometrial fibroblasts," *European Journal of Biochemistry,* vol. 259, no. 1-2, pp. 40-45, 1999.

[8] R. Mirza, L. A. DiPietro, and T. J. Koh, "Selective and specific macrophage ablation is detrimental to wound healing in mice," *The American journal of pathology,* vol. 175, no. 6, pp. 2454-2462, 2009.

[9] F. Grinnell, R. E. Billingham, and L. Burgess, "Distribution of fibronectin during wound healing in vivo," *Journal of Investigative Dermatology,* vol. 76, no. 3, pp. 181-189, 1981.

[10] J. Li, J. Chen, and R. Kirsner, "Pathophysiology of acute wound healing," *Clinics in dermatology,* vol. 25, no. 1, pp. 9-18, 2007.

[11] P. Martin, "Wound healing--aiming for perfect skin regeneration," *Science,* vol. 276, no. 5309, pp. 75-81, 1997.

[12] B. Hinz, D. Mastrangelo, C. E. Iselin, C. Chaponnier, and G. Gabbiani, "Mechanical tension controls granulation tissue contractile activity and myofibroblast differentiation," *The American journal of pathology,* vol. 159, no. 3, pp. 1009-1020, 2001.

[13] I. Boxman, C. Löwik, L. Aarden, and M. Ponec, "Modulation of IL-6 production of IL-1 activity by keratinocyte-fibroblast interaction," *Journal of investigative dermatology,* vol. 101, no. 3, pp. 316-324, 1993.

[14] Z.-Q. Lin, T. Kondo, Y. Ishida, T. Takayasu, and N. Mukaida, "Essential involvement of IL-6 in the skin wound-healing process as evidenced by delayed wound healing in IL-6-deficient mice," *Journal of leukocyte biology,* vol. 73, no. 6, pp. 713-721, 2003.

[15] S. Werner, T. Krieg, and H. Smola, "Keratinocyte–fibroblast interactions in wound healing," *Journal of Investigative Dermatology,* vol. 127, no. 5, pp. 998-1008, 2007.

[16] Z. Khan and J. F. Marshall, "The role of integrins in TGFβ activation in the tumour stroma," *Cell and Tissue Research,* vol. 365, no. 3, pp. 657-673, 2016.

[17] R. A. Rahimi and E. B. Leof, "TGF-β signaling: A tale of two responses," *Journal of cellular biochemistry,* vol. 102, no. 3, pp. 593-608, 2007.

[18] B. Bierie and H. L. Moses, "Transforming growth factor beta (TGF-β) and inflammation in cancer," *Cytokine & growth factor reviews,* vol. 21, no. 1, pp. 49-59, 2010.
[19] M. A. Travis and D. Sheppard, "TGF-β activation and function in immunity," *Annual review of immunology,* vol. 32, p. 51, 2014.
[20] L. E. Gentry and B. W. Nash, "The pro domain of pre-pro-transforming growth factor. beta. 1 when independently expressed is a functional binding protein for the mature growth factor," *Biochemistry,* vol. 29, no. 29, pp. 6851-6857, 1990.
[21] L. Zilberberg *et al.*, "Specificity of latent TGF-β binding protein (LTBP) incorporation into matrix: Role of fibrillins and fibronectin," *Journal of cellular physiology,* vol. 227, no. 12, pp. 3828-3836, 2012.
[22] D. Mu *et al.*, "The integrin αvβ8 mediates epithelial homeostasis through MT1-MMP–dependent activation of TGF-β1," *The Journal of cell biology,* vol. 157, no. 3, pp. 493-507, 2002.
[23] Q. Yu and I. Stamenkovic, "Cell surface-localized matrix metalloproteinase-9 proteolytically activates TGF-β and promotes tumor invasion and angiogenesis," *Genes & development,* vol. 14, no. 2, pp. 163-176, 2000.
[24] F. Klingberg *et al.*, "Prestress in the extracellular matrix sensitizes latent TGF-β1 for activation," *The Journal of cell biology,* vol. 207, no. 2, pp. 283-297, 2014.
[25] H. Hayashi and T. Sakai, "Biological significance of local TGF-β activation in liver diseases," *Frontiers in physiology,* vol. 3, p. 12, 2012.
[26] T. Ebisawa *et al.*, "Smurf1 interacts with transforming growth factor-β type I receptor through Smad7 and induces receptor degradation," *Journal of Biological Chemistry,* vol. 276, no. 16, pp. 12477-12480, 2001.
[27] J. Massagué and D. Wotton, "Transcriptional control by the TGF-β/Smad signaling system," *The EMBO journal,* vol. 19, no. 8, pp. 1745-1754, 2000.
[28] V. J. Thannickal *et al.*, "Myofibroblast differentiation by transforming growth factor-β1 is dependent on cell adhesion and integrin signaling via focal adhesion kinase," *Journal of Biological Chemistry,* vol. 278, no. 14, pp. 12384-12389, 2003.
[29] R. O. Hynes, "Integrins: bidirectional, allosteric signaling machines," *Cell,* vol. 110, no. 6, pp. 673-687, 2002.
[30] M. Barczyk, S. Carracedo, and D. Gullberg, "Integrins," (in eng), *Cell Tissue Res,* vol. 339, no. 1, pp. 269-80, Jan 2010.
[31] J. Emsley, C. G. Knight, R. W. Farndale, M. J. Barnes, and R. C. Liddington, "Structural basis of collagen recognition by integrin α2β1," *Cell,* vol. 101, no. 1, pp. 47-56, 2000.
[32] E. F. Plow, T. A. Haas, L. Zhang, J. Loftus, and J. W. Smith, "Ligand binding to integrins," *Journal of Biological Chemistry,* vol. 275, no. 29, pp. 21785-21788, 2000.
[33] J. Takagi, "Structural basis for ligand recognition by RGD (Arg-Gly-Asp)-dependent integrins," *Biochemical Society Transactions,* vol. 32, no. 3, pp. 403-406, 2004.
[34] B. Hinz and G. Gabbiani, "Fibrosis: recent advances in myofibroblast biology and new therapeutic perspectives," *F1000 Biol Rep,* vol. 2, no. 2, p. 78, 2010.
[35] D. B. Rifkin and D. Sheppard, "The integrin v 6 binds and activates latent TGF 1: a mechanism for regulating pulmonary inflammation and fibrosis," *Cell,* vol. 96, pp. 319-328, 1999.
[36] C. Margadant and A. Sonnenberg, "Integrin–TGF-β crosstalk in fibrosis, cancer and wound healing," *EMBO reports,* vol. 11, no. 2, pp. 97-105, 2010.
[37] J. J. Worthington *et al.*, "Integrin αvβ8-Mediated TGF-β Activation by Effector Regulatory T Cells Is Essential for Suppression of T-Cell-Mediated Inflammation," *Immunity,* vol. 42, no. 5, pp. 903-915, 2015.
[38] N. I. Reed *et al.*, "The αvβ1 integrin plays a critical in vivo role in tissue fibrosis," *Science translational medicine,* vol. 7, no. 288, pp. 288ra79-288ra79, 2015.

[39] P.-J. Wipff, D. B. Rifkin, J.-J. Meister, and B. Hinz, "Myofibroblast contraction activates latent TGF-β1 from the extracellular matrix," *The Journal of cell biology,* vol. 179, no. 6, pp. 1311-1323, 2007.
[40] J.-P. Xiong *et al.*, "Crystal structure of the extracellular segment of integrin αVβ3," *Science,* vol. 294, no. 5541, pp. 339-345, 2001.
[41] J. Takagi, B. M. Petre, T. Walz, and T. A. Springer, "Global conformational rearrangements in integrin extracellular domains in outside-in and inside-out signaling," *Cell,* vol. 110, no. 5, pp. 599-611, 2002.
[42] Y. Su *et al.*, "Relating conformation to function in integrin α5β1," *Proceedings of the National Academy of Sciences,* vol. 113, no. 27, pp. E3872-E3881, 2016.
[43] H. H. Truong *et al.*, "β1 Integrin Inhibition Elicits a Prometastatic Switch Through the TGFβ–miR-200–ZEB Network in E-Cadherin–Positive Triple-Negative Breast Cancer," *Sci. Signal.,* vol. 7, no. 312, pp. ra15-ra15, 2014.
[44] I. D. Campbell and M. J. Humphries, "Integrin structure, activation, and interactions," *Cold Spring Harbor perspectives in biology,* vol. 3, no. 3, p. a004994, 2011.
[45] K. R. Legate, S. A. Wickström, and R. Fässler, "Genetic and cell biological analysis of integrin outside-in signaling," *Genes & development,* vol. 23, no. 4, pp. 397-418, 2009.
[46] E. R. Horton *et al.*, "Definition of a consensus integrin adhesome and its dynamics during adhesion complex assembly and disassembly," *Nature cell biology,* vol. 17, no. 12, pp. 1577-1587, 2015.
[47] M. Theodosiou *et al.*, "Kindlin-2 cooperates with talin to activate integrins and induces cell spreading by directly binding paxillin," *eLife,* vol. 5, p. e10130, 2016.
[48] D. S. Harburger, M. Bouaouina, and D. A. Calderwood, "Kindlin-1 and-2 directly bind the C-terminal region of β integrin cytoplasmic tails and exert integrin-specific activation effects," *Journal of Biological Chemistry,* vol. 284, no. 17, pp. 11485-11497, 2009.
[49] L. Hemmings *et al.*, "Talin contains three actin-binding sites each of which is adjacent to a vinculin-binding site," *Journal of Cell Science,* vol. 109, no. 11, pp. 2715-2726, 1996.
[50] E. A. Cavalcanti-Adam, T. Volberg, A. Micoulet, H. Kessler, B. Geiger, and J. P. Spatz, "Cell spreading and focal adhesion dynamics are regulated by spacing of integrin ligands," *Biophysical journal,* vol. 92, no. 8, pp. 2964-2974, 2007.
[51] D. J. Sieg *et al.*, "FAK integrates growth-factor and integrin signals to promote cell migration," *Nature cell biology,* vol. 2, no. 5, pp. 249-256, 2000.
[52] M. D. Schaller, J. D. Hildebrand, J. D. Shannon, J. W. Fox, R. R. Vines, and J. T. Parsons, "Autophosphorylation of the focal adhesion kinase, pp125FAK, directs SH2-dependent binding of pp60src," *Molecular and cellular biology,* vol. 14, no. 3, pp. 1680-1688, 1994.
[53] D. A. MacKenna, F. Dolfi, K. Vuori, and E. Ruoslahti, "Extracellular signal-regulated kinase and c-Jun NH2-terminal kinase activation by mechanical stretch is integrin-dependent and matrix-specific in rat cardiac fibroblasts," *Journal of Clinical Investigation,* vol. 101, no. 2, p. 301, 1998.
[54] J. Wang, H. Chen, A. Seth, and C. A. McCulloch, "Mechanical force regulation of myofibroblast differentiation in cardiac fibroblasts," *American Journal of Physiology-Heart and Circulatory Physiology,* vol. 285, no. 5, pp. H1871-H1881, 2003.
[55] A. K. Schroer, L. M. Ryzhova, and W. D. Merryman, "Network Modeling Approach to Predict Myofibroblast Differentiation," *Cellular and Molecular Bioengineering,* vol. 7, no. 3, pp. 446-459, 2014.
[56] M. B. Srichai and R. Zent, "Integrin structure and function," in *Cell-Extracellular Matrix Interactions in Cancer*: Springer, 2010, pp. 19-41.

[57] J.-P. Levesque, D. I. Leavesley, S. Niutta, M. Vadas, and P. J. Simmons, "Cytokines increase human hemopoietic cell adhesiveness by activation of very late antigen (VLA)-4 and VLA-5 integrins," *The Journal of experimental medicine,* vol. 181, no. 5, pp. 1805-1815, 1995.

[58] S. J. Ellis *et al.*, "The talin head domain reinforces integrin-mediated adhesion by promoting adhesion complex stability and clustering," *PLoS Genet,* vol. 10, no. 11, p. e1004756, 2014.

[59] Y.-Q. Ma, J. Qin, C. Wu, and E. F. Plow, "Kindlin-2 (Mig-2): a co-activator of β3 integrins," *The Journal of cell biology,* vol. 181, no. 3, pp. 439-446, 2008.

[60] J. Heino, R. A. Ignotz, M. E. Hemler, C. Crouse, and J. Massague, "Regulation of cell adhesion receptors by transforming growth factor-beta. Concomitant regulation of integrins that share a common beta 1 subunit," *Journal of Biological Chemistry,* vol. 264, no. 1, pp. 380-388, 1989.

[61] S. Carracedo, N. Lu, S. N. Popova, R. Jonsson, B. Eckes, and D. Gullberg, "The fibroblast integrin α11β1 is induced in a mechanosensitive manner involving activin A and regulates myofibroblast differentiation," *Journal of Biological Chemistry,* vol. 285, no. 14, pp. 10434-10445, 2010.

[62] Y. Asano, H. Ihn, K. Yamane, M. Kubo, and K. Tamaki, "Increased expression levels of integrin αvβ5 on scleroderma fibroblasts," *The American journal of pathology,* vol. 164, no. 4, pp. 1275-1292, 2004.

[63] Y. Asano, H. Ihn, M. Jinnin, Y. Mimura, and K. Tamaki, "Involvement of αvβ5 integrin in the establishment of autocrine TGF-β signaling in dermal fibroblasts derived from localized scleroderma," *Journal of investigative dermatology,* vol. 126, no. 8, pp. 1761-1769, 2006.

[64] K. A. Lygoe, J. T. Norman, J. F. Marshall, and M. P. Lewis, "αv integrins play an important role in myofibroblast differentiation," *Wound repair and regeneration,* vol. 12, no. 4, pp. 461-470, 2004.

[65] J. C. Horowitz *et al.*, "Combinatorial activation of FAK and AKT by transforming growth factor-β1 confers an anoikis-resistant phenotype to myofibroblasts," *Cellular signalling,* vol. 19, no. 4, pp. 761-771, 2007.

[66] Z. Wang *et al.*, "Mice overexpressing integrin αv in fibroblasts exhibit dermal thinning of the skin," *Journal of dermatological science,* vol. 79, no. 3, pp. 268-278, 2015.

[67] L. Vi, C. de Lasa, G. M. DiGuglielmo, and L. Dagnino, "Integrin-linked kinase is required for TGF-β1 induction of dermal myofibroblast differentiation," *Journal of Investigative Dermatology,* vol. 131, no. 3, pp. 586-593, 2010.

[68] H. Denys *et al.*, "Differential impact of TGF-β and EGF on fibroblast differentiation and invasion reciprocally promotes colon cancer cell invasion," *Cancer letters,* vol. 266, no. 2, pp. 263-274, 2008.

[69] O. M. Rossier *et al.*, "Force generated by actomyosin contraction builds bridges between adhesive contacts," *The EMBO journal,* vol. 29, no. 6, pp. 1055-1068, 2010.

[70] J. J. Tomasek, G. Gabbiani, B. Hinz, C. Chaponnier, and R. A. Brown, "Myofibroblasts and mechano-regulation of connective tissue remodelling," *Nature Reviews Molecular Cell Biology,* vol. 3, no. 5, pp. 349-363, 2002.

[71] J. M. Carthy *et al.*, "Tamoxifen Inhibits TGF-β-Mediated Activation of Myofibroblasts by Blocking Non-Smad Signaling Through ERK1/2," *Journal of cellular physiology,* vol. 230, no. 12, pp. 3084-3092, 2015.

[72] P. Huhtala, M. J. Humphries, J. B. McCarthy, P. M. Tremble, Z. Werb, and C. H. Damsky, "Cooperative signaling by alpha 5 beta 1 and alpha 4 beta 1 integrins regulates metalloproteinase gene expression in fibroblasts adhering to fibronectin," *The Journal of cell biology,* vol. 129, no. 3, pp. 867-879, 1995.

[73] J. E. Koblinski, J. Dosescu, M. Sameni, K. Moin, K. Clark, and B. F. Sloane, "Interaction of human breast fibroblasts with collagen I increases secretion of procathepsin B," *Journal of Biological Chemistry,* vol. 277, no. 35, pp. 32220-32227, 2002.
[74] M. M. Barczyk, N. Lu, S. N. Popova, A. I. Bolstad, and D. Gullberg, "α11β1 integrin-mediated MMP-13-dependent collagen lattice contraction by fibroblasts: Evidence for integrin-coordinated collagen proteolysis," *Journal of cellular physiology,* vol. 228, no. 5, pp. 1108-1119, 2013.
[75] H. Chen *et al.*, "Mechanosensing by the α6-integrin confers an invasive fibroblast phenotype and mediates lung fibrosis," *Nature Communications,* vol. 7, p. 12564, 2016.
[76] X.-K. Zhao *et al.*, "Focal Adhesion Kinase Regulates Fibroblast Migration via Integrin beta-1 and Plays a Central Role in Fibrosis," *Scientific reports,* vol. 6, 2016.
[77] J.-W. Lee *et al.*, "HSP27 regulates cell adhesion and invasion via modulation of focal adhesion kinase and MMP-2 expression," *European journal of cell biology,* vol. 87, no. 6, pp. 377-387, 2008.
[78] (2016). *Deaths Registered in England and Wales - Office for National Statistics*. Available: http://www.ons.gov.uk/peoplepopulationandcommunity/birthsdeathsandmarriages/deaths/bulletins/deathsregistrationsummarytables/2015-07-15#causes-of-death
[79] (2015). *Cancer mortality for common cancers*. Available: http://www.cancerresearchuk.org/health-professional/cancer-statistics/mortality/common-cancers-compared
[80] (2015). *Cancer incidence statistics*. Available: http://www.cancerresearchuk.org/health-professional/cancer-statistics/incidence
[81] (2015, 28/09/16). *Bladder cancer incidence statistics*. Available: http://www.cancerresearchuk.org/health-professional/cancer-statistics/statistics-by-cancer-type/bladder-cancer/incidence
[82] (2015, 28/09/16). *Stomach cancer incidence statistics*. Available: http://www.cancerresearchuk.org/health-professional/cancer-statistics/statistics-by-cancer-type/stomach-cancer/incidence
[83] (2015, 28/09/16). *Cancer incidence for all cancers combined*. Available: http://www.cancerresearchuk.org/health-professional/cancer-statistics/incidence/all-cancers-combined
[84] (2015). *Lung cancer survival statistics*. Available: http://www.cancerresearchuk.org/health-professional/cancer-statistics/statistics-by-cancer-type/lung-cancer/survival
[85] M. J. Bissell and W. C. Hines, "Why don't we get more cancer? A proposed role of the microenvironment in restraining cancer progression," *Nature medicine,* vol. 17, no. 3, pp. 320-329, 2011.
[86] R. M. Bremnes *et al.*, "The role of tumor stroma in cancer progression and prognosis: emphasis on carcinoma-associated fibroblasts and non-small cell lung cancer," *Journal of Thoracic Oncology,* vol. 6, no. 1, pp. 209-217, 2011.
[87] C. Eberlein, C. Rooney, S. J. Ross, M. Farren, H. M. Weir, and S. T. Barry, "E-Cadherin and EpCAM expression by NSCLC tumour cells associate with normal fibroblast activation through a pathway initiated by integrin αvβ6 and maintained through TGFβ signalling," *Oncogene,* vol. 34, no. 6, pp. 704-716, 2015.
[88] M. Groessl *et al.*, "Proteome profiling of breast cancer biopsies reveals a wound healing signature of cancer-associated fibroblasts," *Journal of proteome research,* vol. 13, no. 11, pp. 4773-4782, 2014.
[89] N. A. Bhowmick *et al.*, "TGF-ß signaling in fibroblasts modulates the oncogenic potential of adjacent epithelia," *Science,* vol. 303, no. 5659, pp. 848-851, 2004.

[90] L. Hawinkels *et al.*, "Interaction with colon cancer cells hyperactivates TGF-β signaling in cancer-associated fibroblasts," *Oncogene,* vol. 33, no. 1, pp. 97-107, 2014.
[91] Y. Yu, C. H. Xiao, L. D. Tan, Q. S. Wang, X. Q. Li, and Y. M. Feng, "Cancer-associated fibroblasts induce epithelial–mesenchymal transition of breast cancer cells through paracrine TGF-β signalling," *British journal of cancer,* vol. 110, no. 3, pp. 724-732, 2014.
[92] M. Yamashita *et al.*, "Role of stromal myofibroblasts in invasive breast cancer: stromal expression of alpha-smooth muscle actin correlates with worse clinical outcome," *Breast Cancer,* vol. 19, no. 2, pp. 170-176, 2012.
[93] T. Tsujino *et al.*, "Stromal myofibroblasts predict disease recurrence for colorectal cancer," *Clinical Cancer Research,* vol. 13, no. 7, pp. 2082-2090, 2007.
[94] M. G. Kellermann *et al.*, "Myofibroblasts in the stroma of oral squamous cell carcinoma are associated with poor prognosis," *Histopathology,* vol. 51, no. 6, pp. 849-853, 2007.
[95] A. M. Baker, D. Bird, G. Lang, T. R. Cox, and J. T. Erler, "Lysyl oxidase enzymatic function increases stiffness to drive colorectal cancer progression through FAK," *Oncogene,* vol. 32, no. 14, pp. 1863-1868, 2013.
[96] T. G. Voloshenyuk, E. S. Landesman, E. Khoutorova, A. D. Hart, and J. D. Gardner, "Induction of cardiac fibroblast lysyl oxidase by TGF-β1 requires PI3K/Akt, Smad3, and MAPK signaling," *Cytokine,* vol. 55, no. 1, pp. 90-97, 2011.
[97] H. M. Kagan and W. Li, "Lysyl oxidase: properties, specificity, and biological roles inside and outside of the cell," *Journal of cellular biochemistry,* vol. 88, no. 4, pp. 660-672, 2003.
[98] M. Sakai *et al.*, "Expression of lysyl oxidase is correlated with lymph node metastasis and poor prognosis in esophageal squamous cell carcinoma," *Annals of surgical oncology,* vol. 16, no. 9, pp. 2494-2501, 2009.
[99] S. Reid *et al.*, "Tumour matrix stiffness regulates metastasis by promoting cancer cell interactions with the endothelium," *European Journal of Cancer,* vol. 61, p. S64, 2016.
[100] K. Zhang *et al.*, "Mechanical signals regulate and activate SNAIL1 protein to control the fibrogenic response of cancer-associated fibroblasts," *J Cell Sci,* vol. 129, no. 10, pp. 1989-2002, 2016.
[101] C. D. Madsen *et al.*, "Hypoxia and loss of PHD2 inactivate stromal fibroblasts to decrease tumour stiffness and metastasis," *EMBO reports,* vol. 16, no. 10, pp. 1394-1408, 2015.
[102] C. Gaggioli *et al.*, "Fibroblast-led collective invasion of carcinoma cells with differing roles for RhoGTPases in leading and following cells," *Nature cell biology,* vol. 9, no. 12, pp. 1392-1400, 2007.
[103] L. Alba-Castellón *et al.*, "Snail1-dependent activation of cancer-associated fibroblast controls epithelial tumor cell invasion and metastasis," *Cancer Research,* pp. canres-0176, 2016.
[104] C.-Q. Zhu *et al.*, "Integrin α11 regulates IGF2 expression in fibroblasts to enhance tumorigenicity of human non-small-cell lung cancer cells," *Proceedings of the National Academy of Sciences,* vol. 104, no. 28, pp. 11754-11759, 2007.
[105] H. Lim and A. Moon, "Inflammatory fibroblasts in cancer," *Archives of Pharmacal Research,* vol. 39, no. 8, pp. 1021-1031, 2016.
[106] N. Erez, S. Glanz, Y. Raz, C. Avivi, and I. Barshack, "Cancer associated fibroblasts express pro-inflammatory factors in human breast and ovarian tumors," *Biochemical and biophysical research communications,* vol. 437, no. 3, pp. 397-402, 2013.

[107] J. Liu *et al.*, "Cancer-associated fibroblasts promote hepatocellular carcinoma metastasis through chemokine-activated hedgehog and TGF-β pathways," *Cancer letters,* vol. 379, no. 1, pp. 49-59, 2016.
[108] S.-E. Kuzet and C. Gaggioli, "Fibroblast activation in cancer: when seed fertilizes soil," *Cell and Tissue Research,* vol. 365, no. 3, pp. 607-619, 2016.
[109] E. Hirata *et al.*, "Intravital imaging reveals how BRAF inhibition generates drug-tolerant microenvironments with high integrin β1/FAK signaling," *Cancer Cell,* vol. 27, no. 4, pp. 574-588, 2015.
[110] W. Wang *et al.*, "Crosstalk to stromal fibroblasts induces resistance of lung cancer to epidermal growth factor receptor tyrosine kinase inhibitors," *Clinical Cancer Research,* vol. 15, no. 21, pp. 6630-6638, 2009.
[111] R. Straussman *et al.*, "Tumour micro-environment elicits innate resistance to RAF inhibitors through HGF secretion," *Nature,* vol. 487, no. 7408, pp. 500-504, 2012.
[112] C. Hage *et al.*, "The novel c-Met inhibitor cabozantinib overcomes gemcitabine resistance and stem cell signaling in pancreatic cancer," *Cell death & disease,* vol. 4, no. 5, p. e627, 2013.
[113] C. Bavik, I. Coleman, J. P. Dean, B. Knudsen, S. Plymate, and P. S. Nelson, "The gene expression program of prostate fibroblast senescence modulates neoplastic epithelial cell proliferation through paracrine mechanisms," *Cancer research,* vol. 66, no. 2, pp. 794-802, 2006.
[114] T. Kuilman *et al.*, "Oncogene-induced senescence relayed by an interleukin-dependent inflammatory network," *Cell,* vol. 133, no. 6, pp. 1019-1031, 2008.
[115] J.-P. Coppé, P.-Y. Desprez, A. Krtolica, and J. Campisi, "The senescence-associated secretory phenotype: the dark side of tumor suppression," *Annual review of pathology,* vol. 5, p. 99, 2010.
[116] A. Krtolica, S. Parrinello, S. Lockett, P.-Y. Desprez, and J. Campisi, "Senescent fibroblasts promote epithelial cell growth and tumorigenesis: a link between cancer and aging," *Proceedings of the National Academy of Sciences,* vol. 98, no. 21, pp. 12072-12077, 2001.
[117] K.-H. Kim *et al.*, "Expression of connective tissue growth factor, a biomarker in senescence of human diploid fibroblasts, is up-regulated by a transforming growth factor-β-mediated signaling pathway," *Biochemical and biophysical research communications,* vol. 318, no. 4, pp. 819-825, 2004.
[118] J.-P. Coppé, K. Kauser, J. Campisi, and C. M. Beauséjour, "Secretion of vascular endothelial growth factor by primary human fibroblasts at senescence," *Journal of Biological Chemistry,* vol. 281, no. 40, pp. 29568-29574, 2006.
[119] N. Choices. (2016, 09/10/2016). *Idiopathic pulmonary fibrosis - NHS Choices*. Available: http://www.nhs.uk/conditions/pulmonary-fibrosis/Pages/Introduction.aspx
[120] (2016, 09/10/2016). *Idiopathic pulmonary fibrosis - Treatment - NHS Choices*. Available: http://www.nhs.uk/Conditions/pulmonary-fibrosis/Pages/Treatment.aspx
[121] K. Zhang, M. D. Rekhter, D. Gordon, and S. H. Phan, "Myofibroblasts and their role in lung collagen gene expression during pulmonary fibrosis. A combined immunohistochemical and in situ hybridization study," *The American journal of pathology,* vol. 145, no. 1, p. 114, 1994.
[122] F. Klingberg, B. Hinz, and E. S. White, "The myofibroblast matrix: implications for tissue repair and fibrosis," *The Journal of pathology,* vol. 229, no. 2, pp. 298-309, 2013.

[123] Y. Popov *et al.*, "Integrin αvβ6 is a marker of the progression of biliary and portal liver fibrosis and a novel target for antifibrotic therapies," *Journal of hepatology,* vol. 48, no. 3, pp. 453-464, 2008.
[124] K. Puthawala *et al.*, "Inhibition of integrin αvβ6, an activator of latent transforming growth factor-β, prevents radiation-induced lung fibrosis," *American journal of respiratory and critical care medicine,* vol. 177, no. 1, pp. 82-90, 2008.
[125] V. Sarrazy *et al.*, "Integrins αvβ5 and αvβ3 promote latent TGF-β1 activation by human cardiac fibroblast contraction," *Cardiovascular research,* vol. 102, no. 3, pp. 407-417, 2014.
[126] H. Xia *et al.*, "Pathological integrin signaling enhances proliferation of primary lung fibroblasts from patients with idiopathic pulmonary fibrosis," *The Journal of experimental medicine,* vol. 205, no. 7, pp. 1659-1672, 2008.
[127] E. Patsenker and F. Stickel, "Role of integrins in fibrosing liver diseases," *American Journal of Physiology-Gastrointestinal and Liver Physiology,* vol. 301, no. 3, pp. G425-G434, 2011.
[128] M. T. Milliano and B. A. Luxon, "Initial signaling of the fibronectin receptor (α< sub> 5</sub> β< sub> 1</sub> integrin) in hepatic stellate cells is independent of tyrosine phosphorylation," *Journal of hepatology,* vol. 39, no. 1, pp. 32-37, 2003.
[129] D. Levine, D. C. Rockey, T. A. Milner, J. M. Breuss, J. T. Fallon, and L. M. Schnapp, "Expression of the integrin α8β1 during pulmonary and hepatic fibrosis," *The American journal of pathology,* vol. 156, no. 6, pp. 1927-1935, 2000.
[130] N. C. Henderson *et al.*, "Targeting of [alpha] v integrin identifies a core molecular pathway that regulates fibrosis in several organs," *Nature medicine,* vol. 19, no. 12, pp. 1617-1624, 2013.
[131] K. M. Fries *et al.*, "Evidence of fibroblast heterogeneity and the role of fibroblast subpopulations in fibrosis," *Clinical immunology and immunopathology,* vol. 72, no. 3, pp. 283-292, 1994.
[132] J. M. Sorrell and A. I. Caplan, "Fibroblast heterogeneity: more than skin deep," *Journal of cell science,* vol. 117, no. 5, pp. 667-675, 2004.
[133] I. A. Schafer, M. Pandy, R. Ferguson, and B. R. Davis, "Comparative observation of fibroblasts derived from the papillary and reticular dermis of infants and adults: growth kinetics, packing density at confluence and surface morphology," *Mechanisms of ageing and development,* vol. 31, no. 3, pp. 275-293, 1985.
[134] D. Lindner *et al.*, "Differential expression of matrix metalloproteases in human fibroblasts with different origins," *Biochemistry research international,* vol. 2012, 2012.
[135] M. Nonaka, R. Pawankar, A. Fukumoto, and T. Yagi, "Heterogeneous response of nasal and lung fibroblasts to transforming growth factor-β1," *Clinical & Experimental Allergy,* vol. 38, no. 5, pp. 812-821, 2008.
[136] J. M. Sorrell, M. A. Baber, and A. I. Caplan, "Human dermal fibroblast subpopulations; differential interactions with vascular endothelial cells in coculture: nonsoluble factors in the extracellular matrix influence interactions," *Wound Repair and Regeneration,* vol. 16, no. 2, pp. 300-309, 2008.
[137] A. W. Studebaker *et al.*, "Fibroblasts isolated from common sites of breast cancer metastasis enhance cancer cell growth rates and invasiveness in an interleukin-6–dependent manner," *Cancer research,* vol. 68, no. 21, pp. 9087-9095, 2008.
[138] K. P. Olive *et al.*, "Inhibition of Hedgehog signaling enhances delivery of chemotherapy in a mouse model of pancreatic cancer," *Science (New York, NY),* vol. 324, no. 5933, pp. 1457-1461, 2009.

[139] L. Mei, W. Du, and W. W. Ma, "Targeting stromal microenvironment in pancreatic ductal adenocarcinoma: controversies and promises," *Journal of gastrointestinal oncology,* vol. 7, no. 3, p. 487, 2016.
[140] M. R. Junttila and F. J. de Sauvage, "Influence of tumour micro-environment heterogeneity on therapeutic response," *Nature,* vol. 501, no. 7467, pp. 346-354, 2013.
[141] M. Nguyen, K. K. Lin, M. F. Burbridge, A. D. Simmons, and T. C. Harding, "Nonclinical activity of the FGFR, VEGFR and PDGFR inhibitor lucitanib in FGFR3 translocated tumor models," *Cancer Research,* vol. 75, no. 15 Supplement, pp. 784-784, 2015.
[142] J. M. Hansen, R. L. Coleman, and A. K. Sood, "Targeting the tumour microenvironment in ovarian cancer," *European Journal of Cancer,* vol. 56, pp. 131-143, 2016.
[143] K. E. Hostettler *et al.*, "Anti-fibrotic effects of nintedanib in lung fibroblasts derived from patients with idiopathic pulmonary fibrosis," *Respiratory research,* vol. 15, no. 1, p. 1, 2014.
[144] P. L. McCormack, "Nintedanib: first global approval," *Drugs,* vol. 75, no. 1, pp. 129-139, 2015.
[145] K. Ley, J. Rivera-Nieves, W. J. Sandborn, and S. Shattil, "Integrin-based therapeutics: biological basis, clinical use and new drugs," *Nature Reviews Drug Discovery,* vol. 15, no. 3, pp. 173-183, 2016.
[146] S. L. Goodman and M. Picard, "Integrins as therapeutic targets," *Trends in pharmacological sciences,* vol. 33, no. 7, pp. 405-412, 2012.
[147] A. R. Reynolds *et al.*, "Stimulation of tumor growth and angiogenesis by low concentrations of RGD-mimetic integrin inhibitors," *Nature medicine,* vol. 15, no. 4, pp. 392-400, 2009.
[148] P.-P. Wong *et al.*, "Dual-action combination therapy enhances angiogenesis while reducing tumor growth and spread," *Cancer Cell,* vol. 27, no. 1, pp. 123-137, 2015.
[149] M. Weller *et al.*, "Cilengitide in newly diagnosed glioblastoma: biomarker expression and outcome," *Oncotarget,* vol. 7, no. 12, pp. 15018-15032, 2016.
[150] K. M. Moore *et al.*, "Therapeutic targeting of integrin αvβ6 in breast cancer," *Journal of the National Cancer Institute,* vol. 106, no. 8, p. dju169, 2014.
[151] E. Élez *et al.*, "Abituzumab combined with cetuximab plus irinotecan versus cetuximab plus irinotecan alone for patients with KRAS wild-type metastatic colorectal cancer: the randomised phase I/II POSEIDON trial," *Annals of Oncology,* vol. 26, no. 1, pp. 132-140, 2015.
[152] C. B. Keerthisingam *et al.*, "Cyclooxygenase-2 deficiency results in a loss of the anti-proliferative response to transforming growth factor-β in human fibrotic lung fibroblasts and promotes bleomycin-induced pulmonary fibrosis in mice," *The American journal of pathology,* vol. 158, no. 4, pp. 1411-1422, 2001.
[153] J. J. Gomm, P. J. Browne, R. C. Coope, Q. Y. Liu, L. Buluwela, and R. C. Coombes, "Isolation of pure populations of epithelial and myoepithelial cells from the normal human mammary gland using immunomagnetic separation with Dynabeads," *Analytical biochemistry,* vol. 226, no. 1, pp. 91-99, 1995.
[154] G. J. Thomas *et al.*, "Expression of the &agr; v&bgr; 6 Integrin Promotes Migration and Invasion in Squamous Carcinoma Cells," *Journal of Investigative Dermatology,* vol. 117, no. 1, pp. 67-73, 2001.
[155] M. Sugiyama, P. M. Speight, S. S. Prime, and F. M. Watt, "Comparison of integrin expression and terminal differentiation capacity in cell lines derived from oral squamous cell carcinomas," *Carcinogenesis,* vol. 14, no. 10, pp. 2171-2176, 1993.

[156] (2016, 30/09/16). *NCI-H1299 ATCC Â® CRL-5803â„¢ Homo sapiens lung; derived from m*. Available: https://www.lgcstandards-atcc.org/Products/All/CRL-5803.aspx?geo_country=gb#generalinformation

[157] R. Cailleau, M. Olivé, and Q. V. J. Cruciger, "Long-term human breast carcinoma cell lines of metastatic origin: preliminary characterization," *In vitro,* vol. 14, no. 11, pp. 911-915, 1978.

[158] E. R. Hall, L. I. Bibby, and R. J. Slack, "Characterisation of a novel, high affinity and selective αvβ6 integrin RGD-mimetic radioligand," *Biochemical Pharmacology,* vol. 117, pp. 88-96, 2016.

[159] C. P. Carron *et al.*, "A peptidomimetic antagonist of the integrin αvβ3 inhibits Leydig cell tumor growth and the development of hypercalcemia of malignancy," *Cancer research,* vol. 58, no. 9, pp. 1930-1935, 1998.

[160] C. Mas-Moruno, F. Rechenmacher, and H. Kessler, "Cilengitide: the first anti-angiogenic small molecule drug candidate. Design, synthesis and clinical evaluation," *Anti-Cancer Agents in Medicinal Chemistry (Formerly Current Medicinal Chemistry-Anti-Cancer Agents),* vol. 10, no. 10, pp. 753-768, 2010.

[161] M. W. Miller *et al.*, "Small-molecule inhibitors of integrin α2β1 that prevent pathological thrombus formation via an allosteric mechanism," *Proceedings of the National Academy of Sciences,* vol. 106, no. 3, pp. 719-724, 2009.

[162] K. J. Livak and T. D. Schmittgen, "Analysis of relative gene expression data using real-time quantitative PCR and the 2− ΔΔCT method," *methods,* vol. 25, no. 4, pp. 402-408, 2001.

[163] D. Kim, B. Langmead, and S. L. Salzberg, "HISAT: a fast spliced aligner with low memory requirements," *Nature methods,* vol. 12, no. 4, pp. 357-360, 2015.

[164] Y. Benjamini and Y. Hochberg, "Controlling the false discovery rate: a practical and powerful approach to multiple testing," *Journal of the royal statistical society. Series B (Methodological),* pp. 289-300, 1995.

[165] R. R. Driskell and F. M. Watt, "Understanding fibroblast heterogeneity in the skin," *Trends in cell biology,* vol. 25, no. 2, pp. 92-99, 2015.

[166] C. Zhang, X. Meng, Z. Zhu, X. Yang, and A. Deng, "Role of connective tissue growth factor in renal tubular epithelial-myofibroblast transdifferentiation and extracellular matrix accumulation in vitro," *Life sciences,* vol. 75, no. 3, pp. 367-379, 2004.

[167] S.-J. Chen, W. Yuan, Y. Mori, A. Levenson, M. Trojanowska, and J. Varga, "Stimulation of type I collagen transcription in human skin fibroblasts by TGF-β: involvement of Smad 3," *Journal of investigative dermatology,* vol. 112, no. 1, pp. 49-57, 1999.

[168] R. C. Chambers, P. Leoni, N. Kaminski, G. J. Laurent, and R. A. Heller, "Global Expression Profiling of Fibroblast Responses to Transforming Growth Factor-β< sub> 1</sub> Reveals the Induction of Inhibitor of Differentiation-1 and Provides Evidence of Smooth Muscle Cell Phenotypic Switching," *The American journal of pathology,* vol. 162, no. 2, pp. 533-546, 2003.

[169] E. A. Renzoni *et al.*, "Gene expression profiling reveals novel TGFbeta targets in adult lung fibroblasts," *Respir Res,* vol. 5, no. 1, p. 24, 2004.

[170] C.-M. Lo, D. B. Buxton, G. C. H. Chua, M. Dembo, R. S. Adelstein, and Y.-L. Wang, "Nonmuscle myosin IIb is involved in the guidance of fibroblast migration," *Molecular biology of the cell,* vol. 15, no. 3, pp. 982-989, 2004.

[171] W. Metzger, N. Grenner, S. E. Motsch, R. Strehlow, T. Pohlemann, and M. Oberringer, "Induction of myofibroblastic differentiation in vitro by covalently immobilized transforming growth factor-β1," *Tissue engineering,* vol. 13, no. 11, pp. 2751-2760, 2007.

[172] J. Malmström *et al.*, "Transforming growth factor-β1 specifically induce proteins involved in the myofibroblast contractile apparatus," *Molecular & Cellular Proteomics,* vol. 3, no. 5, pp. 466-477, 2004.
[173] M. Vicente-Manzanares, X. Ma, R. S. Adelstein, and A. R. Horwitz, "Non-muscle myosin II takes centre stage in cell adhesion and migration," *Nature reviews Molecular cell biology,* vol. 10, no. 11, pp. 778-790, 2009.
[174] M. L. Nyström, G. J. Thomas, M. Stone, I. C. Mackenzie, I. R. Hart, and J. F. Marshall, "Development of a quantitative method to analyse tumour cell invasion in organotypic culture," *The Journal of pathology,* vol. 205, no. 4, pp. 468-475, 2005.
[175] J. J. Tomasek, C. J. Haaksma, R. J. Schwartz, and E. W. Howard, "Whole animal knockout of smooth muscle alpha-actin does not alter excisional wound healing or the fibroblast-to-myofibroblast transition," *Wound Repair and Regeneration,* vol. 21, no. 1, pp. 166-176, 2013.
[176] X. Huang *et al.*, "Matrix stiffness–induced myofibroblast differentiation is mediated by intrinsic mechanotransduction," *American journal of respiratory cell and molecular biology,* vol. 47, no. 3, pp. 340-348, 2012.
[177] L. Goffin, Q. Seguin-Estévez, M. Alvarez, W. Reith, and C. Chizzolini, "Transcriptional regulation of matrix metalloproteinase-1 and collagen 1A2 explains the anti-fibrotic effect exerted by proteasome inhibition in human dermal fibroblasts," *Arthritis research & therapy,* vol. 12, no. 2, p. 1, 2010.
[178] O. Eickelberg *et al.*, "Extracellular matrix deposition by primary human lung fibroblasts in response to TGF-β1 and TGF-β3," *American Journal of Physiology-Lung Cellular and Molecular Physiology,* vol. 276, no. 5, pp. L814-L824, 1999.
[179] F. J. Vizoso *et al.*, "Study of matrix metalloproteinases and their inhibitors in breast cancer," *British journal of cancer,* vol. 96, no. 6, pp. 903-911, 2007.
[180] J. García-Alvarez *et al.*, "Tissue inhibitor of metalloproteinase-3 is up-regulated by transforming growth factor-β1 in vitro and expressed in fibroblastic foci in vivo in idiopathic pulmonary fibrosis," *Experimental lung research,* 2009.
[181] C. C. Chipev and M. Simon, "Phenotypic differences between dermal fibroblasts from different body sites determine their responses to tension and TGFβ1," *BMC dermatology,* vol. 2, no. 1, p. 1, 2002.
[182] M. Chiquet, L. Gelman, R. Lutz, and S. Maier, "From mechanotransduction to extracellular matrix gene expression in fibroblasts," *Biochimica et Biophysica Acta (BBA)-Molecular Cell Research,* vol. 1793, no. 5, pp. 911-920, 2009.
[183] N. Merna *et al.*, "Differential β3 integrin expression regulates the response of human lung and cardiac fibroblasts to extracellular matrix and its components," *Tissue Engineering Part A,* vol. 21, no. 15-16, pp. 2195-2205, 2015.
[184] J. H. Tchaicha, S. B. Reyes, J. Shin, M. G. Hossain, F. F. Lang, and J. H. McCarty, "Glioblastoma angiogenesis and tumor cell invasiveness are differentially regulated by β8 integrin," *Cancer research,* vol. 71, no. 20, pp. 6371-6381, 2011.
[185] H. Kitamura *et al.*, "Mouse and human lung fibroblasts regulate dendritic cell trafficking, airway inflammation, and fibrosis through integrin αvβ8–mediated activation of TGF-β," *The Journal of clinical investigation,* vol. 121, no. 7, pp. 2863-2875, 2011.
[186] B. Hinz, G. Celetta, J. J. Tomasek, G. Gabbiani, and C. Chaponnier, "Alpha-smooth muscle actin expression upregulates fibroblast contractile activity," *Molecular biology of the cell,* vol. 12, no. 9, pp. 2730-2741, 2001.
[187] M. M. Ibrahim *et al.*, "Myofibroblasts contribute to but are not necessary for wound contraction," *Laboratory Investigation,* vol. 95, no. 12, pp. 1429-1438, 2015.

[188] X. Fu *et al.*, "Differential regulation of skin fibroblasts for their TGF-β1-dependent wound healing activities by biomimetic nanofibers," *Journal of Materials Chemistry B,* vol. 4, no. 31, pp. 5246-5255, 2016.

[189] C. H. Stuelten, S. D. Byfield, P. R. Arany, T. S. Karpova, W. G. Stetler-Stevenson, and A. B. Roberts, "Breast cancer cells induce stromal fibroblasts to express MMP-9 via secretion of TNF-α and TGF-β," *Journal of cell science,* vol. 118, no. 10, pp. 2143-2153, 2005.

[190] Y. Kojima *et al.*, "Autocrine TGF-β and stromal cell-derived factor-1 (SDF-1) signaling drives the evolution of tumor-promoting mammary stromal myofibroblasts," *Proceedings of the National Academy of Sciences,* vol. 107, no. 46, pp. 20009-20014, 2010.

[191] Y. Asano, H. Ihn, K. Yamane, M. Jinnin, and K. Tamaki, "Increased expression of integrin αvβ5 induces the myofibroblastic differentiation of dermal fibroblasts," *The American journal of pathology,* vol. 168, no. 2, pp. 499-510, 2006.

[192] Y. Asano, H. Ihn, K. Yamane, M. Jinnin, Y. Mimura, and K. Tamaki, "Increased expression of integrin αvβ3 contributes to the establishment of autocrine TGF-β signaling in scleroderma fibroblasts," *The Journal of Immunology,* vol. 175, no. 11, pp. 7708-7718, 2005.

[193] S. Kondo *et al.*, "Transforming growth factor-β1 stimulates collagen matrix remodeling through increased adhesive and contractive potential by human renal fibroblasts," *Biochimica et Biophysica Acta (BBA)-Molecular Cell Research,* vol. 1693, no. 2, pp. 91-100, 2004.

[194] P. Koistinen and J. Heino, "The selective regulation of αvβ1 integrin expression is based on the hierarchical formation of αv-containing heterodimers," *Journal of Biological Chemistry,* vol. 277, no. 27, pp. 24835-24841, 2002.

[195] S. Liu *et al.*, "Expression of integrin β1 by fibroblasts is required for tissue repair in vivo," *J Cell Sci,* vol. 123, no. 21, pp. 3674-3682, 2010.

[196] B. Hu, M. J. Jarzynka, P. Guo, Y. Imanishi, D. D. Schlaepfer, and S.-Y. Cheng, "Angiopoietin 2 induces glioma cell invasion by stimulating matrix metalloprotease 2 expression through the αvβ1 integrin and focal adhesion kinase signaling pathway," *Cancer research,* vol. 66, no. 2, pp. 775-783, 2006.

[197] X. Zhu *et al.*, "Galectin-1 knockdown in carcinoma-associated fibroblasts inhibits migration and invasion of human MDA-MB-231 breast cancer cells by modulating MMP-9 expression," *Acta biochimica et biophysica Sinica,* p. gmw019, 2016.

[198] C. Li *et al.*, "Increased activation of latent TGF-β1 by αVβ3 in human Crohn's disease and fibrosis in TNBS colitis can be prevented by cilengitide," *Inflammatory bowel diseases,* vol. 19, no. 13, p. 2829, 2013.

[199] J.-C. Chen, Y.-C. Fong, and C.-H. Tang, "Novel strategies for the treatment of chondrosarcomas: targeting integrins," *BioMed research international,* vol. 2013, 2013.

[200] P. T. Caswell, M. Chan, A. J. Lindsay, M. W. McCaffrey, D. Boettiger, and J. C. Norman, "Rab-coupling protein coordinates recycling of α5β1 integrin and EGFR1 to promote cell migration in 3D microenvironments," *The Journal of cell biology,* vol. 183, no. 1, pp. 143-155, 2008.

[201] V. H. Lobert *et al.*, "Ubiquitination of α5β1 integrin controls fibroblast migration through lysosomal degradation of fibronectin-integrin complexes," *Developmental cell,* vol. 19, no. 1, pp. 148-159, 2010.

[202] M. Paolillo, M. Serra, and S. Schinelli, "Integrins in glioblastoma: still an attractive target?," *Pharmacological Research,* 2016.

[203] K. R. Levental *et al.*, "Matrix crosslinking forces tumor progression by enhancing integrin signaling," *Cell,* vol. 139, no. 5, pp. 891-906, 2009.

[204] D. C. Rockey, P. D. Bell, and J. A. Hill, "Fibrosis—a common pathway to organ injury and failure," *New England Journal of Medicine,* vol. 372, no. 12, pp. 1138-1149, 2015.
[205] R. Navab *et al.*, "Integrin α11β1 regulates cancer stromal stiffness and promotes tumorigenicity and metastasis in non-small cell lung cancer," *Oncogene,* 2015.
[206] S. Tugues *et al.*, "Tetraspanin CD63 promotes vascular endothelial growth factor receptor 2-β1 integrin complex formation, thereby regulating activation and downstream signaling in endothelial cells in vitro and in vivo," *Journal of Biological Chemistry,* vol. 288, no. 26, pp. 19060-19071, 2013.
[207] F. Wang *et al.*, "Reciprocal interactions between β1-integrin and epidermal growth factor receptor in three-dimensional basement membrane breast cultures: a different perspective in epithelial biology," *Proceedings of the National Academy of Sciences,* vol. 95, no. 25, pp. 14821-14826, 1998.
[208] X. Liu *et al.*, "Smad3 mediates the TGF-β-induced contraction of type I collagen gels by mouse embryo fibroblasts," *Cell motility and the cytoskeleton,* vol. 54, no. 3, pp. 248-253, 2003.
[209] J. Kopp *et al.*, "Abrogation of transforming growth factor-β signaling by SMAD7 inhibits collagen gel contraction of human dermal fibroblasts," *Journal of Biological Chemistry,* vol. 280, no. 22, pp. 21570-21576, 2005.
[210] J.-N. Schulz *et al.*, "Reduced Granulation Tissue and Wound Strength in the Absence of α11β1 Integrin," *Journal of Investigative Dermatology,* vol. 135, no. 5, pp. 1435-1444, 2015.
[211] C. Zeltz and D. Gullberg, "The integrin–collagen connection–a glue for tissue repair?," *J Cell Sci,* vol. 129, no. 4, pp. 653-664, 2016.
[212] L. Wang, C. M. Ly, C.-Y. Ko, E. E. Meyers, D. A. Lawrence, and A. M. Bernstein, "uPA Binding to PAI-1 Induces Corneal Myofibroblast Differentiation on VitronectinuPA Induces Myofibroblasts on Vitronectin," *Investigative ophthalmology & visual science,* vol. 53, no. 8, pp. 4765-4775, 2012.
[213] J. Zhong, H.-C. Yang, V. Kon, A. B. Fogo, D. A. Lawrence, and J. Ma, "Vitronectin-binding PAI-1 protects against the development of cardiac fibrosis through interaction with fibroblasts," *Laboratory Investigation,* vol. 94, no. 6, pp. 633-644, 2014.
[214] B. S. Pedroja, L. E. Kang, A. O. Imas, P. Carmeliet, and A. M. Bernstein, "Plasminogen activator inhibitor-1 regulates integrin αvβ3 expression and autocrine transforming growth factor β signaling," *Journal of biological chemistry,* vol. 284, no. 31, pp. 20708-20717, 2009.
[215] H. Y. Chang *et al.*, "Gene expression signature of fibroblast serum response predicts human cancer progression: similarities between tumors and wounds," *PLoS Biol,* vol. 2, no. 2, p. e7, 2004.
[216] J. A. Nagy, A. M. Dvorak, and H. F. Dvorak, "VEGF-A and the induction of pathological angiogenesis," *Annu. Rev. Pathol. Mech. Dis.,* vol. 2, pp. 251-275, 2007.
[217] S. Bandaru *et al.*, "Targeting filamin B induces tumor growth and metastasis via enhanced activity of matrix metalloproteinase-9 and secretion of VEGF-A," *Oncogenesis,* vol. 3, no. 9, p. e119, 2014.
[218] L. Levy and C. S. Hill, "Alterations in components of the TGF-β superfamily signaling pathways in human cancer," *Cytokine & growth factor reviews,* vol. 17, no. 1, pp. 41-58, 2006.
[219] S. Busch, A. Acar, Y. Magnusson, P. Gregersson, L. Rydén, and G. Landberg, "TGF-beta receptor type-2 expression in cancer-associated fibroblasts regulates breast cancer cell growth and survival and is a prognostic marker in pre-menopausal breast cancer," *Oncogene,* vol. 34, no. 1, pp. 27-38, 2015.

[220] D. Bacman, S. Merkel, R. Croner, T. Papadopoulos, W. Brueckl, and A. Dimmler, "TGF-beta receptor 2 downregulation in tumour-associated stroma worsens prognosis and high-grade tumours show more tumour-associated macrophages and lower TGF-beta1 expression in colon carcinoma: a retrospective study," *BMC cancer,* vol. 7, no. 1, p. 1, 2007.

[221] N. Cheng *et al.*, "Loss of TGF-β type II receptor in fibroblasts promotes mammary carcinoma growth and invasion through upregulation of TGF-α-, MSP-and HGF-mediated signaling networks," *Oncogene,* vol. 24, no. 32, pp. 5053-5068, 2005.

[222] M. P. Lewis *et al.*, "Tumour-derived TGF-β1 modulates myofibroblast differentiation and promotes HGF/SF-dependent invasion of squamous carcinoma cells," *British journal of cancer,* vol. 90, no. 4, pp. 822-832, 2004.

[223] K. Deonarine *et al.*, "Gene expression profiling of cutaneous wound healing," *Journal of translational medicine,* vol. 5, no. 1, p. 1, 2007.

[224] V. Barry-Hamilton *et al.*, "Allosteric inhibition of lysyl oxidase-like-2 impedes the development of a pathologic microenvironment," *Nature medicine,* vol. 16, no. 9, pp. 1009-1017, 2010.

[225] T. R. Spivak-Kroizman *et al.*, "Hypoxia triggers hedgehog-mediated tumor–stromal interactions in pancreatic cancer," *Cancer research,* vol. 73, no. 11, pp. 3235-3247, 2013.

[226] L. J. Vuga *et al.*, "WNT5A is a regulator of fibroblast proliferation and resistance to apoptosis," *American journal of respiratory cell and molecular biology,* vol. 41, no. 5, pp. 583-589, 2009.

[227] N. Erez, M. Truitt, P. Olson, and D. Hanahan, "Cancer-associated fibroblasts are activated in incipient neoplasia to orchestrate tumor-promoting inflammation in an NF-κB-dependent manner," *Cancer cell,* vol. 17, no. 2, pp. 135-147, 2010.

[228] G. Monteleone *et al.*, "Control of matrix metalloproteinase production in human intestinal fibroblasts by interleukin 21," *Gut,* vol. 55, no. 12, pp. 1774-1780, 2006.

[229] V. Michalaki, K. Syrigos, P. Charles, and J. Waxman, "Serum levels of IL-6 and TNF-α correlate with clinicopathological features and patient survival in patients with prostate cancer," *British journal of cancer,* vol. 90, no. 12, pp. 2312-2316, 2004.

[230] G. Scambia *et al.*, "Prognostic significance of interleukin 6 serum levels in patients with ovarian cancer," *British journal of cancer,* vol. 71, no. 2, p. 354, 1995.

[231] P. Chomarat, J. Banchereau, J. Davoust, and A. K. Palucka, "IL-6 switches the differentiation of monocytes from dendritic cells to macrophages," *Nature immunology,* vol. 1, no. 6, pp. 510-514, 2000.

[232] M. Zeisberg *et al.*, "Fibroblasts derive from hepatocytes in liver fibrosis via epithelial to mesenchymal transition," *Journal of Biological Chemistry,* vol. 282, no. 32, pp. 23337-23347, 2007.

[233] F. Balkwill, "Tumour necrosis factor and cancer," *Nature Reviews Cancer,* vol. 9, no. 5, pp. 361-371, 2009.

[234] K. J. Campbell and N. D. Perkins, "Post-translational modification of RelA (p65) NF-κB," *Biochemical Society Transactions,* vol. 32, no. 6, pp. 1087-1089, 2004.

[235] D. J. Abraham, X. Shiwen, C. M. Black, S. Sa, Y. Xu, and A. Leask, "Tumor necrosis factor α suppresses the induction of connective tissue growth factor by transforming growth factor-β in normal and scleroderma fibroblasts," *Journal of Biological Chemistry,* vol. 275, no. 20, pp. 15220-15225, 2000.

[236] H. A. Baarsma *et al.*, "Activation of WNT/β-catenin signaling in pulmonary fibroblasts by TGF-β 1 is increased in chronic obstructive pulmonary disease," *PLoS One,* vol. 6, no. 9, p. e25450, 2011.

[237] M. Menzen, A. Spanjer, R. Gosens, and E. Van Dijk, "Wnt-5b induced inflammatory response in human lung fibroblasts," *Am J Respir Crit Care Med,* vol. 189, p. A6556, 2014.
[238] D. E. Costea *et al.*, "Identification of two distinct carcinoma-associated fibroblast subtypes with differential tumor-promoting abilities in oral squamous cell carcinoma," *Cancer research,* vol. 73, no. 13, pp. 3888-3901, 2013.
[239] Y. P. Moodley *et al.*, "Fibroblasts isolated from normal lungs and those with idiopathic pulmonary fibrosis differ in interleukin-6/gp130-mediated cell signaling and proliferation," *The American journal of pathology,* vol. 163, no. 1, pp. 345-354, 2003.
[240] L. Xiao, Y. Du, Y. Shen, Y. He, H. Zhao, and Z. Li, "TGF-beta 1 induced fibroblast proliferation is mediated by the FGF-2/ERK pathway," *Front Biosci,* vol. 17, no. 1, pp. 2667-2674, 2012.
[241] F. Strutz *et al.*, "Basic fibroblast growth factor expression is increased in human renal fibrogenesis and may mediate autocrine fibroblast proliferation," *Kidney International,* vol. 57, pp. 1521-1538, 2000.
[242] G. Finak *et al.*, "Stromal gene expression predicts clinical outcome in breast cancer," *Nature medicine,* vol. 14, no. 5, pp. 518-527, 2008.
[243] D. D. Hu-Lowe *et al.*, "Nonclinical antiangiogenesis and antitumor activities of axitinib (AG-013736), an oral, potent, and selective inhibitor of vascular endothelial growth factor receptor tyrosine kinases 1, 2, 3," *Clinical Cancer Research,* vol. 14, no. 22, pp. 7272-7283, 2008.
[244] (2016). *Approved Drugs - Axitinib* [WebContent]. Available: http://www.fda.gov/Drugs/InformationOnDrugs/ApprovedDrugs/ucm289439.htm
[245] (2016). *Axitinib for treating advanced renal cell carcinoma after failure of prior systemic treatment | Guidance and guidelines | NICE*. Available: https://www.nice.org.uk/guidance/ta333
[246] H. C. Lin *et al.*, "Beneficial effects of dual vascular endothelial growth factor receptor/fibroblast growth factor receptor inhibitor brivanib alaninate in cirrhotic portal hypertensive rats," *Journal of gastroenterology and hepatology,* vol. 29, no. 5, pp. 1073-1082, 2014.
[247] J. Huang *et al.*, "Nintedanib inhibits fibroblast activation and ameliorates fibrosis in preclinical models of systemic sclerosis," *Annals of the rheumatic diseases,* pp. annrheumdis-2014, 2015.
[248] I. M. Bondarenko, A. Ingrosso, P. Bycott, S. Kim, and C. L. Cebotaru, "Phase II study of axitinib with doublet chemotherapy in patients with advanced squamous non–small-cell lung cancer," *BMC cancer,* vol. 15, no. 1, p. 1, 2015.
[249] E. E. W. Cohen, M. Tortorici, S. Kim, A. Ingrosso, Y. K. Pithavala, and P. Bycott, "A Phase II trial of axitinib in patients with various histologic subtypes of advanced thyroid cancer: long-term outcomes and pharmacokinetic/pharmacodynamic analyses," *Cancer chemotherapy and pharmacology,* vol. 74, no. 6, pp. 1261-1270, 2014.
[250] J.-P. Spano *et al.*, "Efficacy of gemcitabine plus axitinib compared with gemcitabine alone in patients with advanced pancreatic cancer: an open-label randomised phase II study," *The Lancet,* vol. 371, no. 9630, pp. 2101-2108, 2008.
[251] S. Albertini *et al.*, "Genotoxicity of 17 gyrase-and four mammalian topoisomerase II-poisons in prokaryotic and eukaryotic test systems," *Mutagenesis,* vol. 10, no. 4, pp. 343-351, 1995.
[252] E. R. Mondal, S. K. Das, and P. Mukherjee, "Comparative Evaluation of Antiproliferative Activity and Induction of Apoptosis by some Fluoroquinolones on a

Human Non-small Cell Lung Cancer Cell Line in Culture," *Asian Pacific Journal of Cancer Prevention,* vol. 5, no. 2, pp. 196-204, 2004.

[253] M. Yamakuchi, M. Nakata, K.-i. Kawahara, I. Kitajima, and I. Maruyama, "New quinolones, ofloxacin and levofloxacin, inhibit telomerase activity in transitional cell carcinoma cell lines," *Cancer letters,* vol. 119, no. 2, pp. 213-219, 1997.

[254] G. Ouedraogo, P. Morliere, R. Santus, M. A. Miranda, and J. V. Castell, "Damage to mitochondria of cultured human skin fibroblasts photosensitized by fluoroquinolones," *Journal of Photochemistry and Photobiology B: Biology,* vol. 58, no. 1, pp. 20-25, 2000.

[255] J. D. Humphrey, E. R. Dufresne, and M. A. Schwartz, "Mechanotransduction and extracellular matrix homeostasis," *Nature reviews Molecular cell biology,* vol. 15, no. 12, pp. 802-812, 2014.

[256] X.-H. Zhao, C. Laschinger, P. Arora, K. Szászi, A. Kapus, and C. A. McCulloch, "Force activates smooth muscle α-actin promoter activity through the Rho signaling pathway," *Journal of cell science,* vol. 120, no. 10, pp. 1801-1809, 2007.

[257] P. C. Smith, M. Cáceres, and J. Martinez, "Induction of the myofibroblastic phenotype in human gingival fibroblasts by transforming growth factor-β1: role of RhoA-ROCK and c-Jun N-terminal kinase signaling pathways," *Journal of periodontal research,* vol. 41, no. 5, pp. 418-425, 2006.

[258] H. Ji *et al.*, "Rho/Rock cross-talks with transforming growth factor-β/Smad pathway participates in lung fibroblast-myofibroblast differentiation," *Biomedical reports,* vol. 2, no. 6, pp. 787-792, 2014.

[259] E. E. Torr, C. R. Ngam, K. Bernau, B. Tomasini-Johansson, B. Acton, and N. Sandbo, "Myofibroblasts exhibit enhanced fibronectin assembly that is intrinsic to their contractile phenotype," *Journal of Biological Chemistry,* vol. 290, no. 11, pp. 6951-6961, 2015.

[260] N. Amara, D. Goven, F. Prost, R. Muloway, B. Crestani, and J. Boczkowski, "NOX4/NADPH oxidase expression is increased in pulmonary fibroblasts from patients with idiopathic pulmonary fibrosis and mediates TGFβ1-induced fibroblast differentiation into myofibroblasts," *Thorax,* vol. 65, no. 8, pp. 733-738, 2010.

[261] I. Cucoranu *et al.*, "NAD (P) H oxidase 4 mediates transforming growth factor-β1–induced differentiation of cardiac fibroblasts into myofibroblasts," *Circulation research,* vol. 97, no. 9, pp. 900-907, 2005.

[262] N. Sampson *et al.*, "ROS signaling by NOX4 drives fibroblast-to-myofibroblast differentiation in the diseased prostatic stroma," *Molecular endocrinology,* vol. 25, no. 3, pp. 503-515, 2011.

[263] N. Manickam, M. Patel, K. K. Griendling, Y. Gorin, and J. L. Barnes, "RhoA/Rho kinase mediates TGF-β1-induced kidney myofibroblast activation through Poldip2/Nox4-derived reactive oxygen species," *American Journal of Physiology-Renal Physiology,* vol. 307, no. 2, pp. F159-F171, 2014.

[264] C. Jiang, H. Huang, J. Liu, Y. Wang, Z. Lu, and Z. Xu, "Fasudil, a rho-kinase inhibitor, attenuates bleomycin-induced pulmonary fibrosis in mice," *International journal of molecular sciences,* vol. 13, no. 7, pp. 8293-8307, 2012.

[265] Y. Shimizu, K. Dobashi, T. Sano, and M. Yamada, "ROCK activation in lung of idiopathic pulmonary fibrosis with oxidative stress," *International journal of immunopathology and pharmacology,* vol. 27, no. 1, pp. 37-44, 2014.

[266] L. A. Pardo and W. Stühmer, "The roles of K+ channels in cancer," *Nature Reviews Cancer,* vol. 14, no. 1, pp. 39-48, 2014.

[267] J. Selige, A. Hatzelmann, and T. Dunkern, "The differential impact of PDE4 subtypes in human lung fibroblasts on cytokine-induced proliferation and myofibroblast conversion," *Journal of cellular physiology,* vol. 226, no. 8, pp. 1970-1980, 2011.

[268] T. Kohyama *et al.*, "PDE4 inhibitors attenuate fibroblast chemotaxis and contraction of native collagen gels," *American journal of respiratory cell and molecular biology,* vol. 26, no. 6, pp. 694-701, 2002.
[269] M. Abdalla, A. Goc, L. Segar, and P. R. Somanath, "Akt1 mediates α-smooth muscle actin expression and myofibroblast differentiation via myocardin and serum response factor," *Journal of Biological Chemistry,* vol. 288, no. 46, pp. 33483-33493, 2013.
[270] G. Gabbiani, "The myofibroblast in wound healing and fibrocontractive diseases," *The Journal of pathology,* vol. 200, no. 4, pp. 500-503, 2003.
[271] W. Carver, I. Molano, T. A. Reaves, T. K. Borg, and L. Terracio, "Role of the α1β1 integrin complex in collagen gel contraction in vitro by fibroblasts," *Journal of cellular physiology,* vol. 165, no. 2, pp. 425-437, 1995.
[272] Y. Zhou, J. S. Hagood, B. Lu, W. D. Merryman, and J. E. Murphy-Ullrich, "Thy-1-integrin αvβ5 interactions inhibit lung fibroblast contraction-induced latent transforming growth factor-β1 activation and myofibroblast differentiation," *Journal of Biological Chemistry,* vol. 285, no. 29, pp. 22382-22393, 2010.
[273] B. C. Kim *et al.*, "Fibroblasts from chronic wounds show altered TGF-β-signaling and decreased TGF-β Type II Receptor expression," *Journal of cellular physiology,* vol. 195, no. 3, pp. 331-336, 2003.
[274] W. Qiu *et al.*, "No evidence of clonal somatic genetic alterations in cancer-associated fibroblasts from human breast and ovarian carcinomas," *Nature genetics,* vol. 40, no. 5, pp. 650-655, 2008.
[275] T. R. Dunkern, D. Feurstein, G. A. Rossi, F. Sabatini, and A. Hatzelmann, "Inhibition of TGF-β induced lung fibroblast to myofibroblast conversion by phosphodiesterase inhibiting drugs and activators of soluble guanylyl cyclase," *European journal of pharmacology,* vol. 572, no. 1, pp. 12-22, 2007.
[276] B. C. Özdemir *et al.*, "Depletion of carcinoma-associated fibroblasts and fibrosis induces immunosuppression and accelerates pancreas cancer with reduced survival," *Cancer cell,* vol. 25, no. 6, pp. 719-734, 2014.
[277] A. D. Rhim *et al.*, "Stromal elements act to restrain, rather than support, pancreatic ductal adenocarcinoma," *Cancer cell,* vol. 25, no. 6, pp. 735-747, 2014.
[278] M. H. Sherman *et al.*, "Vitamin D receptor-mediated stromal reprogramming suppresses pancreatitis and enhances pancreatic cancer therapy," *Cell,* vol. 159, no. 1, pp. 80-93, 2014.
[279] L. Rønnov-Jessen, O. W. Petersen, V. E. Koteliansky, and M. J. Bissell, "The origin of the myofibroblasts in breast cancer. Recapitulation of tumor environment in culture unravels diversity and implicates converted fibroblasts and recruited smooth muscle cells," *Journal of Clinical Investigation,* vol. 95, no. 2, p. 859, 1995.
[280] D. A. Rider *et al.*, "Autocrine fibroblast growth factor 2 increases the multipotentiality of human adipose-derived mesenchymal stem cells," *Stem cells,* vol. 26, no. 6, pp. 1598-1608, 2008.
[281] G. Ishii *et al.*, "Bone-marrow-derived myofibroblasts contribute to the cancer-induced stromal reaction," *Biochemical and biophysical research communications,* vol. 309, no. 1, pp. 232-240, 2003.
[282] G. Ishii, A. Ochiai, and S. Neri, "Phenotypic and functional heterogeneity of cancer-associated fibroblast within the tumor microenvironment," *Advanced drug delivery reviews,* vol. 99, pp. 186-196, 2016.